HEXOSE SUGAR TRANSPORT AND METABOLISM AT THE PORCINE UTERINE-PLACENTAL INTERFACE

A Dissertation

by

CHELSIE BURROUGHS STEINHAUSER

Submitted to the Office of Graduate and Professional Studies of
Texas A&M University
in partial fulfillment of the requirements for the degree of

DOCTOR OF PHILOSOPHY

Chair of Committee,	Gregory Johnson
Committee Members,	Kayla Bayless
	Fuller Bazer
	Robert Burghardt
Head of Department,	Evelyn Tiffany-Castiglioni

December 2015

Major Subject: Biomedical Sciences

ABSTRACT

Commercial sows experience a high incidence of prenatal loss and substantial variation in birthweight among piglets in a litter. These outcomes negatively impact efficiency and profitability in the swine industry and are hypothesized to result from insufficient endometrial support and placental development during pregnancy. This study examined how glucose and fructose are synthesized, transported, and metabolized at the uterine-placental interface of pigs to support development and growth of the placenta and embryo/fetus.

Total tissue mRNA expression and mRNA or protein cellular localization for glucose transporters and polyol pathway enzymes were determined in endometrial and/or placental tissues collected from gilts throughout the estrous cycle and pregnancy. *SLC2A1* is the most abundant glucose transporter in the endometrium and is expressed by luminal (LE) and glandular epithelia (GE) throughout pregnancy. *SLC2A3* is expressed by trophectoderm/chorion throughout pregnancy. *SLC2A5*, a fructose transporter, is expressed by LE and chorion after Day 30 of gestation. SLC2A8, a glucose and fructose transporter, is expressed by LE, GE, and select fetal tissues during the peri-implantation period of pregnancy. *SLC2A1* mRNA and SLC2A8 protein are upregulated in the uterine epithelia in response to E2 and P4.

The conversion of glucose to fructose involves aldose reductase (AKR1B1) and sorbitol dehydrogenase (SORD). AKR1B1 is expressed by uterine LE during the peri-implantation period, then by chorion after Day 20. SORD is expressed initially by

uterine LE, GE, and trophectoderm, but is barely detectable in the endometrium by Day 20. Ketohexokinase (KHK), which phosphorylates fructose, is expressed by trophectoderm/chorion throughout pregnancy, especially in the tall columnar cells and areolae.

These results establish the presence of the molecular components for hexose sugar transport, conversion of glucose to fructose, and fructose utilization at the uterine-placental interface of pigs. The shift in expression of AKR1B1 and SORD from uterine LE to chorion during pregnancy suggests that the free-floating conceptuses are supported by fructose synthesized and secreted into the uterine lumen by uterine LE. After placentation is initiated, the chorion becomes self-sufficient for fructose synthesis and transport to the conceptus. With this knowledge, future studies can be designed to manipulate the availability and transport of hexose sugars across the uterine-placental interface to decrease prenatal loss and variability in birth weights within litters, leading to increased efficiency and profitability for the swine industry.

ACKNOWLEDGEMENTS

I would like to thank my committee chair, Dr. Greg Johnson, for his guidance and support throughout the course of this research. I would also like to thank my committee members, Drs. Kayla Bayless, Fuller Bazer, and Robert Burghardt, for sharing their knowledge and helping me develop as a scientist throughout my doctoral program.

I would like to acknowledge the Office of Graduate and Professional Studies at Texas A&M University for providing me with a Graduate Diversity Fellowship, which allowed me to pursue this degree.

Thanks also go to my family and friends who have supported me through many years of school, and, specifically, to Dr. Virginia Lehman whose faith and belief in my ability to succeed has always been a driving force for me.

Finally, I would thank my husband, Bryan Steinhauser, for his continual support, faith, and love.

TABLE OF CONTENTS

Page

LIST OF FIGURES

Page

LIST OF TABLES

Page

CHAPTER I

INTRODUCTION

Modern commercial sows have a high incidence of prenatal loss, and individual piglet birthweight varies greatly within a litter, especially with increasing litter size (van der Lende et al., 2001). While sows ovulate 20 to 30 oocytes, only 9 to 15 piglets are delivered at term, and this is due to embryonic/fetal losses at multiple time points during pregnancy. Embryonic/fetal losses occur during four periods of pregnancy, including: 1) the peri-implantation period, prior to Day 16 of pregnancy; 2) between Days 35 to 40; 3) mid-gestation from Days 55 to 75; and, 4) just prior to farrowing (van der Lende and van Rens, 2003). These time points coincide with major changes in placental growth and development, therefore, fetal loss may be in part due to insufficient physical and biochemical development of the interface between endometrial and placental tissues or endometrial development early in pregnancy (Wilson et al., 2001; Vallet et al., 2002).

The large variability in birthweights within a single litter is attributed to intrauterine growth restriction resulting in runt piglets that are only one-half or one-third the size of their largest littermates (Widdowson, 1971). This reduced bodyweight correlates with reduced survival and growth of the runt piglets, making them less cost efficient than larger piglets as they are never able to fully compensate for the intrauterine growth restriction (Ritacco et al., 1997; Tilley et al., 2007). Differences in embryonic development in early pregnancy are noticeable during trophectoderm elongation (Geisert et al., 1982a). Insufficient trophectoderm elongation directly affects placental

development leading to detrimental alterations of the maternal/conceptus interface of small as compared to large fetuses (Vallet and Freking, 2007). While there is evidence that manipulating the maternal diet can reduce variation in birthweight, and improve fetal survivability, advancements in the basic understanding of nutrient transport and metabolism in the endometrium and placenta of pregnant pigs is necessary for further development of strategies to improve placental development and birth weights of piglets for increased economic profitability and sustainability of the swine industry (Wu et al., 2013; De Vos et al., 2014).

Glucose and fructose are abundant hexose sugars in porcine endometria and conceptuses (embryo/fetus and associated placenta). Fructose plays a minor role as an energy source in the placenta and fetus, but fructose can be used as a substrate in a number of metabolic pathways that support conceptus development, including biosynthesis of glycosaminoglycans, phospholipids, and nucleic acids (White et al., 1982). Recently, *in vitro* studies demonstrated that porcine trophectoderm cells utilize fructose through the hexosamine biosynthetic pathway to stimulate mechanistic target of rapamycin (MTOR) cell signaling and cell proliferation, and for the synthesis of hyaluronic acid, a significant glycosaminoglycan in the placenta (Kim et al., 2012).

Fructose is detected in uterine flushings of pregnant gilts as early as Day 12 of pregnancy and is present in greater quantities than glucose in the allantoic fluid and fetal blood (Aherne et al., 1969; Zavy et al., 1982; Bazer et al., 1988). Additionally, fructose is undetectable in maternal blood of pregnant gilts and sows (Pere, 1995). Studies by White *et al.* demonstrated that fructose injected intraperitoneally into an *in utero* fetus

cannot cross the placenta or be converted into glucose, but glucose injected in the same manner can cross the placenta and be converted to fructose (White et al., 1979). Those results suggest that the placenta is the site of fructose production and it is hypothesized that fructose synthesis is a method for the fetus to sequester hexose sugars from the mother (Zavy et al., 1982). However, the cellular localization of fructose synthesis, the cellular use of fructose, and the transport system for both glucose and fructose in placental and endometrial tissues have not been defined in pigs.

The long term research goal is to establish the roles of glucose and fructose in fetal and placental development in pigs, and to determine how they relate to birth weight and fetal survival. The short term goals of the research described in this dissertation were to: 1) identify and localize transporters for hexose sugars in cells of the endometria and placentae; 2) determine which cells synthesize fructose from glucose within endometria and placentae; and 3) determine which endometrial and placental cells utilize fructose.

Our hypothesis was that glucose is transported to the placenta from maternal blood and that a fraction of the glucose is converted to fructose via the polyol pathway. Fructose can then be transported and utilized by the conceptus for synthesis of glycosaminoglycans via the hexosamine pathway and/or for actions as a metabolic regulator. While fructose is found in high concentrations in fetal blood and allantoic fluid, and the conceptus metabolizes fructose, the roles of specific endometrial and placental cell types in synthesizing and metabolizing fructose are unknown.

CHAPTER II

LITERATURE REVIEW

Estrous Cycle

Pigs are polyestrus, spontaneous ovulators with an approximately 21-day estrous cycle. The cycle begins with the onset of estrus, and ovulation of 15-30 oocytes takes place about 40 hours later. At this time the circulating concentration of progesterone is low, but as the corpora lutea (CL) develop, more progesterone is produced until serum levels reach peak quantities around Days 8 to 9 after ovulation. Progesterone levels are maintained until the luteolysin prostaglandin $F_{2\alpha}$ (PGF) is secreted in pulses by the uterine luminal epithelium (LE) towards the utero-ovarian vein in response to pituitary oxytocin binding the oxytocin receptor in the LE on Day 15 or 16 of the estrous cycle (Moeljono et al., 1976; Mirando et al., 1995). The PGF is transported to the ovary and initiates luteolysis of the CL. This results in decreased serum progesterone levels, and the inhibition of progesterone on estrogen action is removed to allow for an ovulatory surge of luteinizing hormone to induce ovulation. Concentrations of estrogen in serum increase, as concentrations of progesterone decrease, and peak about two days before ovulation. During the estrous cycle, the uterus responds to increasing concentrations of progesterone to prepare for the arrival of embryos (Soede et al., 2011).

Pregnancy

The early stages of embryonic development in pigs proceed in a manner similar to that of other mammalian species (Figure 2.1). The pig is a litter bearing species, therefore, multiple oocytes are transported down the oviduct after ovulation. Fertilization occurs within the oviduct, and the zygotes undergo the first cleavage division by 26 hours after fertilization. Cleavage divisions continue, and at the 8-16 cell stage activation of the embryonic transcriptome occurs. The developing embryos enter the uterus at 46 to 56 hours post-fertilization, and form blastocysts. At this point the pluripotent blastomeres begin to differentiate into the inner cell mass (ICM) and trophectoderm to begin the cell lineages that will eventually become the embryo/fetus proper and the placental chorion, respectively, and are collectively termed the conceptus. Blastocysts hatch out of the zona pellucida on Days 6 to 7 as 0.5 to 1 mm spheres, and increase in size to 2 to 6 mm by Day 10 before undergoing a rapid morphological transition called elongation (Figure 2.2). The small spherical blastocysts grow into a long ovoid form (10 to 15 mm) with the trophoblast and endoderm cells migrating toward the ICM to form the elongation zone. The tubular (15 mm by 50 mm) blastocysts then begin to increase in length and decrease in diameter due to the migration of trophectoderm and endoderm cells towards the ends of the blastocyst to produce the filamentous form (1 mm by 100-200 mm). Pig conceptuses elongate at 30 to 40 mm/h during the transition from spherical to filamentous forms primarily due to this trophectoderm remodeling (Geisert et al., 1982a; Mattson et al., 1990). The next phase of rapid growth is dependent on hyperplasia, and the filamentous conceptus grows to 800 to 1000 mm in length by Day

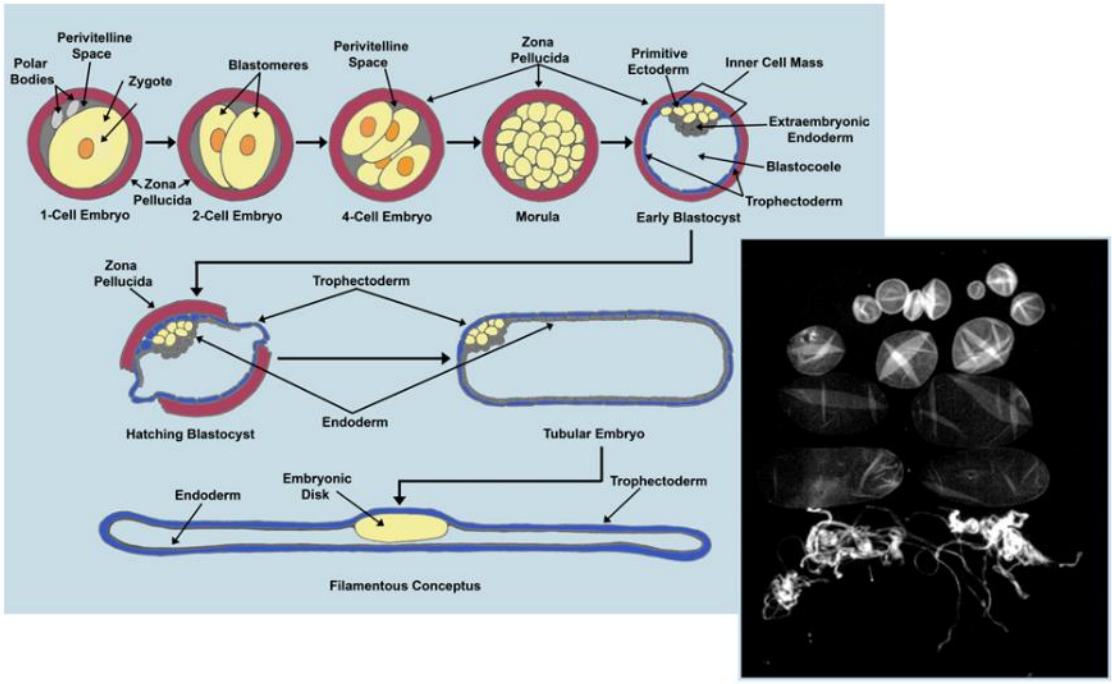

Figure 2.1 Pig embryo pre-implantation development
Pig conceptus pre-implantation development begins with the cleavage stages and the development of the blastocyst. The blastocyst hatches from the zona pellucida and begins to elongate from a small sphere, to a large sphere, to a tubular form, and then to a filamentous form. Reprinted with permission from Bazer and Johnson, 2014.

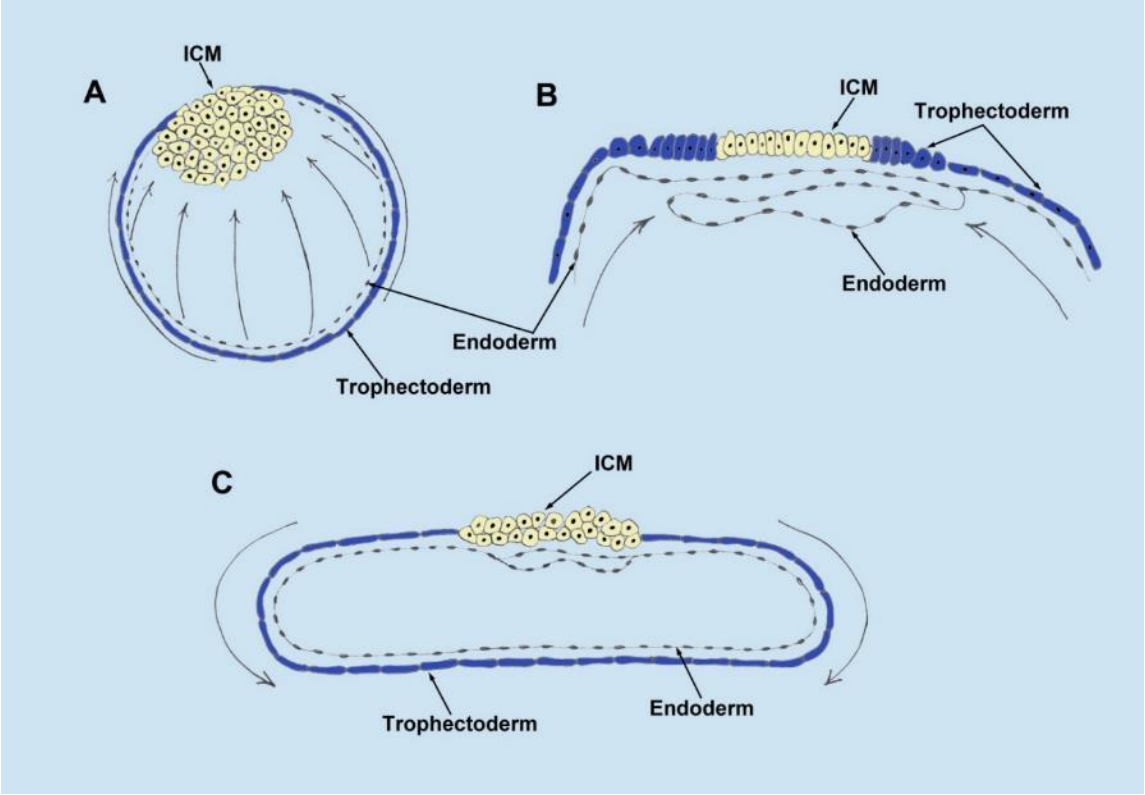

Figure 2.2 Elongation of the pig embryo
Pig embryo elongation is proposed to begin with the (**A**) proliferating trophectoderm and endoderm cells migrating toward the inner cell mass (ICM) to form the elongation zone along the same plane as the ICM along the length of the blastocyst (**B**). The trophectoderm and endoderm cells then migrate towards the tips of the tubular blastocyst (**C**), which reduces the diameter of the blastocyst to eventually develop the filamentous form that can has the maximal surface area for interaction with the uterine luminal epithelium. Reprinted with permission from Bazer and Johnson, 2014.

18 of pregnancy. During the early elongation period, the conceptus remains free-floating and dependent on the uterus for nutrients. Conceptus elongation provides increased surface area for nutrient exchange between the conceptus and uterus and to ensure that estrogens from the conceptus inhibit luteolysis (Dhindsa and Dziuk, 1968). Development of conceptuses within a litter does not happen uniformly as can been seen by the presence of multiple morphological stages at any given time point in a single uterus (Anderson, 1978).

After the blastocyst hatches from the zona pellucida, gastrulation, or formation of three distinct germ layers, ectoderm, mesoderm, and endoderm, begins. The ICM first differentiates into the hypoblast or the primitive endoderm (ventral to the blastocyst cavity, layered against the trophectoderm) and the epiblast (dorsal to the blastocyst cavity). At Day 9 of pregnancy, the trophectoderm overlaying the epiblast (Rauber's layer) gradually disintegrates allowing the epiblast to be exposed to the uterine environment and to form the embryonic disc, which will differentiate into the three distinct germ layers. By Day 11, the mesoderm and endoderm begin to form, and then the remaining epiblast cells differentiate into neural or ectoderm cells (Figure 2.3). The endoderm cells begin to replace the hypoblast cells that line the epiblast and the mesoderm cells localize as an intermediate mesenchymal layer between the epithelial endodermal and ectodermal cell layers. Eventually, the extra-embryonic mesoderm will fuse with the primitive endoderm, the ectoderm, and the trophectoderm to give rise to the yolk sac, amnion, and chorion, respectively, as seen in Figure 2.4 (Perry, 1981; Blomberg et al., 2008; Oestrup et al., 2009).

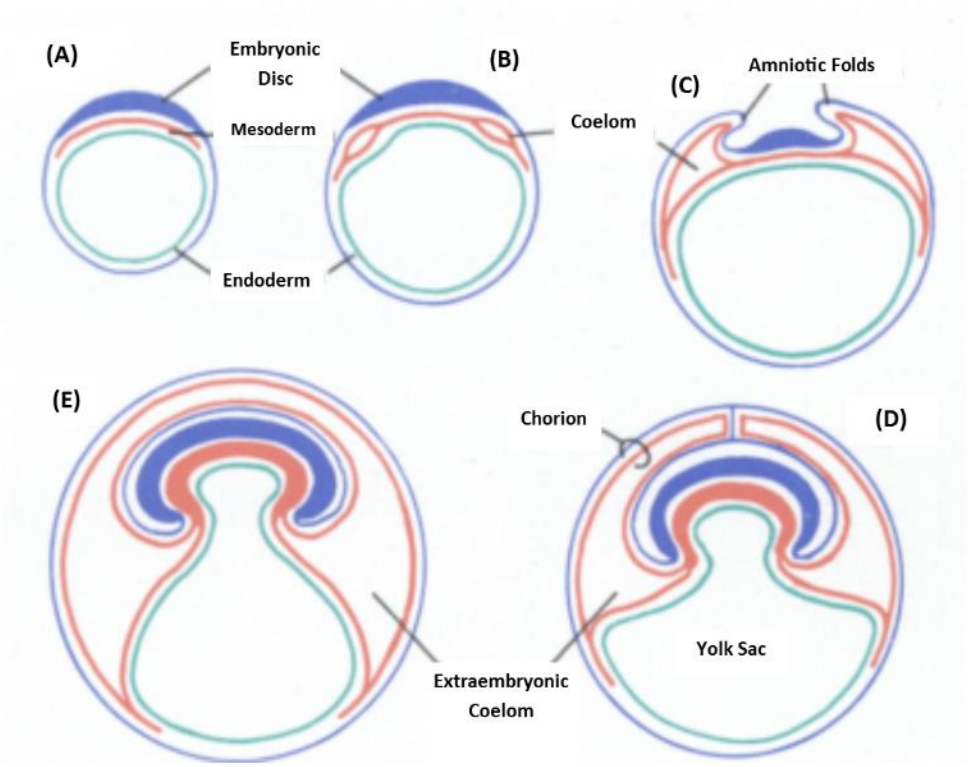

Figure 2.3 Development of the extraembryonic membranes
By Day 11, the embryonic disc has formed, while the mesoderm and endoderm are developing (**A, B**). The trophoblast and mesoderm fold around the embryo to create the amnion (**C**) as the endoderm develops into the yolk sac, and the chorion is formed from the trophoblast and the mesoderm (**D**). By Day 15, the allantoic cavity has formed (**E**) and will continue to enlarge as pregnancy progresses . Reprinted with permission from Perry, 1981.

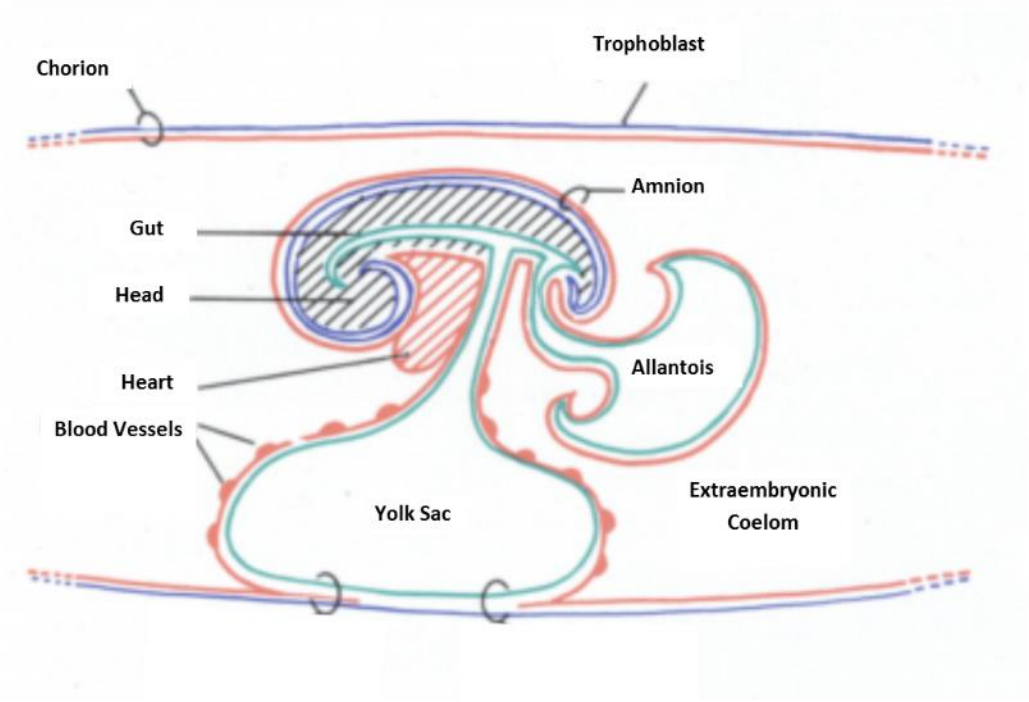

Figure 2.4 Extraembryonic membranes at Day 18 of pregnancy
By Day 18, the amnion completely surrounds the embryo, the allantois has formed and is enlarging to eventually surround the amnion and the embryo, and the yolk sac provides nutrients to the embryo. As placentation proceeds, the yolk sac will recede and the allantois will take over its function in nutrient support for the fetus. Reprinted with permission from Perry, 1981.

As conceptuses undergo these morphological changes, they also produce and secrete estrogen as well as a multitude of other cytokines and growth factors (Geisert et al., 1982b; La Bonnardiere et al., 1991). Many of these factors then act in a paracrine manner, or in an autocrine manner of the trophectoderm, to begin cross-talk between the conceptus and uterus that is necessary for successful implantation.

Maternal Recognition of Pregnancy

In the pig, conceptus trophectoderm secretes estrogen as the signal for maternal recognition of pregnancy (Bazer and Thatcher, 1977). As outlined in the endocrine-exocrine theory, estrogen secretion by the trophectoderm between Days 11 to 12 acts to redirect secretion of prostaglandin $F_{2\alpha}$ (PGF) into the uterine lumen, where it is sequestered and/or metabolized in order to prevent luteolysis (Bazer and Thatcher, 1977; Pusateri et al., 1990). This exocrine secretion of PGF is in contrast to the endocrine secretion that would occur in a normal estrous cycle without the influence of estrogen. Maintenance of the CL is necessary because it produces progesterone, the hormone of pregnancy, which is an essential regulator of uterine functions required for conceptus development, implantation, placentation, and the sustainability of pregnancy. Pseudopregnancy can be achieved in the pig with injection of exogenous 17β-estradiol on Days 11 to 15 of the estrous cycle as the estrogen results in PGF secretion into the uterine lumen and continued maintenance of the corpus luteum for a period of time that is equal to, or slightly longer than, the normal period of gestation for pigs of 114 days (Frank et al., 1977).

Progesterone and Estrogen Receptors in the Uterine Endometrium

Progesterone, from the CL, and estrogen, from the conceptus trophectoderm, mediate their effects on the uterine endometrium through their respective steroid hormone receptors. Expression of these receptors is temporally and spatially variable during the estrous cycle and early pregnancy and allows for the tight control of downstream targets necessary to either maintain a successful pregnancy, or prepare the endometrium for another cycle. Progesterone receptor B (PGRB) protein is expressed in the uterine LE, GE, stroma, and myometrium through Day 7 of the estrous cycle and pregnancy. During both the estrous cycle and pregnancy, prolonged progesterone exposure leads to undetectable levels of PGRB in the uterine LE by Day 10 and in the GE by Day 12, but stromal and myometrial cells continue to express PGRB (Geisert et al., 1994). Progesterone receptor A (PGRA) protein has been detected by Western Blot in endometria between Days 0 to 10 of the estrous cycle and pregnancy (Geisert et al., 1994).

Estrogen receptor (ER) protein localizes to the uterine LE and GE from Days 0 to 12 of the estrous cycle and pregnancy with decreased expression in the LE and GE from Days 5 to 10, and then increased expression between Days 12 and 15 (Ross et al., 2010). Stromal expression of ER is highest at Day 0, decreases by Day 5, and remains low throughout pregnancy, or increases by Day 18 in the estrous cycle (Geisert et al., 1993). ER continues to be expressed in the deep glands through Day 71 of pregnancy with detectable myometrial expression observed from Days 10 through 32 of pregnancy (Knapczyk-Stwora et al., 2011).

Implantation

Implantation involves complex interactions between a developmentally competent conceptus and a receptive uterus (Carson et al., 2000; Burghardt et al., 2002; Lessey, 2002). The phases of the implantation cascade are defined as: (1) shedding of the zona pellucida and elongation of the conceptus trophectoderm; (2) pre-contact and blastocyst orientation; (3) apposition of trophectoderm to uterine LE; and, (4) adhesion of the apical surface of the trophectoderm to the apical surface of the uterine LE (Figure 2.5) (Guillomot, 1995). In the pig, the implantation event is truncated as compared to rodents or humans. That is, after a prolonged pre-attachment period, the conceptus undergoes orientation, apposition, and adhesion, but does not invade through the uterine LE (Dantzer, 1985). The implantation cascade requires the loss of anti-adhesive mucin in the glycocalyx of the uterine LE that sterically inhibits attachment of trophectoderm to uterine LE. This critical event is temporally associated with loss of PGR in the uterine LE (Bowen et al., 1996; Aplin, 1999). Removal of the large anti-adhesive molecules allows smaller carbohydrate molecules, such as selectins and galectins, on the uterine LE to be accessible to the conceptus trophectoderm for initial attachment at Day 13 of pregnancy (Kimber et al., 1995; Farmer et al., 2008). The low stability contact is then replaced by a more stable and comprehensive collection of adhesive interactions between integrins and the extracellular matrix (ECM) that are maintained throughout implantation (Burghardt et al., 1997; Johnson et al., 2001; Lessey, 2002).

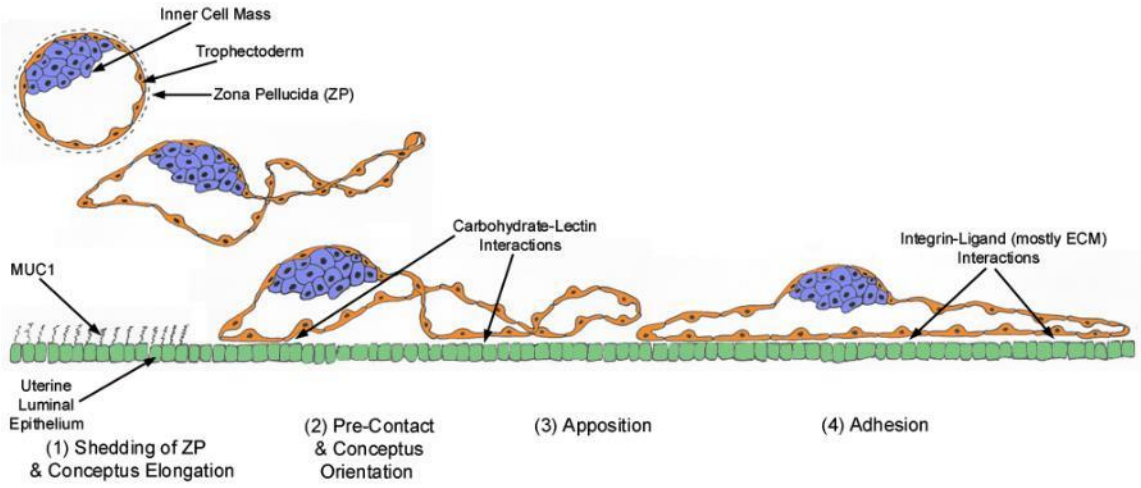

Figure 2.5 Adhesion cascade for implantation
The implantation cascade begins with the blastocyst hatching from the zona pellucida and undergoing the elongation process. During this time, the uterine LE is responding to progesterone to downregulate MUC1 and allow for the initial contact between the conceptus and LE through carbohydrate-lectin interactions. These low stability contacts are then replaced by the more stable integrin-extracellular matrix protein interactions that are maintained throughout implantation.

Placentation

The pig develops a diffuse, epitheliochorial type placenta to support the growth of each individual fetus. This placentation is characterized as being superficial, non-invasive, and having a uterine LE that remains intact. The uterine lamina propria (termed the stroma) underlies the uterine LE to provide structural support and includes fibroblasts, immune cells, and vasculature (endothelial and smooth muscle cells). In the uterus, the LE, GE, and lamina propria are called the endometrium. Outside the endometrium is the myometrium, which contains both inner circular and outer longitudinal layers of smooth muscle. Within the endometrium, invaginations of the LE form tubular compartments, the endometrial glands, which are lined with GE that form a lumen that empties into the uterine lumen and, eventually, into areolae (Fig. 2.6). These areolae are pockets of invaginated chorionic epithelia (CE) that form over the mouths of endometrial glands and are surrounded by a specialized microvasculature (Friess et al., 1981). Underlying the chorion, both in areolar and inter-areolar areas, is the allantoic stroma, which contains fibroblasts and cells of the vasculature. Underlying the allantoic stroma is the allantoic epithelium, which lines the allantoic sac (Figure 2.6).

Areolae form from Days 18 to 30 of pregnancy and the placenta of each piglet will contain about 2,500 areolae (Knight et al., 1977; Leiser and Dantzer, 1994). Secretions from the uterine glands, called histotroph, fill the lumen of the areolae and are then transported through the chorion by fluid phase pinocytosis to the fetal vasculature for use by the placenta and fetus (Renegar et al., 1982; Song et al., 2010). The CE that

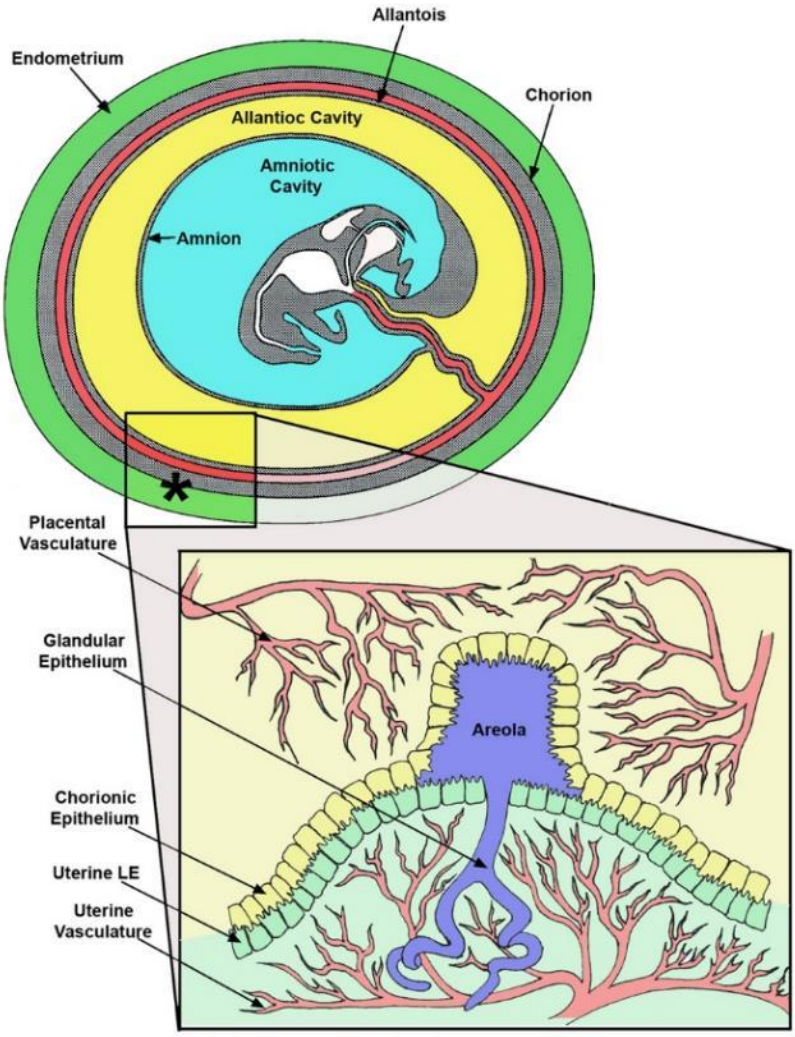

Figure 2.6 The fetal environment
As pregnancy progresses, the fetus resides within the fluid-filled amnion, which is contained inside the allantoic cavity. The allantoic cavity is surrounded by the allantoic membrane and allantoic stroma, which supports the chorion that is interdigitated with the uterine luminal epithelium. At this interface, areolae form over the mouths of glands and are surrounded by a specialized microvasculature. Reprinted with permission from Song et al., 2010.

composes the areola contains tall columnar cells with long microvilli that are optimal for transporting histotroph.

Filamentous conceptuses space out along the uterine horns in order that each conceptus has its own segment of uterine endometrium for implantation/placentation. There is minimal overlap between conceptuses and the areas where the trophoblastic tips do overlap undergo necrosis. There is complete attachment between the uterine LE and trophectoderm by Day 24 of pregnancy. The two adhered epithelia then begin to fold around Day 30 to increase the surface area for nutrient transport and this folding becomes more extensive as gestation progresses (Friess et al., 1980; Vallet and Freking, 2007). The epitheliochorial placenta allows for both histotrophic and hemotrophic support for the developing conceptus. Histotrophic support comes from the GE and is transported through the areolae. Hemotrophic support includes any transport from the maternal blood to the placental blood that occurs in non-areolar regions, across the two adhered epithelia (LE and CE). As pregnancy progresses, the two adhered epithelia and underlying connective tissue become thinner to decrease the distance between the maternal and placental capillaries to as little as 2 microns (Friess et al., 1980). The maternal and fetal capillaries are arranged in a cross-countercurrent manner on opposite sides of the adhered epithelia. If the fetal side of the placenta is “up”, then maternal blood enters at the top of the folds and exits at the bottom. In contrast, the placental blood enters at the bottom of the folds and exits at the top (Leiser and Dantzer, 1988). This arrangement allows for optimum transport of nutrients, especially those dependent on concentration gradients, from mother to fetus. The chorion has two different cell

types. Tall columnar cells are found at the tops of folds, while short cuboidal cells are at the bottoms. The two cell types differ in their transcriptome and may play different roles in both nutrient transport and fold development (Vallet et al., 2014).

After rapid expansion by the chorion and allantois between Days 18 to 30 of pregnancy, they fuse during Days 30 to 60. The placenta grows exponentially through this time until about Day 70 of pregnancy when placental development is completed in terms of placental weight, surface area, and numbers of areolae (Knight et al., 1977). There continues to be angiogenesis and increases in capillary bed volume until parturition to support the exponential growth of the fetus in the last 40 days of gestation (Ullrey et al., 1965; Knight et al., 1977).

Fetal Growth

From Days 15 to 30 of pregnancy, the fetal organs first develop from the three germ layers, endoderm, mesoderm, and ectoderm. As pregnancy progresses, the organs expand in size and weight, but the timing of this expansion is dependent on the organ. The heart, brain, and liver increase exponentially in weight from Days 51 to 114, while lungs and spleen stop enlarging by Day 93 (Ullrey et al., 1965). The bones begin to calcify around Day 30. This represents the time point before which fetuses that are not viable are reabsorbed, while after Day 30, they often result in stillborn mummified fetuses. Overall fetal weight increases exponentially during the last third of pregnancy and this necessitates the increased movement of nutrients through the placenta (Ullrey et al., 1965; McPherson et al., 2004).

Allantoic and Amniotic Fluids

The allantoic cavity is surrounded by the allantoic epithelium and an extensive vasculature that empties into the umbilical artery. The urachus connects the fetal bladder to the allantois allowing for waste from the fetus to be moved into the allantoic cavity (Patten, 1948). Allantoic fluid is a hypotonic solution composed of electrolytes, sugars, proteins, and water that are of maternal and fetal origin, and provide a nutrient reservoir for the fetus (Aherne et al., 1969; Wu et al., 1995). These components are all moved across the allantoic epithelium most likely in a sodium concentration dependent manner. Allantoic fluid is dynamic during pregnancy in terms of changes in both volume and composition. The initial increase in volume from Days 18 to 30 promotes the expansion of the allantois, its apposition with the chorion, and contact with the maternal endometrium. The allantoic fluid volume then decreases until Day 45, again increases until Day 58, and then decreases until parturition (Knight et al., 1977; Goldstein et al., 1980). As the allantoic fluid volume rises, so does the total amounts of glucose and fructose sequestered in allantoic fluid, indicating that the movement of these sugars may be sodium-dependent as is transport of water into the allantoic sac.

The amnion is the fluid-filled sac immediately surrounding the fetus. Suspension in the amnion protects the growing fetus from mechanical injury and allows the fetus to grow symmetrically without pressure points that would lead to abnormal development (Patten, 1948). Additionally, the amnion serves as a nutrient reservoir containing amino acids, sugars, and electrolytes that the fetus may drink during gestation (Aherne et al., 1969; Wu et al., 1995).

Sheep

Fructose has long been detected in the fetal fluids of ruminants, pigs, and, in trace amounts in humans, but the methods used left doubt as to whether the sugar that was being described was actually fructose. By 1946, Cole and Hitchcock used a modified version of the Seliwanoff technique to definitively detect up to 1 mg/ml fructose in the umbilical blood of sheep fetuses between Days 107 and 141 of pregnancy (Cole and Hitchcock, 1946). They also determined that fetal blood fructose levels fall rapidly within 24 hours of birth. Around the same time, Bacon and Bell reported the presence of both glucose and fructose in the blood of fetal sheep late in pregnancy and found greater quantities of fructose than glucose (Bacon and Bell, 1948). This explained the conundrum that total fetal blood sugar concentration was higher than the mother's blood sugar concentration. The glucose concentrations were lower in the fetal blood than in the maternal blood and the rest of the sugar, in the fetus, was fructose.

Barklay et al. then determined fructose quantities in the amniotic and allantoic fluids of sheep. Fructose present in amniotic and allantoic fluids was found in larger quantities than glucose and levels peaked from Days 110 to 130 of pregnancy in both fluids before decreasing substantially just before parturition (Barklay et al., 1949). There was concern that the anaesthetic being given to the ewes was altering their blood glucose levels and, therefore, giving inaccurate results about the differences between maternal and fetal concentrations of glucose in blood. Hitchcock performed a study that accounted

for this concern and concluded that the maternal and fetal concentrations of glucose in blood were less differential than previously thought and that there was a constant loss of glucose from maternal blood to the fetal blood through the placenta (Hitchcock, 1949).

Since the levels of fructose in the maternal blood were undetectable to barely detectable, the question arose as to where the fructose originated. Huggett et al. approached this question by administering intravenous glucose into ewes that were 115 days pregnant and recording both the maternal and fetal blood glucose concentrations. After glucose was administered, there was an immediate rise and peak in maternal blood glucose levels, which then slowly decreased over the course of 3 to 4 hours. There was a concurrent, although less drastic peak in the fetal glucose levels with a similar decrease over time. But, surprisingly, the fetal fructose levels rose slowly, peaked about 3 hours after glucose administration, and slowly fell back to original levels over the course of 3 to 6 hours. The placenta was determined to be the site of fructose production in an experiment using twin lambs at Day 135 of pregnancy, where one lamb was detached from the placenta, one remained attached, and both were given glucose through the umbilical cord. In the attached lamb, circulatory fructose increased, but not in the detached lamb. Blood collected from the umbilical veins and arteries of multiple lambs also indicated that fructose levels were greater in umbilical veins. Taken together, these data implicate the placenta as the site of fructose production, and glucose as the substrate from which fructose is produced in the sheep (Huggett et al., 1951).

It was next determined that fructose production remains constant regardless of fetal blood glucose levels, however, the rate of glucose transport across the placenta

increases with increasing maternal blood glucose levels (Alexander et al., 1955b). When radioactive glucose was administered intravenously to ewes, both radioactive glucose and fructose were detected in the fetus; and it was demonstrated that glucose can be transported from the ewe to the fetus and from the fetus to the ewe, whereas fructose could not be transported back to the maternal blood (Alexander et al., 1955a).

McGowan et al. found that oxidation of fructose only accounted for 16% of the total fetal CO_2 production, which indicates that glucose, not fructose, is utilized as the major energy source in the sheep fetus (McGowan et al., 1995).

Pigs

The literature contains fewer studies concerning fructose in the pregnant pig, but the first report of fructose in the blood of fetal pigs was made by Goodwin in 1956 when he collected blood from piglets just after birth (Goodwin, 1956). Also of note in that article was the report of appreciable fructose in fetal blood of oxen, goats, horses, and whales, which are all animals with epitheliochorial or synepitheliochorial placentae. In contrast, animals with endotheliochorial and hemochorial placentae such as dogs, cats, ferrets, guinea pigs, and rabbits had little to no detectable fructose in the fetal blood (Goodwin, 1956).

In fetal pigs, as seen in fetal lambs, blood fructose levels drop quickly after birth with fructose being non-detectable by 24 hours. Interestingly, although the neonatal pig excretes fructose through the urine, it is very sensitive to decreases in blood glucose levels and easily develops hypothermia within hours of birth in a starved state.

Therefore, any ability that the fetus may have had *in utero* to utilize fructose is rapidly lost after parturition (Goodwin, 1957; Curtis et al., 1966; Aherne et al., 1969).

Aherne et al. determined that fructose levels were substantially higher than glucose levels in the fetal blood, amniotic fluid, and allantoic fluid from Days 82 to 112 of pregnancy. Concentrations of fructose in fetal blood decreased over this time period, while it peaked at both Days 82 and 110 in amniotic and allantoic fluids (Aherne et al., 1969). There were detectable concentrations of fructose in the maternal blood, but they were less than 1% of the concentrations of fructose in fetal blood. Interestingly, the concentrations of fructose in the umbilical artery and vein were equal in this study, which would not be expected if the placenta was the site of fructose production. A more recent study by Pere also found that concentrations of fructose in the umbilical artery and vein are equal, and that fructose is undetectable in maternal blood (Aherne et al., 1969; Pere, 1995).

Fructokinase activity, the enzyme that phosphorylates fructose to produce fructose-1-phosphate, was also measured in the liver, intestine, and placenta by Aherne et al. and enzyme activity was greater in the liver and intestine than the placenta through all days studied (Aherne et al., 1969).

To determine if glucose was a precursor for fructose in the fetal pig, White et al. injected radio-labeled glucose or fructose intraperitoneally into fetal pigs at approximately Day 60 of pregnancy. Results showed that glucose could be converted into fructose, but fructose was not converted into glucose. Also, the radio-labeled carbons from the glucose appeared in the maternal blood, but the radio-labeled carbons

from fructose did not. Therefore, glucose was able to cross the placenta from fetal to maternal blood, but fructose did not (White et al., 1979).

White et al. then asked the question: what is the role of fructose in the fetal pig? Again *in utero* fetal pigs were injected intraperitoneally with radio-labeled fructose at about Day 60 of pregnancy. After 240 min, the fetal pigs were sacrificed and nucleic acids were extracted from skeletal muscle and liver. Both skeletal muscle and liver had radiolabeled carbons incorporated in the nucleic acids indicating that fructose was being used for synthesis of nucleic acids (White et al., 1982).

Recent studies using isolated porcine trophectoderm cells have identified new roles for fructose in stimulating cell proliferation and mRNA translation via activation of the mechanistic target of rapamycin (MTOR) cell signaling pathway. Additionally, fructose is also metabolized via the hexosamine pathway, which is responsible for glycosaminoglycan synthesis, and specifically, hyaluronic acid, an abundant component of the placental stroma (Kim et al., 2012).

In addition to being present in fetal fluids, fructose is also found in the uterine flushings of gilts approximately 48 hours after onset of estrus, and in quantities that were similar to the amount of glucose. Fructose was undetectable by 4 days post-estrus and remained undetectable for the remainder of the estrous cycle (Haynes and Lamming, 1967; Zavy et al., 1982). In contrast, the uterine flushings from pregnant gilts contained detectable fructose as early as Day 14, and the total recoverable fructose increased through Day 18 of pregnancy (Zavy et al., 1982; Bazer et al., 1991).

Hexose Sugar Transport

There are five main roles for soluble sugars in most organisms, including: 1) a source of carbon skeletons for biosynthesis of many compounds; 2) transient energy storage; 3) a driver of osmotic processes; 4) signal transduction; and, 5) molecule transport. In these roles, sugars are essential for growth, development, and maintenance of cells, tissues, organs, and whole organisms. Sugars are either synthesized within special cells or collected from the environment, but with either route of sugar acquisition, there must be a mechanism for transporting the hydrophilic sugars through cell membranes.

The study of sugar transport began with Cori's studies of intestinal sugar absorption, which provided the first evidence for catalyzed transport by showing that the rate of absorption differed depending on the sugar, the transport mechanism could be saturated, and there was competition between glucose and galactose for transporters (Cori, 1925, 1926). Sistrom showed that sugars can be transported against a concentration gradient. This led to the question of how, energetically, this could be achieved (Sistrom, 1958). The evidence for an active transport mechanism for sugars was presented by Crane who described the sodium/glucose cotransport hypothesis, in which the sodium gradient is actually the important driving factor and that the gradient is maintained by the sodium/potassium pump (Crane, 1962, 1965). In 1965, the first purification of a plasma membrane protein that facilitated nutrient transport was published by Fox and Kennedy and described the M (membrane) protein, a component of the β-galactoside transport system in *Escherichia coli* (Fox and Kennedy, 1965). The

first evidence of a proton co-transport mechanism in a eukaryotic cell, using the lactose transport system, was published in 1970 (Komor and Tanner, 1974). Taken together these findings are the basis for our understanding of sugar transport where either sugar or sodium concentration gradients drive the movement of sugar molecules from one compartment to another through proteins located in the plasma membranes.

There are three mechanisms for transporting hexose sugars in mammals and all require plasma membrane transporter proteins. The first mechanism uses the concentration gradient of the sugar and this is facilitated by members of the GLUT family (gene name: solute carrier family 2A; *SLC2A*) of integral membrane proteins. The second mechanism involves sodium-glucose co-transporters that depend on the sodium-potassium ATPase pump to maintain a sodium gradient to drive glucose transport and this is facilitated by members of the sodium-glucose transporter family (SGLT; gene name: *SLC5A*). The third, and relatively newly discovered, mechanism has not been fully defined but uses the SWEET (Sugars Will Eventually be Exported Transporters) transporter of which only one has been defined in mammals.

The GLUT transport family (gene name *SLC2A*) is a subfamily of the major facilitator superfamily (MFS) and consists of 14 members (GLUT1-12, H^+/myo-inositol transporter [HMIT], GLUT14; *SLC2A1-14*) that have a homologous 12-transmembrane domain structure that creates a pore in the plasma membrane (Figure 2.7)(Bell et al., 1993). While family members have common structural features, they vary greatly in kinetic characteristics, substrate specificity, tissue/cell localization, and regulation. The family is divided into three classes with Class I including the traditional glucose

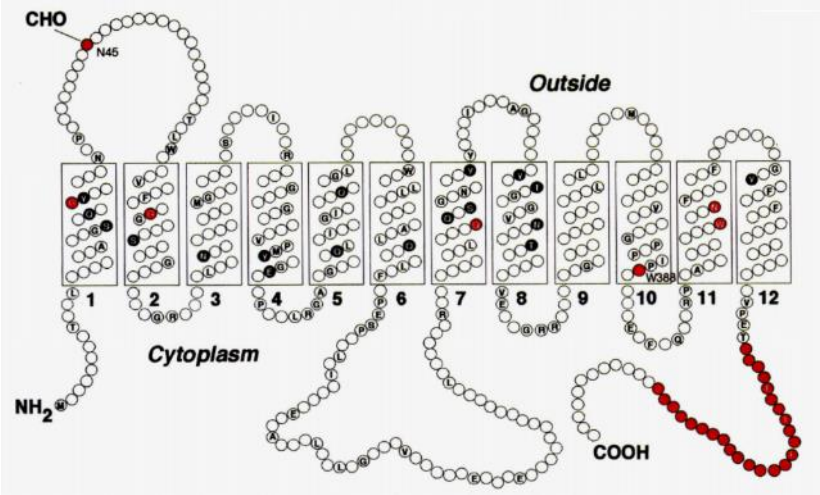

Figure 2.7 GLUT transporter structure
GLUT transporters are composed of 12 transmembrane spanning helices with both termini on the cytoplasmic side. Modifications at different locations give rise to different members of the family. Reprinted with permission from Bell et al., 1993.

transporters GLUT1-4, Class II includes the fructose transporters GLUT5, 7, 9, and 11, and Class III includes GLUT6, 8, 10, 12, 13, and 14 (Bell et al., 1993). Differences in affinities for molecules in part come from certain amino acid or motif changes. For example, affinity for fructose is seen within Class II of the family due to the lack of the QLS motif in the seventh transmembrane domain on the extracellular side. The nomenclature for the GLUT family was defined so that the numbering scheme used for GLUTs is identical to that used for *SLC2A*, as in GLUT1 is the protein and *SLC2A1* is the corresponding gene. The only exception to this is the HMIT protein, which corresponds to the *SLC2A13* gene (Joost et al., 2002).

The sodium-glucose transporter family (SGLT; gene name *SLC5A*) is a subfamily of the sodium solute symporter family (SSF) that consists of 12 members that transport sugars, myo-inositol, iodide, short-chain fatty acids, and choline. All members code for 60-80 kDa proteins that contain 580-718 amino acids and have 14-15 transmembrane helices (Wright et al., 2004). SGLT1, SGLT2, SGLT4, and SGLT5 have been determined to specifically transport glucose. All function as sodium symporters, but there are some differences in mechanism. For instance, SGLT1 couples transport of one glucose molecule to two sodium molecules, while SGLT2 couples one glucose with one sodium molecule. This explains differences in rate of transport between the two isoforms. There is only one post-translational modification found on these proteins, an *N*-linked glycosylation (Wright et al., 2011). SGLT1 and SGLT2, in particular, have been extensively described in the literature as being active in the apical membrane of absorptive epithelia in the intestine and kidney. For this transporter family the

protein/gene nomenclature is identical for SGLT1/*SLC5A1* and SGLT2/*SLC5A2*, but not for SGLT4/*SLC5A9* and SGLT5/*SLC5A10* (Joost et al., 2002).

The SWEET transporters are smaller than the *SLC2A* and *SLC5A* transporters in that they only have seven trans-membrane spanning domains, but they are able to mediate both cellular uptake and efflux. SWEET transporters have an extracellular N-terminus and a long cytosolic C-terminus, which has multiple phosphorylation sites. The sequence of the C-terminus is not well conserved among isoforms or species and has been hypothesized to function in transmission of signals or as a hub for binding of regulatory components (Chen et al., 2015). These transporters have a low affinity for multiple mono- and di-saccharides. The low affinity results in high capacity, so these transporters are most efficient when sugar concentrations are high. SWEET transporters were originally discovered in plants, but have now been found in animals including one transporter in humans (Feng and Frommer, 2015).

Glucose Transporter Characteristics

***SLC2A1*/GLUT1**

GLUT1 is the most studied transporter of the GLUT family and was the first to be isolated and cloned (Mueckler and Thorens, 2013). GLUT1 is responsible for the basal level of glucose uptake into most cells and transports glucose with a K_m=3 mM. Additionally, GLUT1 can transport galactose, mannose, and glucosamine.

SLC2A1 mRNA is ubiquitously expressed throughout the body in multiple species and is upregulated in many cancers (Nishimura and Naito, 2005). In the human placenta, *SLC2A1* mRNA is more abundantly expressed than in any other tissues studied (Nishimura and Naito, 2005). GLUT1 has been reported in both the apical and basal membranes of the syncytiotrophoblast, the cytotrophoblast, and endothelial cells of the human placenta (Jansson et al., 1993; Korgun et al., 2005). Rat and mouse uteri also express GLUT1 protein in the LE, stroma, and decidua (Korgun et al., 2001; Frolova and Moley, 2011b). GLUT1 is detectable in the oocyte through the blastocyst stage in both the inner cell mass and trophectoderm in mice and cattle (Aghayan et al., 1992; Augustin et al., 2001). The *SLC2A1* homozygous knock out is embryonic lethal in mice.

GLUT1 expression in the syncytiotrophoblast of placentae of women is upregulated in women with diabetes (Gaither et al., 1999; Jansson et al., 1999). *SLC2A1* mRNA levels are positively correlated with increasing maternal age (Sciullo et al., 1997). GLUT1 protein is detected in lactating mammary epithelial cells in cattle with the highest levels observed early in lactation, and levels decreasing to barely detectable in non-lactating mammary epithelia (Zhao and Keating, 2007a).

In the sheep, *SLC2A1* mRNA is abundant in the endometrial LE and GE during early pregnancy with a peak in expression occurring during the period of maternal recognition of pregnancy. The protein follows the same profile and is observed in the uterine LE/GE as well as the trophectoderm and endoderm. *SLC2A1* is upregulated by progesterone and that effect is enhanced by interferon tau at the mRNA and protein levels in uterine LE and superficial GE of sheep (Gao et al., 2009a).

SLC2A2/GLUT2

GLUT2 protein is mainly located in enterocytes, hepatocytes, pancreatic β-cells, and the epithelial cells of proximal tubules across multiple species and is responsible for the transport of glucose, fructose, galactose, mannose, and glucosamine across the basolateral and/or apical plasma membranes of cells. *SLC2A2* mRNA is abundant in the human liver, kidney and small intestine, but not in placenta or uterus (von Wolff et al., 2003; Nishimura and Naito, 2005). GLUT2 is located in trophectoderm in mouse blastocysts, but not in the uterus (Aghayan et al., 1992; Frolova and Moley, 2011a). Bovine embryos express *SLC2A2* in the trophectoderm as it elongates (Augustin et al., 2001).

SLC2A3/GLUT3 and *SLC2A14*/GLUT14

GLUT3 and GLUT14 are pseudogenes that share 95% homology. While there is a region of approximately 100 nucleotides in the gene transcript for *SLC2A3*, but not *SLC2A14*, most studies have not differentiated between the two genes. *SLC2A3* mRNA is found in many organs in humans (Nishimura and Naito, 2005) and is particularly abundant in neurons and other tissues that require rapid transport of large amounts of glucose, as it is a high affinity, high capacity transporter for glucose with a K_m=1.5 mM, although it can also transport galactose, mannose, and xylose (Gould et al., 1991; Mueckler and Thorens, 2013). *SLC2A3* has been reported as non-detectable or lowly expressed in human placenta mainly due to samples being taken late in pregnancy, while recent reports indicate that GLUT3 is found at higher levels early in pregnancy in the

extravillous trophoblast cells while invasion is occurring and before a direct connection with the maternal blood has been established (Jansson et al., 1993; Hahn et al., 2001; Brown et al., 2011). GLUT3 expression is higher in placentae of human intrauterine growth restricted (IUGR) fetuses (Janzen et al., 2013). *SLC2A3* expression begins at the morulae stage in bovine embryos and continues to be expressed in the trophectoderm (Augustin et al., 2001). Homozygous knockout of *SLC2A3* in mice is embryonic lethal at the neurulation stage, but the heterozygous knockout survives and displays late gestation fetal growth restriction (Ganguly et al., 2007).

In sheep, *SLC2A3* mRNA is expressed in the conceptus trophectoderm and endoderm early in pregnancy, but has not been studied beyond Day 18 of pregnancy (Gao et al., 2009a).

SLC2A4/GLUT4

GLUT4 is required for systemic glucose homeostasis and is primarily located in skeletal muscle and adipose tissue, although some other tissues, including placenta and uterus express GLUT4 (Nishimura and Naito, 2005; Thorens and Mueckler, 2010). Insulin signaling, in response to high blood glucose, induces the translocation of GLUT4 from an intracellular compartment to the plasma membrane where it can actively transport glucose (K_m=2-10 mM) into cells from the blood (Bryant et al., 2002). Compared to other *SLC2A* family members, *SLC2A4* mRNA is lowly expressed in the endometrial stroma of humans, rats, and mice (Korgun et al., 2001; Frolova and Moley, 2011b). GLUT4 null mice survive past birth and display only perturbations in glucose

and lipid metabolism, indicating that GLUT4 is not required for embryonic development (Charron and Katz, 1998).

In cattle, *SLC2A4* mRNA is lowly expressed in the blastocyst, while in sheep, *SLC2A4* mRNA is lowly detectable in most cell types of the endometrium with protein expression in the uterine LE, GE, and trophectoderm (Augustin et al., 2001; Gao et al., 2009a). *SLC2A4* is not regulated by progesterone, but interferon tau has a suppressive effect on mRNA in uteri of sheep during early pregnancy (Gao et al., 2009a).

SLC2A5/GLUT5

GLUT5 is the only GLUT family member that will only transport fructose (K_m=6mM), not glucose or galactose, and has been mainly studied for its role in transporting fructose across the apical membrane of enterocytes. *SL2A5* mRNA is expressed at high levels in bone marrow, kidney, small intestine, and testes of the human, but not in endometrium (von Wolff et al., 2003; Nishimura and Naito, 2005). *SLC2A5* is expressed in bovine embryos (Augustin 2001). Sperm have high *SLC2A5* expression in multiple species, including humans, mice, cattle, and pigs (Burant et al., 1992; Angulo et al., 1998; Sancho et al., 2007). GLUT5 is upregulated in enterocytes in response to high fructose concentrations in the intestinal lumen. Some cancer cells overexpress GLUT5, specifically in tumors found in brain, breast, liver, uterus, and testes, and fructose uptake is increased in those tumors (Godoy et al., 2006).

SLC2A7/GLUT7

GLUT7 is highly homologous with GLUT5 in terms of amino acid sequence, although it is capable of transporting both glucose and fructose. *SLC2A7* mRNA is only detected in the small intestine and testes in humans (Nishimura and Naito, 2005). GLUT7 protein has been detected in the apical membrane of enterocytes (Cheeseman, 2008).

SLC2A8/GLUT8 (GLUTX1)

GLUT8 has a high affinity for glucose (K_m=2 mM), but can also transport fructose and galactose. GLUT8 localizes to the plasma membrane in some cells, but GLUT8 also contains a specific di-leucine motif in the N-terminus that is conserved across species and believed to be responsible for the transporter localizing to late endosomes, lysosomes, and endoplasmic reticulum (Ibberson et al., 2000; Augustin et al., 2005; DeBosch et al., 2014a). GLUT8 is hypothesized to have a role in providing glucose for glycosylation of proteins in the endoplasmic reticulum. Multiple splice variants have been defined for *SLC2A8* and not all of them have a role in sugar transport since some are truncated and do not have the traditional motifs necessary for transport (Romero et al., 2009). *SLC2A8* mRNA is expressed in human tissues with particular abundance in the liver, spleen, lung, brown adipose tissue, placenta, and testes (Nishimura and Naito, 2005). *SLC2A8* is upregulated in the brain in response to the ovarian hormones estrogen and progesterone (Harrell et al., 2014). *SLC2A8* is ubiquitously expressed throughout the stages of oocyte and embryo development in

cattle (Augustin et al., 2001). GLUT8 protein expression is found in the mouse endometrium during the period of implantation of the blastocyst and decidualization of the uterine stroma and localizes to both the basolateral and apical surfaces of the uterine LE and GE (Kim and Moley, 2009). The mating of two heterozygous *SLC2A8* mice results in lower numbers of *SLC2A8* null pups than would be expected by Mendelian genetics, which indicates that while the knockout is not embryonic lethal, it does a play some role in embryonic development (Augustin, 2010).

SLC2A9/GLUT9

SLC2A9 was first identified through bioinformatics by searching the human genome for sequences similar to those that code for *SLC2A1* and *SLC2A5*. The main difference between *SLC2A9* and other members of the *SLC2A* family is a longer cytoplasmic amino terminus (Phay et al., 2000). GLUT9 is a high capacity uric acid transporter (K_m=0.6 mM) that helps maintain uric acid homeostasis in multiple tissues (DeBosch et al., 2014b). *SLC2A9* mRNA is most abundant in the kidney proximal tubule and liver hepatocytes, but has also been localized to the basolateral and apical surfaces of enterocytes where it is responsible for the clearance of uric acid from the blood (Augustin et al., 2004; DeBosch et al., 2014b).

SLC2A11/GLUT11

GLUT11 exhibits a high degree of similarity to GLUT5, but can transport both glucose and fructose. *SLC2A11* mRNA is abundantly expressed in the human kidney,

pancreas, and placenta (Nishimura and Naito, 2005; Scheepers et al., 2005). Interestingly, mice and rats do not have the *SLC2A11* gene.

SLC2A12/GLUT12

GLUT12 transports glucose and fructose, but it has some unique characteristics. First, GLUT12 is insulin-sensitive in muscle and adipose tissue and may work in concert with GLUT4 for glucose uptake in those tissues. Second, GLUT12 sugar transport is influenced by protons and Na^+ ions, and there is a "sodium leak" associated with these transporters even when sugar is not present, although exactly how these ions mechanistically work with GLUT12 is still unknown. Therefore, GLUT12 appears to have characteristics of both the GLUT and SGLT glucose transporter families (Pujol-Gimenez et al., 2015). *SLC2A12* mRNA is ubiquitously expressed in human tissues and GLUT12 protein has been localized to cardiac muscle, skeletal muscle, adipose tissue, and mammary glands (Nishimura and Naito, 2005). GLUT12 protein has also been localized to human trophoblast cells from first trimester placentae and villous stromal cells from term placentae (Gude et al., 2003; Gude et al., 2005).

SLC2A13/HMIT

HMIT is an H^+/myo-inositol co-transporter and does not transport glucose. *SLC2A13* mRNA is abundantly expressed in human brain, but is also detectable in adipose tissue, placenta and uterus (Uldry and Thorens, 2004; Nishimura and Naito, 2005).

SLC5A1/SGLT1

SGLT1 is a high affinity transporter that has an apparent coupling stoichiometry of two sodium ions to one sugar molecule with a K_m=0.5 mM (Turner and Moran, 1982). This transporter was the first of the family to be cloned and was determined to have no homology with other sugar transporters in the GLUT family (Hediger et al., 1987). SGLT1 is abundant in the apical membrane of enterocytes, but is also found in the kidney, heart, brain, testes, and pancreas. There is low expression of *SLC5A1* mRNA in human uterus and placenta (Nishimura and Naito, 2005). *SLC5A1* is also expressed throughout the stages of embryo development, but is most abundant in the oocyte (Augustin et al., 2001).

In sheep, *SLC5A1* mRNA and protein are expressed in the uterine LE and GE during early pregnancy and this expression is upregulated by progesterone (Gao et al., 2009a).

SGLT1 protein is expressed in bovine mammary glands and is more abundant in lactating glands than non-lactating glands (Zhao and Keating, 2007a). Additionally, SGLT1 is expressed in human mammary epithelial cells during lactation (Obermeier et al., 2000). SGLT1 may be necessary for providing sugars to the cell for energy and molecule production or may be necessary for secretion of milk products.

SGLT1 null mice survive to weaning, but die within 2 days post-weaning on a normal diet with loss of glucose in the feces and urine. However, these mice survive if given a diet with no free monosaccharides or disaccharides. SGLT1 null mouse models have been used to demonstrate that SGLT1 is necessary for large uptake of glucose from

the intestinal lumen. In addition to overall uptake by enterocytes, SGLT1 in the apical membrane of the enteroendocrine L-cells and K-cells stimulates production and secretion of glucagon-like peptide 1 (GLP-1) and glucose-dependent insulinotropic peptide (GIP), which in turn enter the systemic blood and act to increase the pancreatic production of insulin (Gorboulev et al., 2012). SGLT1 is also necessary for reabsorption of glucose in the kidney, specifically in the straight descending portion of the proximal tubule (Gorboulev et al., 2012).

Mutations in the human *SLC5A1* gene can occur and result in the glucose-galactose malabsorption syndrome where SGLT1 does not function properly to absorb glucose in the intestine or kidney, but fetuses develop normally and symptoms are not seen until after birth (Wright et al., 2011; Raja and Kinne, 2012).

SGLT1 can be transcriptionally and post-transcriptionally regulated by regulatory solute carrier protein (RSC1) to increase SGLT1 in response to a glucose-rich diet (Filatova et al., 2009). Protein kinases A and C can stimulate the trafficking of SGLT1 to the plasma membrane, and this can occur either through phosphorylation of the transporter, or independently of phosphorylation (Raja et al., 2012).

***SLC5A2*/SGLT2**

SGLT2 is a low affinity glucose transporter that has an apparent coupling stoichiometry of one sodium ion to one sugar molecule with a K_m=6 mM (Turner and Moran, 1982). SGLT2 was originally isolated from the kidney and *SLC5A2* mRNA is

abundant in that organ with low to non-detectable expression in other human organs (Nishimura and Naito, 2005).

SLC5A9/SGLT4

SGLT4 is a sodium/glucose co-transporter that has been localized in intestine, kidney, liver, lung, uterus, and pancreas of multiple species (Wright et al., 2004).

SLC5A10/SGLT5

SGLT5 is a sodium/glucose co-transporter that has been localized to the kidney cortex. *SLC5A10* mRNA is abundant in the kidney, but is very low in other human tissues (Nishimura and Naito, 2005).

Regulation of Transporters

Glucose transport can be regulated by a variety of factors including hormones, substrate concentration, and oxidative stress. Growth hormone stimulates the uptake of glucose by villous tissue of the placenta during late pregnancy in women, but has no effect in early pregnancy (Ericsson et al., 2005a). Corticotropin releasing hormone can increase GLUT1 expression and decrease GLUT3 expression. Since CRH is produced by the human placenta, this represents a paracrine/autocrine regulation of glucose transport (Goland et al., 1993; Gao et al., 2012).

The literature on the effects of insulin on glucose uptake in human pregnancy is variable. Insulin has very little effect on glucose transport by placental samples at term,

but glucose transport in villous fragments of placentae can be stimulated with insulin early in pregnancy (Challier et al., 1986; Ericsson et al., 2005b). GLUT4 and GLUT12, two insulin-sensitive GLUT isoforms, are found in placentae from humans early in pregnancy, but not late, and may be responsible for insulin sensitivity (Gude et al., 2003; Ericsson et al., 2005b).

The steroid hormones progesterone and estrogen regulate glucose transporters in multiple species and tissues. Progesterone upregulates GLUT1 protein in the epithelial cells of the mouse uterus as well as mouse and human endometrial stromal cells (Frolova et al., 2009). Estradiol upregulates glucose utilization in the rat uterus (Smith and Gorski, 1968). Indeed, GLUT1 protein in the uterus is increased within 4-6 h after estrogen administration (Welch and Gorski, 1999). In the sheep, progesterone upregulates GLUT1 protein in uterine LE and superficial GE with the increase being augmented by the cytokine interferon tau (Gao et al., 2009a). Progesterone and interferon tau also increased the localization of GLUT4 protein to the uterine LE. SGLT1 protein was upregulated by progesterone in the uterine LE of sheep, but interferon tau had a suppressive effect (Gao et al., 2009a).

Maternal nutrition can regulate glucose transporter expression. In a mouse model of maternal obesity where dams were fed diets composed of high amounts of sugar, placental trophoblast cells from obese dams showed increased expression of GLUT1 and GLUT3 proteins compared to the controls (Rosario et al., 2015). In intrauterine growth restriction models, GLUT8 protein is decreased in whole sheep placentae (Limesand et al., 2004), as is GLUT3 protein in whole rat placentae (Lesage et al., 2002). GLUT3 is

also upregulated in human pregnancies with intrauterine growth restricted fetuses in trophoblast cells at term (Janzen et al., 2013). While the effects of maternal diet on placental glucose transporters are varied, mainly due to differences in maternal diet in the models or the uncontrolled diet in human studies, the consistency between studies is that glucose transporters can be affected by nutrient availability.

Under hypoxic conditions, *SLC2A1* and *SLC2A3* transcription is increased through the HIF-1 pathway and there is a decreased amount of transcript degradation in placental tissues from humans and mice (Iyer et al., 1998; Baumann et al., 2002).

Sugar Transport in the Intestine

In the small intestine, polarized enterocytes absorb sugars from the intestinal lumen, and deliver them into the vasculature in order to provide these sugars to the rest of the body. When luminal glucose concentrations are high, and a large disparity between luminal and blood concentrations exists, such as after a meal, sodium transport through SGLT1 causes apical membrane depolarization, which stimulates Ca^{2+} entry and allows GLUT2 to be rapidly trafficked to the apical surface of enterocytes. GLUT2 facilitates glucose transport at a rate 3-5 times greater than SGLT1 (Raja et al., 2012). GLUT2 is also located basolaterally in enterocytes to facilitate the transport of glucose and fructose through the basal membrane and into the circulation (Uldry and Thorens, 2004). After a meal, insulin binding to its enterocyte receptor rapidly traffics GLUT2 out of the apical membrane (Hahn et al., 2001). SGLT1 is continuously localized to the apical surface to maximize sugar absorbance from the lumen as luminal concentrations

decrease. The sodium concentration gradient that drives glucose transport by SGLT1 is created and maintained by the Na-K-ATPase primary active transport system in the basal membrane (Schultz and Curran, 1970). Fructose is transported through the apical surface of enterocytes using mainly GLUT5 and GLUT2, although GLUT7 and GLUT9 may also play a role. Fructose is transported through the basolateral surface using GLUT2 (Uldry and Thorens, 2004).

Sugar Transport in the Kidney

In the kidney, sugar transport is necessary to retrieve sugars from the filtrate generated in the glomerulus so that they can be returned to the peritubular blood and not lost through the urine. The early and late proximal tubules have different glucose transport characteristics. The early proximal tubule has high-capacity, low affinity glucose transport mainly facilitated by SGLT2 in the apical membrane, while the late proximal tubule uses the higher affinity SGLT1 to move glucose against the concentration gradient that is increasing with movement down the tubule (Balen et al., 2008; Sabolic et al., 2012). GLUT2 is located basolaterally in the renal epithelia to transport glucose out of the cells and into the blood.

Water Transport by Sugar Transporters

In addition to transport of sugars, members of both the GLUT and SGLT families also transport water molecules. For each sugar molecule transported by SGLT1, there are 260 molecules of water transported (Loo et al., 1996). GLUT transporters are also

capable of transporting water, but with only 35 molecules of water translocated per sugar molecule (Zeuthen et al., 2007). The total volume of water moved by GLUT transporters is probably greater than that by SGLT1 due to the great volume of sugar molecules being moved by the GLUTs. GLUT1 and GLUT3 are also capable of moving water (Tomioka, 2012). Water transported by co-transporters such as SGLT1 and GLUT2 can be moved with or against an osmotic gradient (Zeuthen, 2010). These transporters may play a role in the dynamic fluid volume changes that are seen in pig conceptuses during pregnancy (Knight et al., 1977).

Fructose Synthesis and Metabolism

The Polyol Pathway

Fructose can be synthesized from glucose via the polyol pathway, which is also known as the sorbitol-aldose reductase pathway. This pathway has mostly been studied for its role in pathological complications associated with the metabolic disorder diabetes mellitus, although it is active in the normal liver, kidney, and male reproductive tract (Kobayashi et al., 2002; Pruneda et al., 2006; Alexiou et al., 2009; Pastel et al., 2012).

The polyol pathway is a minor metabolic pathway for glucose that is activated when intracellular concentrations of glucose are high. In the first, and rate limiting step, aldose reductase uses NADPH as a co-factor to reduce glucose to its alcohol, sorbitol. Sorbitol is then metabolized to fructose by the enzyme sorbitol dehydrogenase using the co-factor NAD^+. Sorbitol is a polyhydroxylated, strongly hydrophilic alcohol that does

not readily diffuse through membranes and can act as an osmotic regulator. A transport system for sorbitol has not been elucidated in animals, although in plants there are specific plasma membrane transporters for sorbitol movement. Therefore, it is hypothesized that, in animals, sorbitol is either converted to another metabolite in the cell in which it is synthesized or it accumulates in cells. Sorbitol accumulation is often toxic to cells. Sorbitol has been hypothesized to be synthesized in the placentae of sheep, cattle, and humans due to greater concentrations in the uterine vein than in the uterine artery (Teng et al., 2002; Brusati et al., 2005).

In the liver, aldose reductase and sorbitol dehydrogenase in hepatocytes catalyze the conversion of glucose, from blood, into fructose that is used to produce fatty acids (Lanaspa et al., 2013). In the kidney, these enzymes localize to epithelia of the renal tubules (Corder et al., 1977; Zopf et al., 2009). Aldose reductase has been localized to the uterine LE from Days 12 to 15 of pregnancy in pigs (Seo et al., 2014). Sorbitol dehydrogenase, also known as ketose reductase, has been localized to the trophectoderm of bovine placenta (Rama et al., 1973). Overall, the polyol pathway is not a major metabolic pathway nor has it been well studied, but the pig epitheliochorial placenta is a potential site for the polyol pathway to have a major metabolic role.

Metabolism

Fructose metabolism begins with phosphorylation, which can occur at multiple carbons on the fructose molecule. Phosphorylation of fructose results in it being sequestered in the cell and requires ATP to donate the phosphate group. Hexokinase

adds a phosphate group to the 6-carbon to produce fructose-6-phosphate (F-6-P). Ketohexokinase (KHK; also known as fructokinase) adds a phosphate group to the 1-carbon to produce fructose-1-phosphate (F-1-P) and cannot act on glucose. Fructose-3-phosphate can also be produced (Feinman and Fine, 2013).

Aldolase B and triosekinase catalyze the cleavage of F-1-P into dihydroxyacetone phosphate and glyceraldehyde-3-phosphate. These two substrates can either enter into the glycolytic pathway for use in the TCA cycle, the gluconeogenic pathway, or triglyceride synthesis. Dihydroxyacetone phosphate and glyceraldehyde-3-phosphate enter into the glycolytic pathway below the step where phosphofructokinase converts fructose-6-phosphate into fructose-1,6,-bisphosphate, which is the main regulation point in glycolysis. Therefore, fructose is not regulated as tightly as glucose, which results in greater lipogenesis when fructose levels are high. The metabolic pathway used depends on the cell type (Feinman and Fine, 2013). In the liver, fructose is used for glycogen and triglyceride synthesis, while in sperm, fructose is utilized as the main energy source (Aalbers et al., 1961).

F-1-P can also regulate glucose metabolism by binding glucokinase regulatory protein (GKRP) and allowing glucokinase to be released, then translocate to the cytoplasm from the nucleus (Brown et al., 1997). This release of inhibition on glucokinase increases the amount of glucose that can enter the cell and be sequestered.

Ketohexokinase (KHK)

KHK has two isoforms, A and C (Hayward and Bonthron, 1998). KHK-C is

expressed in small intestine, liver, and kidney and has a K_m=0.8. KHK-A is more ubiquitously expressed throughout tissues and has a K_m=8.0. High amounts of KHK activity result in ATP depletion because one molecule of ATP is necessary to phosphorylate each fructose molecule. This results in increased levels of uric acid, which can induce oxidative stress in vascular smooth muscle and endothelial cells (Corry et al., 2008; Lanaspa et al., 2012). Additionally, cytokines, chemokines, and transcription factors such as IL-1β, IL-6, MCP-1, and NFκB can be activated in a KHK-dependent manner in renal proximal tubule cells (Cirillo et al., 2009; Lanaspa et al., 2014).

KHK has greater expression in liver hepatocytes than in any other tissue (Adelman et al., 1967). This is hypothesized to be because the liver is removing fructose from the portal blood, especially after a meal. KHK has been detected in uteri of mice and placentae of humans, but the cellular localization is unknown (Funari et al., 2005; Diggle et al., 2009).

Summary

The pig has a diffuse, fructogenic, epitheliochorial type placenta that develops to support the growth of each individual fetus after the conceptus has undergone elongation and implantation. Elongation requires vast morphological remodeling of the blastocyst, which temporally overlaps with attachment of the trophectoderm to the uterine LE in a truncated implantation process where the trophectoderm never invades the uterine LE. During these events, the conceptus trophectoderm also secretes estrogen, the maternal recognition of pregnancy signal, to maintain the CL, progesterone production, and,

therefore, pregnancy. The placenta utilizes both histotrophic and hemotrophic support, which contain sugars, amino acids, proteins, and electrolytes, to provide for the developing fetus until the end of gestation.

Sugars are essential for growth, development, and maintenance of cells and tissues, including those that compose the endometrium and conceptus. Sugars are mainly transported either in a sodium-dependent manner by the SGLT family or by facilitated diffusion by the GLUT family of transporter proteins. Different members of these two families localize to different cell types throughout the body and are regulated by a variety of factors. GLUT1, GLUT3, and SGLT1 have been the most studied in the reproductive tract during pregnancy and can be regulated by the steroid hormones estrogen and progesterone.

Concentrations of fructose are substantially higher than those for glucose in fetal blood, amniotic fluid, allantoic fluid, and uterine flushings during pregnancy in the pig, although the roles of fructose have not been fully elucidated. The polyol pathway is a minor metabolic pathway for glucose that converts glucose into fructose. Our hypothesis is that glucose is transported to the placenta from maternal blood and that a fraction of the glucose is converted to fructose via the polyol pathway. Fructose can then be transported and utilized by the conceptus via pathways such as the hexosamine pathway or for production of fatty acids and lipids. The studies described in this dissertation were aimed at defining the transport mechanisms for glucose and fructose as well as identification of tissues which synthesize and utilize fructose at the uterine-placental interface during pregnancy in pigs.

CHAPTER III

APPROPRIATE REFERENCE GENE SELECTION FOR QPCR DEMONSTRATES THAT PORCINE PLACENTA EXPRESSES *SLC7A3* AND INDUCES ENDOMETRIAL *SLC5A1* EXPRESSION

Introduction

Dynamic changes occur in the porcine endometrium and the developing placenta that allow for the exchange of gases, micronutrients (including glucose and amino acids), and macromolecules (proteins) necessary for the growth and development of the conceptus (embryo/fetus and associated extraembryonic membranes). Our long-term goal is to understand interactions between the uterus and placenta that provide the necessary support for embryonic/fetal development; however, these vast structural, metabolic, and angiogenic changes can alter the expression of genes that are often considered stable reference genes for qPCR in less dynamic tissues. The aims of this study were to identify genes that are stable across the estrous cycle and pregnancy to be used as reference genes for qPCR, and then use them to examine mRNA expression of select glucose and amino acid transporters in the porcine endometrium and placenta. A comparison was made between the mRNA profiles from qPCR and *in situ* hybridization to verify that the reference genes were appropriate for future use in porcine endometrial and placental tissues.

After entering the uterus on Days 4 to 5 post-fertilization, pig blastocysts remain free-floating within the uterine lumen for an extended period of time that allows them to

elongate prior to attaching to the uterine wall and implanting between Days 13 and 25 of pregnancy (Bazer and Johnson, 2014). The conceptus undergoes major structural remodeling during this period as it elongates from a 10 mm spherical blastocyst to a 1000 mm long filamentous blastocyst in order to maximize the surface area for attachment to the uterine endometrium for exchange of molecules (Geisert et al., 1982a; Bazer and Johnson, 2014). Additionally, the conceptus secretes multiple factors at this time, including interferons, growth factors, and estrogens, the maternal recognition of pregnancy signal in the pig (Bazer and Thatcher, 1977; Mirando et al., 1990; Johnson et al., 2009). Many of the changes incurred in the endometrium early in pregnancy can be attributed to estrogens and cytokines secreted by the conceptus, which regulate transcription of multiple genes, including those for glucose transporters, osteopontin, growth factors, and interferon-stimulated genes in the endometrium (White et al., 2005; Joyce et al., 2007; Ka et al., 2007; Bazer and Johnson, 2014). Progesterone, the hormone of pregnancy, is also present in high concentrations in blood and can affect gene expression in both the placenta and endometrium (Bailey et al., 2010b; Mathew et al., 2011).

This rapid growth and remodeling of the conceptus requires a substantial amount of nutrient support from the endometrium (Geisert et al., 1982b). In order to support the conceptus as it attaches to the uterine luminal epithelium (LE) for implantation, the endometrium undergoes substantial cellular restructuring to increase angiogenesis and nutrient transport. Pigs develop a true epitheliochorial placenta where the apical surface of the uterine LE attaches to the apical surface of the conceptus trophectoderm and this

interface is maintained throughout pregnancy (Dantzer, 1985). There is never invasion of the maternal endometrium by the conceptus and multiple cell layers separate the maternal and placental circulations (Wislocki and Dempsey, 1946; Friess et al., 1980).

The placenta exponentially increases in weight from Day 20 to approximately Day 70 of pregnancy and angiogenesis continues to increase capillary bed volume until the end of gestation at 114 days (Michael et al., 1983; Freking et al., 2007). The placenta is responsible for nutrient, ion, gas, and waste transport between the mother and fetus, and is dynamic in terms of metabolism and structure. The interface between the maternal LE and the conceptus chorion (outer placental epithelium) begins folding around Day 25 and continues to remodel throughout pregnancy in order to increase surface area available for transport of nutrients and gases (Dantzer and Leiser, 1994; Vallet et al., 2009). Also, between Days 25 and 30, the endometrial glandular epithelia (GE) become more active in the synthesis and secretion of histotroph (composed of proteins, carbohydrates, sugars, lipids, and ions that nourish and sustain the conceptus) that is transported to placental areolae that form over the uterine gland openings for absorption of histotroph into the placenta (Friess et al., 1981; Bailey et al., 2010c).

Significant amounts of glucose are transported across the pig placental membranes either by facilitated diffusion solute carrier family 2A (SLC2A) transporters, which move glucose down its concentration gradient, or by sodium-dependent solute carrier family 5A (SLC5A) transporters, which move glucose using the sodium gradient maintained by the sodium-potassium ATPase pump. The two most studied sodium-glucose co-transporters are SLC5A1 and SLC5A2. *SLC5A1* mRNA is expressed on the

luminal surface of large intestine, small intestine, and stomach of mice (Yoshikawa et al., 2011) and by the uterine LE and GE of the ovine endometrium (Gao et al., 2009a).

Amino acids, particularly arginine, profoundly impact conceptus development in pigs (Wu et al., 2013). Similar to glucose, amino acids are also delivered across cellular membranes, but use a subfamily of the solute carrier 7 (SLC7) cationic amino acid transporter proteins. The four known transporter proteins for cationic amino acids include SLC7A1, SLC7A2A, SLC7A2B, and SLC7A3. Cationic amino acids are transported into cells for protein synthesis, and arginine is also converted into nitric oxide by nitric oxide synthase 2, and polyamines by arginase and ornithine decarboxylase (Fotiadis et al., 2013).

Quantitative PCR is an efficient, sensitive, and reliable method for estimating expression of gene transcripts. However, qPCR depends on finding stable endogenous genes to use as a reference in order to minimize problems arising from RNA extraction or cDNA synthesis efficiency (Lanoix et al., 2012; Kozera and Rapacz, 2013). Reference genes that have been used widely include glyceraldehydes-3-phosphate dehydrogenase (*GAPDH*), β-actin (*ACTB*), and 18S rRNA, but these genes are involved in many major cellular processes and are not stable in all tissues (Kuijk et al., 2007; Mamo et al., 2007). Beta-2-microglobulin (*B2M*), a commonly used reference gene, has been shown to increase in the pig endometrium in response to interferons secreted by conceptuses (Joyce et al., 2008). Jalali et al. determined that ACTB and TUBA1B proteins increase from Days 9 to 12 of pregnancy, which may indicate changes in expression of mRNAs for those genes (Jalali et al., 2015). Use of either an inappropriate or an individual

reference gene can lead to inaccurate interpretation of target gene expression (Vandesompele et al., 2002a). A few studies have determined stable reference genes for short periods of time or individual days during the estrous cycle and pregnancy in the pig (Kuijk et al., 2007; Wang et al., 2011), but not throughout pregnancy. Studying gene expression throughout the estrous cycle and pregnancy is important for understanding both normal and pathological pregnancies, which in the pig, a livestock species, can lead to increased production and profit.

In this study, we identified a trio of genes with stable expression across the estrous cycle (Days 5 to 15) and pregnancy (Days 9 to 85) for which their geometric mean serves as an acceptable endogenous reference for analysis of qPCR gene expression profiles from pig endometrial tissues. Further, we identified the geometric mean of a second trio of genes that can serve as an acceptable endogenous reference for qPCR in placental tissues. Lastly, we compared the mRNA localization by *in situ* hybridization to the results of mRNA quantification from qPCR across the estrous cycle and pregnancy for a glucose transporter, *SLC5A1*, and an amino acid transporter, *SLC7A3*, to determine if the chosen qPCR reference genes were appropriate.

Materials and Methods

Animals and Tissue Collection

Sexually mature, 8-month-old crossbred gilts were observed daily for estrus (Day 0) and exhibited at least two estrous cycles of normal duration (18 to 21 days) before

being used in these studies. All experimental and surgical procedures were in compliance with the Guide for Care and Use of Agricultural Animals in Teaching and Research and approved by the Institutional Animal Care and Use Committee of Texas A&M University.

To evaluate gene expression in normal endometrial and placental tissues, gilts were detected in estrus, and then assigned randomly to either cyclic or pregnant status. Gilts in the pregnant group were bred naturally to boars with proven fertility. Then, gilts were ovariohysterectomized on either Day 5, 9, 11, 12, 13, 15 or 17 of the estrous cycle or Day 9, 11, 12, 13, 14, 15, 17, 20, 25, 30, 40, 60, or 85 of pregnancy (n = 3 or 4 gilts/day/status). Conceptuses and several cross-sections of uterus and placenta from the middle of each uterine horn (~1 cm) were fixed in fresh 4% paraformaldehyde in PBS (pH 7.2) and embedded in Paraplast-Plus (Oxford Laboratory, St. Louis, MO). Additionally, endometrium was physically dissected from the myometrium, snap-frozen in liquid nitrogen, and stored at -80°C for RNA extraction. Chorioallantoic tissue was physically dissected from uterine tissues and frozen in a similar manner. For Day 60 placenta, areolae were carefully dissected from inter-areolar chorioallantois and both tissue compartments were immediately subjected to procedures to assess arginine transport.

To evaluate effects of estrogen (E2) and E2-induced pseudopregnancy on uterine *SLC5A1* gene expression, gilts were detected in estrus (Day 0) and assigned randomly to receive daily intramuscular injections of 5 mg 17β-estradiol benzoate in 5ml corn oil (Sigma-Aldrich, St. Louis, MO; n = 4) or 5ml corn oil alone (CO; n = 4) on Days 11, 12,

13, and 14 of the estrous cycle (Joyce et al., 2007). All gilts were ovariohysterectomized on Day 15 of pseudopregnancy. Tissues were collected as described above.

To evaluate effects of long-term progesterone (P4) treatment without the influence of other ovarian hormones on uterine *SLC5A1* gene expression, gilts were ovariectomized on Day 12 of the estrous cycle and assigned randomly to receive daily 4 ml intramuscular injections of either P4 (200 mg in corn-oil; CO) or CO alone on Days 12 through 39 post-estrus (n=3/treatment) (Bailey et al., 2010c). All gilts were hysterectomized on Day 40 post-estrus and tissues collected as above.

RNA Extraction and cDNA Synthesis

Total RNA from endometrial and placental tissues was isolated using Trizol reagent (Life Technologies, Carlsbad, CA, USA) according to manufacturer's instructions (Appendix B). RNA yield and purity were determined using a Nanodrop spectrophotometer (Thermo Scientific, Waltham, MA, USA). First strand cDNA was synthesized from 5µg of total RNA using Superscript III First Strand Kit (Life Technologies) following the manufacturer's instructions (Appendix B). The cDNA was subjected to a 1:5 dilution with nuclease-free water and stored at -20°C.

Gene Selection and Primer Design

Ten candidate reference genes were selected (*ACTB, B2M, GAPDH, HPRT1, PPIA, RPL7, SDHA, TBP, TUBA1B, YWHAZ*) based on common usage in endometrial, placental, and other pig tissues (Table 3.1). Primers for reference genes not present in the

Gene Name	*Genbank Reference Sequence*	*Sequence*	*Product Length*	*Reference*
ACTB	XM_003124280	5'-TCCCTGGAGAAGAGCTACGA-3' 5'-TGT TGG CGT AGA GGT CCT TC-3'	187	Designed
B2M	NM_213978	5'-TTCACACCGCTCCAGTAG-3' 5'-CCAGATACATAGCAGTTCAGG-3'	166	(Kuijk et al., 2007)
GAPDH	NM_001206359	5'-GGTGAAGGTCGGAGTGAACG-3' 5'-TGACTGTGCCGTGGAATTTG-3'	173	Designed
HPRT1	NM_001032376	5'-GGACTTGAATCATGTTTGTG-3' 5'-CAGATGTTTCCAAACTCAAC-3'	91	(Kuijk et al., 2007)
PPIA	NM_214353	5'-CCAACACAAACGGTTCCCAG-3' 5'-GCCATCCAACCACTCAGTCT-3'	59	Designed
RPL7	NM_001113217	5'-AAGCCAAGCACTATCACAAGGAATACA-3' 5'-TGCAACACCTTTCTGACCTTTGG-3'	171	(Seo et al., 2012)
SDHA	XM_003362140	5'-CTACAAGGGGCAGGTTCTGA-3' 5'-AAGACAACGAGGTCCAGGAG-3'	141	(Nygard et al., 2007)
SLC5A1 (qPCR)	NM_001164021.1	5'-GGCTGGACGGAAGTATGGTGT-3' 5'-ACAACCACCCAAATCAGAGC-3'	158	Designed
SLC5A1 (ISH)	NM_001164021.1	5'-TCTCATGAGCTCCCTGACCT-3' 5'-GAGACGACCAGGACGATGAT-3'	468	Designed
SLC7A3 (qPCR)	NM_001130973.1	5'-CACTCAACTCCATCCCCACT-3' 5'-CTGTGGCTGTCTCCAGATGA-3'	206	Designed
SLC7A3 (ISH)	NM_001130973.1	5'-CTGGAGGATTTGTGCCATTT-3' 5'-AAAGAGGAATGCCATGAACG-3'	479	Designed
SLC16A6	XM_005674551.1	5' –AGGAGTTTGGGTATGGCAGAAA-3' 5' –ACTTACTCCCTGGGTTGACATC-3'	143	Designed
TBP	XM_003361418	5'-AACAGTTCAGTAGTTATGAGCCAGA-3' 5'-AGATGTTCTCAAACGCTTCG-3'	153	(Nygard et al., 2007)
TUBA1B	NM_001044544	5'-GCTGCCAATAACTATGCCCG-3' 5'-ACCAAGAAGCCCTGAAGACC-3'	116	Designed
YWHAZ	XM_001927228	5'-TGATGATAAGAAAGGGATTGTGG-3' 5'-GTTCAGCAATGGCTTCATCA-3'	203	(Nygard et al., 2007)

Table 3.1 Primer information for qPCR and *in situ* hybridization analyses

literature and for *SLC16A6*, *SLC5A1*, and *SLC7A3* were designed using Genbank sequences inserted into Primer3Plus software (Untergasser et al., 2007). Primers were submitted to NCBI BLAST to test for specificity against the known pig genome. All primer sequences and product lengths are presented in Table 3.1.

Quantitative PCR

All qPCR reactions were performed in triplicate, in 10 µl reactions using PerfeCta SYBR Green Mastermix (Quanta Biosciences, Gaithersburg, MD, USA) and 2.5 mM of each specific primer, on a Roche 480 Lightcycler (Roche) with approximately 75 ng of cDNA per reaction (Appendix B). The PCR program began with 5 min at 95°C followed by 40 cycles of 95°C denaturation for 10 sec and 60°C annealing/extension for 30 sec. A dissociation curve was produced with every run after the 40^{th} cycle to verify a single gene-specific peak. Additionally, qPCR products were run in a 2.5% agarose electrophoresis gel to confirm primer specificity. Standard curves with 4-fold serial dilutions of pooled cDNA samples were run to determine primer efficiencies. All primer slopes were -3.30 to -3.48 with efficiencies of 97-100%.

Gene Stability

Analysis of the stability of candidate reference genes was performed using NormFinder and GeNorm algorithms.

In situ *Hybridization Analysis*

Cell-specific expression of mRNAs in sections (5 µm) of porcine endometria and placentae were determined using radioactive *in situ* hybridization analysis as described previously (Johnson et al., 1999)(Appendix B). Briefly, partial cDNAs for porcine *SLC5A1* and *SLC7A3* mRNAs were cloned beginning with PCR amplification using total RNA from Day 15 pregnant porcine endometrial tissues by specific primers (Table 3.1). PCR amplification was conducted as follows: 1) 95°C for 5 min; 2) 95°C for 45 sec, 60°C for 30 sec, and 72°C for 1 min for 35 cycles; and 3) 72°C for 10 min. The partial cDNAs of the correct predicted size were cloned into a pCRII plasmid using a T/A Cloning Kit (Life Technologies) and the sequence of each verified using an ABI PRISM Dye Terminator Cycle Sequencing Kit and ABI PRISM automated DNA sequencer (Perkin-Elmer Applied Biosystems).

Radiolabeled antisense or sense cRNA probes were generated by *in vitro* transcription using linearized plasmid templates, RNA polymerases, and [α-^{35}S]-UTP. Deparaffinized, rehydrated, and deproteinated uterine tissue sections (5µm thick) were hybridized with radiolabeled antisense or sense cRNA probes. After hybridization, washing, and ribonuclease A digestion, slides were dipped in NTB-2 liquid photographic emulsion (Kodak, Rochester, NY), and exposed at 4°C for seven to ten days. Slides were developed in Kodak D-19 developer, counterstained with Gill's hematoxylin (Fisher Scientific, Fairlawn, NJ), and then dehydrated through a graded series of alcohol to xylene. Coverslips were affixed with Permount (Fisher Scientific, Fairlawn, NJ). Digital images of representative fields recorded under brightfield or darkfield

illumination were evaluated using an Axioplan 2 microscope (Carl Zeiss, Thornwood, NY) interfaced with an Axioplan HR digital camera and Axiovision 4.3 software. Photographic plates were assembled using Adobe Photoshop (version 6.0, Adobe Systems Inc., San Jose, CA).

Arginine Transport in Placenta

Arginine transport in pig placenta was determined using L-[U-^{14}C]-arginine (American Radiolabeled Chemicals, St. Louis, MO) as described previously for branched-chain amino acids (Self et al., 2004). Placental samples (~200 mg of areolar or inter-areolar chorioallantois; n=4 placentae) were washed three times in oxygenated (95% O_2/5% CO_2, v/v) Krebs-Henseleit bicarbonate (KHB) buffer containing 20 mM HEPES (pH 7.4) and 5 mM glucose. Samples were then incubated at 37°C for 5 min in 1 ml of oxygenated KHB buffer plus 20 mM HEPES, 2 mM glutamate, 5 mM glucose, 0.5 mM arginine, 0.05 μCi L-[U-^{14}C]-arginine, and 0.05 μCi [^{3}H] inulin. After a 5 min incubation, the tissues were rinsed thoroughly with fresh KHB buffer and solubilized in 0.5 ml Soluene 350. The ^{14}C and ^{3}H radioactivities were measured using a dual-channel counting program in a Packard 1900 liquid scintillation counter (Meriden, CT). The specific activity of L-[U-^{14}C]-arginine was used to calculate arginine uptake by the placentae.

Statistical Analyses

For all qPCR data, fold changes were determined using the $2^{-\Delta\Delta Ct}$ Method with raw Ct values normalized to either *B2M* or the geometric mean of *TBP*, *SDHA*, and *ACTB* for endometrial tissue and the geometric mean of *TBP*, *HPRT1*, and *TUBA1B* for placental tissue (Livak and Schmittgen, 2001). The qPCR data for normal tissues were analyzed for effect of day, pregnancy status, and their interaction for Days 9, 11, 13, 15 and 17 by 2-way ANOVA via the General Linear Models (GLM) procedures of the Statistical Analysis System (SAS Institute, Cary, NC) with the least significant difference (LSD) multiple testing method. The qPCR data were also subjected to a sliding time window linear regression analysis to determine if there was an effect of day of gestation on the gene expression for the genes of interest throughout pregnancy (Days 9 to 85). The sliding time windows of the analysis were designed to detect effect of day on gene expression during three biologically relevant periods of time: the beginning, the middle, and the end of the study period. Each window analyzed contained a minimum of three days. Some windows contained greater than three days as long as the regression model showed a non-decreased performance in terms of the r^2 and the p-value of the F-statistics.

The data from the hormone therapy studies were analyzed by Students t-test. The arginine transport data were subjected to a least-squares regression analysis (ANOVA) using the GLM procedures of the Statistical Analysis System. All data are presented as mean±standard error with significance at $p<0.05$.

Results

Primer Specificity and Efficiency

Ten genes were chosen as candidate reference genes based on their previous published use in pig tissues and their involvement in diverse cellular processes. The first step to determining stable reference genes was to ensure that the selected genes were expressed in the pig endometrium and placenta and that the primers were both specific and efficient for the pig genes. The ten selected genes (beta-actin, *ACTB*; beta-2-microglobulin, *B2M*; glyceraldehydes-3-phosphate dehydrogenase, *GAPDH*; hypoxanthine phosphoribosyl transferase 1, *HPRT1*; peptidylprolyl isomerase A, *PPIA*; ribosomal protein L7, *RPL7*; succinate dehydrogenase complex protein A, *SDHA*; TATA-box binding protein, *TBP*; alpha tubulin 1B, *TUBA1B*; tyrosine 3-monooxygenase/tryptophan 5-monooxygenase activation protein zeta, *YWHAZ*) were expressed in endometrial and placental tissues with the expected amplicon size as seen with agarose gel electrophoresis (Figure 3.1). The presence of only one band in the agarose gel and a single peak in the dissociation curves confirmed amplification specificity of the primers. Standard curves were generated to determine amplification efficiencies, which ranged from 97-100%.

Gene Stability Analyses

Raw Cq values from endometrial tissues of pregnant and cyclic gilts were used to determine optimal stability with both NormFinder and GeNorm algorithms (Table 3.2).

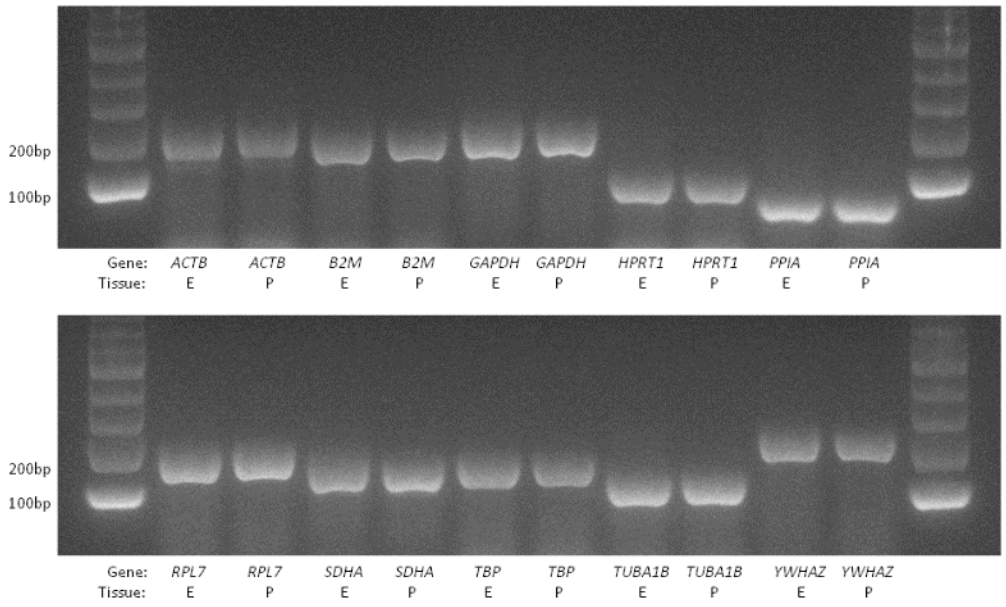

Figure 3.1 PCR of candidate reference genes

Agarose gels (2.5%) showing PCR products for candidate reference genes from endometrial or placental tissues. Amplicons were of expected sizes (*ACTB* 187bp, *B2M* 166bp, *GAPDH* 173bp, *HPRT1* 91bp, *PPIA* 59bp, *RPL7* 171bp, *SDHA* 141bp, *TBP* 153bp, *TUBA1B* 116bp, *YWHAZ* 203bp). Legend: Endometrium (E); Placenta (P).

Raw Cq values for placental tissues were analyzed separately (Table 3.3). For this particular set of data, NormFinder is the more appropriate algorithm because it takes into consideration both intra- and inter-day sources of variation. *TBP* was the most stable gene for both analyses, and both tissues, with *YWHAZ* being the least stable gene overall (Table 3.2, endometrium; Table 3.3, placenta). The genes ranked differently in degree of stability between endometrial and placental tissues. They also ranked differently between the two algorithms. For endometrial tissue, *SDHA* and *TUBA1B* ranked in the top half of genes, while *GAPDH* and *B2M* ranked in the bottom half (Table 3.2). For placental tissue, *HPRT1* and *RPL7* ranked in the top half, while *GAPDH* and *B2M* ranked in the bottom half for stability (Table 3.3).

The acceptable standard for calculation of normalization factors includes a geometric mean of the top three most stable genes (Vandesompele et al., 2002b; Gu et al., 2011). Therefore, the candidate genes were ranked by combining the ranks from the two algorithms for each tissue type. For endometrial tissue, the geometric mean of *TBP*, *SDHA*, and *ACTB* is recommended, while the geometric mean of *TBP*, *HPRT1*, and *TUBA1B* are recommended for placenta (Table 3.4).

Influence of Reference Gene Choice on Target Gene Expression

As mentioned previously, the choice of reference gene can influence the conclusions that are made about the target gene. In order to demonstrate the benefit of normalizing with the most stable reference genes when analyzing gene expression in a specific tissue, the mRNA expression profile for the monocarboxylate transporter

Gene	NormFinder Stability (±SE)	GeNorm Stability
ACTB	0.478±0.079	0.086
B2M	0.627±0.093	0.108
GAPDH	0.886±0.123	0.089
HPRT1	0.616±0.092	0.080
PPIA	1.027±0.139	0.084
RPL7	0.584±0.089	0.079
SDHA	0.556±0.086	0.074
TBP	0.454±0.077	0.069
TUBA1B	0.568±0.087	0.079
YWHAZ	1.120±0.150	0.099

Table 3.2 Stability values for candidate reference genes in endometrial tissue

Gene	NormFinder Stability (±SE)	GeNorm Stability
ACTB	0.380±0.071	0.058
B2M	0.686±0.110	0.063
GAPDH	0.552±0.092	0.053
HPRT1	0.333±0.066	0.046
PPIA	0.543±0.091	0.048
RPL7	0.380±0.071	0.047
SDHA	0.417±0.075	0.047
TBP	0.225±0.058	0.043
TUBA1B	0.373±0.070	0.050
YWHAZ	1.081±0.166	0.073

Table 3.3 Stability values for candidate reference genes in placental tissue

Rank	Endometrium	Placenta
1	*TBP*	*TBP*
2	*SDHA*	*HPRT1*
3	*ACTB*	*TUBA1B*
4	*TUBA1B*	*RPL7*
5	*HPRT1*	*SDHA*
6	*RPL7*	*PPIA*
7	*PPIA*	*ACTB*
8	*GAPDH*	*GAPDH*
9	*B2M*	*B2M*
10	*YWHAZ*	*YWHAZ*

Table 3.4 Recommended ranking of candidate reference genes for endometrial and placental tissue

SLC16A6 in endometrial tissue was determined via qPCR and normalized using the geometric mean of *TBP*, *SDHA*, and *ACTB* or the single gene, *B2M* (Figure 3.2). The data normalized to the trio of genes indicates little difference in *SLC16A6* gene expression between the estrous cycle and pregnancy from Days 5 to 20 with the greatest expression occurring on Day 17 of the estrous cycle. The data normalized to only *B2M* indicates that the gene has significantly higher expression in pregnant gilts than cycling gilts on Days 15 and 17 (Figure 3.2b; $p<0.05$). In the pig, this is a critical period of pregnancy because maternal recognition of pregnancy has recently occurred, while elongation and attachment are proceeding. The conclusions drawn from these two profiles would be opposites. In Figure 3.2b, expression of *SLC16A6* mRNA is higher during pregnancy than the estrous cycle, but this expression is being influenced by the reference gene, *B2M*, which is also higher during pregnancy than the estrous cycle. From Figure 3.2a, the conclusion would be that the conceptus has no influence on expression of mRNA for this gene in the endometrium during the peri-implantation period, while Figure 3.2b indicates that the conceptus, possibly conceptus secreted estrogens or cytokines, could be increasing gene expression in the endometrium.

Expression of SLC5A1 mRNA in Porcine Endometria and Placentae

Analysis by qPCR, using the geometric mean of *TBP*, *SDHA*, and *ACTB* for normalization, determined that *SLC5A1* mRNA increased between Days 5 and 9, then decreased between Days 9 and 11 in endometria from both the estrous cycle and pregnancy (Fig. 3.3a). In contrast, there was a significant increase in the expression of

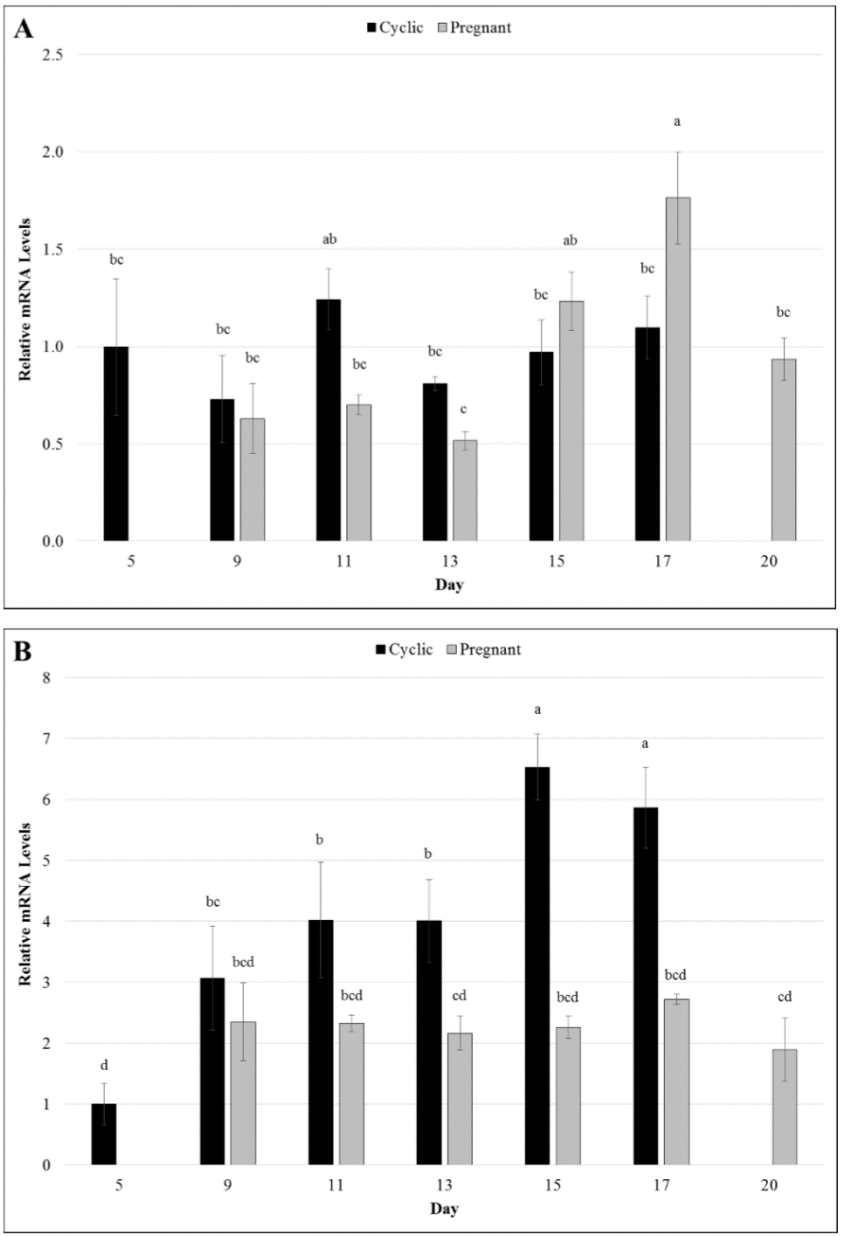

Figure 3.2 Expression of *SLC16A6* mRNA in endometrial tissues normalized using optimal and suboptimal reference genes

Expression of *SL16A5* mRNA across the estrous cycle and pregnancy in endometria normalized to the geometric mean of *TBP*, *ACTB*, and *SDHA* (**A**) or to *B2M* (**B**). Relative mRNA expression values are expressed as a ratio to Day 5 of the estrous cycle. Differing superscript letters indicate significant differences ($p<0.05$). Values are presented as mean±SEM.

SLC5A1 mRNA between Days 11 and 13 of pregnancy, and *SLC5A1* mRNA was more abundant in the endometria from Day 13 pregnant as compared to Day 13 cyclic gilts (Fig. 3.3a; $p<0.001$). After Day 13, expression of *SLC5A1* mRNA decreased and remained lowly abundant with no changes in expression for the duration of pregnancy (Fig. 3.3a; $p>0.05$; $r^2=0.173$).

Analysis by qPCR using the geometric mean of *TBP, HPRT1,* and *TUBA1B* for normalization determined that expression of *SLC5A1* mRNA was unchanged in placental tissue from Days 30 to 85 of pregnancy expression (Fig. 3.3b; $p>0.05$; $r^2=0.008$). *In situ* hybridization analysis localized *SLC5A1* mRNA to uterine LE and GE of both cyclic and pregnant gilts as well as the placental chorion and areolae (Fig. 3.3c). *SLC5A1* was expressed in the uterine LE and GE of both cyclic and pregnant gilts on Day 9, and then appeared to decrease in those cells between Days 9 and 12 of the estrous cycle (Fig. 3.3). In contrast to the estrous cycle, expression of *SLC5A1* mRNA appeared to further increase in the uterine LE between Days 9 and 12 of pregnancy (Fig. 3.3c). Expression of *SLC5A1* mRNA then appeared to decrease to background levels in uterine LE and GE between Days 13 and 14 of gestation and remained at that level for the duration of gestation (Fig. 3.3c).

Results of qPCR analysis indicated that expression of *SLC5A1* mRNA was greater in endometria of pseudopregnant as compared to cyclic gilts ($p<0.01$) and expression was unaffected by long-term P4 treatment (Fig. 3.4a,b; $p>0.05$). *In situ* hybridization analysis localized *SLC5A1* mRNA to uterine LE of Day 15 pseudopregnant, but not cyclic gilts, suggesting that E2 induces *SLC5A1* mRNA in

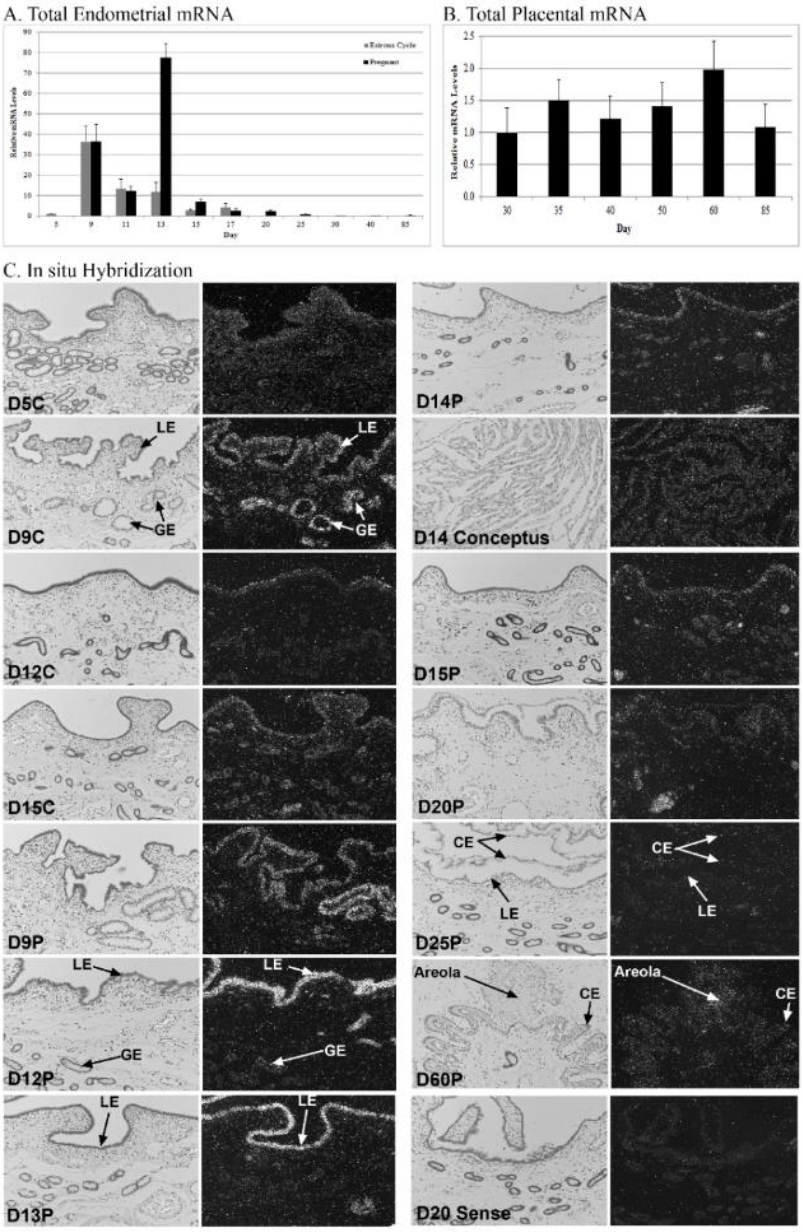

Figure 3.3 Expression *SLC5A1* mRNA in endometria and placentae
Expression of *SLC5A1* mRNA was higher in endometria (**A**) from pregnant than cyclic gilts on Day 13 ($p<0.05$), but placental expression of *SLC5A1* mRNA (**B**) showed no change from Days 30 to 85 ($p>0.05$). Corresponding bright-field and dark-field images from *in situ* hybridization (**C**) reveal expression of *SLC5A1* mRNA in uterine LE and GE at Day 9 of the estrous cycle and pregnancy and only in uterine LE by Day 12 of pregnancy. The D20 sense panel is the negative control. Width of field is 870 µm. Legend: LE, luminal epithelium; GE, glandular epithelium; Tr, trophectoderm; CE, chorion.

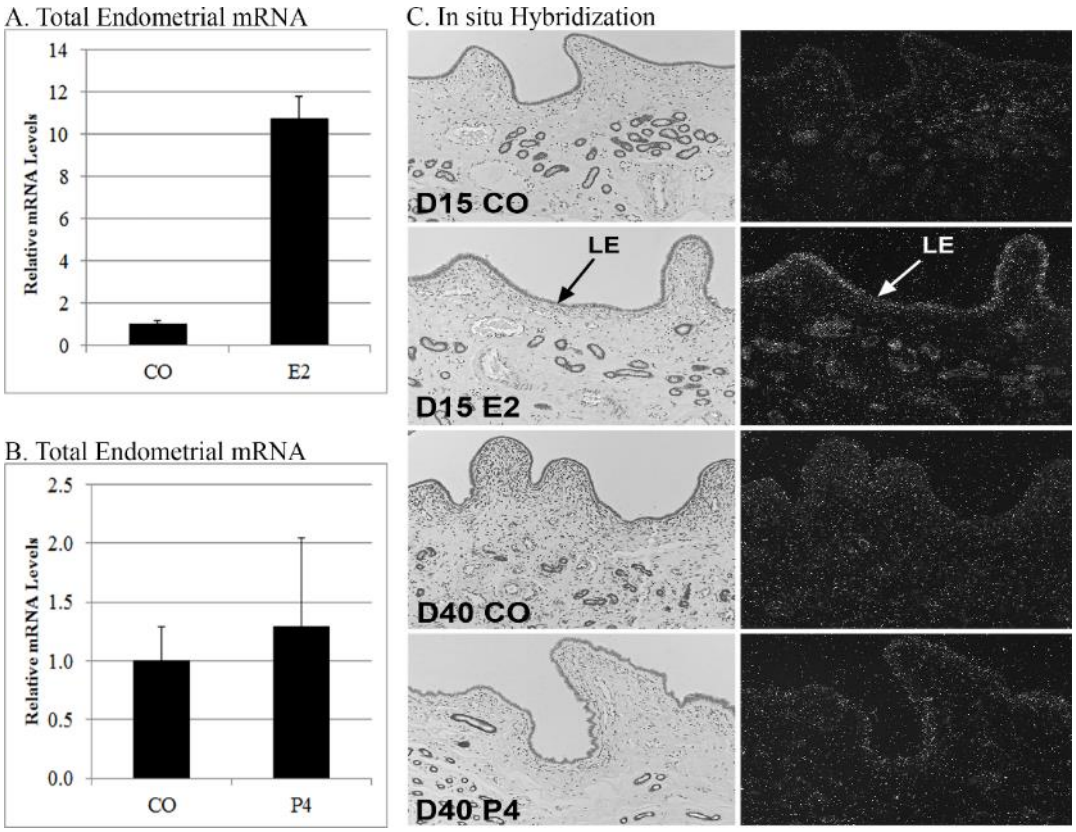

Figure 3.4 Estradiol induces expression of *SLC5A1* mRNA in uterine LE
SLC5A1 mRNA expression is higher in endometria from E2-treated as compared to control gilts (**A**; $p<0.05$), but was not different in endometria from P4-treated compared to control gilts (**B**; $p>0.05$). Corresponding bright-field and dark-field images from *in situ* hybridization (**C**) depict *SLC5A1* mRNA expression increases in the uterine LE and GE in response to E2, while P4 treatment had no detectable effect on gene expression. The D20 Sense panel in Figure 3.3 is the negative control. Legend: LE, luminal epithelium.

uterine LE (Fig. 3.4c). Long-term P4 treatment of ovariectomized gilts did not induce expression of *SLC5A1* mRNA in the endometrium (Fig. 3.4c).

Expression of SLC7A3 mRNA in Porcine Endometria and Placentae

Analysis by qPCR, using the geometric mean of *TBP*, *SDHA*, and *ACTB* for normalization, determined that *SLC7A3* mRNA was not detectable in endometrial tissues at any day of the estrous cycle and pregnancy (data not shown).

Analysis by qPCR, using the geometric mean of *TBP*, *HPRT1*, and *TUBA1B* for normalization, determined that *SLC7A3* mRNA expression in placental tissue increased from Days 30 to 40 ($p<0.001$; $r^2=0.999$) and then expression remained unchanged through Day 85 of pregnancy (Fig. 3.5a; $p>0.05$; $r^2=0.086$). *In situ* hybridization analyses localized *SLC7A3* mRNA to the chorion (Fig. 3.5b). *SLC7A3* mRNA was not detectable in trophectoderm through Day 20, but was detectable in the chorion by Day 25 of gestation. The hybridization signal for *SLC7A3* mRNA expression appeared to increase in placental tissues through Day 85, and was present in both the chorionic epithelia of areolae and non-areolar regions of placentae with distinctly higher expression in the tall columnar cells at the tops of uterine folds (Fig. 3.5b). *SLC7A3* mRNA was not detected in endometria from any day of the estrous cycle or pregnancy (Fig. 3.5b).

Radiolabeled arginine was transported from culture medium into the chorioallantoic cells of Day 60 pig placentae (Fig. 3.5c). As predicted from results of *in*

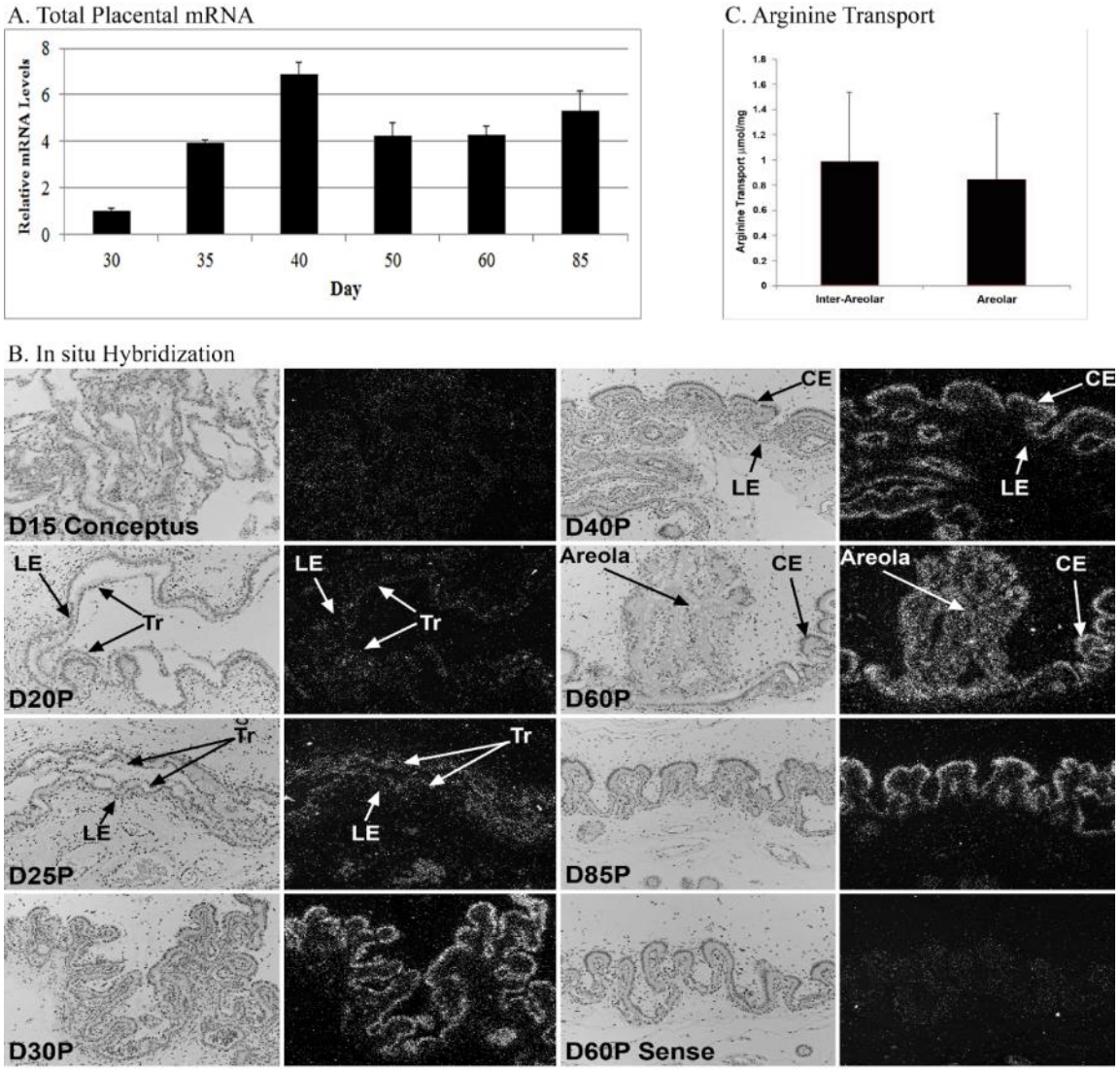

Figure 3.5 Expression of *SLC7A3* mRNA and arginine transport in placentae
Expression of *SLC7A3* mRNA in placenta (**A**) increases from Days 30 to 40 of pregnancy ($p<0.001$; $r^2=0.999$) and then remains unchanged through Day 85 of pregnancy ($p>0.05$; $r^2=0.086$). Corresponding bright-field and dark-field images from *in situ* hybridization (**B**) depict *SLC7A3* mRNA localization to the trophectoderm, CE, and areolae. There is no difference in arginine transport between areolar and inter-areolar regions (**C**; $p>0.05$). The D60P Sense panel is the *in situ* hybridization negative control. Legend: LE, luminal epithelium; Tr, trophectoderm; CE, chorion.

situ hybridization analyses to determine cell-specific localization of *SLC7A3* mRNA, no significant difference in arginine transport was found between areolae and inter-areolar regions of the chorioallantois (Fig. 3.5c; $p<0.05$).

Discussion

Gene expression analysis applied over the duration of the estrous cycle and pregnancy is a useful tool for studying the myriad of changes that occur in both the maternal endometrium and fetal placenta. In the pig, protein analysis is restricted by the availability of commercial antibodies that cross-react with pig proteins, making gene expression analysis by qPCR one of the main tools for documenting changes in gene expression. Care must be given to determine which genes are reliable and optimal for selection as reference genes in order to provide the most accurate data (Peters et al., 2004).

A serious issue with measuring gene expression over the duration of pregnancy is the potential gene regulation of traditional reference genes because the pig endometrium and placenta undergo temporal remodeling as they develop throughout pregnancy. Another consideration, specifically for the use of *B2M* or any other immune-related gene, is that pregnancy influences changes in the maternal immune system so that it will not reject the fetal allograft. In the epitheliochorial placenta of the pig, this can be seen in the down regulation of MHC class I molecules at the maternal/fetal interface (Huddleston and Schust, 2004; Joyce et al., 2008). This example shows that the

physiology of the tissue being analyzed should be considered when choosing reference genes.

Previous studies have identified optimal reference genes for use in pig tissues, including: *TBP, ACTB, HPRT1, YWHAZ, HSPCB* (Nygard et al., 2007; Gu et al., 2011), but these studies did not include endometrium and placenta. Martinez-Giner *et al*. concluded that *TBP, SDHA,* and *UBC* were optimal reference genes in pig endometrium across pregnancy, but endometrial tissue from non-pregnant gilts during the estrous cycle was not considered in the analysis (Martinez-Giner et al., 2013). The present results agree with Martinez-Giner *et al*. in that *TBP* and *SDHA* were also found to be the most stable reference genes when tissues from non-pregnant cycling gilts were included in the analyses. The ability to compare tissue from pregnant and cycling gilts is important for understanding gene expression during establishment of pregnancy in pigs.

The ribosomal protein *18S* is often used as a reference gene, but it was excluded in the present study because of the disadvantages that ribosomal genes can have when used as reference genes. First, rRNA genes have a much higher abundance than most target genes and this imbalance can negatively impact the accuracy of the qPCR analysis (Vandesompele et al., 2002b). Second, regulation of rRNA synthesis is different than for mRNA, as it is transcribed by RNA polymerase I (Radonic et al., 2004). Ribosomal protein *RPL7* was included in this analysis, but was not found to be optimal, most likely due to the issues noted.

In order to provide evidence that the reference genes chosen were appropriate, both qPCR and *in situ* hybridization were performed for two genes over the duration of

the estrous cycle and pregnancy in the pig. *SLC5A1* mRNA expression from the qPCR analyses closely followed the results from *in situ* hybridization analyses indicating that expression was high on both Day 9 of the estrous cycle and pregnancy, then decreased in the estrous cycle, while increasing and peaking on Day 15 of pregnancy. The data from the pseudopregnant model further confirmed the biological significance of this peak by determining that it was induced by E2, the maternal recognition of pregnancy signal. In the pig, the corpora lutea can be maintained without any conceptuses when injections of exogenous E2 are administered during Days 11 to 14 of the estrous cycle to mimic secretion of estrogen by the conceptus. This psuedopregnant state provides an opportunity to determine the effects of E2 on the endometrium independent of other conceptus-secreted factors. *SLC7A3* mRNA expression also followed a similar pattern between the two techniques with increasing expression in the chorion as pregnancy progressed and the areolar development most likely driving the increase seen in placental tissue from Days 30 to 40 of pregnancy.

In addition to being models for determining the appropriateness of reference genes for qPCR, *SLC5A1* and *SLC7A3* also have biologically significant roles at the uterine-placental interface in the pig. Pig embryos enter the uterus, develop into blastocysts, and then shed the zona pellucida. The presumptive placental membranes (trophectoderm and endoderm) elongate at a rate of 30-45 mm/h from a 10 mm blastocyst to a 150-200 mm long filamentous form, after which further elongation occurs until conceptuses are 800-1,000 mm in length by Day 16 of pregnancy. This process provides maximum surface area for contact between trophectoderm and uterine LE to

facilitate the uptake of nutrients from uterine LE and uterine GE (Bazer and Johnson, 2014). Significant energy is required to drive those extreme morphological changes in the conceptus. Glucose is essential to conceptus survival, growth, and development, and substantial amounts of glucose are transported across the placental membranes of pigs (White et al., 1979; Ramsay et al., 1984; Pere, 2003). Although little is known about the role(s) of sodium-dependent glucose transporters in uterine physiology, *SLC5A1* mRNA and protein are present in ovine uterine LE and GE during the peri-implantation period, making SLC5A1 a potential candidate for glucose transport into the uterine lumen during conceptus elongation in pigs (Gao et al., 2009a).

Messenger RNA for the sodium-dependent glucose transporter *SLC5A1* was localized to the uterine LE coinciding with conceptus elongation, pregnancy recognition, and early attachment of conceptuses to the uterine wall for implantation. *SLC5A1* mRNA expression was greatest in uterine LE on Days 12 and 13 of pregnancy, then decreased precipitously to undetectable levels by Day 14, suggesting that a paracrine factor(s) from the conceptus regulates expression of *SLC5A1* mRNA. Pig conceptuses secrete E2 on Days 11 and 12 to signal initiation of pregnancy to the uterus. Conceptus E2 also induces or upregulates expression of a number of endometrial growth factors and cytokines as components of histotroph that are released by uterine LE and GE into the uterine lumen to support development of free-floating conceptuses (Geisert et al., 1982c; Johnson et al., 2009). In this study, results from Day 15 psuedopregnant pigs provide strong evidence that E2 increases expression of *SLC5A1* mRNA in uterine LE. We hypothesize that as porcine conceptuses begin to elongate, an energy-dependent event,

they secrete E2 that increases the number of SLC5A1 transporters in uterine LE, thereby increasing potential transport of glucose into the uterine lumen to nourish free-floating conceptuses. Accordingly, recoverable glucose in uterine flushings increases between Days 12 and 14 of pregnancy in Large White and Meishan gilts (Bazer et al., 1991).

Another hallmark of pregnancy in pigs is epitheliochorial placentation. Porcine placental trophectoderm/chorion directly attaches to uterine LE, and these epithelia serve as the conduit for maternal hemotrophic and histotrophic support for conceptus growth and development. The formidable barrier to nutrient transport presented by two adhered epithelial cell layers separating uterine and placental vasculatures must be overcome in both the inter-areolar regions of placental attachment and in areolae that form only over the openings of uterine glands to maintain sufficient hemotrophic and histotrophic nutrition, respectively (Bazer and Johnson, 2014). Results from the present study provide evidence that both the inter-areolar and areolar chorion at the uterine-placental interface express *SLC7A3*, a transporter capable of moving arginine, and other amino acids, to the placental vasculature for transport to the embryo/fetus.

We reported an abundance of ornithine and arginine in the allantoic fluids of pigs at levels never before reported in any other biological fluid (Wu et al., 1995). On Days 45 and 60 of gestation, ornithine and arginine account for 34-36% of total free α-amino acids in allantoic fluid, and arginine increased 4.5 fold between Days 30 and 45 of pregnancy (Wu et al., 1995). The potential for arginine to positively influence conceptus development is profound as arginine is a precursor for synthesis of ornithine, polyamines, proline, glutamine, creatine, agmatine, NO, and proteins. Further, arginine-

derived ornithine serves as a precursor for synthesis of polyamines and proline in porcine maternal and conceptus tissues where proline and ornithine play an important role in polyamine synthesis (Wu and Morris, 1998; Wu et al., 2013). This biochemical potential has been realized in real-world application where arginine supplementation of the diet of pregnant gilts between Days 30 and 114 of pregnancy significantly increased litter birth-weight and the number of live-born piglets (Mateo et al., 2007), and a number of studies have provided additional support for a beneficial role for arginine supplementation in reducing embryonic deaths in gestating pigs (Berard and Bee, 2010; Wu et al., 2013). Although the importance of placental arginine to pregnancy success in pigs is well established, little is known about how arginine is transported across the placental chorion for access to the placental vasculature, tissues for metabolism, and routes for diffusion through the allantois for storage in allantoic fluid before being taken up again into the circulation of the conceptus. This study identifies SLC7A3 as an excellent candidate for arginine transport across the placental chorion of pigs.

The mRNA for the cationic amino acid transporter *SLC7A3* was localized to the chorionic epithelium coinciding with increased abundance of arginine in porcine allantoic fluid (Wu et al., 1995). *In situ* hybridization and qPCR analyses demonstrated that *SLC7A3* mRNA significantly increases between Days 30 and Day 60 in the chorion and support a role for SLC7A3 transport of amino acids across the placenta. Further, when chorioallantois from Day 60 of pregnancy was isolated and areolae separated from inter-areolar regions of placentation, both areolae and inter-areolar tissues exhibited a comparable ability to transport radioactive arginine across cell membranes and into the

cells of the tissues. We hypothesize that as the attachment phase of implantation in pigs is completed and mature placentation proceeds between Days 25 and 40 of pregnancy, the number of SLC7A3 transporters increase in the placental chorionic epithelium for transport of arginine across the chorioallantois and into the fetal-placental vasculature and/or allantoic fluid. This enables arginine to be used immediately to support development and growth of the conceptus, but particularly the fetus during the second and third trimesters of gestation in gilts. However, the allantois serves as a reservoir for storage of nutrients such as amino acids, glucose, and fructose that are available for subsequent uptake into the placental circulation as needed to support development and growth of the conceptus.

In conclusion, these data would recommend use of *TBP* as an acceptable stable reference gene for qPCR in pig endometrial and placental tissues. The geometric mean of *TBP, HPRT1,* and *TUBA1B* is the optimal reference value for placental tissue, while the geometric mean of *TBP, ACTB,* and *SDHA* is optimal for endometrial tissue. *YWHAZ, B2M,* and *GAPDH* are not acceptable reference genes for pig endometrial or placental tissues. Additionally, using these recommended reference genes, this study has identified *SLC5A1* and *SLC7A3* as excellent candidate genes for glucose and arginine transport, respectively, during pregnancy to aid in growth and development of the porcine conceptus.

CHAPTER IV

ESTROGEN AND PROGESTERONE REGULATE SLC2A FACILITATED GLUCOSE TRANSPORTER GENE EXPRESSION IN PORCINE ENDOMETRIA DURING PREGNANCY

Introduction

Glucose is an abundant hexose sugar that is transported through endometrial and placental tissues and utilized as a major energy substrate for growth and development of porcine conceptuses (embryo/fetus and associated extraembryonic membranes) during pregnancy (White et al., 1979; Pere, 2003). There is minimal gluconeogenesis in the placenta and fetus of pigs (Fowden et al., 1997). Therefore, glucose from maternal blood must be transported into the uterine lumen early in pregnancy where the free-floating conceptus can access the sugar and transport it across the trophectoderm. As implantation and placentation progress, the adherence of the uterine luminal epithelium (LE) to the placental chorion creates the uterine-placental interface of the epitheliochorial pig placenta that nutrients must traverse to reach the placental vasculature (Dantzer, 1984, 1985).

Glucose can be transported by either facilitated diffusion transporters of the solute carrier 2A (SLC2A; GLUT) family or sodium-dependent transporters of the solute carrier 5A (SLC5A; SGLT) family. The pig primarily depends on a glucose concentration gradient to transport glucose as indicated by the concentrations of glucose in fetal blood that are 40-70% lower than concentrations of glucose in maternal blood

(Randall, 1977; Pere, 1995), therefore, this study focused on the SLC2A family of glucose transporters. There are 14 members of the SLC2A family (SLC2A1-14) responsible for transporting multiple sugars in addition to glucose. Different members of the family have differing affinities for glucose, some are regulated by insulin or steroid hormones, and all have a distinct tissue-specific expression (Augustin, 2010). SLC2A1 is ubiquitously expressed throughout the body and is responsible for the basal glucose uptake into cells. SLC2A2 is a low affinity, high capacity glucose transporter often found in the basal plasma membrane of transporting epithelia. SLC2A3 is a high affinity, high capacity glucose transporter found in tissues such as the brain where glucose needs to be moved quickly and in large quantities. SLC2A4 is an insulin-sensitive glucose transporter mostly found in skeletal muscle and adipose tissues (Olson and Pessin, 1996; Zhao and Keating, 2007b).

The transporters SLC2A1, SLC2A3, and SLC2A4 have been localized to endometrial or conceptus tissues of humans, mice, and sheep. SLC2A1 has been localized to human placental syncytiotrophoblasts and the LE, glandular epithelium (GE), and stroma of human and mouse endometrium (Jansson et al., 1993; Yamaguchi et al., 1996; von Wolff et al., 2003)). SLC2A1 protein has also been detected in the LE and GE of the sheep endometrium during the estrous cycle and early pregnancy, as well as in the conceptus trophectoderm (Gao et al., 2009a). SLC2A3 has been detected in the stroma and decidua of human and mouse endometria in addition to the placenta (Yamaguchi et al., 1996; Hahn et al., 2001; Brown et al., 2011). SLC2A3 mRNA is expressed in the trophectoderm of sheep as early as Day 14 of pregnancy, but there is no

endometrial expression detected through Day 20 (Gao et al., 2009a). SLC2A4 has been detected in LE, GE and stroma of human and mouse endometria as well as sheep uterine LE and GE throughout the estrous cycle and early pregnancy (von Wolff et al., 2003; Gao et al., 2009a). SLC2A2 has not been detected in either human or mouse endometria (von Wolff et al., 2003; Frolova and Moley, 2011b).

Glucose transport from mother to conceptus can be influenced by several factors, including utero-placental blood flow, concentration gradients, surface area for exchange, placental metabolism, transporter expression, maternal hormones, and placental hormones. The true epitheliochorial placenta of the pig represents a significant barrier to nutrient transport because nutrients must traverse multiple cell layers between the maternal and fetal microvasculatures (Dantzer, 1985). This barrier to nutrient transport is overcome by folding of the adhered interface, comprised of the maternal uterine epithelia and placental chorion and underlying connective tissue, to increase surface area. Areolae, invaginations of the chorioallantois that receive and transport the secretions from uterine GE to the vasculature of the conceptus also develop (Friess et al., 1981; Dantzer, 1984).

Steroid hormone regulation of expression of SLC2A transporters has been described in the sheep where progesterone (P4) upregulates SLC2A1 protein in the uterine LE, but has no effect on expression of SLC2A4 protein (Gao et al., 2009a). Additionally, estrogen (E2) treatment increases glucose uptake and the expression of SLC2A1 protein in the rat uterus (Smith and Gorski, 1968; Welch and Gorski, 1999).

SLC2A1 protein is also upregulated in mouse uterine epithelia in response to P4 (Frolova et al., 2009).

While the glucose transporters SLC2A1, SLC2A2, SLC2A3, and SLC2A4 have been studied in the endometrial and placental tissues of non-pregnant and early pregnant humans, mice, and sheep, there is no information regarding the temporal and cell-specific expression of these transporters in pig endometria and placentae or their regulation by steroid hormones. Therefore, this study aimed to quantify temporal and cell-specific changes in expression of glucose transporters throughout the estrous cycle and pregnancy in the pig and determine whether their expression is regulated by E2 and/or P4, two important hormones of pregnancy in pigs.

Material and Methods

Animals and Tissue Collection

Sexually mature, 8-month-old crossbred gilts were observed daily for estrus (Day 0) and exhibited at least two estrus cycles of normal duration (18 to 21 days) before being used in these studies. All experimental and surgical procedures were in compliance with the Guide for Care and Use of Agricultural Animals in Teaching and Research and approved by the Institutional Animal Care and Use Committee of Texas A&M University.

To evaluate the effects of pregnancy on expression of *SLC2A1*, *SLC2A2*, *SLC2A3* and *SLC2A4* genes, gilts were assigned randomly to either cyclic or pregnant status.

Gilts in the pregnant group were bred naturally to boars with proven fertility. Cyclic gilts were ovariohysterectomized on either Day 5, 9, 11, 12, 13, 15 or 17 of the estrous cycle, while pregnant gilts were ovaiohysterectomized on either Day 9, 11, 12, 13, 15, 17, 20, 25, 30, 35, 40, 50, 60, or 85 of pregnancy (n = 3 or 4 gilts/day/status). For uterine lumen fluid collection, the lumen of each uterine horn from Days 9 through 17 of the estrous cycle and pregnancy were flushed with 20 ml physiological saline. Pregnancy was confirmed in the mated gilts by the presence of morphologically normal conceptuses. Tissue sections (uterus or uterus with attached placenta ~1cm thick) from the middle of each uterine horn of all hysterectomized gilts were fixed in fresh 4% paraformaldehyde in PBS (pH 7.2) and embedded in Paraplast-Plus (Oxford Laboratory, St. Louis, MO). Additionally, endometrium was physically dissected from the myometrium, snap-frozen in liquid nitrogen, and stored at -80°C for RNA extraction. Chorioallantoic tissue was physically dissected from endometrium and frozen in a similar manner.

Progesterone and Estrogen Models

To evaluate effects of E2 and E2-induced pseudopregnancy on expression of *SLC2A1*, *SLC2A2*, *SLC2A3*, and *SLC2A4* mRNAs in endometria, gilts were detected in estrus (Day 0) and assigned randomly to receive daily intramuscular injections of either estradiol benzoate (E2 in corn oil (E2); n = 4) or corn oil alone (CO; n = 4) on Days 11, 12, 13, and 14 of the estrous cycle (Joyce et al., 2007). All gilts were ovariohysterectomized on Day 15 of pseudopregnancy. Tissues were collected as described previously.

To evaluate effects of long-term P4 treatment, without ovarian hormones, on expression of *SLC2A1*, *SLC2A2*, *SLC2A3* and *SLC2A4* mRNAs in endometria, gilts were ovariectomized on Day 12 of the estrous cycle and assigned randomly to receive daily intramuscular injections of either CO (4 ml) or P4 (200 mg in 4 ml CO) on Days 12 through 39 post-estrus (n = 3/treatment) (Bailey et al., 2010c). All gilts were hysterectomized on Day 40 post-estrus and tissues collected as previously described.

Concentrations of Glucose in Uterine Flushings

Uterine flushings were purified by centrifugation at 3000 x g for 15 min at 4°C, and the supernatants aliquoted and stored at –80°C. Uterine flushings (0.5 ml) were deproteinized with an equal volume of 1.5M $HClO_4$ followed by addition of 0.25 ml of 2 M K_2CO_3. Extracts were analyzed for glucose using a fluorometric method utilizing hexokinase and glucose-6-phosphate dehydrogenase as described previously (Bergmeyer et al., 1974).

RNA Extraction, cDNA Synthesis, and Primer Design

Total RNA was extracted from endometrial and chorioallantoic tissue samples using Trizol reagent (Life Technologies, Carlsbad, CA) according to the manufacturer's recommendations (see Appendix B). First strand cDNA was synthesized using a Superscript III First Strand Kit (Life Technologies, Carlsbad, CA) according to the manufacturer's instructions (see Appendix B). First strand cDNA was diluted 10x for the qPCR reaction. Primers for qPCR and *in situ* hybridization were designed using NCBI

Gene Name	Method	Gene ID	Sequence	Product Length
SLC2A1	qPCR	XM_005665507.1	F: 5'-TCCTTTACCCACATCCCACG-3' R: 5'-AAGGCAAGTGTCTAGGCAGG-3'	82
SLC2A1	ISH	X17058	F: 5'-TGGCCTTCATATCTGCTGTG-3' R: 5'-AACAGCTCCAGGATGGTGAC-3'	484
SLC2A2	qPCR	NM_001097417.1	F: 5'-CCCTGCTGCTTTAGCAATGG-3' R: 5'-TAAGGTCCACAGAAGTCCGC-3'	96
SLC2A3	qPCR	XM_003355585.3	F: 5'-ATCTTGGTATGGCCACTCGG-3' R: 5'-GCAAGGCAATCCACTAAGGC-3'	130
SLC2A3	ISH	NM_001009770.1	F: 5'-CCACACATGAGCCGTAAATG-3' R: 5'-TGAAGAGCCCAGTCTCCACT-3'	477
SLC2A4	qPCR	NM_001128433.1	F: 5'-GAGAGCCAGTTCTCTCCACC-3' R: 5'-CTCCACCCTGGAAGTAACGG-3'	88
SLC2A4	ISH	NM_001128433.1	F: 5'-CAACAGATAGGCTCCGAAGA-3' R: 5'-CACGTACATGGGCACCAG	465
ACTB	qPCR	XM_003124280.3	F: 5'-TCCCTGGAGAAGAGCTACGA-3' R: 5'-TGTTGGCGTAGAGGTCCTTC-3'	187
HPRT1	qPCR	DQ845175	F: 5'-GGACTTGAATCATGTTTGTG-3' R: 5'-CAGATGTTTCCAAACTCAAC-3'	91
SDHA	qPCR	DQ845177	F: 5'-CTACAAGGGGCAGGTTCTGA-3' R: 5'-AAGACAACGAGGTCCAGGAG-3'	141
TBP	qPCR	DQ845178	F: 5'-AACAGTTCAGTAGTTATGAGCCAGA-3' R: 5'-AGATGTTCTCAAACGCTTCG-3'	153
TUBA1B	qPCR	NM_001044544.1	F: 5'-GCTGCCAATAACTATGCCCG-3' R: 5'-ACCAAGAAGCCCTGAAGACC-3'	116

Table 4.1 Primer information for *SLC2A* genes

Genbank sequences and Primer-BLAST (http://www.ncbi.nlm.nih.gov/). Primers were submitted to BLAST to test for specificity against the known porcine genome. Primer information is summarized in Table 4.1.

Quantitative PCR

Quantitative PCR assays were performed as previously described (Chapter III and Appendix B of this dissertation). Briefly, PerfeCta SYBR Green Mastermix (Quanta) was used in 10 µl reactions with 2.5 mM of each specific primer, on a Roche 480 Lightcycler (Roche) with approximately 60 ng cDNA per reaction. The PCR program began with 5 min at 95°C followed by 40 cycles of 95°C denaturation for 10 sec and 60°C annealing/extension for 30 sec. A melt curve was produced with every run to verify a single gene-specific peak. Standard curves with 2-fold serial dilutions were run to determine primer efficiencies. All primer correlation coefficients were greater than 0.95 and efficiencies were 95-102%. The geometric mean of *TBP*, *SDHA*, and *ACTB* was used to normalize endometrial tissue, while the geometric mean of *TBP*, *HPRT1*, and *TUBA1B* was used for chorioallantoic tissue.

In situ *Hybridization Analysis*

Cell-specific expression of mRNAs in sections of porcine endometria and placentae were determined by radioactive *in situ* hybridization analysis as described previously (Johnson et al., 1999)(Appendix B). Briefly, partial cDNAs for porcine *SLC2A1*, *SLC2A2*, *SLC2A3* and *SLC2A4* mRNAs were cloned beginning with PCR

amplification using total RNA from Day 15 pregnant porcine endometrial tissues using specific primers (Table 3.1). PCR amplification was conducted as follows: 1) 95°C for 5 min; 2) 95°C for 45 sec, 60°C for 30 sec, and 72°C for 1 min for 35 cycles; and 3) 72°C for 10 min. The partial cDNAs of the correct predicted size were cloned into a pCRII plasmid using a T/A Cloning Kit (Life Technologies) and the sequence of each verified using an ABI PRISM Dye Terminator Cycle Sequencing Kit and ABI PRISM automated DNA sequencer (Perkin-Elmer Applied Biosystems).

Radiolabeled antisense or sense cRNA probes were generated by *in vitro* transcription using linearized plasmid templates, RNA polymerases, and [α-^{35}S]-UTP. Deparaffinized, rehydrated, and deproteinated uterine tissue sections (5 µm thick) were hybridized with radiolabeled antisense or sense cRNA probes. After hybridization, washing, and ribonuclease A digestion, slides were dipped in NTB-2 liquid photographic emulsion (Kodak, Rochester, NY), and exposed at 4°C for seven to ten days. Slides were developed in Kodak D-19 developer, counterstained with Harris modified hematoxylin (Fisher Scientific, Fairlawn, NJ), dehydrated through a graded series of alcohol to Citrisolv (Fisher Scientific) and coverslips were affixed with Permount (Fisher Scientific). Slides were evaluated using an Axioplan 2 microscope (Carl Zeiss, Thornwood, NY) interfaced with an Axioplan HR digital camera and Axiovision 4.3 software, and digital images of representative fields recorded under brightfield or darkfield illumination. Photographic plates were assembled using Adobe Photoshop (version 6.0, Adobe Systems Inc., San Jose, CA).

Statistical Analyses

Data for concentrations of glucose were analyzed for effects of day, pregnancy status (cyclic or pregnant), and their interaction using a 2-way ANOVA via the General Linear Models (GLM) procedures of the Statistical Analysis System (SAS Institute, Cary, NC). For all qPCR data, fold changes were determined using the $2^{-\Delta\Delta Ct}$ Method with raw Ct values normalized to the geometric mean of *TBP*, *SDHA*, and *ACTB* for endometrial tissue and the geometric mean of *TBP, HPRT1,* and *TUBA1B* for placental tissue. The qPCR data for normal tissues were analyzed for effects of day, pregnancy status, and their interaction for Days 9, 11, 13, 15 and 17 by 2-way ANOVA via the General Linear Models (GLM) procedures of the Statistical Analysis System (SAS Institute, Cary, NC) with the least significant difference (LSD) multiple testing method. The qPCR data were also subjected to a sliding time window linear regression analysis to determine if there was an effect of day of gestation on the gene expression for the genes of interest throughout pregnancy (Days 9 to 85). The sliding time windows of the analysis were designed to detect effect of day on gene expression during three biologically relevant periods of time: the beginning, the middle, and the end of the study period. Each window analyzed contained a minimum of three days. Some windows contained greater than three days as long as the regression model showed a non-decreased performance in terms of the r^2 and the p-value of the F-statistics.

The data from the hormone therapy studies were analyzed using the Students t-test. All data are presented as mean±standard error of the means with significance at $p<0.05$.

Results

Glucose in Uterine Flushings

Total recoverable glucose increased in the uterine flushings of both cyclic and pregnant gilts between Days 9 and 15 (Figure 4.1; $p<0.05$). This indicates that the free-floating conceptus is exposed to increasing levels of glucose during development; however, there was no effect of pregnancy status, and no interaction between day and pregnancy status on total recoverable glucose (Figure 4.1; $p>0.05$).

SLC2A1 mRNA Localizes to Uterine LE During Pregnancy and Is Upregulated by E2 and P4

To determine the total endometrial expression of *SLC2A1* mRNA, qPCR was used on tissue samples from Days 5 to 17 of the estrous cycle and Days 9 to 85 of pregnancy. Expression of *SLC2A1* mRNA increased from Days 11 to 15 in endometrial tissue from cycling and pregnant gilts, but expression was more abundant in endometrial tissue from pregnant than cyclic gilts (Figure 4.2A; day x status, $p<0.001$). When endometrial expression of *SLC2A1* mRNA from pregnant gilts was analyzed from Days 9 to 85, there was an increase in expression from Days 9 to 17 ($r^2=0.864$; $p<0.05$), and there was no change in expression of *SLC2A1* between Days 17 and 25 ($r^2=0.108$; $p>0.05$) or Days 30 and 85 ($r^2=0.578$; $p>0.05$) of pregnancy. Expression of *SLC2A1* mRNA in the chorioallantois did not change between Days 30 and 85 of pregnancy (Figure 4.2B; $r^2=0.143$; $p>0.05$).

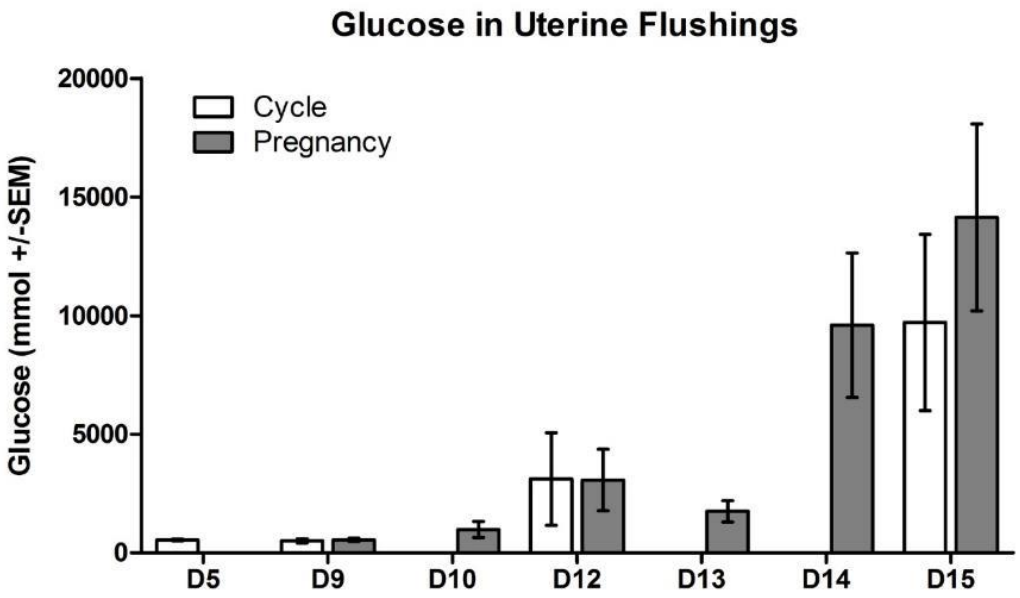

Figure 4.1 Total recoverable glucose in porcine uterine flushings increased from Days 9 to 15 of the estrous cycle and pregnancy

Glucose increased in the uterine flushings from Day 9 through 15 during the estrous cycle and pregnancy ($p<0.01$). There was no interaction between Day and Status or effect of Status alone ($p>0.05$). Values are means ± SEM.

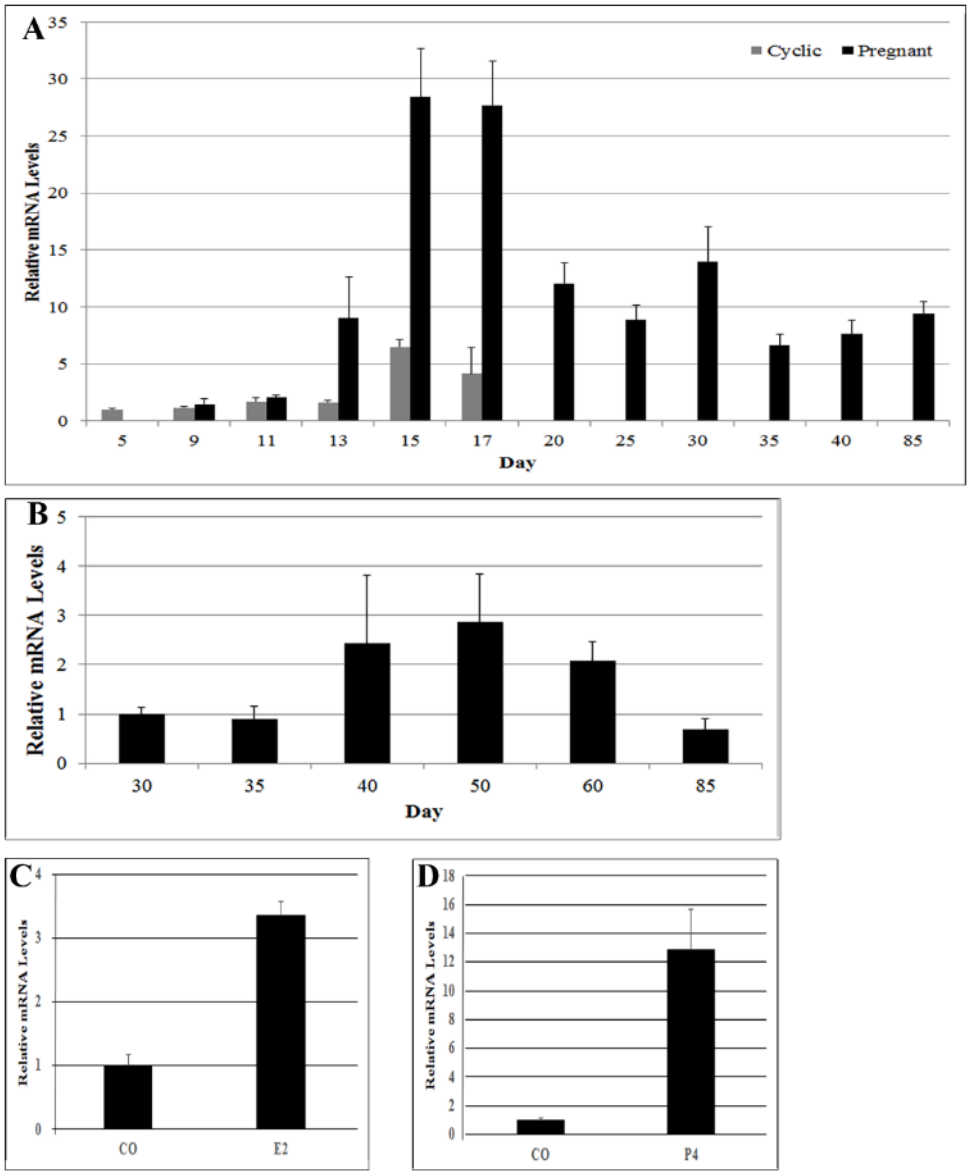

Figure 4.2 Expression of *SLC2A1* mRNA in endometria and placentae
(A) Expression of *SLC2A1* mRNA increased from Days 11 to 15 in endometrial tissue from cycling and pregnant gilts, and expression was more abundant in endometrial tissue from pregnant than cyclic gilts (day x status, $p<0.001$); **(B)** Expression of *SLC2A1* mRNA in placenta did not change between Days 30 and 85 ($r^2=0.143$; $p>0.05$); **(C)** Exogenous E2 upregulated expression of *SLC2A1* mRNA in endometria ($p<0.05$); **(D)** Exogenous P4 upregulated expression of *SLC2A1* mRNA in endometria ($p<0.05$). Values presented are means±SEM and $p<0.05$ is significant.

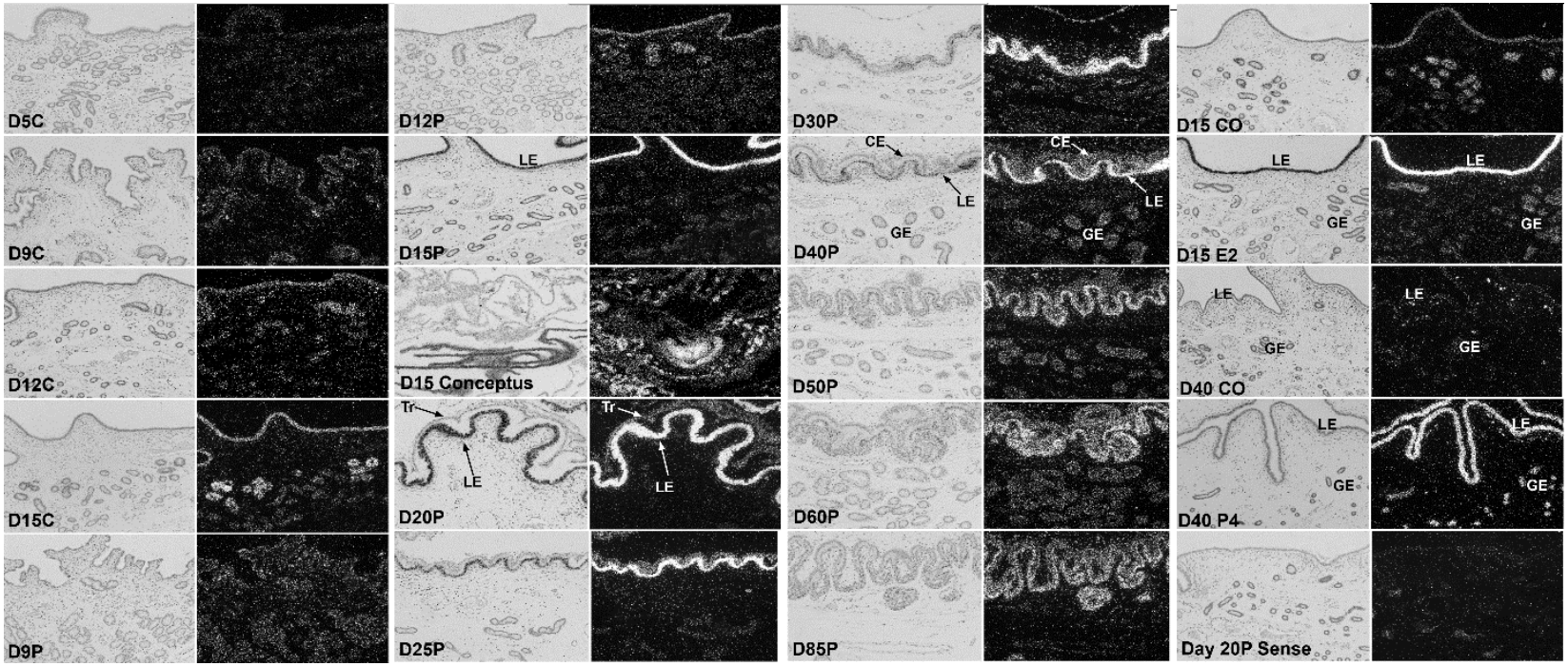

Figure 4.3 Cell-specific expression of *SLC2A1* mRNA in endometria and placentae
Corresponding bright-field and dark-field images from *in situ* hybridization show that *SLC2A1* mRNA localizes predominantly to uterine LE during the estrous cycle and early pregnancy with some expression in the uterine GE and trophectoderm/chorion. Exogenous E2 induced expression of *SLC2A1* mRNA in the LE, while exogenous P4 induced expression in the LE and GE. Width of field is 870 µm. The Day 20P Sense panel is the negative control. Legend: LE, luminal epithelium; GE, glandular epithelium; Tr, trophectoderm; CE, chorion.

Cell-specific expression of *SLC2A1* mRNA was determined by *in situ* hybridization analysis of tissues from the estrous cycle and pregnancy. *SLC2A1* mRNA localized to the uterine LE and GE on all days of the estrous cycle and pregnancy studied. On Day 15, expression of *SLC2A1* mRNA appeared to be greater in uterine LE from pregnant gilts as compared to cyclic gilts (Figure 4.3). *SLC2A1* mRNA was also detected in the conceptuses from Day 15 of pregnancy. From Days 25 to 85 of pregnancy, expression of *SLC2A1* remained localized to the uterine LE with expression appearing to increase in the GE at Day 30, which then decreased by Day 85. Expression of *SLC2A1* mRNA was also detected in the chorion, although at lower levels than in uterine LE (Figure 4.3).

Endometria from gilts treated with exogenous E2 or P4 were analyzed for expression of *SLC2A1* mRNA and its cell-specific localization. Expression of *SLC2A1* mRNA increased in uterine LE in response to E2 (Figure 4.2C; $p<0.05$), which was similar to the expression pattern in uterine tissues from Day 15 of pregnancy (Figure 4.3). Endometrial expression of *SLC2A1* mRNA increased in uterine LE and GE of gilts treated with exogenous P4 as compared to control gilts ($p<0.05$; Figure 4.2D and Figure 4.3).

SLC2A2 mRNA Is Expressed During Late Pregnancy

Expression of *SLC2A2* mRNA in endometria was low during the estrous cycle and early pregnancy compared to other *SLC2A* transporters studied with no significant effect of day or status during the peri-implantation period of pregnancy (Figure 4.4A;

p>0.05). However, expression of *SLC2A2* mRNA increased in endometrium from Days 9 to 85 of pregnancy (r^2=0.774; p<0.001) and in the placenta from Days 30 to 85 of pregnancy (Figure 4.4B; r^2=0.810; p<0.001).

SLC2A2 mRNA was detected in the trophectoderm of Day 15 conceptuses using *in situ* hybridization analysis (Figure 4.4C). By Day 40, *SLC2A2* mRNA was detected in areolae and this expression appeared to increase through Day 60. *SLC2A2* mRNA was barely detectable in non-areolar regions of the chorion from Days 60 to 85 of pregnancy.

There was no effect of E2 or P4 on expression of *SLC2A2* mRNA in the pseudopregnancy or long-term P4 studies performed (data not shown).

SLC2A3 mRNA Localizes Primarily to the Placenta Throughout Pregnancy

Expression of *SLC2A3* mRNA in endometria decreased from Days 9 to 13 (p<0.001) in both pregnant and cycling gilts (Figure 4.5A; p>0.05). When expression of *SLC2A3* mRNA in endometria from pregnant gilts was analyzed, there was no change in expression between Days 9 and 15 (r^2=0.884; p>0.05) or Days 17 and 25 (r^2=0.185; p>0.05) of pregnancy, but expression increased between Days 30 and 85 (r^2=0.964; p<0.01). There was no change in expression of *SLC2A3* mRNA in chorioallantois between Days 30 and 85 of pregnancy (Figure 4.5B; r^2=0.04; p>0.05).

SLC2A3 mRNA was barely detectable in the LE and GE of uteri from cycling and pregnant gilts, although expression was detected in the tips of the uterine villi on Day 60 (Figure 4.6). Expression of *SLC2A3* mRNA by trophectoderm was detected as

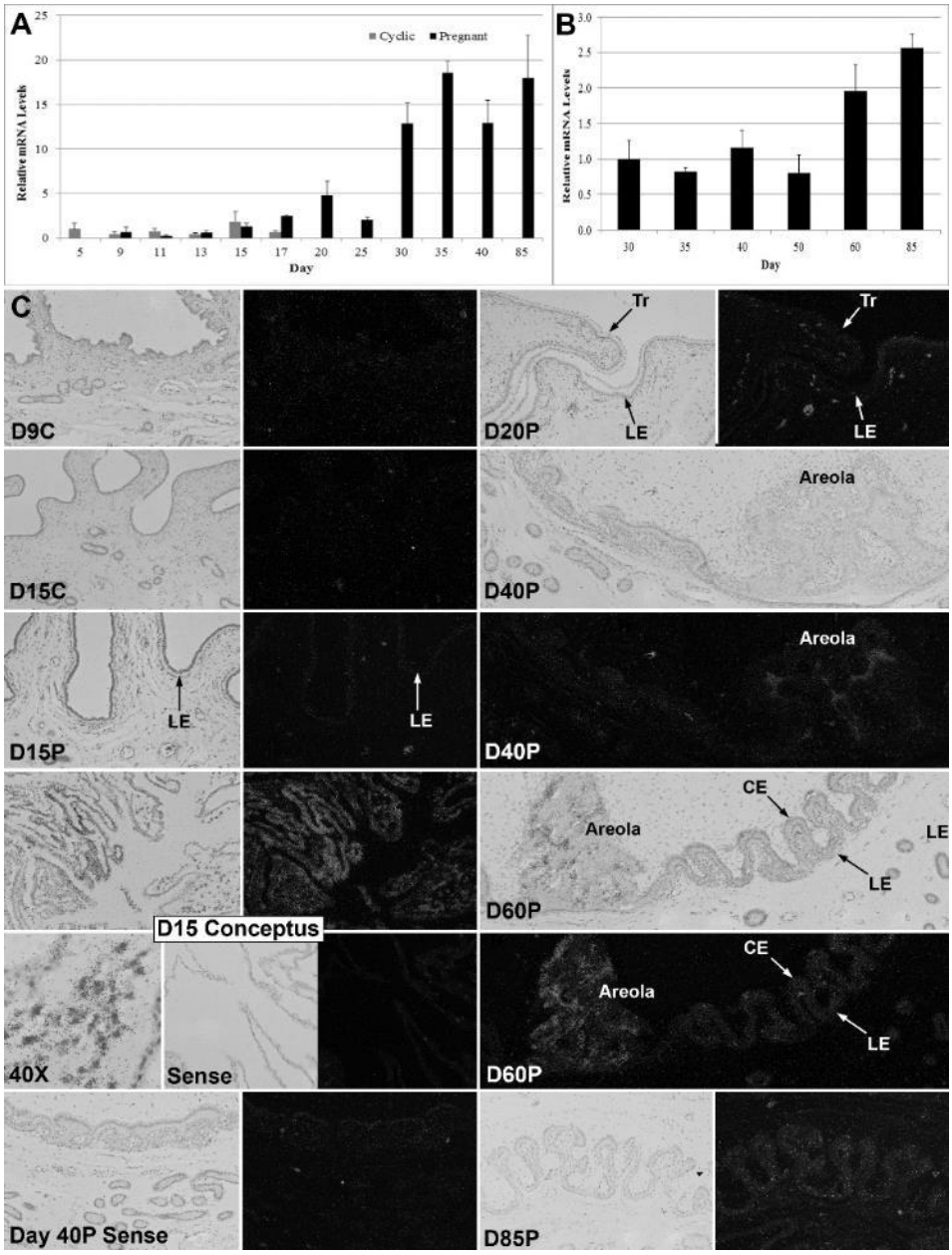

Figure 4.4 Expression of *SLC2A2* mRNA in endometria and placentae
(A) Endometrial expression of *SLC2A2* mRNA increased from Days 9 to 85 of pregnancy (r^2=0.774; p<0.001); **(B)** Placental expression of *SLC2A2* mRNA increased from Days 30 to 85 of pregnancy (r^2=0.810; p<0.001); **(C)** Corresponding bright-field and dark-field images detected *SLC2A2* mRNA in the trophectoderm at Day 15 and in the areolae, uterine LE, and CE on Days 60 to 85 of pregnancy. Values presented are means±SEM and p<0.05 is significant. Width of field is 870 µm except D15 Conceptus 40X and Sense (580 µm) and D40P, D60P (1740 µm). The Day 40P Sense panel is the negative control. Legend: LE, luminal epithelium; Tr, trophectoderm; CE, chorion.

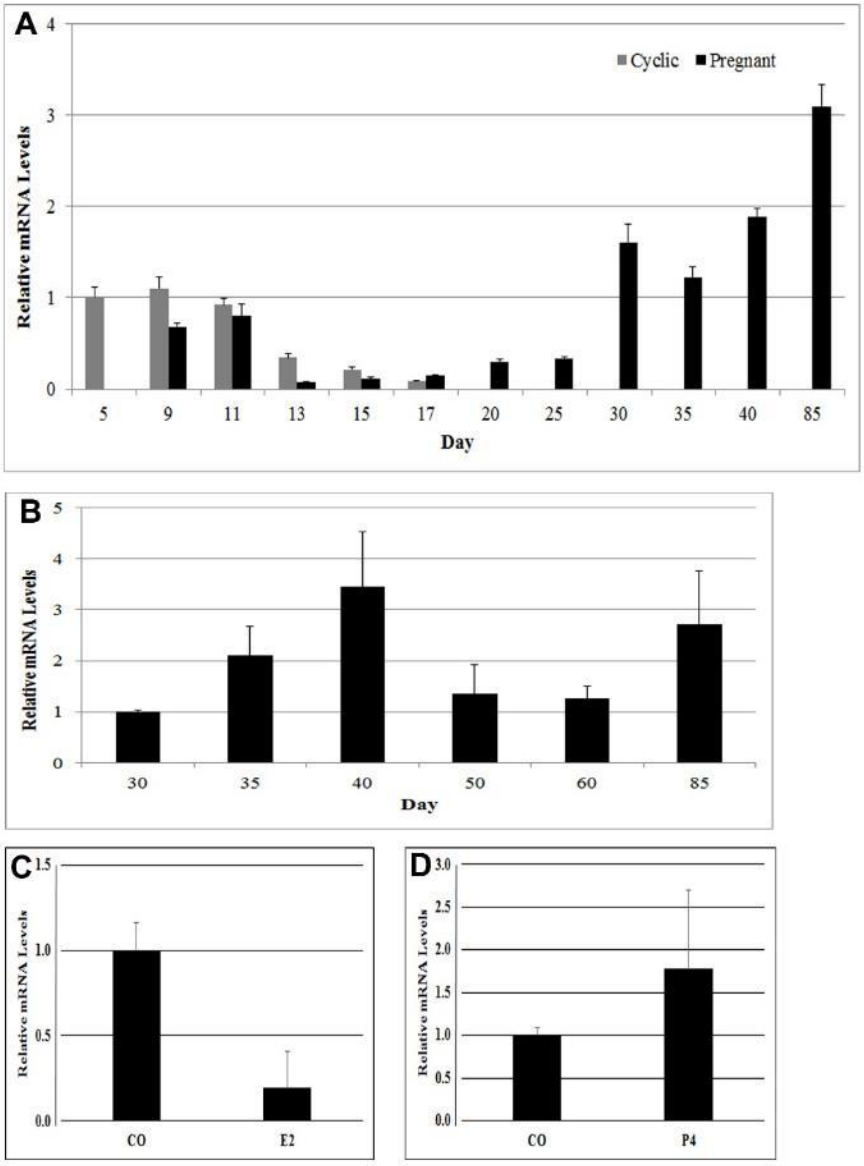

Figure 4.5 Expression of *SLC2A3* mRNA in endometria and placentae
(A) Endometrial expression of *SLC2A3* mRNA was low during the estrous cycle and early pregnancy, and then increased between Days 30 and 85 of pregnancy (r^2=0.964; $p<0.01$). **(B)** Placental expression of *SLC2A3* mRNA was not different between Days 30 and 85 (r^2=0.04; $p>0.05$). **(C)** Endometrial expression of *SLC2A3* mRNA decreased in response to E2 ($p<0.05$) and **(D)** was not affected by P4 ($p>0.05$). Values presented are means±SEM and $p<0.05$ is significant.

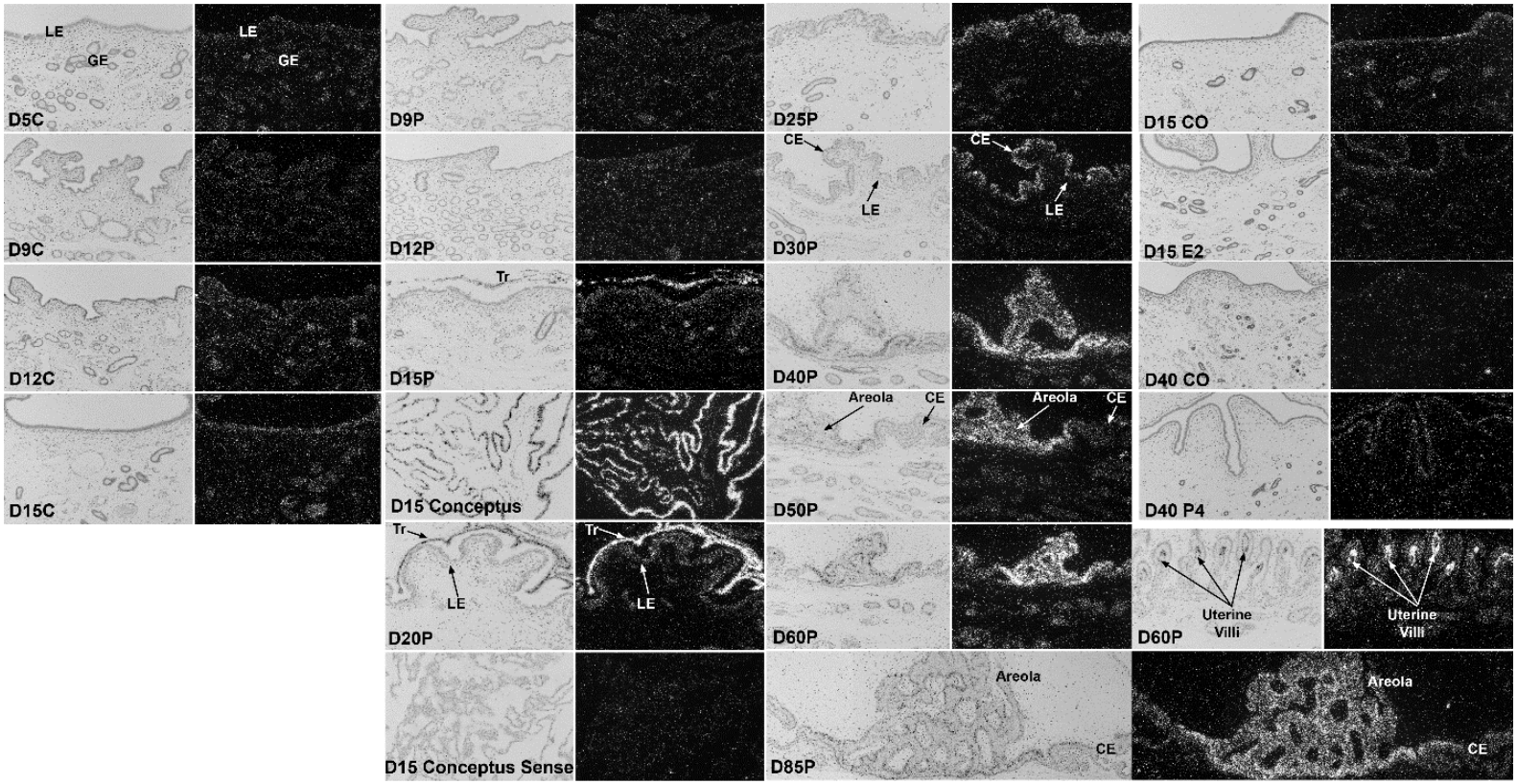

Figure 4.6 Cell-specific localization of *SLC2A3* mRNA in endometria and placentae
Corresponding bright-field and dark-field images revealed low endometrial expression of *SLC2A3* mRNA in the endometrium during the estrous cycle and early pregnancy. However, there was abundant expression of *SLC2A3* in the trophectoderm on Day 15 of pregnancy, which was maintained in the chorion and areolae through Day 85 of pregnancy. Width of field is 870 µm. The D15 Conceptus Sense panel is the negative control. Legend: LE, luminal epithelium; GE, glandular epithelium; Tr, trophectoderm; CE, chorion.

early as Day 15 and expression was maintained in the chorion through Day 85 of pregnancy. Chorion expression of *SLC2A3* mRNA was greater in the areolae than in non-areolar regions of the chorion from Days 40 to 85 of pregnancy.

Endometrial expression of *SLC2A3* mRNA decreased in uterine LE and GE in response to E2 ($p<0.05$; Figure 4.5C and Figure 4.6), but there was no effect of P4 on expression of *SLC2A3* mRNA in uterine LE (Figure 4.5D and Figure 4.6).

SLC2A4 mRNA Is Expressed Lowly in Endometria and Localizes to the Uterine LE

Endometrial expression of *SLC2A4* mRNA was lower than for the other three *SLC2A* genes studied and was not affected by day, status, or the day by status interaction during the peri-implantation period of pregnancy (Figure 4.7A; $p>0.05$). Endometrial expression of *SLC2A4* mRNA was not different between Days 9 and 85 of pregnancy ($r^2=0.005$; $p<0.05$) and placental expression of *SLC2A4* mRNA was not different between Days 30 and 85 of pregnancy (Figure 4.7B; $r^2=0.019$; $p<0.05$).

Endometrial expression of *SLC2A4* mRNA was barely detectable by *in situ* hybridization analysis between Days 9 and 12, but was detectable in uterine LE by Day 15 in cycling and pregnant gilts (Figure 4.8). Expression of *SLC2A4* mRNA by uterine LE was maintained through Day 40 of gestation, and there was an increase in expression in uterine GE on Day 30. Placental expression of *SLC2A4* mRNA was barely detectable by *in situ* hybridization analysis.

Endometrial expression of *SLC2A4* mRNA decreased in endometria of gilts in response to E2 ($p<0.05$; Figure 4.7C). Interestingly, localization of *SLC2A4* mRNA

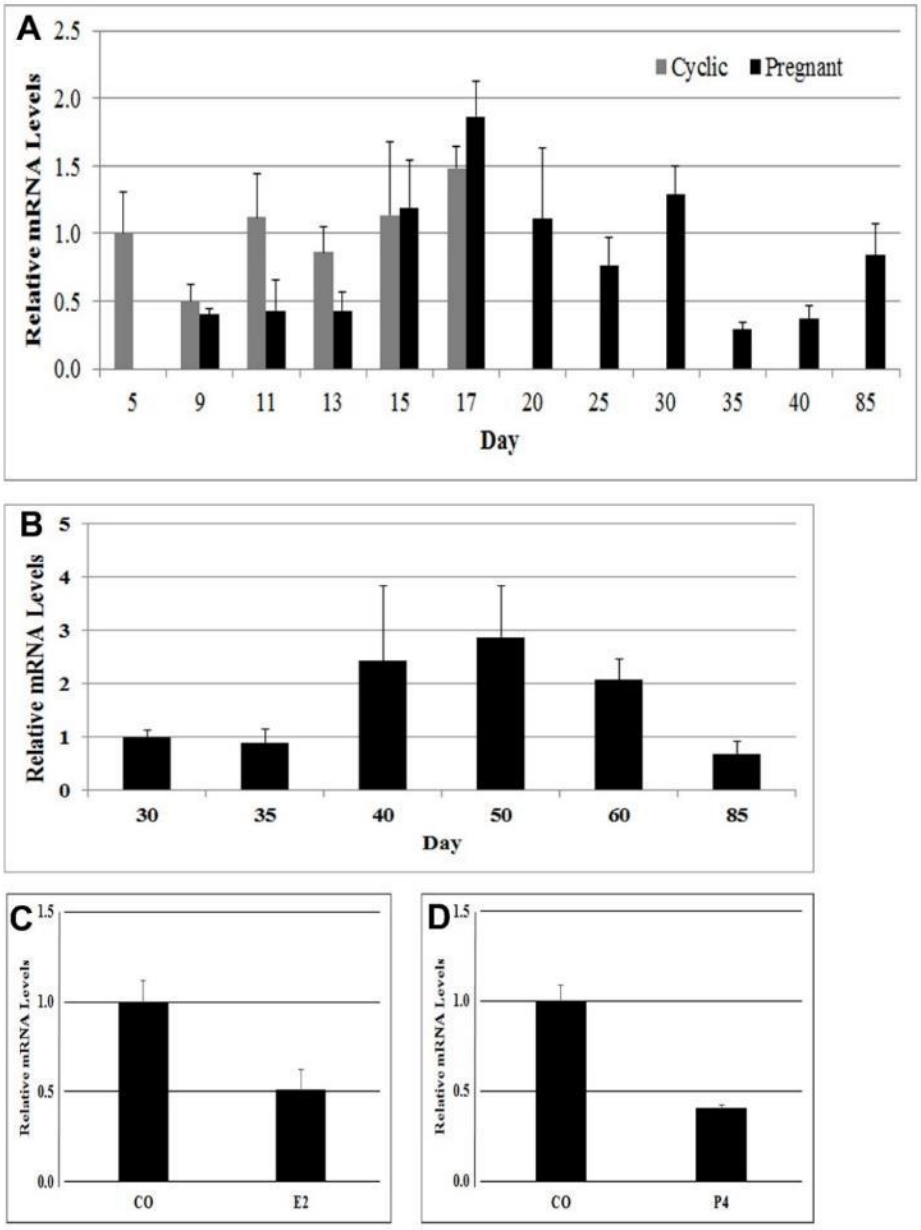

Figure 4.7 Expression of *SLC2A4* mRNA in endometria and placentae

(A) Endometrial and **(B)** placental expression of *SLC2A4* mRNA was not affected by day of the estrous cycle or pregnancy ($p>0.05$). **(C,D)** Endometrial expression of *SLC2A4* mRNA increased in response to E2 and P4 ($p<0.05$). Values presented are means±SEM and $p<0.05$ is significant.

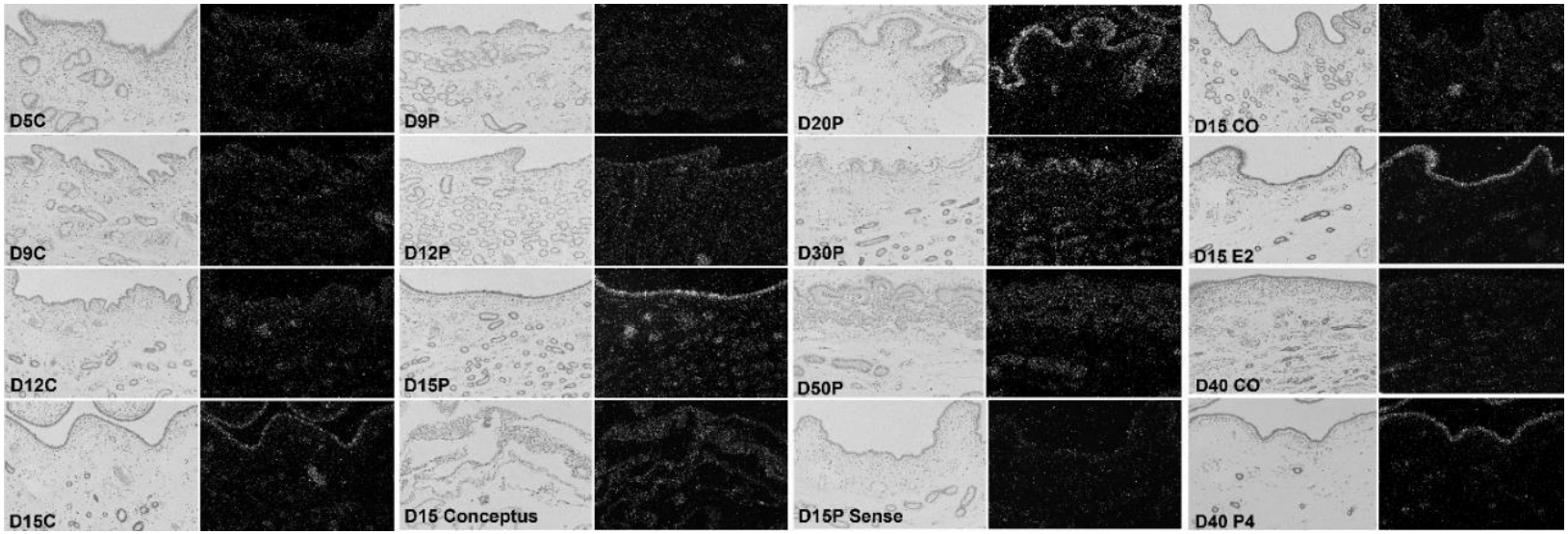

Figure 4.8 Cell-specific localization of *SLC2A4* mRNA in endometria and placentae

Corresponding bright-field and dark-field images detected *SLC2A4* mRNA in uterine LE on Day 15 of the estrous cycle and pregnancy and in uterine LE through Day 50 of pregnancy. *SLC2A4* mRNA localized to the uterine LE in response to both E2 and P4. Width of field is 870 µm. The D15P Sense panel is the negative control.

suggested a decrease in abundance in uterine GE and an increase in expression in uterine LE (Figure 4.8). Since the uterine GE represents a greater percentage of cells in total endometrial tissue, the decrease seen in total endometrial tissue mRNA is not surprising. P4 also induced expression of *SLC2A4* mRNA in uterine LE, although again, the abundance of *SLC2A4* mRNA was greater in endometria from control gilts ($p<0.05$; Figure 4.7).

SLC2A mRNAs Localize to Endometrial and Placental Endothelia During Pregnancy

In addition to being expressed in epithelia at the uterine-placental interface, *SLC2A* transporter mRNAs were expressed in endothelia of blood vessels in both endometrial and placental tissues. The presence of *SLC2A* transporters in these endothelial cell layers is important for movement of glucose out of and into the endometrial and placental vasculatures. *SLC2A1* mRNA was expressed in both endometrial and placental endothelia (Figure 4.9). *SLC2A3* and *SLC2A4* mRNAs were also present in endometrial and placental endothelia, although expression was lower than for *SLC2A1*. *SLC2A4* mRNA appears to have higher expression in the placental endothelium than in the endometrial endothelium.

SLC2A mRNAs Localize to Areolae and the Allantoic Epithelium During Pregnancy

SLC2A1, *SLC2A3*, and *SLC2A4* mRNAs were expressed in areolae, but *SLC2A3* appeared to have the greatest expression in areolae (Figure 4.10). The allantoic epithelium also expressed *SLC2A1*, *SLC2A2*, *SLC2A3*, and *SLC2A4* mRNAs.

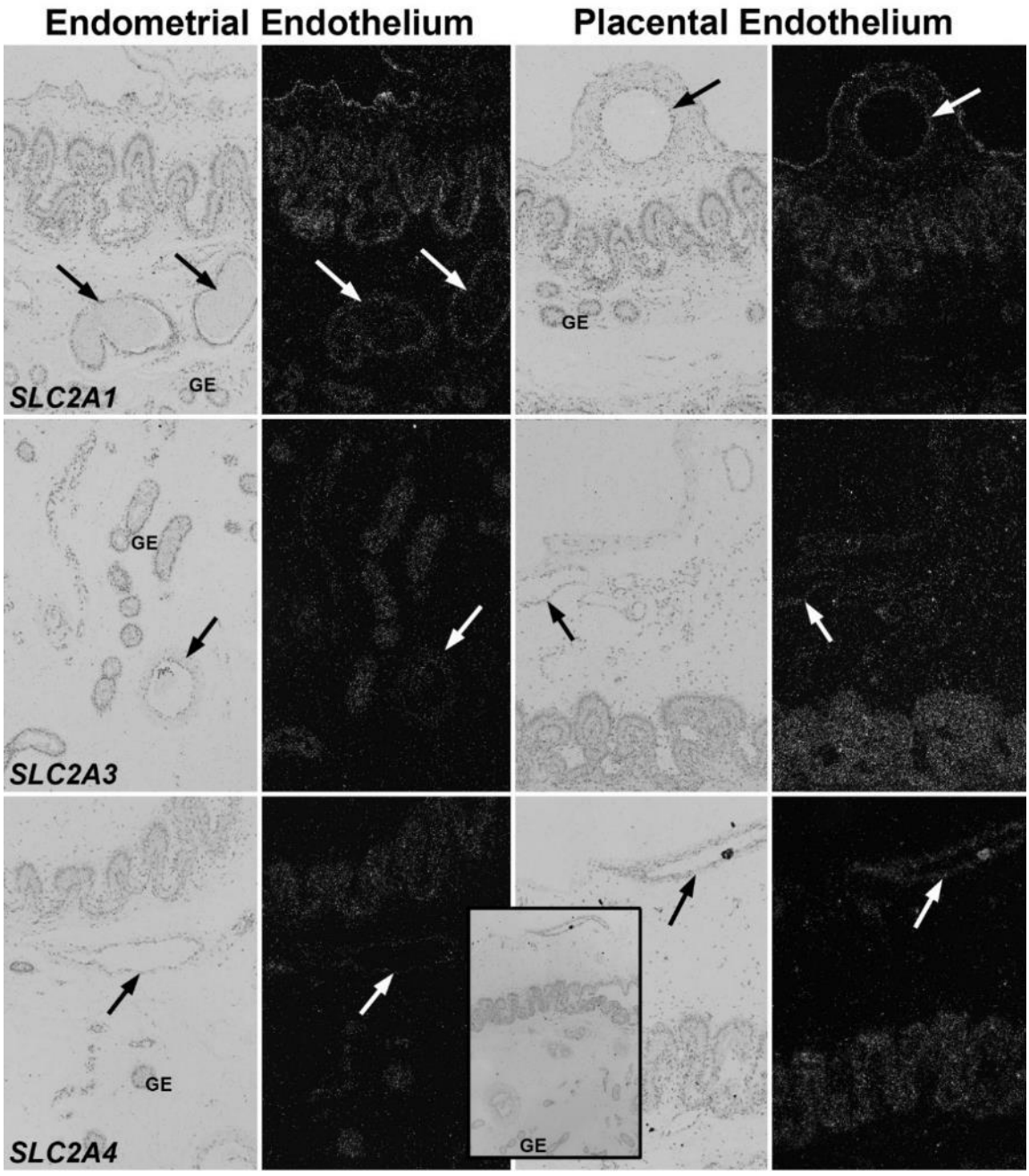

Figure 4.9 *SLC2A* transporter mRNAs localize to the endometrial and placental endothelia during pregnancy

Corresponding bright-field and dark-field images from *in situ* hybridization analysis show *SLC2A1*, *SLC2A3*, and *SLC2A4* mRNAs in endothelia of endometrial and chorioallantoic blood vessels, which would allow movement of glucose out of and into the respective endometrial and placental vasculatures. Arrows indicate mRNA expression by blood vessels. Height of field is 870 μm. Legend: LE, luminal epithelium; GE, glandular epithelium.

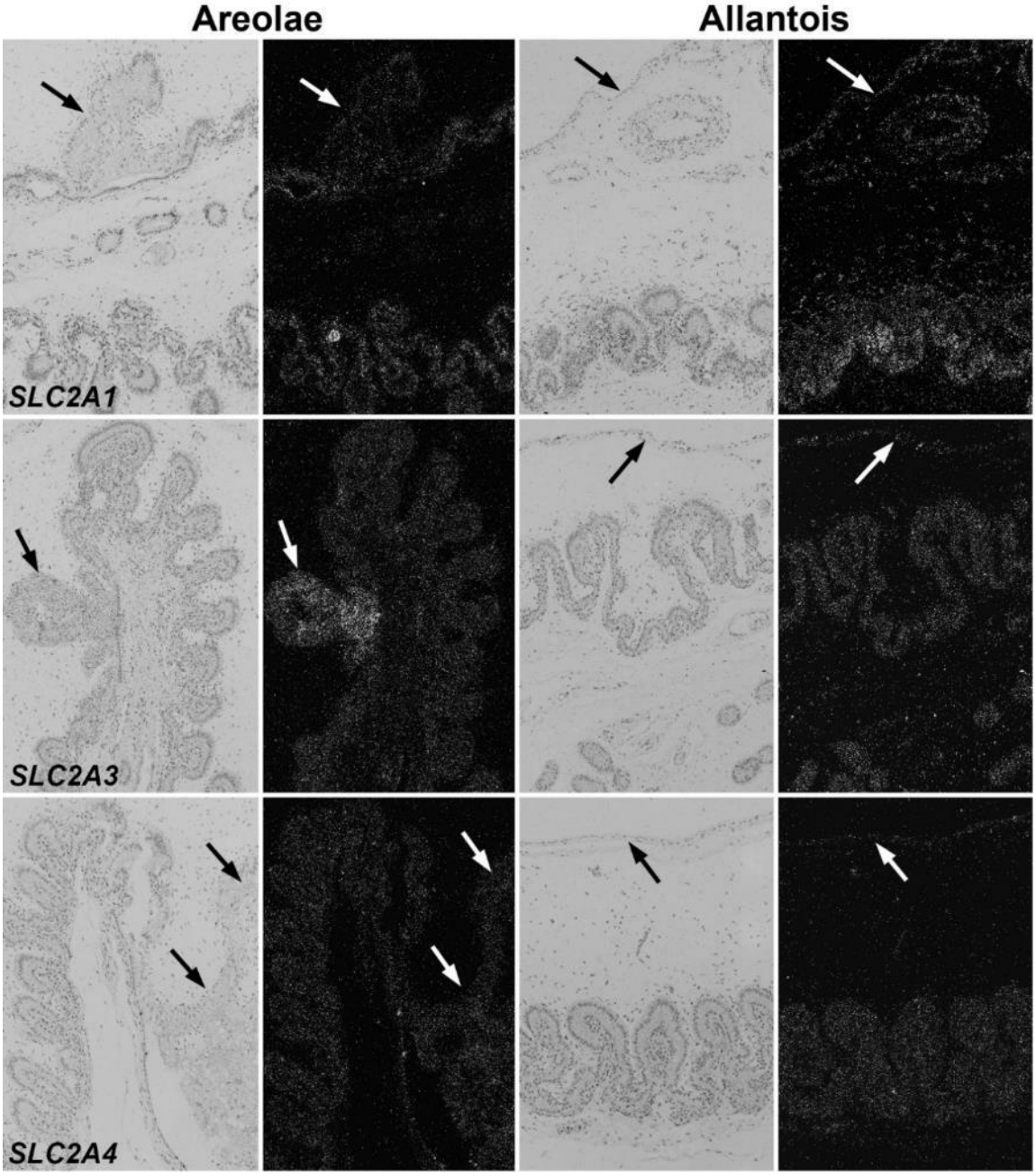

Figure 4.10 *SLC2A* transporter mRNAs localize to areolae and the allantoic epithelium during pregnancy

Corresponding bright-field and dark-field images from *in situ* hybridization analyis show *SLC2A1*, *SLC2A3*, and *SLC2A4* mRNAs in the chorionic epithelium of areolae and in the allantoic epithelium. Expression of *SLC2A3* mRNA was greater in areolar epithelia than in non-areolar chorion. Arrows indicate areolae and allantoic epithelium. Height of field is 870 µm.

Discussion

Glucose is an essential nutrient for conceptus growth and development, but little is known about how glucose is transported in the pig endometrium and placenta. This study is the first to determine that: 1) *SLC2A1*, *SLC2A2*, *SLC2A3*, and *SLC2A4* mRNAs are all expressed at the pig uterine-placental interface; 2) their individual temporal and spatial patterns of expression suggest that each has a unique role in glucose transport from the mother to the conceptus; and, 3) P4, the hormone of pregnancy secreted by the ovary, and E2, the maternal recognition of pregnancy signal secreted by the conceptus, likely act to increase *SLC2A1* mRNA expression in the uterine epithelia. Figure 4.11 is a model depicting the multiple cell layers found at the pig uterine-placental interface and where transporters must be located, both by cell type and cell surface, to effectively transport glucose from mother to conceptus. The present results indicate that the endometrial endothelium expresses *SLC2A1* and *SLC2A3*, which can transport glucose out of the maternal vasculature in pigs. The uterine LE expresses *SLC2A1* and *SLC2A4*, although *SLC2A1* expression is greatest. This is not surprising as *SLC2A4* is insulin dependent. The conceptus removes glucose from the maternal blood continually, not just after meals, so having *SLC2A1* as the prominent isoform would result in a more continuous movement of glucose into the conceptus. Early in pregnancy, the trophectoderm expresses *SLC2A1*, *SLC2A2*, and *SLC2A3*, but as pregnancy progresses, *SLC2A3* becomes the most dominant isoform in the chorion. The allantoic epithelium expresses *SLC2A1*, *SLC2A3*, and *SLC2A4* mRNAs, which would allow for movement of glucose either into or out of the glucose-rich allantoic fluid (Bazer et al., 1988). Finally,

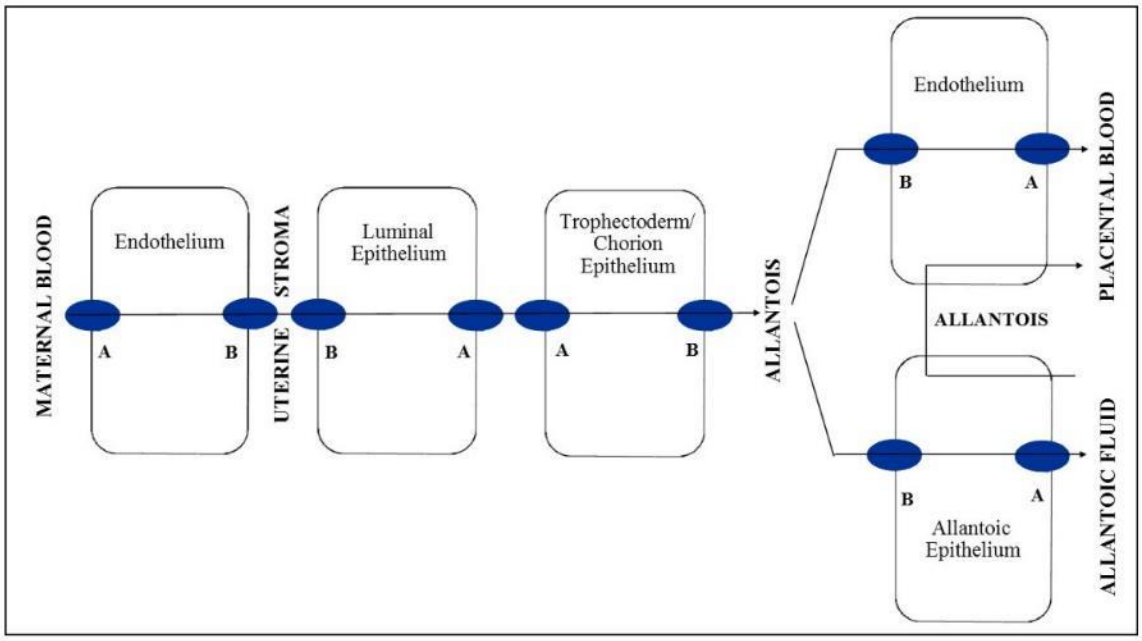

Figure 4.11 A model for glucose transport from maternal to placental blood in pigs
In an epitheliochorial placenta, glucose is transported from the maternal vasculature to the placental vasculature through multiple cell layers that comprise the uterine-placental interface. Movement of glucose requires GLUT transporters (ovals) on the apical (A) and basolateral (B) cell surfaces of each cell. Starting from the maternal blood, glucose is transported through an endothelium and into the uterine LE. The endothelial cells of the vasculature and the LE are in close proximity to facilitate this transport of glucose. Glucose is then transported out of the uterine LE and into the trophectoderm/chorion. Close proximity of the placental vasculature then facilitates movement of glucose from the trophectoderm/chorion, through the placental endothelium, and into the placental vasculature for use by the placenta and fetus. Glucose can also be transported into and out of the allantoic fluid through the allantoic epithelium. The arrows depict the direction of glucose movement.

the placental endothelium also expresses *SLC2A1*, *SLC2A3*, and *SLC2A4* mRNAs for transport of glucose into the placental circulation.

SLC2A1 and *SLC2A3* are the prominent glucose transporters in the pig uterus and placenta, similar to what is observed in mice and humans (Jansson et al., 1995; Frolova and Moley, 2011a). Interestingly, *SLC2A1* is the most abundant glucose transporter in the endometrium of most mammals studied, but the cell-specific localization of the transporter differs (Korgun et al., 2001; von Wolff et al., 2003; Gao et al., 2009a; Frolova and Moley, 2011b). In mice and humans, *SLC2A1* is more abundant in the uterine stroma than epithelia, especially as decidualization progresses, while in the pig, *SLC2A1* localizes to the uterine LE and GE. These differences in localization can be explained by major differences in type of implantation among species. The invading mouse and human blastocysts are supported by the decidualizing stromal cells immediately surrounding them, while the free-floating pig and sheep conceptuses must rely on molecules secreted or transported by uterine LE and GE into the uterine lumen during the peri-implantation period of pregnancy.

The trophoblast cells of most mammalian species studied predominantly express the glucose transporter *SLC2A3*, although in mice and humans this expression is high in the first trimester, but decreases with advancing stage of gestation, while in the pig, *SLC2A3* appears to be the prominent placental transporter in the trophectoderm/chorion through the beginning of the third trimester (Hahn et al., 2001; Ganguly et al., 2007; Brown et al., 2011). Similar to the endometrium, differences in expression of *SLC2A3* over time, and among species, can be attributed to utilization of different types of

implantation and placentation. *SLC2A3* is a high-affinity transporter that will transport glucose efficiently even at low concentrations of glucose. During the first trimester in the mouse and human, the conceptus is in the process of establishing a connection with the maternal vasculature, but until this is firmly established, glucose has to be efficiently accrued from the surrounding decidualized stroma. In contrast, the pig conceptus never develops an intimate contact with the maternal vasculature since it develops an epitheliochorial placenta and, therefore, must continue to maximize the efficiency of glucose transport throughout pregnancy.

Pig conceptuses remain free-floating within the uterine lumen for a protracted period of time prior to implantation as compared to humans or rodents. Pig embryos enter the uterus, develop into blastocysts, shed the zona pellucida, and then the presumptive placental membranes (trophectoderm and endoderm) elongate at a rate of 30 to 40 mm/h from a 10 mm diameter sphere to a filamentous form that is 800-1,000 mm in length by Day 16 of pregnancy. During this time, the free-floating conceptus is dependent upon the composition of uterine luminal fluid, including glucose, to support this extensive morphological remodeling of trophectoderm and endoderm during elongation. Glucose in the luminal fluid originates in the endometrium and has to be transported in through the uterine LE from the maternal vasculature in order to support this nutrient intensive process and allow the conceptus to survive and develop past this stage. The present data indicate that *SLC2A1* is upregulated during this crucial period in the uterine LE and may be responsible for glucose transport into the uterine luminal fluid. Results of the present study also indicate that glucose in the uterine luminal fluid is

potentially transported into the conceptus through *SLC2A2* and *SLC2A3* transporters expressed by the trophectoderm.

The maternal recognition of pregnancy signal in pigs is E2, which is secreted by the conceptus trophectoderm. In the pig, the corpora lutea can be maintained without any conceptuses present in the uterine horns when injections of exogenous E2 are administered daily between Days 11 to 14 of the estrous cycle, which mimics the maternal recognition of pregnancy signal. The present data clearly show that E2 upregulates expression of *SLC2A1* mRNA in uterine LE of pseudopregnant gilts, suggesting that estrogens secreted by the conceptus itself direct increased expression of this key glucose transporter in the endometrium. Previous studies have indicated that conceptus E2 upregulates gene expression of SPP1, STAT1, CD24, and FGF7 in the endometrium of pigs (White et al., 2005; Joyce et al., 2007; Ka et al., 2007; Ross et al., 2007). These genes are specifically upregulated in the uterine LE between Days 12 and 15 of pregnancy, which is also shown for *SLC2A1* mRNA in this study. The psuedopregnant state provides an opportunity to determine the effects of E2 on the endometrium independent of other conceptus-secreted factors, but in an environment that is still under the influence of ovarian P4. Therefore, *SLC2A1* mRNA can be upregulated by E2, independent of other conceptus-secreted factors, but may still rely on the presence of P4.

When exogenous P4 was administered to ovariectomized gilts, there was upregulation of *SLC2A1* mRNA in the uterine LE and GE. Therefore, it is reasonable to hypothesize that P4 induces *SLC2A1* mRNA expression in uterine LE, while E2

amplifies this expression. A similar physiology has been demonstrated for the sheep where *SLC2A1* mRNA is upregulated by P4, but enhanced by interferon tau (IFNT), the pregnancy recognition signal in sheep (Gao et al., 2009a). Both pigs and sheep enhance P4 induced *SLC2A1* mRNA, and potentially glucose transport, with a conceptus-secreted signal. Regardless of whether a steroid hormone or a cytokine enhances expression of *SLC2A1* mRNA, the observation that both species have this mechanism indicates that *SLC2A1* is a particularly important glucose transporter for conceptus growth and development in species with a protracted period of development of the conceptus before implantation.

Expression of *SLC2A1* mRNA by GE was not upregulated by E2, but only by P4. This indicates a differential regulation of *SLC2A1* expression by these two epithelia. The P4 nuclear receptor (PGR) is downregulated in the uterine LE by Day 10 and only partially downregulated in the GE by Day 12, although the endometrial stromal cells continue to express PGR (Geisert et al., 1994). Therefore, increased *SLC2A1* mRNA expression in the uterine LE is potentially due to a downregulation of PGR, which allows E2 to have an effect through the estrogen receptor (ESR1). Alternatively, increased expression of *SLC2A1* mRNA in uterine GE is potentially due to paracrine-acting growth factors (progestamedins) being produced by the PGR-positive stromal cells in response to P4 (Johnson et al., 2000). This regulation of a glucose transporter in the uterine LE and GE illustrates the complex interactions that take place between the uterus, conceptus, and ovary to orchestrate successful conceptus development through the peri-implantation period of pregnancy in pigs. Further studies will be necessary to

determine if other SLC2A glucose transporters, and other nutrient transporters in general, can also be regulated by the steroid hormones, E2 and P4.

The pig develops a diffuse, epitheliochorial type placenta to support the growth of each individual fetus. This placentation is characterized as superficial, non-invasive, and having a uterine LE that remains intact throughout pregnancy. By Day 24 of pregnancy, there is complete attachment between the uterine LE and the conceptus trophectoderm and these adhered epithelia begin to fold around Day 30 to increase surface area for nutrient transport (Friess et al., 1980). The trophectoderm expresses *SLC2A3* mRNA from Day 15 when attachment is just beginning, and continues to be expressed in the chorion through Day 85 of pregnancy. *SLC2A3* is also expressed in the tips of the uterine villi in the uterine LE at Day 60 of pregnancy (Figure 4.6), which is a site where the maternal and placental vasculatures are within 2 microns of each other, the closest they ever come together during pregnancy (Friess et al., 1980). Additionally, the maternal and fetal capillaries are arranged in a cross-countercurrent manner on opposite sides of the adhered, folded epithelia. If the fetal side of the placenta is "up", then maternal blood enters at the top of the folds and exits at the bottom. In contrast, the placental blood enters at the bottom of the folds and exits at the top (Leiser and Dantzer, 1988). This arrangement allows for optimum transport of nutrients, especially those dependent on concentration gradients, such as glucose, from mother to fetus. By localizing to the LE at the top of the uterine folds, *SLC2A3*, as a high-capacity and high-affinity transporter, is in an optimal position for transporting the maximal amount of glucose across the uterine-placental interface at a period of pregnancy when placental

growth is slowing, but fetal growth is beginning to increase exponentially (Ullrey et al., 1965; Knight et al., 1977).

SLC2A1 mRNA also localized to the trophectoderm and chorion on all days of pregnancy studied, although with less abundance than in the endometrium. Our laboratory has not developed a model to explore the regulation of genes in the placenta, although the same molecules that regulate gene expression in the endometrium, E2 and P4, may also drive gene expression in the placenta. Tung et al. demonstrated that SLC2A1 protein was expressed in the chorion and placental endothelia of gilts at Day 50 of pregnancy and that expression was upregulated by exogenous growth hormone (Tung et al., 2012). These findings suggest that there are a number of different regulators of expression of the glucose transporters at the uterine-placental interface and indicate an area where further study in necessary.

In the pig, areolar structures form over the mouths of endometrial glands to transport large amounts of nutrients from the glandular epithelia into the specialized microvasculature on the placental side of areolar chorion cells (Renegar et al., 1982; Leiser and Dantzer, 1994). *SLC2A2* and *SLC2A3* are highly expressed in the areolae and this is an optimal location for these high capacity transporters to move glucose from the uterine GE to the placental vasculature.

Once glucose is transported across the chorion by *SLC2A3*, it is necessary that transporters be strategically placed to move glucose both into the placental vasculature and into the allantoic cavity, which is filled with a hypotonic solution composed of electrolytes, sugars, proteins, and water that are of maternal and fetal origin, which

provide a nutrient reservoir for the fetus (Aherne et al., 1969; Wu et al., 1995). Glucose is found in substantial amounts in this fluid and, therefore, must be transported through the allantoic epithelium (Bazer et al., 1988). The present data indicate that *SLC2A1, SLC2A3,* and *SLC2A4* mRNAs localize to the placental endothelium, although *SLC2A1* appears to be the most abundant transporter in this cell type. Further, *SLC2A1, SLC2A3,* and *SLC2A4* mRNAs have the potential to transport glucose through the allantoic epithelium (see Figure 4.11).

In summary, results of this study indicate differential temporal and spatial expression, localization, and hormonal regulation of the facilitative diffusion glucose transporters SLC2A1, SLC2A2, SLC2A3, and SLC2A4 at the uterine-placental interface of pigs during pregnancy (see Figure 4.11). The localization of these transporters indicates that glucose can be transported from the maternal endometrial blood by SLC2A1, and then through the chorioallantois to the placental blood by SLC2A3, which is clearly demonstrated by comparing the *in situ* hybrization panels at Day 20 of pregnancy in Figure 4.3 and Figure 4.6. The SLC2A transporters necessary to transport glucose, a nutrient necessary for survival and development of the conceptus, are upregulated by E2 from the conceptus trophectoderm, and P4 from the maternal ovary, indicating that glucose transport is dependent on steroid hormones during pregnancy in pigs.

CHAPTER V

FRUCTOSE SYNTHESIS AND TRANSPORT AT THE UTERINE-PLACENTAL INTERFACE OF PIGS: CELL-SPECIFIC LOCALIZATION OF SLC2A5, SLC2A8, AND COMPONENTS OF THE POLYOL PATHWAY

Introduction

Glucose and fructose are abundant hexose sugars in porcine endometria and conceptuses (embryo/fetus and associated placenta), but little is known about the synthesis, transport, and metabolism of fructose at the uterine-placental interface. The presence of fructose in conceptuses is unique to species with epitheliochorial or synepitheliochorial placentae, indicating that fructose may be important for growth and development of fetuses supported by these types of placentation (Goodwin, 1956). Fructose plays a minor role as an energy source in the placenta and fetus, because fructose is oxidized to CO_2 at only ~20% the rate of glucose (Meznarich et al., 1987). However, studies indicate that fructose can be used as a substrate in a number of metabolic pathways that could support conceptus development, including biosynthesis of glycosaminoglycans, phospholipids, and nucleic acids (White et al., 1982). Recently, *in vitro* studies demonstrated that porcine trophectoderm cells can metabolize fructose through the hexosamine biosynthetic pathway to stimulate the mechanistic target of rapamycin (mTOR) cell signaling and cell proliferation, and for the synthesis of hyaluronic acid, a significant glycosaminoglycan in the placenta (Kim et al., 2012).

Fructose is detected in uterine flushings of pregnant gilts as early as Day 12 and is present in greater quantities than glucose in allantoic fluid and fetal blood (Aherne et al., 1969; Zavy et al., 1982; Bazer et al., 1988). Additionally, fructose is undetectable in blood of pregnant gilts and sows (Pere, 1995). Studies by White et al. demonstrated that fructose injected intraperitoneally into an *in utero* fetus cannot cross the placenta or be converted into glucose, but glucose injected in the same manner can cross the placenta and be converted to fructose (White et al., 1979). Those results suggest the placenta is the site of fructose production, and it is hypothesized that fructose synthesis from glucose is a method for the conceptus to sequester a hexose sugar from the mother (Zavy et al., 1982).

Glucose can be transported from maternal blood into pig endometrial luminal epithelium (LE), conceptus trophectoderm/chorion, and placental blood by solute carrier transporters SLC2A1, SLC2A3, and SLC2A4 (see Chapter IV). It is reasonable to hypothesize that fructose can then be synthesized from this glucose via the polyol pathway, through which glucose and NADPH are first converted to sorbitol and $NADP^+$ by aldose reductase (AKR1B1), then sorbitol and NAD^+ are converted to fructose and NADH, respectively, by sorbitol dehydrogenase (SORD). The intermediate, sorbitol, is found in high concentrations in ovine, bovine, and human placentae, especially during early pregnancy (Teng et al., 2002; Brusati et al., 2005; Jauniaux et al., 2005) and the enzyme that converts sorbitol to fructose, SORD, has been localized to the trophectoderm of bovine conceptuses (Rama et al., 1973), but there is nothing known about the polyol pathway or its components in pigs.

After synthesis, fructose can be transported across cell membranes by members of the facilitative diffusion solute carrier 2A family of glucose transporters (SLC2A). Two members, SLC2A5 and SLC2A8, have an affinity for fructose. SLC2A8 is necessary for decidualization of the uterus in mice during implantation of blastocysts, most likely due to its ability to transport glucose into the differentiating stromal cells, but SLC2A5 has not been detected in human or rodent endometria or placentae (Kim and Moley, 2009; Frolova and Moley, 2011a; Adastra et al., 2012). Since humans and rodents, unlike pigs, do not have fructogenic placentae, differences would be expected in expression of these particular transporters.

Once fructose enters into a cell, the first metabolic step is the addition of a phosphate group, which is catalyzed by ketohexokinase (KHK) to produce the metabolite fructose-1-phosphate (F-1-P). F-1-P can either be catalyzed into glyceraldehyde-3-phosphate and dihydroxyacetone phosphate for entry into the glycolytic pathway or it can act as a signaling molecule to induce NFkB activation and subsequent production of cytokines (Feinman and Fine, 2013; Lanaspa et al., 2014).

Our hypothesis is that specific cell types in the endometrium and chorioallantois utilize the polyol pathway to convert glucose to fructose to support growth and development of the conceptus. This aims of this study were to determine the cellular localization of enzymes required for synthesis of fructose, the transport system for fructose, and the cells of the placenta and endometrium of pigs that use fructose.

Material and Methods

Tissue Collection

Sexually mature, 8-month-old crossbred gilts were observed daily for estrus (Day 0) and exhibited at least two estrous cycles of normal duration (18 to 21 days) before being used in these studies. All experimental and surgical procedures were in compliance with the Guide for Care and Use of Agricultural Animals in Teaching and Research and approved by the Institutional Animal Care and Use Committee of Texas A&M University.

To evaluate the effects of pregnancy on expression of mRNAs and cell-specific localization of the proteins AKR1B1, SORD, KHK, SLC2A5, and SLC2A8, gilts were assigned randomly to either cyclic or pregnant status. Cyclic gilts were ovariohysterectomized on either Day 5, 9, 11, 13, 15 or 17 of the estrous cycle. Gilts in the pregnant group were bred and ovariohysterectomized on either Day 9, 11, 13, 15, 17, 20, 30, 40, 50, 60, or 85 of pregnancy (n = 3 or 4 gilts/day/status). The lumen of each uterine horn in each gilt was flushed with 20 ml physiological saline for those collected on Days 5 to 17 post-estrus. Pregnancy was confirmed in mated gilts by the presence of morphologically normal conceptuses in uterine flushings. The uterine flushings were frozen for storage at -80°C until analysis. Tissue sections (~1 cm thick) from the middle of each uterine horn of all hysterectomized gilts were fixed in fresh 4% paraformaldehyde in PBS (pH 7.2) and embedded in Paraplast-Plus (Oxford Laboratory, St. Louis, MO). Additionally, endometrium was physically dissected from the

myometrium, snap-frozen in liquid nitrogen, and stored at -80°C for RNA extraction. Chorioallantoic tissue was physically dissected from endometrium and frozen in a similar manner.

Progesterone and Estrogen Models

To evaluate effects of estrogen (E2) and E2-induced pseudopregnancy on endometrial expression of AKR1B1, SORD, KHK, SLC2A5, and SLC2A8 mRNAs and cell-specific localization of their proteins, gilts were detected in estrus (Day 0) and assigned randomly to receive daily intramuscular injections of estradiol benzoate (E2; 5 mg in corn oil; n = 4) or corn oil alone (CO; n = 4) on Days 11, 12, 13, and 14 of the estrous cycle (Joyce et al., 2007). All gilts were ovariohysterectomized on Day 15 of pseudopregnancy. Tissues were collected as described previously.

To evaluate effects of long-term progesterone (P4) treatment without ovarian hormones on endometrial expression of AKR1B1, SORD, KHK, SLC2A5, and SLC2A8 mRNAs and cell-specific localization of their respective proteins, gilts were ovariectomized on Day 12 of the estrous cycle and assigned randomly to receive daily intramuscular injections of either CO (4 ml) or P4 (200 mg P4 in 4 ml CO) on Days 12 through 39 post-estrus (n = 3/treatment) (Bailey et al., 2010c). All gilts were hysterectomized on Day 40 post-estrus and tissues collected as previously noted.

To evaluate effects of E2, P4, and their interaction independent of ovarian hormones on endometrial expression of AKR1B1, SORD, KHK, SLC2A5, and SLC2A8 mRNAs and cell-specific localization of their respective proteins, gilts were

ovariectomized on Day 4 of the estrous cycle and assigned randomly to be treated daily from Day 4 through Day 12 as follows: 1) 200 mg P4 in CO (P4); 2) 5 mg E2 in CO (E2); 3) 200 mg P4 + 5 mg E2 in CO (P4+E2); or 4) CO alone (CO) (Ka et al., 2007). All gilts were hysterectomized on Day 12 and tissues collected as previously described.

Total Recoverable Fructose

Uterine flushings from Day 11 and Day 15 of the estrous cycle and pregnancy were analyzed for total recoverable fructose. The High Sensitivity Fructose Assay Kit (Sigma-Aldrich, St. Louis, MO) was used to determine concentrations of fructose in uterine flushings according to the manufacturer's instructions. Briefly, samples were deproteinated using a 10kDa MWCO spin filter (VWR) at 15,000 x g for 5 min. Sample Clean-up Mix was added to each sample to remove glucose. To account for high background levels, a sample blank without the Conversion Enzyme was run for each sample and subtracted from the sample readings during calculations. Total recoverable fructose was calculated by multiplying the concentration of fructose (determined with the kit) by total recoverable volume of uterine flushings (recorded at the time of sample collection).

RNA Extraction and cDNA Synthesis

Total RNA was extracted from endometrial and chorioallantoic tissue samples using Trizol reagent (Life Technologies, Carlsbad, CA) according to manufacturer's recommendations. First strand cDNA was synthesized using Superscript III First Strand

Kit (Life Technologies, Carlsbad, CA) according to the manufacturer's instructions. First strand cDNA was diluted 10x before use in the qPCR reaction.

Primers for qPCR and *in situ* hybridization were designed using NCBI Genbank sequences and Primer-BLAST (http://www.ncbi.nlm.nih.gov/). Primers were submitted to BLAST to test for specificity against the known porcine genome. Primer information can be found in Table 1.

Quantitative PCR

The qPCR assays were performed as described previously (Chapters III and IV of this dissertation). Briefly, PerfeCta SYBR Green Mastermix (Quanta) was used in 10 µl reactions with 2.5 mM of each specific primer, on a Roche 480 Lightcycler (Roche) with approximately 60 ng of cDNA per reaction. The PCR program began with 5 min at 95°C followed by 40 cycles of 95°C denaturation for 10 sec and 60°C annealing/extension for 30 sec. A melt curve was produced with every run to verify a single gene-specific peak. Standard curves with 2-fold serial dilutions were run to determine primer efficiencies. All primer correlation coefficients were greater than 0.95 and efficiencies were 95-102%. The geometric mean of *TBP*, *SDHA,* and *ACTB* was used to normalize data from endometrial tissue, while the geometric mean of *TBP*, *HPRT1,* and *TUBA1B* used to normalize data from chorioallantoic tissue. The $2^{-\Delta\Delta Ct}$ Method was used to normalize data and those fold changes were subjected to statistical analyses.

Gene Name	Method	Gene ID	Sequence	Product Length
AKR1B1	qPCR	NM_001001539.2	F: 5'- CTGAACGCATTGCCGAGAAC -3' R: 5'- AGCTCATCAAGGCACAGACC -3'	111
KHK	qPCR	XM_003125300.3	F: 5'-GCTCTTGCTGCATCGTCAAC-3' R: 5'-TTCCGGCCCTCAATGTGGAT-3'	139
SLC2A5	qPCR	XM_003361556.2	F: 5'-CGGCTCCTCCTTCCAGTATG-3' R: 5'-GGACACAGACACAGACCACA-3'	151
SLC2A5	ISH	XM_003361556.2	F: 5'-AGACCAAAGATCTGGGCCAC-3' R: 5'-CGGCTCCTCCTTCCAGTATG-3'	468
SLC2A8	qPCR	XM_003480608.2	F: 5'-GTCAGGTGTGGTCATGGTGT-3' R: 5'-TTGACGTGCAGAGGGAAGA-3'	246
SORD	qPCR	NM_001244162.1	F: 5'-TGGTGTCTGATCTGTCTGCG -3' R: 5'-GGCTCTCGTTGGAGATCTGG-3'	84
ACTB	qPCR	XM_003124280.3	F: 5'-TCCCTGGAGAAGAGCTACGA-3' R: 5'-TGTTGGCGTAGAGGTCCTTC-3'	187
HPRT1	qPCR	DQ845175	F: 5'-GGACTTGAATCATGTTTGTG-3' R: 5'-CAGATGTTTCCAAACTCAAC-3'	91
SDHA	qPCR	XM_005659031.1	F: 5'-CTACAAGGGGCAGGTTCTGA-3' R: 5'-AAGACAACGAGGTCCAGGAG-3'	141
TBP	qPCR	DQ845178	F: 5'-AACAGTTCAGTAGTTATGAGCCAGA-3' R: 5'-AGATGTTCTCAAACGCTTCG-3'	153
TUBA1B	qPCR	NM_001044544.1	F: 5'-GCTGCCAATAACTATGCCCG-3' R: 5'-ACCAAGAAGCCCTGAAGACC-3'	116

Table 5.1 Primer information for genes of interest

In situ *Hybridization*

Cell-specific expression of *SLC2A5* mRNA in the porcine endometrium and placenta was determined by radioactive *in situ* hybridization analysis as described previously (Johnson et al., 1999). Briefly, a partial cDNA for porcine *SLC2A5* mRNA was cloned from total RNA from Day 15 pregnant porcine endometrial tissue using specific primers (Table 5.1) and PCR amplification was conducted as follows: 1) 95°C for 5 min; 2) 95°C for 45 sec, 60°C for 30 sec, and 72°C for 1 min for 35 cycles; and 3) 72°C for 10 min. The partial cDNA of the correct predicted size was cloned into a pCRII plasmid using a T/A Cloning Kit (Life Technologies) and the sequence verified using an ABI PRISM Dye Terminator Cycle Sequencing Kit and ABI PRISM automated DNA sequencer (Perkin-Elmer Applied Biosystems).

Radiolabeled antisense or sense cRNA probes were generated by *in vitro* transcription using linearized plasmid templates, RNA polymerases, and [α-^{35}S]-UTP. Deparaffinized, rehydrated, and deproteinated uterine tissue sections (5µm thick) were hybridized with radiolabeled antisense or sense cRNA probes. After hybridization, washing, and ribonuclease A digestion, slides were dipped in NTB-2 liquid photographic emulsion (Kodak, Rochester, NY), and exposed at 4°C for ten days. Slides were developed in Kodak D-19 developer, counterstained with Harris modified hematoxylin (Fisher Scientific, Fairlawn, NJ), and then dehydrated through a graded series of alcohol to Citrosolv (Fisher Scientific). Coverslips were affixed with Permount (Fisher). Slides were evaluated using an Axioplan 2 microscope (Carl Zeiss, Thornwood, NY) interfaced with an Axioplan HR digital camera and Axiovision 4.3 software, and digital images of

representative fields recorded under brightfield or darkfield illumination. Photographic plates were assembled using Adobe Photoshop (version 6.0, Adobe Systems Inc., San Jose, CA).

Immunohistochemistry

AKR1B1, SORD, KHK, and SLC2A8 proteins were immunolocalized in porcine uterine and conceptus tissues as described previously (Joyce et al., 2005). A rabbit anti-human AKR1B1 polyclonal immunoglobulin (IgG; catalog no. GTX113381; GeneTex, Inc., Irvine, CA), a rabbit anti-human SORD polyclonal IgG (catalog no. sc-366370; Santa Cruz Biotechnology, Inc., Dallas, TX), a rabbit anti-human KHK polyclonal IgG (catalog no. GTX109591; GeneTex, Inc.), and a rabbit anti-mouse SLC2A8 IgG (catalog no. GTX12394; GeneTex, Inc.) were used at 8.9 µg/ml, 5 µg/ml, 8.7 µg/ml, and 5 µg/ml, respectively. Antigen retrieval was performed using a boiling citrate buffer for anti-SORD and anti-SLC2A8, protease for anti-AKR1B1, and no retrieval for anti-KHK. Additionally a rabbit anti-pig interferon gamma (IFNG) polyclonal IgG (catalog no. I7662-16N8; United States Biologicals, Salem, MA) was used at 5 µg/ml with the boiling citrate buffer antigen retrieval for identification of trophectoderm tissue. Purified non-relevant rabbit IgG, at the same concentration as the corresponding primary IgG, was used as the negative control. Immunoreactive protein was visualized in paraffin-embedded sections (5µm thick) using the Vectastain ABC Kit (catalog no. PK-4001; Vector Laboratories, Inc., Burlingame, CA) according to kit instructions with 3,3'-diaminobenzidine tetrahydrochloride (catalog no. D5637; Sigma-Aldrich, St. Louis,

MO) as the color substrate. Sections were counterstained with Harris modified hematoxylin (Fisher Scientific) and coverslips were affixed using Permount mounting medium (Fisher Scientific). Digital images of representative fields of immune-stained tissue were recorded under bright-field illumination and photographic plates assembled as described for *in situ* hybridization.

Statistical Analyses

The qPCR data for normal tissues were analyzed for effects of day, pregnancy status, and their interaction for Days 9, 11, 13, 15 and 17 by 2-way ANOVA via the General Linear Models (GLM) procedures of the Statistical Analysis System (SAS Institute, Cary, NC) with the least significant difference (LSD) multiple testing method. The qPCR data were also subjected to a sliding time window linear regression analysis to determine if there was an effect of day of gestation on the gene expression for the genes of interest throughout pregnancy (Days 9 to 85). The sliding time windows of the analysis were designed to detect effect of day on gene expression during three biologically relevant periods of time: the beginning, the middle, and the end of the study period. Each window analyzed contained a minimum of three days. Some windows contained greater than three days as long as the regression model showed a non-decreased performance in terms of the r^2 and the p-value of the F-statistics.

The data from the hormone therapy studies were analyzed using the Students t-test. Data on total recoverable fructose in uterine flushing were analyzed for effects of day, pregnancy status, and their interaction for Days 11 and 15 by 2-way ANOVA via

the GLM procedures of SAS with the least significant difference (LSD) multiple testing method. All data are presented as mean±standard errors of the mean with significance at $p<0.05$.

Results

Total Recoverable Fructose Increases in Uterine Flushings From Pregnant Gilts

Total recoverable fructose in the uterine flushings from Days 11 and 15 of the estrous cycle and early pregnancy was determined (Figure 5.1). Total fructose was significantly higher in fluid from Day 15 pregnant compared to Day 11 or 15 cycling and Day 11 pregnant gilts (day x status $p<0.01$) indicating that the free-floating conceptus is exposed to increasing levels of fructose during the peri-implantation period of pregnancy.

SLC2A8 Is Expressed in Uterine LE During the Peri-Implantation Period, and Is Expressed By the Placenta For the Majority of Pregnancy

SLC2A8 is a fructose and glucose transporter that is highly expressed during the estrous cycle and early pregnancy in pigs. Endometrial mRNA for *SLC2A8* increased from Days 5 through 11, then decreased through Day 20 with no differences between cyclic and pregnant gilts (Figure 5.2a; day $p<0.01$). There was a decrease in expression of *SLC2A8* mRNA in endometria from Days 9 to 85 of pregnancy ($r^2=0.198$; $p<0.01$), but expression increased in the placenta from Days 30 to 50, and then decreased to Day

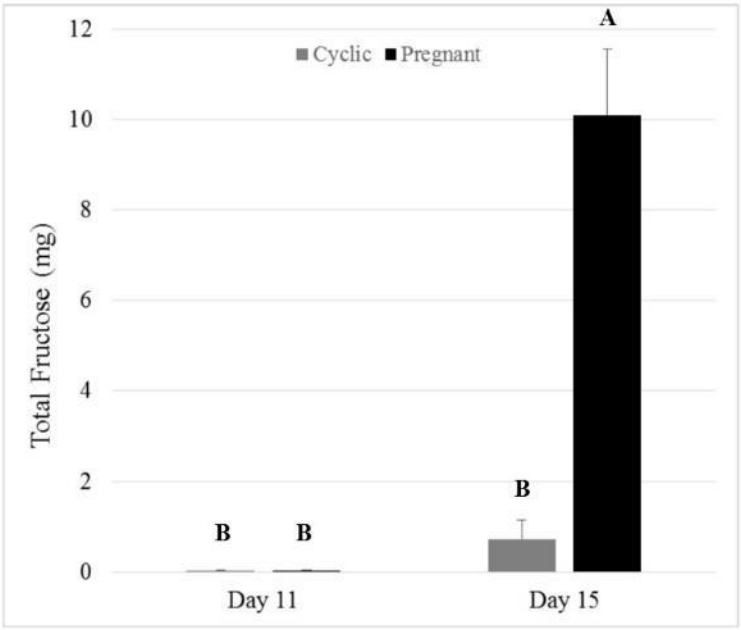

Figure 5.1 Total recoverable fructose in uterine flushings from cyclic and pregnant gilts

Fructose increased in the uterine flushings between Days 11 and 15 of pregnancy with no change during the estrous cycle (day x status $p<0.01$). Differing letters indicate significant differences. Values are presented as mean±SEM.

85 of pregnancy (Figure 5.2b; r^2=0.909; $p<0.05$). In endometria from gilts treated with exogenous E2, expression of *SLC2A8* mRNA was less than for control gilts (Figure 5.2c; $p<0.05$) and there was no effect of P4 on expression of *SLC2A8* mRNA (Figure 5.2d; $p>0.05$). SLC2A8 protein was expressed in uterine GE of cyclic and pregnant gilts by Day 9 after onset of estrus. SLC2A8 protein was first observed in uterine LE of pregnant gilts on Day 13, and was maintained though Day 15. Expression of SLC2A8 protein in uterine LE was limited to Day 15 in cyclic gilts (Figure 5.3). SLC2A8 was detected in uterine LE until Day 30 of pregnancy after which time expression transitioned from uterine LE to chorion, and specifically in the tall columnar cells at the top of the uterine folds. Expression of SLC2A8 protein in uterine GE decreased from Days 20 to 25 and remained detectable at very low abundance through Day 85 of pregnancy. Placental areolae and blood vessels in the placental stroma expressed SLC2A8 from Day 30 to Day 85.

Since *SLC2A8* mRNA expression peaked on Day 11 of both the estrous cycle and early pregnancy, an additional hormone therapy model was utilized to elucidate regulation of expression of SLC2A8. In this model, ovariectomized gilts were given exogenous E2, P4, E2+P4, or neither, to mimic the normal exposure of the endometrium to these hormones during early pregnancy, then endometrium was collected on Day 12 after onset of estrus. Endometrial expression of *SLC2A8* mRNA was greatest in response to P4 treatment (Figure 5.4a). The effect of P4 to stimulate expression of *SLC2A8* mRNA decreased when administered in combination with E2, while treatment with CO or E2 alone decreased expression of *SLC2A8* mRNA ($p<0.05$). Using

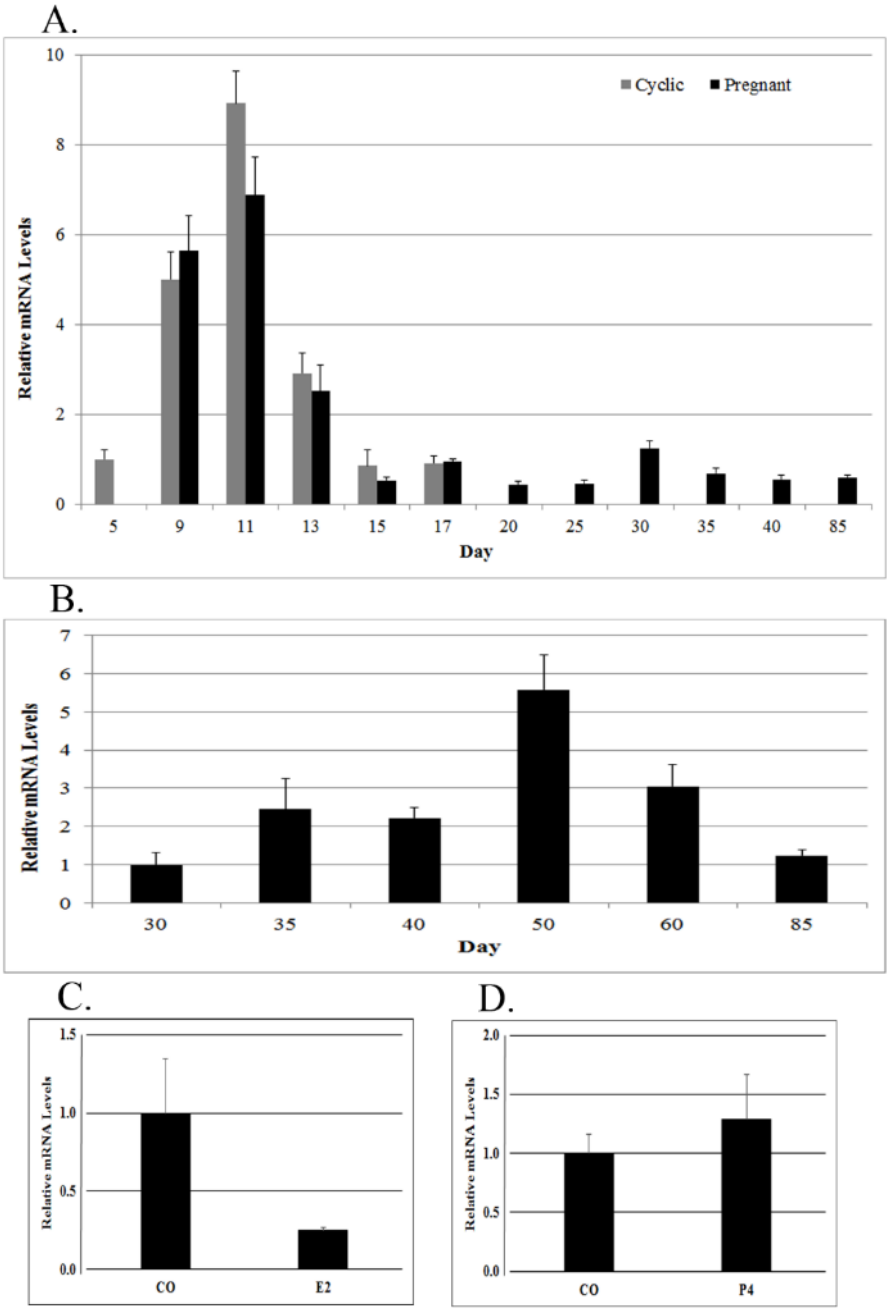

Figure 5.2 Expression of *SLC2A8* mRNA in endometria and placentae
Endometrial expression of *SLC2A8* mRNA (**A**) increased from Day 5 to Day 11 during both the estrous cycle and pregnancy, then decreased through Day 20 of gestation ($p<0.01$). Placental expression of *SLC2A8* mRNA (**B**) increased from Day 30 to Day 50, then decreased to Day 85 of pregnancy ($r^2=0.909$; $p<0.05$). E2-treatment decreased *SLC2A8* mRNA levels compared to controls (**C**; $p<0.05$), while there was no effect of P4 treatment (**D**; $p>0.05$). Values presented are mean±SEM with $p<0.05$ as significant.

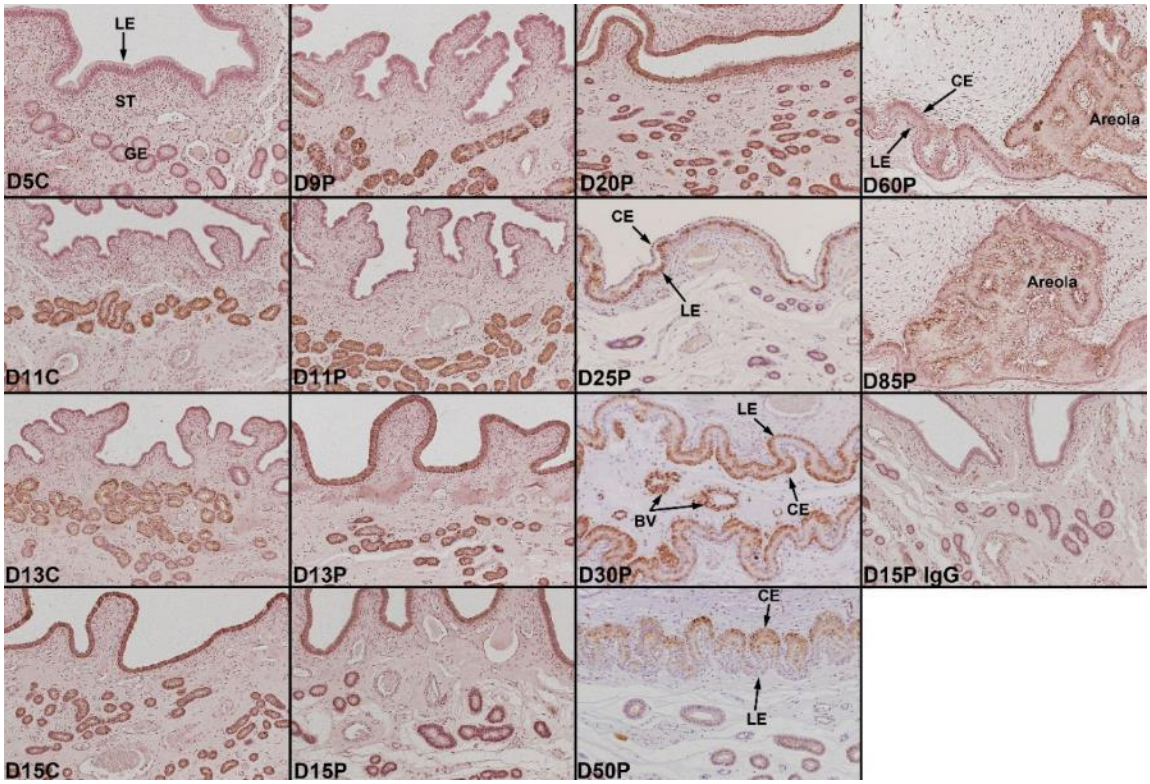

Figure 5.3 Immunohistochemical localization of SLC2A8 at the uterine-placental interface

SLC2A8 protein was detected by Day 9 in the GE of endometria from the estrous cycle and pregnancy, while LE expression was observed on Day 13 of pregnancy and Day 15 of the estrous cycle. SLC2A8 was detected in LE until Day 30 when the localization transitioned to the CE. SLC2A8 was observed in the smooth muscle surrounding the placental blood vessels at Day 30. By Day 60, SLC2A8 was only detected in the areolae and placental blood vessels. Rabbit IgG was used as a negative control. Width of field is 890 µm. Legend: LE, luminal epithelium; GE, glandular epithelium; ST, stroma; CE, chorion; BV, blood vessel.

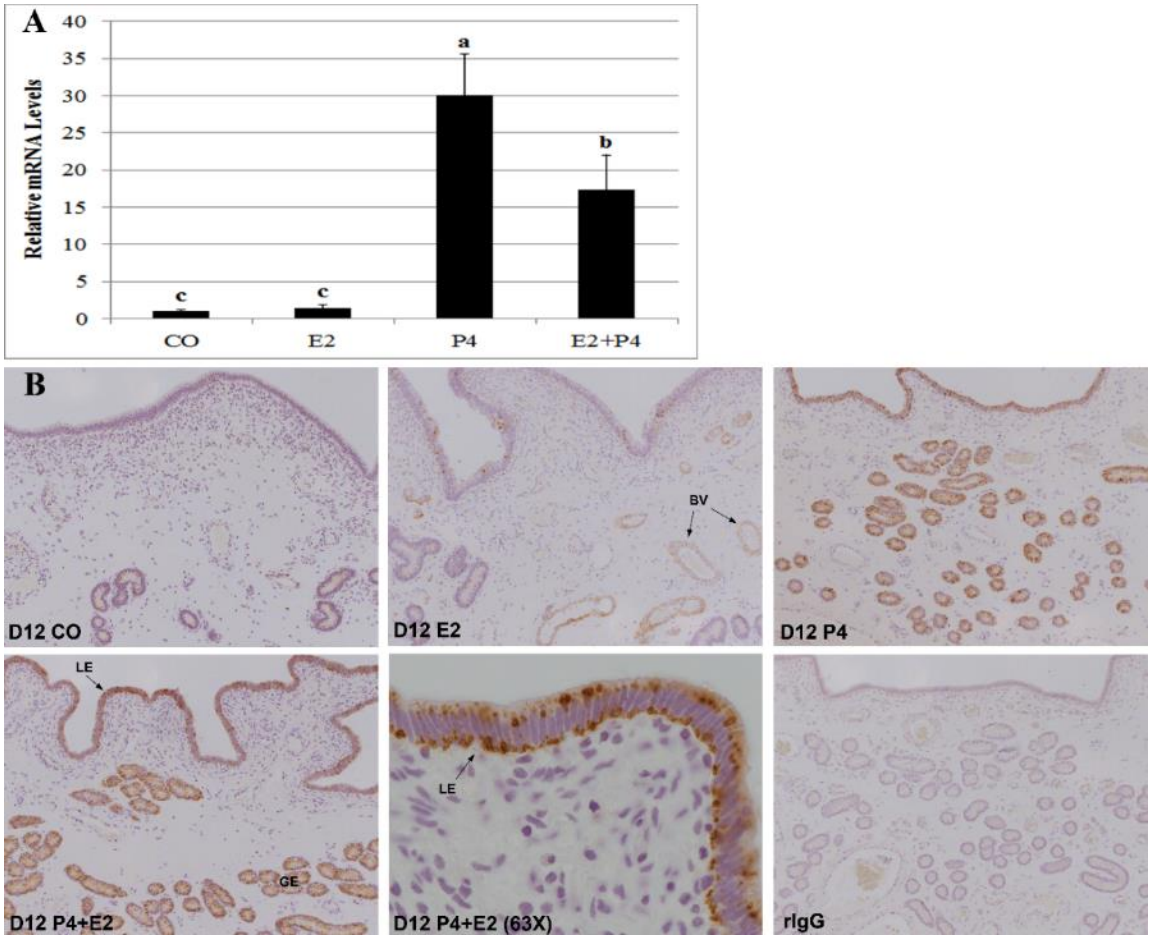

Figure 5.4 Regulation of expression of SLC2A8 by P4 and E2

Endometrial expression of *SLC2A8* mRNA (**A**) was greatest in endometria of P4-treated gilts, was suppressed in E2+P4-treated gilts as compared to P4-treatment alone, and was lowest in E2- and CO-treated gilts. Differing letters represent significant differences ($p<0.05$). Values are presented as means±SEM. Immunostaining (**B**) detected SLC2A8 protein in the uterine LE and GE of P4-treated gilts and endometria from P4+E2-treated gilts had apical and basal cell surface staining in the uterine LE. In E2-treated gilts, immunostaining was observed in the smooth muscle surrounding blood vessels in the endometrium, while in CO-treated gilts immunostaining was barely detectable in uterine GE. Width of field is 870 µm except 63X (140 µm). Rabbit IgG was used as a negative control. Legend: LE, luminal epithelium; GE, glandular epithelium; BV, blood vessel.

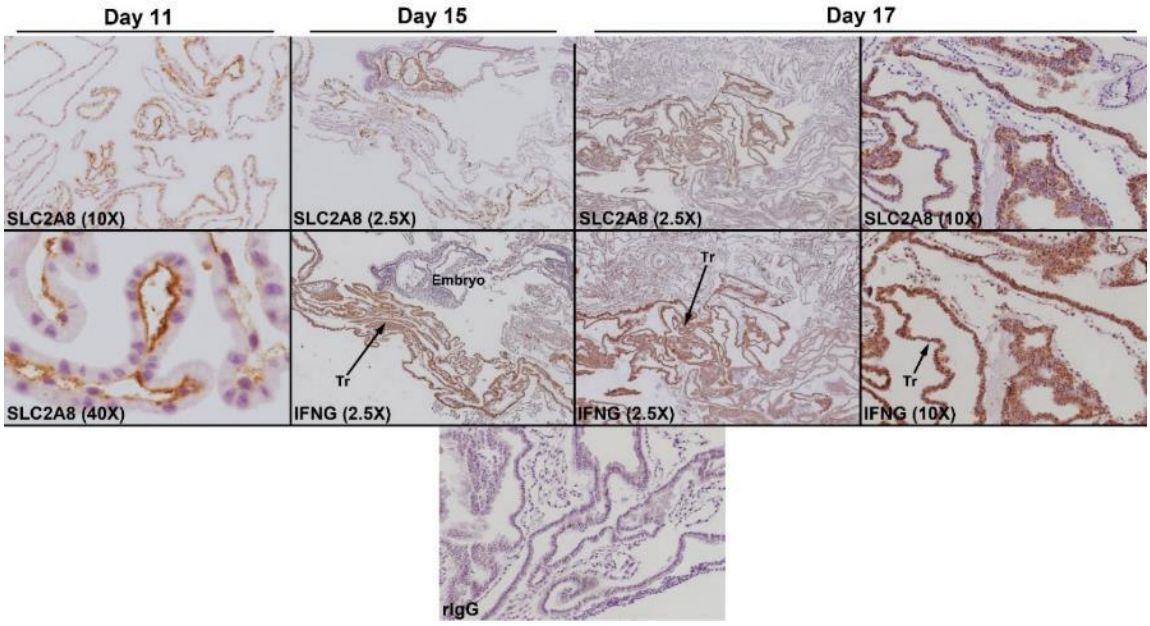

Figure 5.5 Localization of SLC2A8 protein in the pig conceptus
SLC2A8 protein was detected in the conceptus trophectoderm on Day 11 of pregnancy. At Day 15 and 17, SLC2A8 was co-distributed with IFNG, indicating expression by trophectoderm, but not endoderm. Width of field is 5.45 mm (2.5X), 890 µm (10X), and 230 µm (40X). Legend: Tr, trophectoderm.

immunohistochemistry, SLC2A8 localized to the apical and basal cell surfaces of uterine LE and GE from gilts treated with P4 or P4+E2 (Figure 5.4b). The E2 treated gilts had a marked decrease in overall expression of SLC2A8 in the endometrium compared to that for gilts treated with P4, but there was detectable SLC2A8 protein in the smooth muscle surrounding the blood vessels. The CO treated gilts had no detectable SLC2A8 protein in uterine LE, sporadic protein in uterine GE, and no detectable protein in any other cell type. Results from this experiment suggest that P4, either directly or indirectly, is a positive regulator of expression of SLC2A8 in uterine LE and GE, while E2 may modulate induction of expression of SLC2A8 by P4 and increase expression of SLC2A8 in the tunica media of blood vessels in the uterus.

SLC2A8 protein was detected in conceptuses beginning at Day 11 (Figure 5.5). At Day 15, SLC2A8 was detected in the same cells that express IFNG, which are has previously been reported to localize only to the trophectoderm, not the endoderm, cells (Lefèvre et al., 1998). The embryo at Day 15 also expressed SLC2A8 in what appears to be the somites. SLC2A8 continued to be expressed in the trophectoderm on Day 17 of pregnancy.

Expression of SLC2A5 Increases in Uterine LE and GE, and Placental CE as Pregnancy Progresses

The abundance of endometrial mRNA for the fructose transporter *SLC2A5* increased from Day 25 to Day 85 of pregnancy (Figure 5.6a; $r^2=0.869$; $p<0.01$). From Days 11 to 13, mRNA expression was higher in endometria from cycling gilts compared

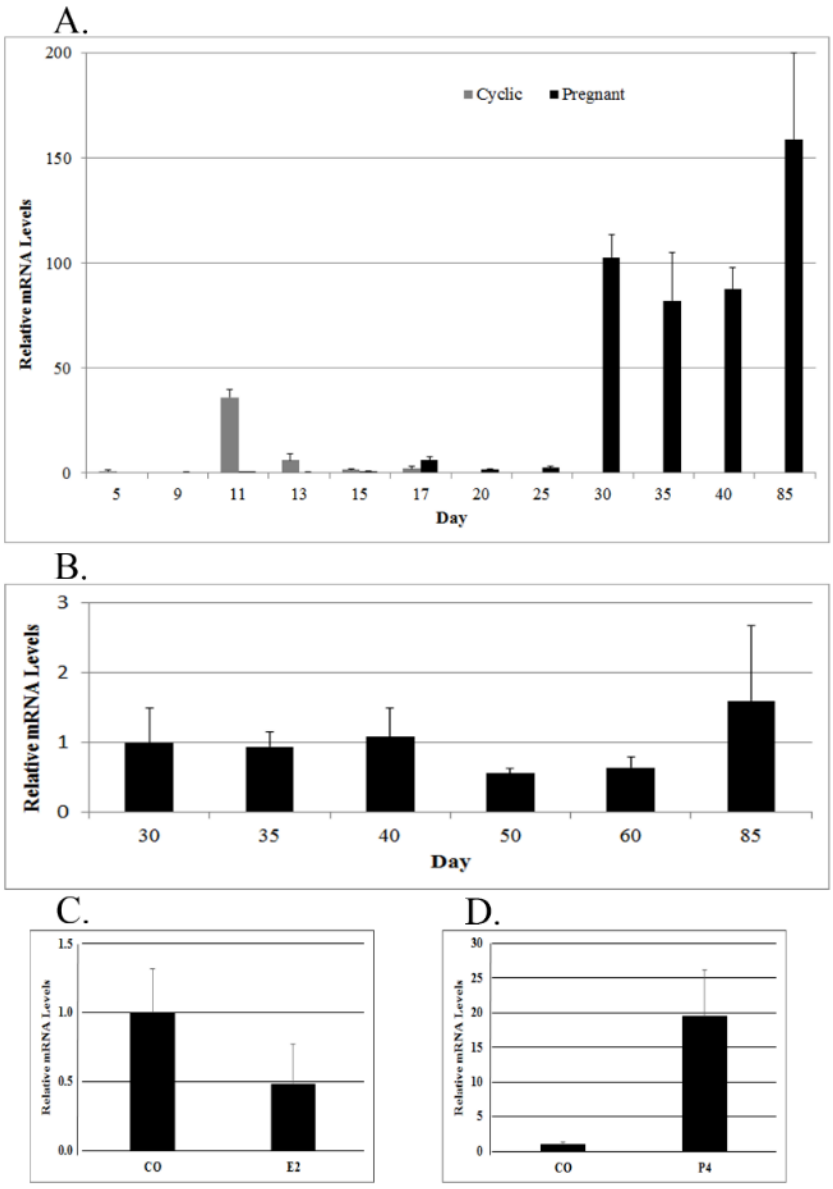

Figure 5.6 Expression of *SLC2A5* mRNA in endometria and placentae
Endometrial expression of *SLC2A5* mRNA (**A**) increased from Day 25 to Day 85 of pregnancy (r^2=0.869; p<0.01). Expression of *SLC2A5* mRNA in placentae (**B**) did not change from Days 30 through 85 (p>0.05). E2-treatment of gilts had no effect (**C**; p>0.05), but P4-treatment increased *SLC2A5* mRNA in endometria compared to control gilts (**D**; p<0.01). Values presented are mean±SEM with p<0.05 as significant.

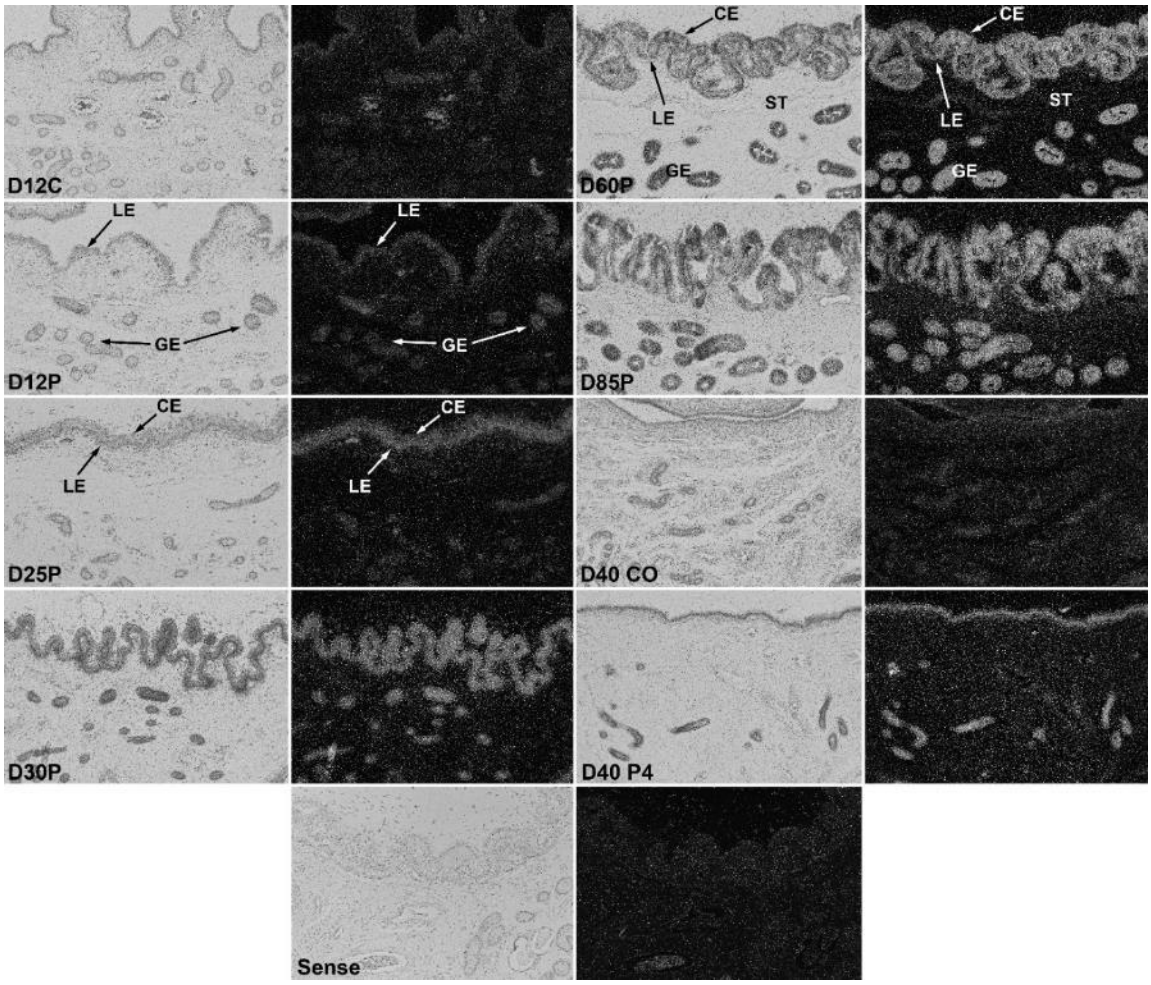

Figure 5.7 Cell-specific localization of *SLC2A5* mRNA by *in situ* hybridization at the uterine-placental interface

Corresponding bright-field and dark-field images indicated that *SLC2A5* mRNA was lowly expressed in uterine LE and GE during the estrous cycle and early pregnancy. By Day 25 of pregnancy, expression increased in uterine LE and continued to increase through Day 85 of pregnancy in both uterine LE and GE. *SLC2A5* mRNA also localized to the chorion from Day 25 through Day 85 of pregnancy. In endometria from the P4-treated gilts, *SLC2A5* mRNA localized to the uterine LE and GE. The sense panels are the negative control. Width of field is 890 μm. Legend: LE, luminal epithelium; GE, glandular epithelium; ST, stroma; CE, chorion.

to the corresponding Days of pregnancy (day x status $p<0.05$). Placental expression of *SLC2A5* mRNA did not change from Days 30 to 85 of pregnancy (Figure 5.6b; $p>0.05$). E2 had no effect on endometrial expression of *SLC2A5* mRNA ($p>0.05$; Figure 5.6c), but P4 increased expression of *SLC2A5* mRNA compared to CO treated gilts ($p<0.01$; Figure 5.6d). *In situ* hybridization analysis localized *SLC2A5* mRNA to the uterine LE and GE at low levels during the estrous cycle and early pregnancy with increasing expression in those cells and the CE through Day 85 of pregnancy (Figure 5.7). Additionally, treatment with exogenous P4 increased the expression of *SLC2A5* mRNA in uterine LE and GE.

AKR1B1 Is Expressed in Uterine LE During the Peri-Implantation Period, and in Trophectoderm/Chorion For the Majority of Pregnancy

Aldose reductase (AKR1B1) catalyzes the conversion of glucose to sorbitol as the first step in the polyol pathway. Endometrial expression of *AKR1B1* mRNA increased from Days 9 to 11, and then decreased through Day 15 with higher expression in endometria from pregnant gilts (Figure 5.8a; day x status, $p<0.05$). Endometrial expression of *AKR1B1* mRNA did not change from Days 9 to 20 ($p>0.05$), but increased from Days 25 to Day 85 of pregnancy ($r^2=0.924$; $p<0.01$). Placental expression of *AKR1B1* mRNA was not different between Days 30 and 85 (Figure 5.8b; $p>0.05$). Treatment of gilts with E2 decreased endometrial expression of *AKR1B1* mRNA compared to that for endometria from cycling control gilts ($p<0.05$; Figure 5.8c), and P4 had no effect ($p>0.05$; Figure 5.8d).

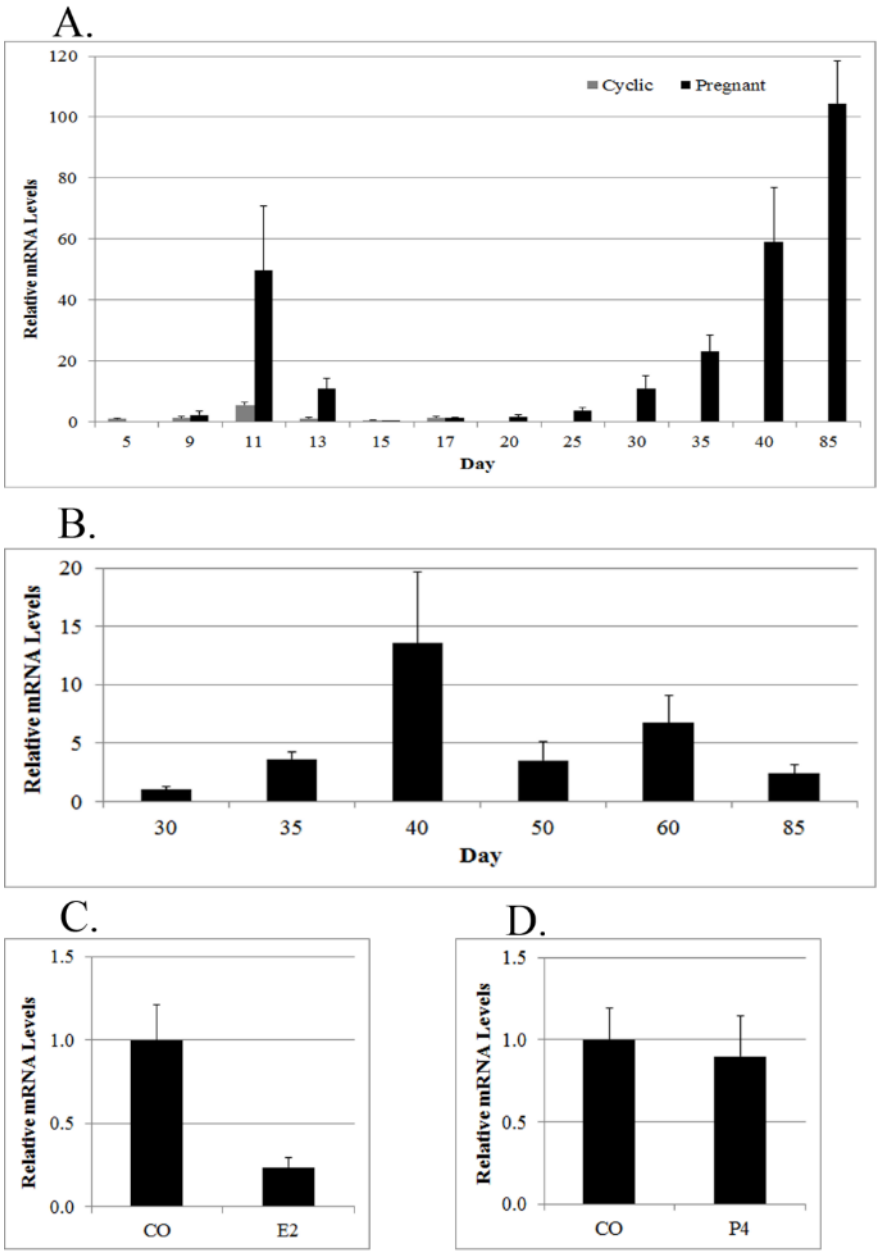

Figure 5.8 Expression of *AKR1B1* mRNA in endometria and placentae
Endometrial expression of *AKR1B1* mRNA (**A**) increased from Day 9 to Day 11, decreased until Day 15 (day x status $p<0.05$), then increased from Day 25 to Day 85 of pregnancy ($r^2=0.924$; $p<0.01$). Placental expression of *AKR1B1* mRNA (**B**) did not change between Days 30 and 85 of gestation ($p>0.05$). E2-treatment of gilts decreased *AKR1B1* mRNA compared to controls (**C**; $p<0.05$), while P4-treatment had no effect (**D**; $p>0.05$). Values presented are mean±SEM with $p<0.05$ as significant.

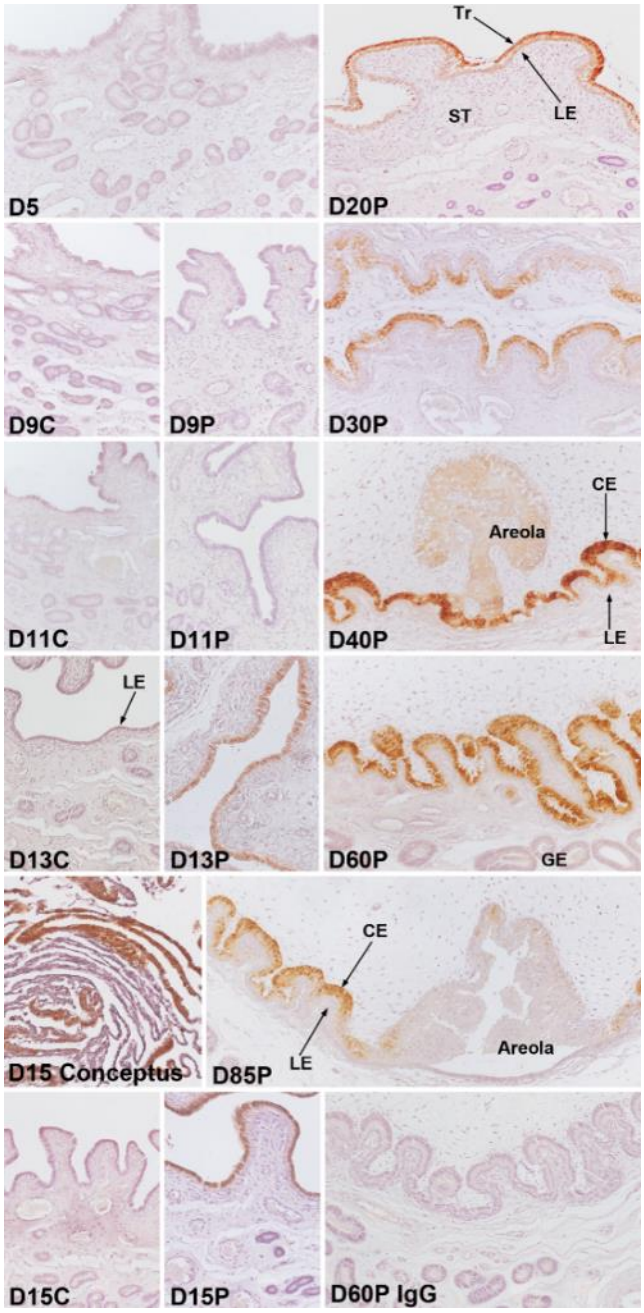

Figure 5.9 Immunohistochemical localization of AKR1B1 at the uterine-placental interface

AKR1B1 localized to uterine LE from Day 13 through Day 15 of pregnancy and to the trophectoderm as early as Day 15. Expression of AKR1B1 continued in the chorion through Day 85 of pregnancy. Rabbit IgG was used as a negative control. Width of field is: 890 µm for D5, D20P, D30P, D40P, D60P, D60P IgG; 445 µm for D9, D11, D13, D15; 572 µm for D15 conceptus; 1208 µm for D85P. Legend: LE, luminal epithelium; GE, glandular epithelium; ST, stroma; Tr, trophectoderm; CE, chorion.

AKR1B1 protein was localized to the uterine LE of pregnant gilts and to placental trophectoderm/chorion. AKR1B1 was first observed in uterine LE on Day 13 of pregnancy, but not the estrous cycle (Figure 5.9). By Day 20, AKR1B1 was barely detectable in the endometrium, and was not observed in uterine LE through Day 85. In contrast, the conceptus trophectoderm expressed AKR1B1 as early as Day 15 and expression continued in the chorion through Day 85 of pregnancy. There was low abundance of AKR1B1 protein in the areolae at Day 40, but not at Day 85 of pregnancy.

SORD Is Expressed in Uterine LE and GE During the Peri-Implantation Period, and Is Expressed in Trophectoderm/Chorion For the Majority of Pregnancy

Sorbitol is converted to fructose by the enzyme sorbitol dehydrogenase (SORD). Endometrial expression of *SORD* mRNA peaked on Day 5 of the estrous cycle and then decreased from Days 9 to 17 (Figure 5.10a; $p<0.01$), but there was no significant Day x Status interaction ($p>0.05$). When expression of *SORD* mRNA was analyzed across pregnancy, there were no significant changes from Days 9 to 13 ($r^2=0.858$; $p>0.05$), but expression increased from Days 15 to 30 ($r^2=0.828$; $p<0.05$). Placental expression of *SORD* mRNA increased from Day 30 to Day 40 (Figure 5.10b, $r^2=0.999$; $p<0.05$). For E2- and P4-treated gilts, there was no effect on expression of *SORD* mRNA ($p>0.05$; Figure 5.10c,d). SORD protein was expressed in the uterine GE at Day 5 through Day 17 of both the estrous cycle and pregnancy (Figure 5.11). Uterine LE began to express SORD at Day 13 of the estrous cycle and pregnancy, and then expression decreased to low levels by Day 20 of pregnancy. The trophectoderm expressed SORD as early as

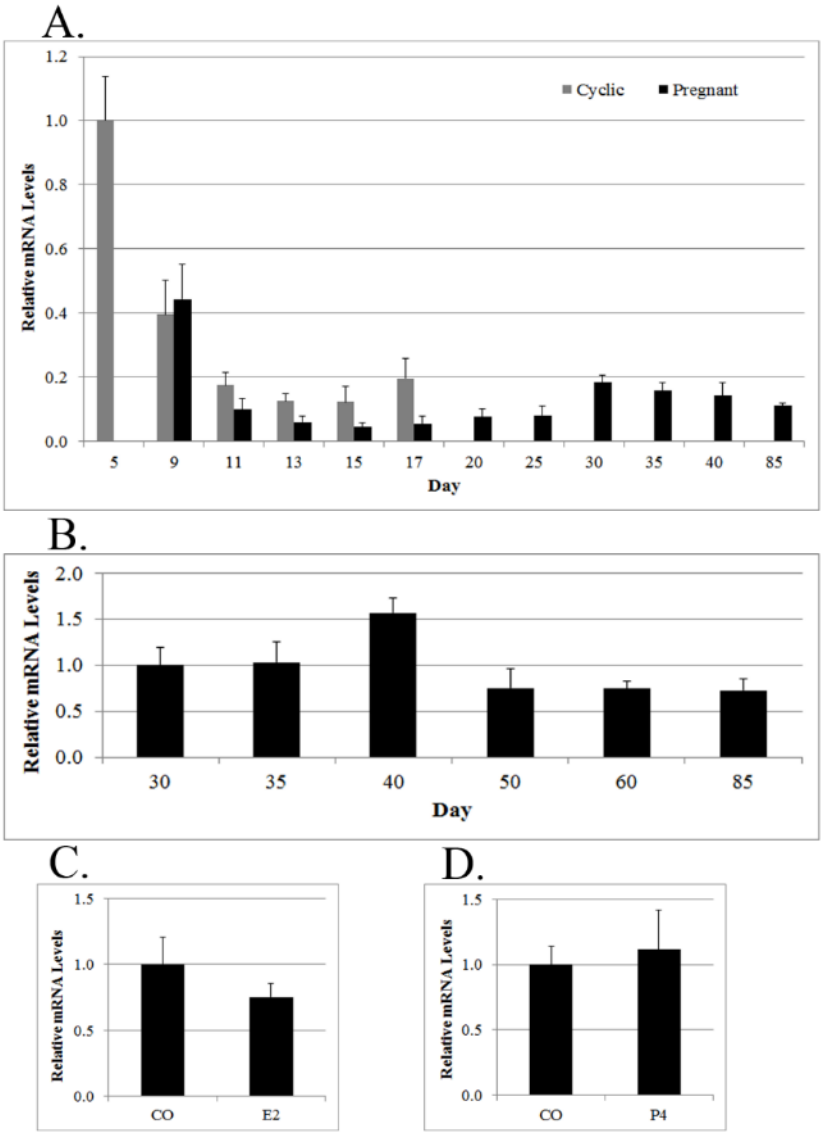

Figure 5.10 Expression of *SORD* mRNA in endometria and placentae
Endometrial expression of *SORD* mRNA (**A**) peaked at Day 5 of gestation, then decreased through Day 15 ($p<0.01$). Placental expression of *SORD* mRNA (**B**) increased from Day 30 to Day 40 of gestation ($r^2=0.999$; $p<0.05$). Treatment of gilts with E2 or P4 had no effect on endometrial expression of *SORD* mRNA compared to control gilts (**C**,**D**; $p>0.05$). Values presented are mean±SEM with $p<0.05$ as significant.

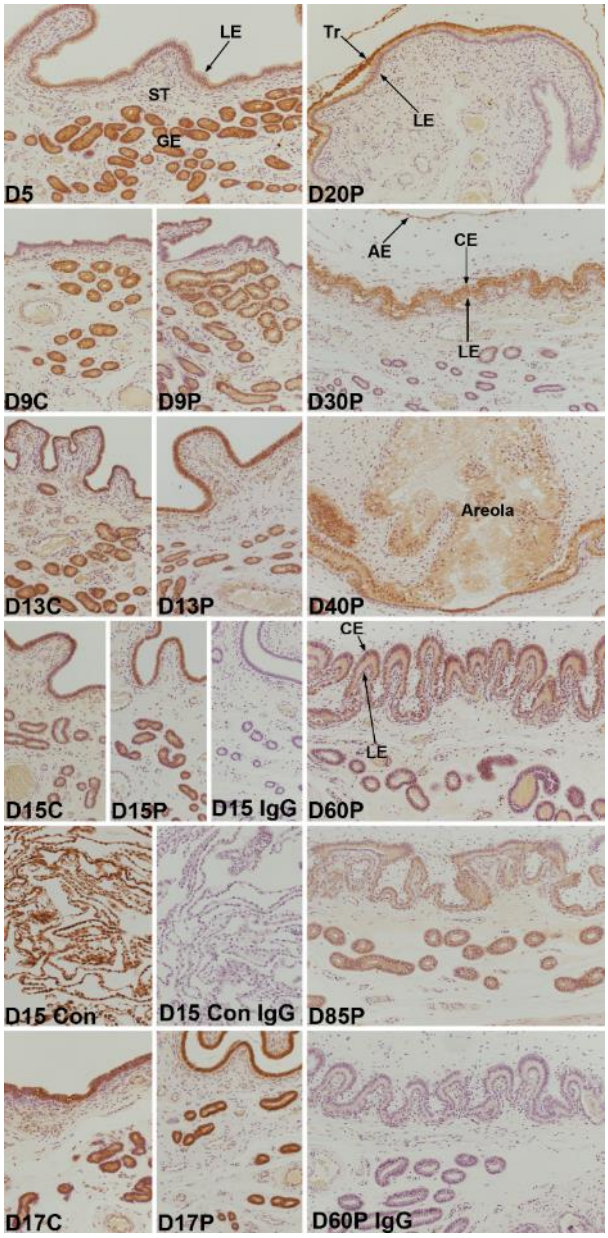

Figure 5.11 Immunohistochemical localization of SORD protein at the uterine-placental interface

SORD protein was detected in uterine GE by Day 5 and in uterine LE by Day 13 of both the estrous cycle and pregnancy. Trophectoderm expression of SORD protein was detected by Day 15 and expression continued in trophectoderm/chorion through Day 85. Areolae also expressed SORD protein. Rabbit IgG was used as the negative control. Width of field is: 890 µm for D5, D20P, D30P, D40P, D60P, D85P, D60P IgG; 445 µm for D9, D13, D15 conceptus, D17; 286 µm for D15C, D15P, D15 IgG. Legend: LE, luminal epithelium; GE, glandular epithelium; ST, stroma; Tr, trophectoderm; CE, chorion; AE, allantoic epithelium.

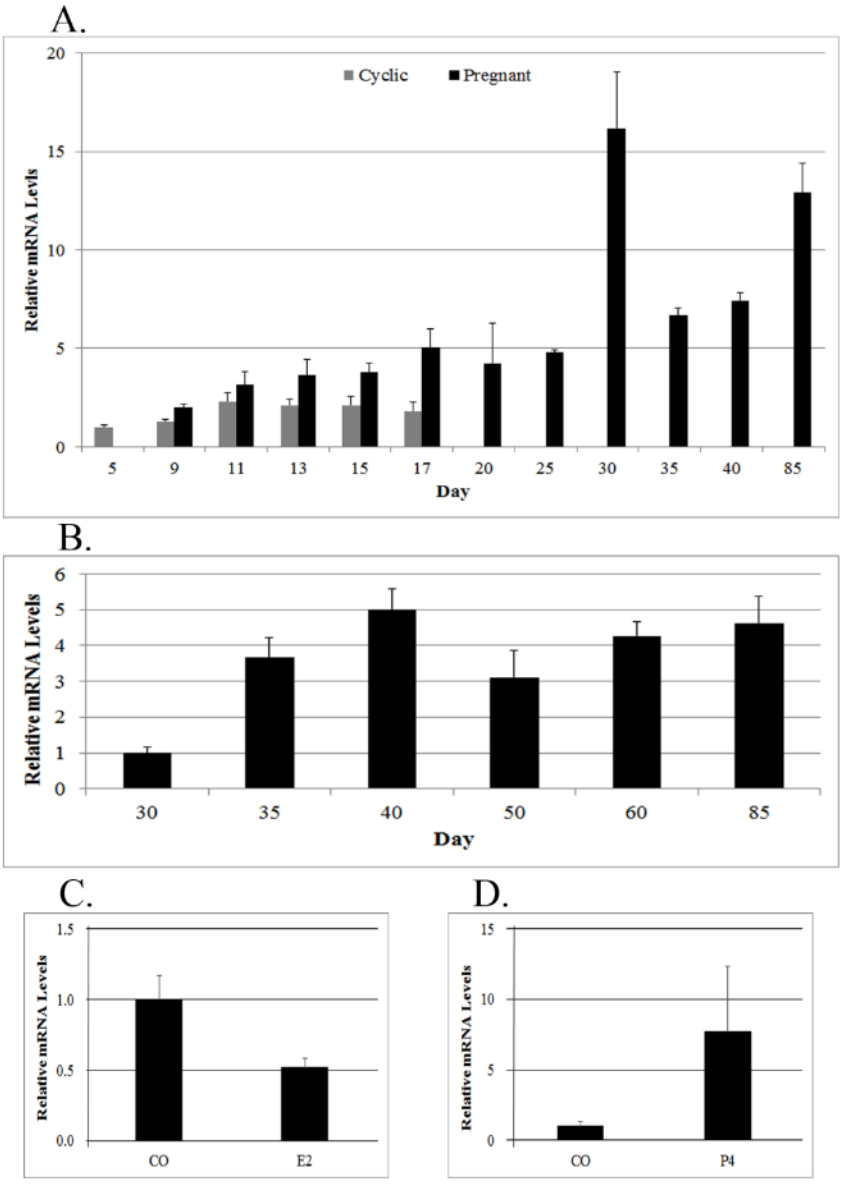

Figure 5.12 Expression of *KHK* mRNA in endometria and placentae
Endometrial expression of *KHK* mRNA (**A**) was greater in pregnant than cyclic gilts from Days 9 through 17 (Day x Status $p<0.01$) and expression increased continually through Day 85 ($r^2=0.478$; $p<0.05$). Placental expression of *KHK* mRNA (**B**) did not change from Days 30 to 85 of pregnancy ($r^2=0.433$, $p>0.05$). Treatment of gilts with either E2 or P4 had no significant effect on expression of *KHK* mRNA compared to controls (**C**,**D**; $p>0.05$). Values presented are mean±SEM with $p<0.05$ as significant.

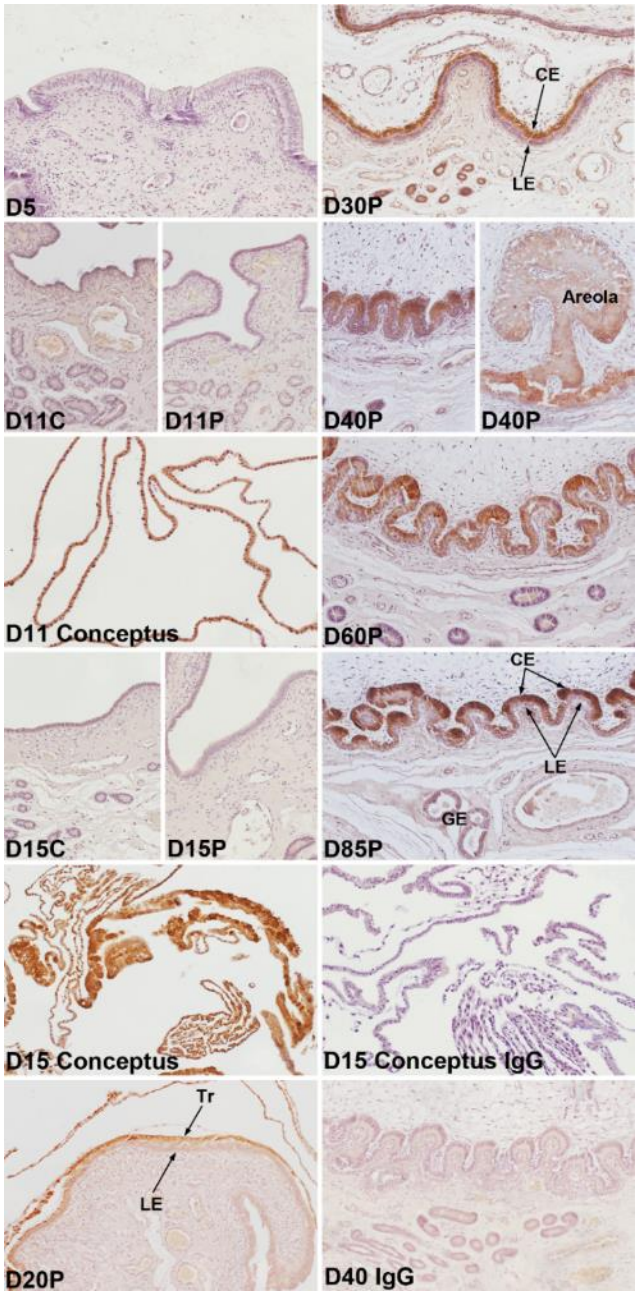

Figure 5.13 Immunohistochemical localization of KHK at the uterine-placental interface

KHK protein was detected as early as Day 11 in conceptus trophectoderm and trophectoderm/chorion expression continued through Day 85 of pregnancy with areolae also expressing KHK. Endometrial expression was limited to uterine GE at Day 30 of gestation. Rabbit IgG was used as a negative control. Width of field is 890 µm for all images except D11, D15, D40, which are 445 µm. Legend: LE, luminal epithelium; GE, glandular epithelium; Tr, trophectoderm; CE, chorion.

Day 15 and the chorion, including the areolae, expressed SORD through Day 85 of gestation when uterine GE also had higher expression than during mid-pregnancy (Figure 5.11).

KHK Is Expressed Primarily by the Trophectoderm/Chorion

Ketohexokinase (KHK) catalyzes the addition of a phosphate group to fructose to produce fructose-1-phosphate. Endometrial expression of *KHK* mRNA was higher in tissues from Days 9 through 17 of pregnancy compared to the corresponding Days of the estrous cycle ($p<0.01$; Figure 5.12a). There was an increase in expression throughout pregnancy with a peak at Day 30 ($r^2=0.478$; $p<0.05$). Placental expression of KHK mRNA did not significantly change from Days 30 to 85 of pregnancy ($p>0.05$; Figure 5.12b). Treatment of gilts with either E2 or P4 did not affect expression of *KHK* mRNA ($p>0.05$; Figure 5.12c,d). KHK protein was only detectable in GE of the endometrium at Day 30 of pregnancy (Figure 5.13). KHK protein was detected in the trophectoderm as early as Day 11 and in the chorion, including the areolae, at all stages of gestation studied through Day 85. There was stronger immunostaining in the tall columnar cells at the tops of the uterine-placental folds.

Discussion

There is an unusual abundance of fructose in pig fetal fluids and uterine flushings. Fructose has long been known to be synthesized in the placenta of ungulates and cetaceans during pregnancy, but the pathway by which fructose is synthesized, the transport

mechanisms involved, and the cells that may use fructose have not been described previously. Indeed, fructose has, for the most part, been ignored in research regarding ungulate species, possibly because fructose is not metabolized through the glycolytic pathway in the fetus or placenta (Battaglia and Meschia, 1978; McGowan et al., 1995; Bell and Ehrhardt, 2002). Results from this study indicate that fructose increases in uterine flushings of pregnant gilts from Days 11 to 15, that there are two transporters, SLC2A5 and SLC2A8, which can transport fructose from the uterus to the conceptus, and that the components of the polyol pathway, by which fructose can be synthesized from glucose, are present at the uterine-placental interface during pregnancy in pigs (Figure 5.14).

The transporters capable of transporting fructose from uterus to placenta localize to different cell types in a stage of pregnancy dependent manner. SLC2A8 localizes to uterine LE and GE during the peri-implantation period of pregnancy (Figure 5.14a), and to the chorion at Day 30 (Figure 5.14b). In contrast, *SLC2A5* mRNA increases significantly by Day 30, and remains high through Day 85 of pregnancy in uterine LE and CE at the uterine-placental interface (Figure 5.14b). The results also indicated an interesting stage-dependent change in the cellular localization of the enzymes involved in the polyol pathway. From Day 13 through Day 17, AKR1B1 and SORD localize to the uterine LE (Figure 5.14a), but by Day 20, the proteins are undetectable in uterine LE, but are abundant in the chorion through Day 85 of pregnancy (Figure 5.14b). This intriguing shift in expression of the polyol enzymes from uterine LE to chorion during pregnancy suggests that the free-floating, elongating conceptuses are supported by fructose that is synthesized by the uterus. However, after implantation is initiated and placentation is

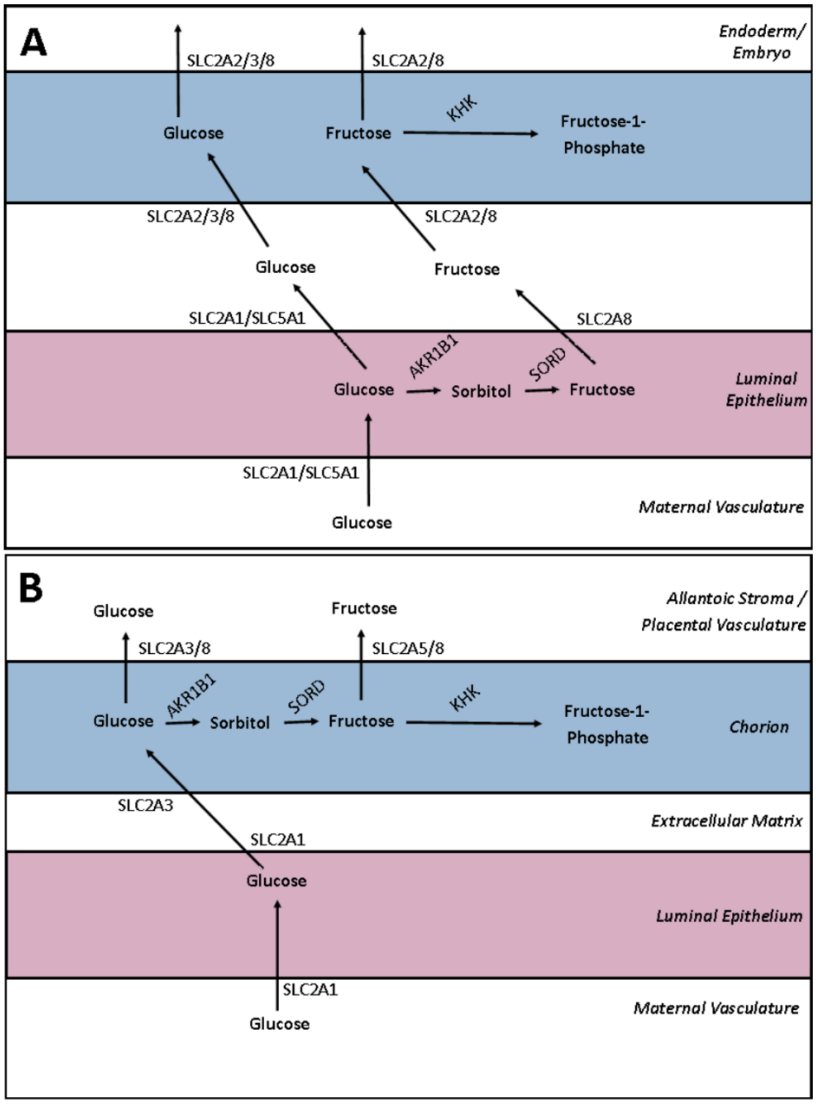

Figure 5.14 Current working model for fructose transport at the uterine-placental interface of pigs

During the peri-implantation period of pregnancy (**A**), glucose is transported into uterine LE from the maternal vasculature by SLC2A1. The polyol pathway converts glucose to fructose in uterine LE, then fructose, and glucose, are transported into the uterine lumen by SLC2A8, SLC2A1, and SLC5A1. Fructose can be utilized in the trophectoderm after being transported in by SLC2A2 or SLC2A8, or be further transported to other extraembryonic tissues or the embryo proper, while glucose can be transported into trophectoderm by SLC2A3 or SLC2A8. As placentation progresses, during mid-pregnancy (**B**), glucose is transported into and through uterine LE by SLC2A1, but the polyol pathway enzymes do not localize to that cell type. Rather, glucose is transported into the chorion by SLC2A3 and SLC2A8 where conversion to fructose can occur. Fructose can either be used by the chorion or be transported by SLC2A5 to the placental vasculature in mid- to late-pregnancy.

established at the maternal/conceptus interface, the placenta becomes self-sufficient for synthesis and transport of fructose.

Pig embryos enter the uterus, develop into blastocysts, and then shed the zona pellucida. The presumptive placental membranes (trophectoderm and endoderm) elongate at a rate of 30-45 mm/h from a 10 mm blastocyst to a 150-200 mm long filamentous form, after which further elongation occurs until conceptuses are 800-1,000 mm in length by Day 16 of pregnancy. This process provides maximum surface area for contact between trophectoderm and uterine LE to facilitate the uptake of nutrients from uterine LE and GE (Bazer and Johnson, 2014). Significant energy is required to drive these extreme morphological changes. Glucose is essential to conceptus survival, growth, and development, and substantial amounts of glucose are transported across the placental membranes of pigs and mice (Goldstein et al., 1980). SLC2A8 is an outstanding candidate for fructose and glucose transport during these important events of early pregnancy because of its localization to both uterine LE and trophectoderm while the conceptus is free-floating.

SLC2A8 protein localizes to the apical and basal cell surfaces of hepatocytes and uterine epithelia as well as the endoplasmic reticulum and lysosomes in spermatocytes (Diril et al., 2009; Kim and Moley, 2009; DeBosch et al., 2014a). SLC2A8 can transport glucose and fructose into and out of cells when it is located in the apical or basal plasma membranes, but when SLC2A8 is located in the endoplasmic reticulum, it is hypothesized to be for transporting glucose into the endoplasmic reticulum to be used for glycosylation of new proteins, especially in cells with high secretory activity. In this study, SLC2A8

localized to the apical and basal surfaces of the plasma membrane in uterine LE, GE, and Day 11 trophectoderm, but it also localized intracellularly in Day 15 trophectoderm and in the embryo. The change of localization within the trophectoderm is interesting because the Day 15 trophectoderm is more active in secretion of molecules than the Day 11 trophectoderm and SLC2A8 may help facilitate increased synthesis of proteins for secretion.

Amongst the roles of the steroid hormones P4 and E2 in pregnancy, are their ability to regulate expression of multiple genes and proteins at the uterine-placental interface in mice, sheep, and pigs, including those involved in nutrient transport and metabolism (Gao et al., 2009a; Gao et al., 2009b; Kim and Moley, 2009). SLC2A8 protein expression is suppressed in uterine LE of ovariectomized mice treated with E2, while mice treated with P4 had an increase in expression of SLC2A8 protein in uterine LE (Kim and Moley, 2009). These results are similar to those from the ovariectomized pig model as E2 alone, or when administered with P4, suppressed endometrial expression of *SLC2A8* mRNA compared to treatment with P4 alone, although the cellular localization of SLC2A8 to uterine LE and GE was not affected by hormone treatments. Interestingly, treatment of gilts with E2 alone resulted in endometrial expression of *SLC2A8* mRNA equal to those of control endometria; however, expression was localized to smooth muscle surrounding the blood vessels. While this was not observed when E2 and P4 were administered together, SLC2A8 protein was expressed in the smooth muscle and endothelium of placental blood vessels from Days 30 to 85 of pregnancy. Since concentrations of E2 in both placental blood and the allantoic fluid increase as pregnancy progresses, E2 could be responsible

for the expression of SLC2A8 mRNA and protein in placental blood vessels (Knight et al., 1977).

The high expression of SORD in uterine GE early in the estrous cycle may be attributed to one of two reasons. SORD may have a function other than converting sorbitol to fructose and fructose to sorbitol, or there is another aldose reductase family member that localizes to the GE to catalyze the first step in the polyol pathway. There are more than 190 known enzymes in the aldo/keto reductase family, each with their own specificities for different substrates, but most, especially those in the AKR1B family, are defined as NADPH-dependent oxidoreductases (Pastel et al., 2012; Penning, 2015). AKR1B1, specifically, has a high affinity for glucose and is active in the polyol pathway in other tissues (Pruneda et al., 2006; Alexiou et al., 2009). Additionally, AKR1B1 protein in the endometrium of pregnant pigs localizes to uterine LE beginning on Day 12 of pregnancy (Seo et al., 2014). We detected AKR1B1 protein in uterine LE from Days 13 through 17 of gestation (Figure 5.9), but did not analyze uteri from Day 12 of pregnancy. This could account for the discrepancy as to when AKR1B1 is initially detected in uterine LE.

The pig develops a diffuse, epitheliochorial type placenta to support the growth of each individual fetus. This placentation is characterized as being superficial, non-invasive, and having a uterine LE that remains intact. By Day 24 of pregnancy, there is complete attachment between the uterine LE and the conceptus trophectoderm and these adhered epithelia begin to fold around Day 30 to increase surface area for nutrient transport (Friess et al., 1980). Interestingly, the results of this study show that multiple proteins, SLC2A8,

AKR1B1, and SORD, are expressed in the uterine LE during early pregnancy, but expression by uterine LE begins to downregulate as folding commences and expression of those genes is limited to the placental chorion (see Figure 5.3 for an example of the temporal/spatial shift in the expression of SLC2A8). Additionally, the fructose transporter, *SLC2A5*, becomes highly expressed in uterine LE and chorion during the same period of gestation. As the placenta develops, there is a transition from uterine LE support of the conceptus to placental chorion support of the conceptus that is exemplified by changes in cell-specific expression of the proteins involved in synthesis and transport of fructose.

P4 increased expression of *SLC2A5* mRNA in uterine LE and GE of gilts treated with P4 from Day 12 to Day 40 post-estrus; therefore, P4 may induce the increase in expression of *SLC2A5* at Day 30 of pregnancy. The receptor for P4, PGR, is not present in uterine LE and GE of the P4-treated gilts or in LE and GE of the pig uterus at Day 40 of pregnancy (Figure A.5 and A.6). Therefore, the expression of *SLC2A5* could increase due to removal of repression by PGR in uterine GE, or via actions of a paracrine-acting growth factor (progestamedin) produced by the PGR-positive stromal cells responding to P4 (Johnson et al., 2000).

Another characteristic of the epitheliochorial placenta is the development of chorionic areola. Areolae form over the mouths of uterine glands and are comprised of folded chorion containing tall columnar cells with long microvilli that are optimal for transporting histotroph secreted from uterine GE (Renegar et al., 1982; Leiser and Dantzer, 1994). In addition to transporting histotroph, these cells may also play a role in synthesis of nutrients from precursor molecules in histotroph or from the placental

vasculature. SLC2A5 and SLC2A8 were detected in the areolae and could provide transport for glucose and fructose. Additionally, AKR1B1, SORD and KHK localized to areolae on Day 40, indicating that areolae are potential sites for synthesis and phosphorylation of fructose. The tall columnar cells at the tops of uterine folds in the inter-areolar regions also are hypothesized to be highly active in transporting molecules as compared to the more cuboidal cells at the bottom of the uterine folds (Vallet et al., 2014). The localization of SLC2A8 to the tall columnar cells supports to this hypothesis, although, the localization of KHK to those cells, an enzyme that phosphorylates fructose to sequester it for use in the cell that KHK localizes to, raises questions regarding the role fructose may play at the uterine-placental interface.

The polyol pathway is upregulated by hyperglycemia and, therefore, has been studied intensively in the pathological states of diabetes and cancer. In those states, activation of the pathway can result in: 1) accumulation of the intermediate sorbitol, which functions as an osmoregulator; 2) reduced ability to modulate oxidative stress due to consumption of NADPH; and, 3) production of fructose. Organ systems where the polyol pathway is normally active and functional include the liver, kidney, and male reproductive tract where fructose is produced in abundance by the seminal vesicles and the epididymis (Kobayashi et al., 2002; Pruneda et al., 2006). While the sow is not hyperglycemic during pregnancy, glucose accumulates at the uterine-placental interface in the pig due to the presence of both sodium-dependent (SGLT1; see Figure 3.3) and sodium-independent (SLC2A1, SLC2A4, SLC2A8; see Figures 4.2, 4.5, 5.10) glucose transporters and an appreciably lower concentration of glucose than that in the placental blood. This

accumulation of glucose could activate the polyol pathway. Conversion of glucose to fructose would then not only sequester the sugar in the conceptus (fructose cannot be transported back to the maternal blood), but it would maintain the disparity in concentrations of glucose between maternal and fetal-placental blood to enhance transport of glucose to the conceptus.

Shibutani et al. reported that KHK mRNA is present in parthenogenetic pig embryos as early as the 5- to 8-cell stage and that expression continues through the blastocyst stage (Shibutani et al., 2015). Those embryos are also unable to utilize fructose as the only carbohydrate source before the 5- to 8- cell stage of development. Results of the present study indicate that the pig conceptuses continue to express KHK protein to Day 11 in trophectoderm and to Day 85 of gestation in the chorion (Figure 5.6).

In the liver, fructose is used for glycogen and triglyceride synthesis, neither of which are synthesized in substantial amounts by the pig placenta (Ramsay et al., 1984; Feinman and Fine, 2013). Also, sperm use fructose as an energy source, but this too is minimal in the placenta (Aalbers et al., 1961). While recent *in vitro* data using porcine trophectoderm cells indicate that fructose activates the hexosamine biosynthetic pathway to stimulate mechanistic target of rapamycin (mTOR) cell signaling and cell proliferation, and the synthesis of hyaluronic acid, a significant glycosaminoglycan in the placenta, there are still questions about the role of fructose in the placenta (Kim et al., 2012). Results of the present research indicate that the trophectoderm has the potential to utilize fructose due to the presence of KHK in those cells; however, the downstream molecules or regulatory targets will need to be determined in future studies.

In conclusion, the components for the synthesis of fructose via the polyol pathway and for fructose transport are present at the uterine-placental interface during pregnancy in pigs (Figure 5.14). Additionally, those components are expressed in a temporal and spatial manner that is, at least in part, regulated by the steroid hormones progesterone and estrogen. Early in development, the free-floating conceptus can be supported by fructose synthesized by the uterine LE and transported into the uterine lumen. As pregnancy and placentation progress, the chorion takes over the synthesis of fructose, and the conceptus becomes self-sufficient for fructose production. Additionally, the localization of SLC2A8 to uterine LE and trophectoderm during the peri-implantation period provides a mechanism for transport of fructose between the tissues synthesizing fructose and the tissues metabolizing fructose, particularly the conceptus trophectoderm and chorioallantois.

CHAPTER VI

SUMMARY AND CONCLUSION

Summary

Glucose and fructose are abundant hexose sugars in porcine endometria and conceptuses that play differing roles in supporting growth and development of the conceptus during pregnancy. Glucose is a major source of energy to the conceptus while fructose likely has a minor role as an energy source; however, fructose may be: 1) a precursor to other metabolites; 2) able to help establish concentration gradients for glucose between the maternal and fetal circulations; and 3) a regulator of non-metabolic cellular processes. The research for this dissertation has determined potential transport pathways for moving glucose and fructose to tissues where they can serve functional roles. Additionally, the localization of key enzymes involved in fructose synthesis has been determined, which is a major advancement because fructose is not supplied by the maternal blood to the conceptus.

Before qPCR could be used as a tool for analysis of gene expression in the endometria and placentae of pigs, it was necessary to optimize the choice of reference genes. Analysis of mRNA expression is only possible when there is a stable expression of a reference gene with which to compare expression of the gene of interest. Therefore, in order to determine a set of three appropriate reference genes for endometrial and placental tissues, a group of 10 reference genes, selected due to their stability in other tissues, were analyzed by performing qPCR on endometrial and placental tissues from

time points throughout the estrous cycle and pregnancy. After analysis using the algorithms GeNorm and NormFinder, the geometric mean of *TBP, HPRT1,* and *TUBA1B* was determined to be appropriate for normalization of data from placental tissue while the geometric mean of *TBP, ACTB,* and *SDHA* was appropriate for normalization of data from endometrial tissue. *YWHAZ, GAPDH,* and *B2M* were not appropriately stable in those tissues for use as reference genes according to the algorithms.

In order to determine that the chosen reference genes provided reliable results, qPCR analysis for two genes, *SLC5A1* and *SLC7A3,* was compared to results from *in situ* hybridization analysis in which each mRNA was localized to specific cells within a tissue. Results of both the qPCR and the *in situ* hybridization analyses revealed that the sodium-dependent glucose transporter *SLC5A1* was expressed predominantly early in pregnancy during the peri-implantation period and that expression was induced by trophectoderm-derived E2 (Figures 3.3 and 3.4). The amino acid transporter, *SLC7A3,* was expressed in the trophectoderm/chorion, expression increased from Days 30 to 40 of pregnancy, and the chorion was capable of transporting arginine (Figure 3.5).

Quantification and localization of mRNAs for the glucose transporters *SLC2A1, SLC2A2, SLC2A3,* and *SLC2A4* were performed using endometrial and placental tissues from the estrous cycle and pregnancy in pigs. Those four transporters are the most studied in other tissues and species and play major roles in whole body glucose homeostasis, insulin-driven glucose uptake, and rapid transport of glucose. *SLC2A1* and *SLC2A3* in particular have roles during pregnancy in other species. Indeed, this study

found *SLC2A1* to be the prominent glucose transporter in the endometrium and *SLC2A3* to be prominent in the conceptus (Figure 4.2 and 4.4). Expression of *SLC2A1* mRNA was also upregulated specifically in uterine LE of gilts treated with E2 or P4 (Figure 4.2). Expression of *SLC2A2* mRNA was only in trophectoderm and areolae, while *SLC2A4* was lowly expressed in uterine LE and GE in a similar manner to *SLC2A1* (Figures 4.3 and 4.5). *SLC2A1*, *SLC2A3*, and *SLC2A4* mRNAs were also localized to the endothelia of the endometrium and placenta as well as the areolae and the allantoic epithelium (Figures 4.6 and 4.7). These results indicate that glucose transporters are present in all cell types necessary for transport of glucose from maternal to placental blood (Figure 4.8).

Two transporters that can transport fructose, SLC2A5 and SLC2A8, were examined. *SLC2A5* mRNA localized to uterine LE, GE, and chorion with expression increasing to Day 30 of pregnancy (Figure 5.7). In contrast, expression of *SLC2A8* mRNA peaked in endometria around Day 11 of the estrous cycle and pregnancy with the protein localizing to uterine GE by Day 9 and to uterine LE by Day 13 (Figures 5.2 and 5.3). SLC2A8 protein was expressed in uterine LE until Day 30 of pregnancy, but then transitioned to being expressed in the chorion. In non-pregnant gilts, SLC2A8 protein was upregulated by P4 in uterine LE and GE, and by E2 in endometrial blood vessels (Figure 5.4).

After determining that glucose and fructose transporters were present in endometrial and placental tissues, the next step was to determine if the components necessary for fructose synthesis and metabolism were not only present, but where they

localized within uterine and placental tissues. The enzymes involved in the polyol pathway, AKR1B1 and SORD, were detected at both the mRNA and protein levels. AKR1B1 protein was expressed in uterine LE beginning at Day 13 of pregnancy, but expression was undetectable in uterine LE by Day 20, although the protein was expressed in the trophectoderm/chorion through Day 85 of pregnancy (Figure 5.9). SORD protein was also detectable at Day 13 of pregnancy in uterine LE and in uterine GE as early as Day 5, but expression transitioned to the chorion through Day 85 of pregnancy (Figure 5.11). KHK, the enzyme that adds a phosphate group to fructose, localized to conceptus tissue on each of the days of pregnancy studied, specifically to trophectoderm and the tall columnar cells of the chorion (Figure 5.13).

Conclusion

These studies provide evidence that transporters necessary for the movement of glucose from maternal blood to placental blood are present at the uterine-placental interface in pigs throughout pregnancy. Additionally, the enzymes and transporters necessary to produce fructose via the polyol pathway, and to transport fructose, are present in a temporal and cell-type specific manner during pregnancy (Figure 5.14). The transport of glucose and fructose in the endometrium is regulated by progesterone and estrogen, which increase transcriptional or translational effects for expression of multiple transporters of the *SLC2A* and *SLC5A* families. This basic knowledge can be used to manipulate transport of hexose sugars for metabolism at the uterine-placental interface to increase birthweights of piglets, decrease variation among piglets within litters with

respect to growth and development, and improve survivability of piglets for increased efficiency and profitability of the swine industry.

REFERENCES

Aalbers, J. G., T. Mann, and C. Polge. 1961. Metabolism of boar semen in relation to sperm motility and survival. J. Reprod. Fertil. 2: 42-53.

Adastra, K. L. et al. 2012. Slc2a8 deficiency in mice results in reproductive and growth impairments. Biol. Reprod. 87: 49.

Adelman, R. C., F. J. Ballard, and S. Weinhouse. 1967. Purification and Properties of Rat Liver Fructokinase. J. Biol. Chem. 242: 3360-3365.

Aghayan, M. et al. 1992. Developmental expression and cellular localization of glucose transporter molecules during mouse preimplantation development. Development 115: 305-312.

Aherne, F., V. W. Hays, R. C. Ewan, and V. C. Speer. 1969. Absorption and utilization of sugars by the baby pigs. J. Anim. Sci. 29: 444-450.

Alexander, D. P., R. D. Andrews, A. S. Huggett, D. A. Nixon, and W. F. Widdas. 1955a. The placental transfer of sugars in the sheep: studies with radioactive sugar. J. Physiol. 129: 352-366.

Alexander, D. P., A. S. Huggett, D. A. Nixon, and W. F. Widdas. 1955b. The placental transfer of sugars in the sheep: the influence of concentration gradient upon the rates of hexose formation as shown in umbilical perfusion of the placenta. J. Physiol. 129: 367-383.

Alexiou, P., K. Pegklidou, M. Chatzopoulou, I. Nicolaou, and V. J. Demopoulos. 2009. Aldose reductase enzyme and its implication to major health problems of the 21(st) century. Curr. Med. Chem. 16: 734-752.

Anderson, L. L. 1978. Growth, protein content and distribution of early pig embryos. Anat. Rec. 190: 143-153.

Angulo, C. et al. 1998. Hexose transporter expression and function in mammalian spermatozoa: cellular localization and transport of hexoses and vitamin C. J. Cell. Biochem. 71: 189-203.

Aplin, J. D. 1999. MUC-1 glycosylation in endometrium: possible roles of the apical glycocalyx at implantation. Hum. Reprod. 14 Suppl 2: 17-25.

Augustin, R. 2010. The protein family of glucose transport facilitators: It's not only about glucose after all. IUBMB Life 62: 315-333.

Augustin, R. et al. 2004. Identification and characterization of human glucose transporter-like protein-9 (GLUT9): alternative splicing alters trafficking. J. Biol. Chem. 279: 16229-16236.

Augustin, R. et al. 2001. Glucose transporter expression is developmentally regulated in in vitro derived bovine preimplantation embryos. Mol. Reprod. Dev. 60: 370-376.

Augustin, R., J. Riley, and K. H. Moley. 2005. GLUT8 contains a [DE]XXXL[LI] sorting motif and localizes to a late endosomal/lysosomal compartment. Traffic (Copenhagen, Denmark) 6: 1196-1212.

Bacon, J. S., and D. J. Bell. 1948. Fructose and glucose in the blood of the foetal sheep. Biochem. J. 42: 397-405.

Bailey, D. W. et al. 2010a. Effects of long-term progesterone exposure on porcine uterine gene expression: progesterone alone does not induce secreted phosphoprotein 1 (osteopontin) in glandular epithelium. Reproduction 140: 595-604.

Bailey, D. W. et al. 2010b. Effects of long-term progesterone on developmental and functional aspects of porcine uterine epithelia and vasculature: progesterone alone does not support development of uterine glands comparable to that of pregnancy. Reproduction 140: 583-594.

Bailey, D. W. et al. 2010c. Effects of long-term progesterone on developmental and functional aspects of porcine uterine epithelia and vasculature: progesterone

alone does not support development of uterine glands comparable to that of pregnancy. Reproduction 140: 583-594.

Balen, D. et al. 2008. Revised immunolocalization of the Na+-D-glucose cotransporter SGLT1 in rat organs with an improved antibody. Am. J. Physiol. Cell Physiol. 295: C475-489.

Barklay, H., P. Haas, and et al. 1949. The sugar of the foetal blood, the amniotic and allantoic fluids. J. Physiol. 109: 98-102.

Basha, S. M., F. W. Bazer, R. D. Geisert, and R. M. Roberts. 1980. Progesterone-induced uterine secretions in pigs. Recovery from pseudopregnant and unilaterally pregnant gilts. J. Anim. Sci. 50: 113-123.

Battaglia, F. C., and G. Meschia. 1978. Principal substrates of fetal metabolism. Physiol. Rev. 58: 499-527.

Baumann, M. U., S. Deborde, and N. P. Illsley. 2002. Placental glucose transfer and fetal growth. Endocrine 19: 13-22.

Bazer, F. W., and G. A. Johnson. 2014. Pig blastocyst-uterine interactions. Differentiation 87: 52-65.

Bazer, F. W., and W. W. Thatcher. 1977. Theory of maternal recognition of pregnancy in swine based on estrogen controlled endocrine versus exocrine secretion of prostaglandin F2alpha by the uterine endometrium. Prostaglandins 14: 397-400.

Bazer, F. W., W. W. Thatcher, F. Martinat-Botte, and M. Terqui. 1988. Conceptus development in large white and prolific Chinese Meishan pigs. J. Reprod. Fertil. 84: 37-42.

Bazer, F. W. et al. 1991. Composition of uterine flushings from Large White and prolific Chinese Meishan gilts. Reprod. Fertil. Dev. 3: 51-60.

Bell, A. W., and R. A. Ehrhardt. 2002. Regulation of placental nutrient transport and implications for fetal growth. Nutr Res Rev 15: 211-230.

Bell, G. I., C. F. Burant, J. Takeda, and G. W. Gould. 1993. Structure and function of mammalian facilitative sugar transporters. J. Biol. Chem. 268: 19161-19164.

Berard, J., and G. Bee. 2010. Effects of dietary l-arginine supplementation to gilts during early gestation on foetal survival, growth and myofiber formation. Animal 4: 1680-1687.

Bergmeyer, H., E. Bernt, F. Schmidt, and H. Stork. 1974. Determination of hexokinase and glucose-6-phosphate dehydrogenase. In: B. HU (ed.) Methods of Enzymatic Analysis. p 1196-1201. Academic Press, New York.

Blomberg, L., K. Hashizume, and C. Viebahn. 2008. Blastocyst elongation, trophoblastic differentiation, and embryonic pattern formation. Reproduction 135: 181-195.

Bowen, J. A., F. W. Bazer, and R. C. Burghardt. 1996. Spatial and temporal analyses of integrin and Muc-1 expression in porcine uterine epithelium and trophectoderm in vivo. Biol. Reprod. 55: 1098-1106.

Brown, K., D. S. Heller, S. Zamudio, and N. P. Illsley. 2011. Glucose transporter 3 (GLUT3) protein expression in human placenta across gestation. Placenta 32: 1041-1049.

Brown, K. S., S. S. Kalinowski, J. R. Megill, S. K. Durham, and K. A. Mookhtiar. 1997. Glucokinase Regulatory Protein May Interact With Glucokinase in the Hepatocyte Nucleus. Diabetes 46: 179-186.

Brusati, V. et al. 2005. Fetal and maternal non-glucose carbohydrates and polyols concentrations in normal human pregnancies at term. Pediatr. Res. 58: 700-704.

Bryant, N. J., R. Govers, and D. E. James. 2002. Regulated transport of the glucose transporter GLUT4. Nat. Rev. Mol. Cell Biol. 3: 267-277.

Burant, C. F., J. Takeda, E. Brot-Laroche, G. I. Bell, and N. O. Davidson. 1992. Fructose transporter in human spermatozoa and small intestine is GLUT5. J. Biol. Chem. 267: 14523-14526.

Burghardt, R. C., J. A. Bowen, G. R. Newton, and F. W. Bazer. 1997. Extracellular matrix and the implantation cascade in pigs. J. Reprod. Fertil. Suppl. 52: 151-164.

Burghardt, R. C. et al. 2002. Integrins and extracellular matrix proteins at the maternal-fetal interface in domestic animals. Cells Tissues Organs 172: 202-217.

Carson, D. D. et al. 2000. Embryo implantation. Dev. Biol. 223: 217-237.

Challier, J. C., S. Hauguel, and V. Desmaizieres. 1986. Effect of insulin on glucose uptake and metabolism in the human placenta. J. Clin. Endocrinol. Metab. 62: 803-807.

Charron, M. J., and E. B. Katz. 1998. Metabolic and therapeutic lessons from genetic manipulation of GLUT4. Mol. Cell. Biochem. 182: 143-152.

Cheeseman, C. 2008. GLUT7: a new intestinal facilitated hexose transporter. Am. J. Physiol. Endocrinol. Metab. 295: E238-241.

Chen, L.-Q., L. S. Cheung, L. Feng, W. Tanner, and W. B. Frommer. 2015. Transport of Sugars. Annu. Rev. Biochem. 84: 865-894.

Chen, T. T., F. W. Bazer, J. J. Cetorelli, W. E. Pollard, and R. M. Roberts. 1973. Purification and properties of a progesterone-induced basic glycoprotein from the uterine fluids of pigs. J. Biol. Chem. 248: 8560-8566.

Chen, T. T., F. W. BAZER, B. M. GEBHARDT, and R. M. ROBERTS. 1975. Uterine Secretion in Mammals: Synthesis and Placental Transport of a Purple Acid Phosphatase in Pigs. Biol. Reprod. 13: 304-313.

Cirillo, P. et al. 2009. Ketohexokinase-Dependent Metabolism of Fructose Induces Proinflammatory Mediators in Proximal Tubular Cells. J. Am. Soc. Nephrol. 20: 545-553.

Cole, S. W., and M. W. Hitchcock. 1946. Sugars in the foetal and maternal bloods of sheep. Biochem. J. 40: li.

Corder, C. N., J. G. Collins, T. S. Brannan, and J. Sharma. 1977. Aldose reductase and sorbitol dehydrogenase distribution in rat kidney. J. Histochem. Cytochem. 25: 1-8.

Cori, C. 1925. The fate of sugar in the animal body: The rate of absorption of hexoses and pentoses from the intestinal tract. J. Biol. Chem. 66: 691-715.

Cori, C. 1926. The rate of absorption of a mixture of glucose and galactose. Proc. Soc. Exp. Biol. Med. 23.

Corry, D. B. et al. 2008. Uric acid stimulates vascular smooth muscle cell proliferation and oxidative stress via the vascular renin-angiotensin system. J. Hypertens. 26: 269-275.

Crane, R. K. 1962. Hypothesis for mechanism of intestinal active transport of sugars. Fed. Proc. 21: 891-895.

Crane, R. K. 1965. Na+ -dependent transport in the intestine and other animal tissues. Fed. Proc. 24: 1000-1006.

Curtis, S. E., C. J. Heidenreich, and C. W. Foley. 1966. Carbohydrate assimilation and utilization by newborn pigs. J. Anim. Sci. 25: 655-662.

Dantzer, V. 1984. Scanning electron microscopy of exposed surfaces of the porcine placenta. Acta Anat. (Basel) 118: 96-106.

Dantzer, V. 1985. Electron microscopy of the initial stages of placentation in the pig. Anat. Embryol. (Berl.) 172: 281-293.

Dantzer, V., and R. Leiser. 1994. Initial vascularisation in the pig placenta: I. Demonstration of nonglandular areas by histology and corrosion casts. Anat. Rec. 238: 177-190.

De Vos, M. et al. 2014. Nutritional interventions to prevent and rear low-birthweight piglets. J. Anim. Physiol. Anim. Nutr. (Berl.) 98: 609-619.

DeBosch, B. J., Z. Chen, J. L. Saben, B. N. Finck, and K. H. Moley. 2014a. Glucose Transporter 8 (GLUT8) Mediates Fructose-induced de Novo Lipogenesis and Macrosteatosis. J. Biol. Chem. 289: 10989-10998.

DeBosch, B. J., O. Kluth, H. Fujiwara, A. Schürmann, and K. Moley. 2014b. Early-onset metabolic syndrome in mice lacking the intestinal uric acid transporter SLC2A9. Nat Commun 5.

Dhindsa, D. S., and P. J. Dziuk. 1968. Influence of varying the proportion of uterus occupied by embryos on maintenance of pregnancy in the pig. J. Anim. Sci. 27: 668-672.

Diggle, C. P. et al. 2009. Ketohexokinase: expression and localization of the principal fructose-metabolizing enzyme. J. Histochem. Cytochem. 57: 763-774.

Diril, M. K. et al. 2009. Lysosomal localization of GLUT8 in the testis--the EXXXLL motif of GLUT8 is sufficient for its intracellular sorting via AP1- and AP2-mediated interaction. FEBS J 276: 3729-3743.

Ericsson, A. et al. 2005a. Hormonal regulation of glucose and system A amino acid transport in first trimester placental villous fragments. Am. J. Physiol. Regul. Integr. Comp. Physiol. 288: R656-662.

Ericsson, A., B. Hamark, T. L. Powell, and T. Jansson. 2005b. Glucose transporter isoform 4 is expressed in the syncytiotrophoblast of first trimester human placenta. Hum. Reprod. 20: 521-530.

Farmer, J. L. et al. 2008. Galectin 15 (LGALS15) functions in trophectoderm migration and attachment. FASEB J. 22: 548-560.

Feinman, R. D., and E. J. Fine. 2013. Fructose in perspective. Nutr. Metab. 10: 45-45.

Feng, L., and W. B. Frommer. 2015. Structure and function of SemiSWEET and SWEET sugar transporters. Trends Biochem. Sci.

Filatova, A. et al. 2009. Novel shuttling domain in a regulator (RSC1A1) of transporter SGLT1 steers cell cycle-dependent nuclear location. Traffic (Copenhagen, Denmark) 10: 1599-1618.

Fotiadis, D., Y. Kanai, and M. Palacin. 2013. The SLC3 and SLC7 families of amino acid transporters. Mol. Aspects Med. 34: 139-158.

Fowden, A. L., A. J. Forhead, M. Silver, and A. A. MacDonald. 1997. Glucose, lactate and oxygen metabolism in the fetal pig during late gestation. Exp. Physiol. 82: 171-182.

Fox, C. F., and E. P. Kennedy. 1965. Specific labeling and partial purification of the M protein, a component of the beta-galactoside transport system of Escherichia coli. Proc. Natl. Acad. Sci. U. S. A. 54: 891-899.

Frank, M., F. W. Bazer, W. W. Thatcher, and C. J. Wilcox. 1977. A study of prostaglandin F2alpha as the luteolysin in swine: III effects of estradiol valerate on prostaglandin F, progestins, estrone and estradiol concentrations in the utero-ovarian vein of nonpregnant gilts. Prostaglandins 14: 1183-1196.

Freking, B. A., K. A. Leymaster, J. L. Vallet, and R. K. Christenson. 2007. Number of fetuses and conceptus growth throughout gestation in lines of pigs selected for ovulation rate or uterine capacity. J. Anim. Sci. 85: 2093-2103.

Friess, A. E., F. Sinowatz, R. Skolek-Winnisch, and W. Traautner. 1980. The placenta of the pig. I. Finestructural changes of the placental barrier during pregnancy. Anat. Embryol. (Berl.) 158: 179-191.

Friess, A. E., F. Sinowatz, R. Skolek-Winnisch, and W. Trautner. 1981. The placenta of the pig. II. The ultrastructure of the areolae. Anat. Embryol. (Berl.) 163: 43-53.

Frolova, A. et al. 2009. Facilitative glucose transporter type 1 is differentially regulated by progesterone and estrogen in murine and human endometrial stromal cells. Endocrinology 150: 1512-1520.

Frolova, A. I., and K. H. Moley. 2011a. Glucose transporters in the uterus: an analysis of tissue distribution and proposed physiological roles. Reproduction 142: 211-220.

Frolova, A. I., and K. H. Moley. 2011b. Quantitative analysis of glucose transporter mRNAs in endometrial stromal cells reveals critical role of GLUT1 in uterine receptivity. Endocrinology 152: 2123-2128.

Funari, V. A., V. L. Herrera, D. Freeman, and D. R. Tolan. 2005. Genes required for fructose metabolism are expressed in Purkinje cells in the cerebellum. Brain Res. Mol. Brain Res. 142: 115-122.

Gabler, C., D. Chapman, and G. Killian. 2003. Expression and presence of osteopontin and integrins in the bovine oviduct during the oestrous cycle. Reproduction 126: 721-729.

Gaither, K., A. N. Quraishi, and N. P. Illsley. 1999. Diabetes alters the expression and activity of the human placental GLUT1 glucose transporter. J. Clin. Endocrinol. Metab. 84: 695-701.

Ganguly, A. et al. 2007. Glucose transporter isoform-3 mutations cause early pregnancy loss and fetal growth restriction. Am. J. Physiol. Endocrinol. Metab. 292: E1241-1255.

Gao, H., G. Wu, T. E. Spencer, G. A. Johnson, and F. W. Bazer. 2009a. Select Nutrients in the Ovine Uterine Lumen. II. Glucose Transporters in the Uterus and Peri-Implantation Conceptuses. Biol. Reprod. 80: 94-104.

Gao, H., G. Wu, T. E. Spencer, G. A. Johnson, and F. W. Bazer. 2009b. Select nutrients in the ovine uterine lumen. III. Cationic amino acid transporters in the ovine uterus and peri-implantation conceptuses. Biol. Reprod. 80: 602-609.

Gao, L. et al. 2012. Differential regulation of glucose transporters mediated by CRH receptor type 1 and type 2 in human placental trophoblasts. Endocrinology 153: 1464-1471.

Garlow, J. E. et al. 2002. Analysis of Osteopontin at the Maternal-Placental Interface in Pigs. Biol. Reprod. 66: 718-725.

Geisert, R. D. et al. 1993. Changes in oestrogen receptor protein, mRNA expression and localization in the endometrium of cyclic and pregnant gilts. Reprod. Fertil. Dev. 5: 247-260.

Geisert, R. D., J. W. Brookbank, R. M. Roberts, and F. W. Bazer. 1982a. Establishment of pregnancy in the pig: II. Cellular remodeling of the porcine blastocyst during elongation on day 12 of pregnancy. Biol. Reprod. 27: 941-955.

Geisert, R. D., T. N. Pratt, F. W. Bazer, J. S. Mayes, and G. H. Watson. 1994. Immunocytochemical localization and changes in endometrial progestin receptor protein during the porcine oestrous cycle and early pregnancy. Reprod. Fertil. Dev. 6: 749-760.

Geisert, R. D., R. H. Renegar, W. W. Thatcher, R. M. Roberts, and F. W. Bazer. 1982b. Establishment of pregnancy in the pig: I. Interrelationships between preimplantation development of the pig blastocyst and uterine endometrial secretions. Biol. Reprod. 27: 925-939.

Geisert, R. D., W. W. Thatcher, R. M. Roberts, and F. W. Bazer. 1982c. Establishment of pregnancy in the pig: III. Endometrial secretory response to estradiol valerate administered on day 11 of the estrous cycle. Biol. Reprod. 27: 957-965.

Giangrande, P. H., G. Pollio, and D. P. McDonnell. 1997. Mapping and characterization of the functional domains responsible for the differential activity of the A and B isoforms of the human progesterone receptor. J. Biol. Chem. 272: 32889-32900.

Godoy, A. et al. 2006. Differential subcellular distribution of glucose transporters GLUT1-6 and GLUT9 in human cancer: ultrastructural localization of GLUT1 and GLUT5 in breast tumor tissues. J. Cell. Physiol. 207: 614-627.

Goland, R. S. et al. 1993. Elevated levels of umbilical cord plasma corticotropin-releasing hormone in growth-retarded fetuses. J. Clin. Endocrinol. Metab. 77: 1174-1179.

Goldstein, M. H., F. W. Bazer, and D. H. Barron. 1980. Characterization of changes in volume, osmolarity and electrolyte composition of porcine fetal fluids during gestation. Biol. Reprod. 22: 1168-1180.

Goodwin, R. F. 1956. Division of the common mammals into two groups according to the concentration of fructose in the blood of the foetus. J. Physiol. 132: 146-156.

Goodwin, R. F. 1957. The relationship between the concentration of blood sugar and some vital body functions in the new-born pig. J. Physiol. 136: 208-217.

Gorboulev, V. et al. 2012. Na(+)-D-glucose cotransporter SGLT1 is pivotal for intestinal glucose absorption and glucose-dependent incretin secretion. Diabetes 61: 187-196.

Gould, G. W., H. M. Thomas, T. J. Jess, and G. I. Bell. 1991. Expression of human glucose transporters in Xenopus oocytes: kinetic characterization and substrate specificities of the erythrocyte, liver, and brain isoforms. Biochemistry 30: 5139-5145.

Gu, Y. R. et al. 2011. Evaluation of endogenous control genes for gene expression studies across multiple tissues and in the specific sets of fat- and muscle-type samples of the pig. Journal of animal breeding and genetics = Zeitschrift fur Tierzuchtung und Zuchtungsbiologie 128: 319-325.

Gude, N. M. et al. 2005. Expression of GLUT12 in the fetal membranes of the human placenta. Placenta 26: 67-72.

Gude, N. M. et al. 2003. GLUT12 expression in human placenta in first trimester and term. Placenta 24: 566-570.

Guillomot, M. 1995. Cellular interactions during implantation in domestic ruminants. J. Reprod. Fertil. Suppl. 49: 39-51.

Hahn, D. et al. 2001. From maternal glucose to fetal glycogen: expression of key regulators in the human placenta. Mol. Hum. Reprod. 7: 1173-1178.

Harrell, C. S., J. Burgado, S. D. Kelly, and G. N. Neigh. 2014. Ovarian Steroids Influence Cerebral Glucose Transporter Expression in a Region- and Isoform-Specific Pattern. J. Neuroendocrinol. 26: 217-225.

Haynes, N. B., and G. E. Lamming. 1967. The carbohydrate content of sow uterine flushings. J. Reprod. Fertil. 14: 335-337.

Hayward, B. E., and D. T. Bonthron. 1998. Structure and alternative splicing of the ketohexokinase gene. Eur. J. Biochem. 257: 85-91.

Hediger, M. A., M. J. Coady, T. S. Ikeda, and E. M. Wright. 1987. Expression cloning and cDNA sequencing of the Na+/glucose co-transporter. Nature 330: 379-381.

Henricks, D. M., H. D. Guthrie, and D. L. Handlin. 1972. Plasma estrogen, progesterone and luteinizing hormone levels during the estrous cycle in pigs. Biol. Reprod. 6: 210-218.

Hitchcock, M. W. 1949. Fructose in the sheep foetus. J. Physiol. 108: 117-126.

Huddleston, H., and D. J. Schust. 2004. Immune interactions at the maternal-fetal interface: a focus on antigen presentation. Am. J. Reprod. Immunol. 51: 283-289.

Huggett, A. S., F. L. Warren, and N. V. Warren. 1951. The origin of the blood fructose of the foetal sheep. J. Physiol. 113: 258-275.

Ibberson, M., M. Uldry, and B. Thorens. 2000. GLUTX1, a novel mammalian glucose transporter expressed in the central nervous system and insulin-sensitive tissues. J. Biol. Chem. 275: 4607-4612.

Ing, N. H., and M. B. Tornesi. 1997. Estradiol up-regulates estrogen receptor and progesterone receptor gene expression in specific ovine uterine cells. Biol. Reprod. 56: 1205-1215.

Iyer, N. V. et al. 1998. Cellular and developmental control of O2 homeostasis by hypoxia-inducible factor 1 alpha. Genes Dev. 12: 149-162.

Jalali, B. M., M. Bogacki, M. Dietrich, P. Likszo, and M. Wasielak. 2015. Proteomic analysis of porcine endometrial tissue during peri-implantation period reveals altered protein abundance. J. Proteomics.

Jansson, T., E. A. Cowley, and N. P. Illsley. 1995. Cellular localization of glucose transporter messenger RNA in human placenta. Reprod. Fertil. Dev. 7: 1425-1430.

Jansson, T., M. Wennergren, and N. P. Illsley. 1993. Glucose transporter protein expression in human placenta throughout gestation and in intrauterine growth retardation. J. Clin. Endocrinol. Metab. 77: 1554-1562.

Jansson, T., M. Wennergren, and T. L. Powell. 1999. Placental glucose transport and GLUT 1 expression in insulin-dependent diabetes. Am. J. Obstet. Gynecol. 180: 163-168.

Janzen, C. et al. 2013. Placental glucose transporter 3 (GLUT3) is up-regulated in human pregnancies complicated by late-onset intrauterine growth restriction. Placenta 34: 1072-1078.

Jauniaux, E., J. Hempstock, C. Teng, F. C. Battaglia, and G. J. Burton. 2005. Polyol Concentrations in the Fluid Compartments of the Human Conceptus during the First Trimester of Pregnancy: Maintenance of Redox Potential in a Low Oxygen Environment. The Journal of Clinical Endocrinology & Metabolism 90: 1171-1175.

Johnson, G. A. et al. 2009. Conceptus-uterus interactions in pigs: endometrial gene expression in response to estrogens and interferons from conceptuses. Society of Reproduction and Fertility supplement 66: 321-332.

Johnson, G. A. et al. 2001. Muc-1, Integrin, and Osteopontin Expression During the Implantation Cascade in Sheep. Biol. Reprod. 65: 820-828.

Johnson, G. A. et al. 2000. Progesterone modulation of osteopontin gene expression in the ovine uterus. Biol. Reprod. 62: 1315-1321.

Johnson, G. A. et al. 1999. Expression of the Interferon Tau Inducible Ubiquitin Cross-Reactive Protein in the Ovine Uterus. Biol. Reprod. 61: 312-318.

Joost, H.-G. et al. 2002. Nomenclature of the GLUT/SLC2A family of sugar/polyol transport facilitators.

Joyce, M. M. et al. 2008. Uterine MHC Class I Molecules and β2-Microglobulin Are Regulated by Progesterone and Conceptus Interferons during Pig Pregnancy. The Journal of Immunology 181: 2494-2505.

Joyce, M. M. et al. 2007. Pig conceptuses secrete estrogen and interferons to differentially regulate uterine STAT1 in a temporal and cell type-specific manner. Endocrinology 148: 4420-4431.

Joyce, M. M. et al. 2005. Interferon stimulated gene 15 conjugates to endometrial cytosolic proteins and is expressed at the uterine-placental interface throughout pregnancy in sheep. Endocrinology 146: 675-684.

Ka, H. et al. 2007. Regulation of expression of fibroblast growth factor 7 in the pig uterus by progesterone and estradiol. Biol. Reprod. 77: 172-180.

Kim, J., G. Song, G. Wu, and F. W. Bazer. 2012. Functional roles of fructose. Proceedings of the National Academy of Sciences 109: E1619–E1628.

Kim, S. T., and K. H. Moley. 2009. Regulation of facilitative glucose transporters and AKT/MAPK/PRKAA signaling via estradiol and progesterone in the mouse uterine epithelium. Biol. Reprod. 81: 188-198.

Kimber, S. J., I. M. Illingworth, and S. R. Glasser. 1995. Expression of carbohydrate antigens in the rat uterus during early pregnancy and after ovariectomy and steroid replacement. J. Reprod. Fertil. 103: 75-87.

Knapczyk-Stwora, K. et al. 2011. Expression of Oestrogen Receptor α and Oestrogen Receptor β in the Uterus of the Pregnant Swine. Reproduction in Domestic Animals 46: 1-7.

Knight, J. W., F. W. Bazer, W. W. Thatcher, D. E. Franke, and H. D. Wallace. 1977. Conceptus development in intact and unilaterally hysterectomized-ovariectomized gilts: interrelations among hormonal status, placental development, fetal fluids and fetal growth. J. Anim. Sci. 44: 620-637.

Knight, J. W., F. W. Bazer, and H. D. Wallace. 1973. Hormonal regulation of porcine uterine protein secretion. J. Anim. Sci. 36: 546-553.

Knight, J. W., F. W. Bazer, and H. D. Wallace. 1974. Effect of Progesterone Induced Increase in Uterine Secretory Activity on Development of the Porcine Conceptus. J. Anim. Sci. 39: 743-746.

Kobayashi, T. et al. 2002. Localization and physiological implication of aldose reductase and sorbitol dehydrogenase in reproductive tracts and spermatozoa of male rats. J. Androl. 23: 674-683.

Komor, E., and W. Tanner. 1974. The hexose-proton symport system of Chlorella vulgaris. Specificity, stoichiometry and energetics of sugar-induced proton uptake. Eur. J. Biochem. 44: 219-223.

Korgun, E. T., C. Celik-Ozenci, Y. Seval, G. Desoye, and R. Demir. 2005. Do glucose transporters have other roles in addition to placental glucose transport during early pregnancy? Histochem. Cell Biol. 123: 621-629.

Korgun, E. T. et al. 2001. Glucose transporter expression in rat embryo and uterus during decidualization, implantation, and early postimplantation. Biol. Reprod. 65: 1364-1370.

Kozera, B., and M. Rapacz. 2013. Reference genes in real-time PCR. J Appl Genetics 54: 391-406.

Kuijk, E. et al. 2007. Validation of reference genes for quantitative RT-PCR studies in porcine oocytes and preimplantation embryos. BMC Dev Biol 7: 58.

La Bonnardiere, C. et al. 1991. Production of two species of interferon by Large White and Meishan pig conceptuses during the peri-attachment period. J. Reprod. Fertil. 91: 469-478.

Lanaspa, M. A. et al. 2014. Endogenous fructose production and fructokinase activation mediate renal injury in diabetic nephropathy. J. Am. Soc. Nephrol. 25: 2526-2538.

Lanaspa, M. A. et al. 2013. Endogenous fructose production and metabolism in the liver contributes to the development of metabolic syndrome. Nat Commun 4: 2434.

Lanaspa, M. A. et al. 2012. Uric acid stimulates fructokinase and accelerates fructose metabolism in the development of fatty liver. PLoS One 7: e47948.

Lanoix, D. et al. 2012. Quantitative PCR Pitfalls: The Case of the Human Placenta. Mol. Biotechnol. 52: 234-243.

Lefèvre, F., M. Guillomot, S. D'Andréa, S. Battegay, and C. La Bonnardière. 1998. Interferon-delta: The first member of a novel type I interferon family. Biochimie 80: 779-788.

Leiser, R., and V. Dantzer. 1988. Structural and functional aspects of porcine placental microvasculature. Anat. Embryol. (Berl.) 177: 409-419.

Leiser, R., and V. Dantzer. 1994. Initial vascularisation in the pig placenta: II. Demonstration of gland and areola-gland subunits by histology and corrosion casts. Anat. Rec. 238: 326-334.

Lesage, J. et al. 2002. Maternal undernutrition during late gestation-induced intrauterine growth restriction in the rat is associated with impaired placental GLUT3 expression, but does not correlate with endogenous corticosterone levels. J. Endocrinol. 174: 37-43.

Lessey, B. A. 2002. Adhesion molecules and implantation. J. Reprod. Immunol. 55: 101-112.

Limesand, S. W., T. R. H. Regnault, and W. W. Hay Jr. 2004. Characterization of Glucose Transporter 8 (GLUT8) in the Ovine Placenta of Normal and Growth Restricted Fetuses. Placenta 25: 70-77.

Livak, K. J., and T. D. Schmittgen. 2001. Analysis of relative gene expression data using real-time quantitative PCR and the 2(-Delta Delta C(T)) Method. Methods 25: 402-408.

Loo, D. D., T. Zeuthen, G. Chandy, and E. M. Wright. 1996. Cotransport of water by the Na+/glucose cotransporter. Proc. Natl. Acad. Sci. U. S. A. 93: 13367-13370.

Mamo, S., A. B. Gal, S. Bodo, and A. Dinnyes. 2007. Quantitative evaluation and selection of reference genes in mouse oocytes and embryos cultured in vivo and in vitro. BMC Dev. Biol. 7: 14.

Martinez-Giner, M., J. L. Noguera, I. Balcells, A. Fernandez-Rodriguez, and R. N. Pena. 2013. Selection of internal control genes for real-time quantitative PCR in ovary and uterus of sows across pregnancy. PLoS One 8: e66023.

Mateo, R. D. et al. 2007. Dietary L-arginine supplementation enhances the reproductive performance of gilts. J. Nutr. 137: 652-656.

Mathew, D. J. et al. 2011. Uterine progesterone receptor expression, conceptus development, and ovarian function in pigs treated with RU 486 during early pregnancy. Biol. Reprod. 84: 130-139.

Mattson, B. A., E. W. Overstrom, and D. F. Albertini. 1990. Transitions in trophectoderm cellular shape and cytoskeletal organization in the elongating pig blastocyst. Biol. Reprod. 42: 195-205.

McGowan, J. E., P. W. Aldoretta, and W. W. Hay, Jr. 1995. Contribution of fructose and lactate produced in placenta to calculation of fetal glucose oxidation rate. Am. J. Physiol. 269: E834-839.

McPherson, R. L., F. Ji, G. Wu, J. R. Blanton, Jr., and S. W. Kim. 2004. Growth and compositional changes of fetal tissues in pigs. J. Anim. Sci. 82: 2534-2540.

Meznarich, H. K., W. W. Hay, Jr., J. W. Sparks, G. Meschia, and F. C. Battaglia. 1987. Fructose disposal and oxidation rates in the ovine fetus. Q. J. Exp. Physiol. 72: 617-625.

Michael, K., B. S. Ward, and W. M. Moore. 1983. Gestational changes in pig placental weight, area and DNA content in the second half of pregnancy. Placenta 4: 369-378.

Mirando, M. A. et al. 1990. Onset of secretion of proteins with antiviral activity by pig conceptuses. J. Reprod. Fertil. 88: 197-203.

Mirando, M. A. et al. 1995. A proposed role for oxytocin in regulation of endometrial prostaglandin F2 alpha secretion during luteolysis in swine. Adv. Exp. Med. Biol. 395: 421-433.

Moeljono, M. P., F. W. Bazer, and W. W. Thatcher. 1976. A study of prostaglandin F2alpha as the luteolysin in swine: I. Effect of prostaglandin F2alpha in hysterectomized gilts. Prostaglandins 11: 737-743.

Mueckler, M., and B. Thorens. 2013. The SLC2 (GLUT) family of membrane transporters. Mol. Aspects Med. 34: 121-138.

Mulac-Jericevic, B., and O. M. Conneely. 2004. Reproductive tissue selective actions of progesterone receptors. Reproduction 128: 139-146.

Nishimura, M., and S. Naito. 2005. Tissue-specific mRNA expression profiles of human ATP-binding cassette and solute carrier transporter superfamilies. Drug Metab. Pharmacokinet. 20: 452-477.

Nygard, A.-B., C. Jorgensen, S. Cirera, and M. Fredholm. 2007. Selection of reference genes for gene expression studies in pig tissues using SYBR green qPCR. BMC Mol. Biol. 8: 67.

Obermeier, S., B. Huselweh, H. Tinel, R. H. Kinne, and C. Kunz. 2000. Expression of glucose transporters in lactating human mammary gland epithelial cells. Eur. J. Nutr. 39: 194-200.

Oestrup, O. et al. 2009. From Zygote to Implantation: Morphological and Molecular Dynamics during Embryo Development in the Pig. Reproduction in Domestic Animals 44: 39-49.

Olson, A. L., and J. E. Pessin. 1996. Structure, function, and regulation of the mammalian facilitative glucose transporter gene family. Annu. Rev. Nutr. 16: 235-256.

Pastel, E., J. C. Pointud, F. Volat, A. Martinez, and A. M. Lefrancois-Martinez. 2012. Aldo-Keto Reductases 1B in Endocrinology and Metabolism. Front. Pharmacol. 3: 148.

Patten, B. 1948. Embryology of the Pig. Third ed. McGraw-Hill Book Company, New York.

Penning, T. M. 2015. The aldo-keto reductases (AKRs): Overview. Chem. Biol. Interact. 234: 236-246.

Pere, M. C. 1995. Maternal and fetal blood levels of glucose, lactate, fructose, and insulin in the conscious pig. J. Anim. Sci. 73: 2994-2999.

Pere, M. C. 2003. Materno-foetal exchanges and utilisation of nutrients by the foetus: comparison between species. Reprod. Nutr. Dev. 43: 1-15.

Perry, J. S. 1981. The mammalian fetal membranes. J. Reprod. Fertil. 62: 321-335.

Perry, J. S., and P. R. Crombie. 1982. Ultrastructure of the uterine glands of the pig. J. Anat. 134: 339-350.

Peters, I. R., C. R. Helps, E. J. Hall, and M. J. Day. 2004. Real-time RT-PCR: considerations for efficient and sensitive assay design. J. Immunol. Methods 286: 203-217.

Phay, J. E., H. B. Hussain, and J. F. Moley. 2000. Cloning and expression analysis of a novel member of the facilitative glucose transporter family, SLC2A9 (GLUT9). Genomics 66: 217-220.

Pruneda, A., E. Pinart, S. Bonet, C. H. Yeung, and T. G. Cooper. 2006. Study of the polyol pathway in the porcine epididymis. Mol. Reprod. Dev. 73: 859-865.

Pujol-Gimenez, J., A. Perez, A. M. Reyes, D. D. Loo, and M. P. Lostao. 2015. Functional characterization of the human facilitative glucose transporter 12 (GLUT12) by electrophysiological methods. Am. J. Physiol. Cell Physiol. 308: C1008-1022.

Pusateri, A. E., M. F. Rothschild, C. M. Warner, and S. P. Ford. 1990. Changes in morphology, cell number, cell size and cellular estrogen content of individual

littermate pig conceptuses on days 9 to 13 of gestation. J. Anim. Sci. 68: 3727-3735.

Radonic, A. et al. 2004. Guideline to reference gene selection for quantitative real-time PCR. Biochem. Biophys. Res. Commun. 313: 856-862.

Raja, M., and R. K. Kinne. 2012. Structural insights into genetic variants of Na(+)/glucose cotransporter SGLT1 causing glucose-galactose malabsorption: vSGLT as a model structure. Cell Biochem. Biophys. 63: 151-158.

Raja, M., T. Puntheeranurak, P. Hinterdorfer, and R. Kinne. 2012. SLC5 and SLC2 transporters in epithelia-cellular role and molecular mechanisms. Curr Top Membr 70: 29-76.

Rama, F., M. A. Castellano, N. I. Germino, M. Micucci, and C. Ohanian. 1973. Histochemical location of ketose-reductase in the placenta and fetal tissues. J. Anat. 114: 109-113.

Ramsay, T. G., J. A. Sheahan, and R. J. Martin. 1984. Comparison of lactate and glucose metabolism in the developing porcine placenta. Am. J. Physiol. 247: R755-760.

Randall, G. C. 1977. Daily changes in the blood of conscious pigs with catheters in foetal and uterine vessels during late gestation. J. Physiol. 270: 719-731.

Renegar, R. H., F. W. Bazer, and R. M. Roberts. 1982. Placental transport and distribution of uteroferrin in the fetal pig. Biol. Reprod. 27: 1247-1260.

Ritacco, G., S. V. Radecki, and P. A. Schoknecht. 1997. Compensatory growth in runt pigs is not mediated by insulin-like growth factor I. J. Anim. Sci. 75: 1237-1243.

Roberts, R. M., and F. W. Bazer. 1988. The functions of uterine secretions. J. Reprod. Fertil. 82: 875-892.

Romero, A., O. Gomez, J. Terrado, and J. E. Mesonero. 2009. Expression of GLUT8 in mouse intestine: identification of alternative spliced variants. J. Cell. Biochem. 106: 1068-1078.

Rosario, F. J., Y. Kanai, T. L. Powell, and T. Jansson. 2015. Increased placental nutrient transport in a novel mouse model of maternal obesity with fetal overgrowth. Obesity (Silver Spring) 23: 1663-1670.

Ross, J. W. et al. 2010. Activation of the transcription factor, nuclear factor kappa-B, during the estrous cycle and early pregnancy in the pig. Reprod. Biol. Endocrinol. 8: 39.

Ross, J. W. et al. 2007. Premature estrogen exposure alters endometrial gene expression to disrupt pregnancy in the pig. Endocrinology 148: 4761-4773.

Sabolic, I. et al. 2012. Expression of Na+-D-glucose cotransporter SGLT2 in rodents is kidney-specific and exhibits sex and species differences. Am. J. Physiol. Cell Physiol. 302: C1174-1188.

Sancho, S. et al. 2007. Effects of cryopreservation on semen quality and the expression of sperm membrane hexose transporters in the spermatozoa of Iberian pigs. Reproduction 134: 111-121.

Sartorius, C. A. et al. 1994. A third transactivation function (AF3) of human progesterone receptors located in the unique N-terminal segment of the B-isoform. Mol. Endocrinol. 8: 1347-1360.

Scheepers, A. et al. 2005. Characterization of the human SLC2A11 (GLUT11) gene: alternative promoter usage, function, expression, and subcellular distribution of three isoforms, and lack of mouse orthologue. Mol. Membr. Biol. 22: 339-351.

Schultz, S. G., and P. F. Curran. 1970. Coupled transport of sodium and organic solutes. Physiol. Rev. 50: 637-718.

Sciullo, E. et al. 1997. Glucose transporter (Glut1, Glut3) mRNA in human placenta of diabetic and non-diabetic pregnancies. Early Pregnancy 3: 172-182.

Self, J. T. et al. 2004. Glutamine synthesis in the developing porcine placenta. Biol. Reprod. 70: 1444-1451.

Seo, H., Y. Choi, J. Shim, M. Kim, and H. Ka. 2012. Analysis of the Lysophosphatidic Acid-Generating Enzyme ENPP2 in the Uterus During Pregnancy in Pigs. Biol. Reprod. 87: 77, 71-78.

Seo, H., Y. Choi, J. Shim, I. Yoo, and H. Ka. 2014. Comprehensive Analysis of Prostaglandin Metabolic Enzyme Expression During Pregnancy and the Characterization of AKR1B1 as a Prostaglandin F Synthase at the Maternal-Conceptus Interface in Pigs. Biol. Reprod. 90: 99, 91-13.

Shibutani, M., J. Lee, T. Miyano, and M. Miyake. 2015. Demands for carbohydrates as major energy substrates depend on the preimplantation developmental stage in pig embryos: Differential use of fructose by parthenogenetic diploids before and after the 4-cell stage in the pig. J Reprod Dev 61: 106-115.

Sistrom, W. R. 1958. On the physical state of the intracellularly accumulates substrates of beta-galactoside-permease in Escherichia coli. Biochim. Biophys. Acta 29: 579-587.

Smith, D. E., and J. Gorski. 1968. Extrogen control of uterine glucose metabolism. An analysis based on the transport and phosphorylation of 2-deoxyglucose. J. Biol. Chem. 243: 4169-4174.

Soede, N. M., P. Langendijk, and B. Kemp. 2011. Reproductive cycles in pigs. Anim. Reprod. Sci. 124: 251-258.

Song, G. et al. 2010. Cathepsin B, cathepsin L, and cystatin C in the porcine uterus and placenta: potential roles in endometrial/placental remodeling and in fluid-phase transport of proteins secreted by uterine epithelia across placental areolae. Biol. Reprod. 82: 854-864.

Spencer, T. E., R. C. Burghardt, G. A. Johnson, and F. W. Bazer. 2004. Conceptus signals for establishment and maintenance of pregnancy. Anim. Reprod. Sci. 82-83: 537-550.

Sukjumlong, S., A.-M. Dalin, L. Sahlin, and E. Persson. 2005. Immunohistochemical studies on the progesterone receptor (PR) in the sow uterus during the oestrous cycle and in inseminated sows at oestrus and early pregnancy. Reproduction 129: 349-359.

Teng, C. C., S. Tjoa, P. V. Fennessey, R. B. Wilkening, and F. C. Battaglia. 2002. Transplacental Carbohydrate and Sugar Alcohol Concentrations and Their Uptakes in Ovine Pregnancy. Exp. Biol. Med. 227: 189-195.

Thorens, B., and M. Mueckler. 2010. Glucose transporters in the 21st Century.

Tilley, R. E., C. J. McNeil, C. J. Ashworth, K. R. Page, and H. J. McArdle. 2007. Altered muscle development and expression of the insulin-like growth factor system in growth retarded fetal pigs. Domest. Anim. Endocrinol. 32: 167-177.

Tomioka, S. 2012. Water transport by glucose transporter type 3 expressed in Xenopus oocytes. Neuroreport 23: 21-25.

Tung, E. et al. 2012. Increased placental nutrient transporter expression at midgestation after maternal growth hormone treatment in pigs: a placental mechanism for increased fetal growth. Biol. Reprod. 87: 126.

Turner, R. J., and A. Moran. 1982. Further studies of proximal tubular brush border membrane D-glucose transport heterogeneity. J. Membr. Biol. 70: 37-45.

Uldry, M., and B. Thorens. 2004. The SLC2 family of facilitated hexose and polyol transporters. Pflugers Arch. 447: 480-489.

Ullrey, D. E., J. I. Sprague, D. E. Becker, and E. R. Miller. 1965. GROWTH OF THE SWINE FETUS. J. Anim. Sci. 24: 711-717.

Untergasser, A. et al. 2007. Primer3Plus, an enhanced web interface to Primer3. Nucleic Acids Res. 35: W71-74.

Vallet, J. L., and B. A. Freking. 2007. Differences in placental structure during gestation associated with large and small pig fetuses. J. Anim. Sci. 85: 3267-3275.

Vallet, J. L., H. G. Klemcke, and R. K. Christenson. 2002. Interrelationships among conceptus size, uterine protein secretion, fetal erythropoiesis, and uterine capacity. J. Anim. Sci. 80: 729-737.

Vallet, J. L., A. K. McNeel, J. R. Miles, and B. A. Freking. 2014. Placental accommodations for transport and metabolism during intra-uterine crowding in pigs. Journal of animal science and biotechnology 5: 55.

Vallet, J. L., J. R. Miles, and B. A. Freking. 2009. Development of the pig placenta. Society of Reproduction and Fertility supplement 66: 265-279.

van der Lende, T., E. F. Knol, and J. I. Leenhouwers. 2001. Prenatal development as a predisposing factor for perinatal losses in pigs. Reproduction (Cambridge, England) Supplement 58: 247-261.

van der Lende, T., and B. T. van Rens. 2003. Critical periods for foetal mortality in gilts identified by analysing the length distribution of mummified foetuses and frequency of non-fresh stillborn piglets. Anim. Reprod. Sci. 75: 141-150.

Vandesompele, J. et al. 2002a. Accurate normalization of real-time quantitative RT-PCR data by geometric averaging of multiple internal control genes. Genome Biol 3: 34.

Vandesompele, J. et al. 2002b. Accurate normalization of real-time quantitative RT-PCR data by geometric averaging of multiple internal control genes. Genome Biol. 3: RESEARCH0034.

von Wolff, M., S. Ursel, U. Hahn, R. Steldinger, and T. Strowitzki. 2003. Glucose transporter proteins (GLUT) in human endometrium: expression, regulation, and function throughout the menstrual cycle and in early pregnancy. J. Clin. Endocrinol. Metab. 88: 3885-3892.

Wang, S., J. Li, A. Zhang, M. Liu, and H. Zhang. 2011. Selection of reference genes for studies of porcine endometrial gene expression on gestational day 12. Biochem. Biophys. Res. Commun. 408: 265-268.

Wei, L. L., B. M. Norris, and C. J. Baker. 1997. An N-terminally truncated third progesterone receptor protein, PR(C), forms heterodimers with PR(B) but interferes in PR(B)-DNA binding. J. Steroid Biochem. Mol. Biol. 62: 287-297.

Welch, R. D., and J. Gorski. 1999. Regulation of glucose transporters by estradiol in the immature rat uterus. Endocrinology 140: 3602-3608.

Wetendorf, M., and F. J. DeMayo. 2014. Progesterone receptor signaling in the initiation of pregnancy and preservation of a healthy uterus. Int. J. Dev. Biol. 58: 95-106.

White, C. E., E. L. Piper, and P. R. Noland. 1979. Conversion of Glucose to Fructose in the Fetal Pig. J. Anim. Sci. 48: 585-590.

White, C. E., E. L. Piper, P. R. Noland, and L. B. Daniels. 1982. Fructose Utilization for Nucleic Acid Synthesis in the Fetal Pig. J. Anim. Sci. 55: 73-76.

White, F. J. et al. 2005. Steroid regulation of cell specific secreted phosphoprotein 1 (osteopontin) expression in the pregnant porcine uterus. Biol. Reprod. 73: 1294-1301.

Widdowson, E. M. 1971. Intra-uterine growth retardation in the pig. I. Organ size and cellular development at birth and after growth to maturity. Biol. Neonate 19: 329-340.

Wilson, M. E., K. A. Vonnahme, and S. P. Ford. 2001. The role of altered uterine-embryo synchrony on conceptus growth in the pig. J. Anim. Sci. 79: 1863-1867.

Wislocki, G. B., and E. W. Dempsey. 1946. Histochemical reactions of the placenta of the pig. Am. J. Anat. 78: 181-225.

Wright, E. M., D. D. Loo, and B. A. Hirayama. 2011. Biology of human sodium glucose transporters. Physiol. Rev. 91: 733-794.

Wright, E. M., D. D. Loo, B. A. Hirayama, and E. Turk. 2004. Surprising versatility of Na+-glucose cotransporters: SLC5. Physiology (Bethesda) 19: 370-376.

Wu, G. et al. 2013. Impacts of arginine nutrition on embryonic and fetal development in mammals. Amino Acids 45: 241-256.

Wu, G., F. W. Bazer, and W. Tou. 1995. Developmental changes of free amino acid concentrations in fetal fluids of pigs. J. Nutr. 125: 2859-2868.

Wu, G., and S. M. Morris, Jr. 1998. Arginine metabolism: nitric oxide and beyond. Biochem. J. 336 (Pt 1): 1-17.

Yamaguchi, M., M. Sakata, K. Ogura, and A. Miyake. 1996. Gestational changes of glucose transporter gene expression in the mouse placenta and decidua. J. Endocrinol. Invest. 19: 567-569.

Yoshikawa, T. et al. 2011. Comparative expression of hexose transporters (SGLT1, GLUT1, GLUT2 and GLUT5) throughout the mouse gastrointestinal tract. Histochem. Cell Biol. 135: 183-194.

Zavy, M. T., W. R. Clark, D. C. Sharp, R. M. Roberts, and F. W. Bazer. 1982. Comparison of glucose, fructose, ascorbic acid and glucosephosphate isomerase enzymatic activity in uterine flushings from nonpregnant and pregnant gilts and pony mares. Biol. Reprod. 27: 1147-1158.

Zeuthen, T. 2010. Water-transporting proteins. J. Membr. Biol. 234: 57-73.

Zeuthen, T., E. Zeuthen, and N. Macaulay. 2007. Water transport by GLUT2 expressed in Xenopus laevis oocytes. J. Physiol. 579: 345-361.

Zhao, F. Q., and A. F. Keating. 2007a. Expression and regulation of glucose transporters in the bovine mammary gland. J. Dairy Sci. 90 Suppl 1: E76-86.

Zhao, F. Q., and A. F. Keating. 2007b. Functional properties and genomics of glucose transporters. Curr Genomics 8: 113-128.

Zopf, S. et al. 2009. Localization of the polyol pathway in the human kidney. Histol. Histopathol. 24: 447-455.

APPENDIX A

EXPRESSION OF PROGESTERONE RECEPTOR, PHOSPHATASE ACID TYPE 5 TARTRATE-RESISTANT, AND SECRETED PHOSPOPROTEIN 1 PROTEINS IN THE UTERUS AND PLACENTA OF PIGS THROUGHOUT GESTATION

Introduction

Progesterone (P4), the hormone of pregnancy, is produced by the corpus luteum and is required to maintain a successful pregnancy in the pig. P4 is a steroid hormone that exerts its actions on tissues through the progesterone receptor (PGR), which is encoded by a single gene, *PGR*, but has three isoforms (A, B, and C) with differing lengths and activities (Wetendorf and DeMayo, 2014). PGR is a classical nuclear receptor that binds P4, dimerizes, enters the nucleus, and binds DNA at progesterone response element domains to promote transcription of target genes, although P4 acting via its PGR can also inhibit transcription of some target genes (Mulac-Jericevic and Conneely, 2004).

Of the three PGR isoforms, B is the most transcriptionally active due to an additional activation domain (AF-3) in the amino terminus (Sartorius et al., 1994). PGRA has more inhibitory effects due to an active transcription inhibitory domain, which is blocked in PGRB (Giangrande et al., 1997). The third isoform, PGRC, is a truncated version of PGRA and PGRB with no amino terminus containing the main activation domain or the DNA binding domain. Therefore, PGRC cannot bind DNA directly, but can still bind P4 and dimerize, leading to the hypothesis that it has a role in sequestering ligand or the other isoforms to decrease P4 signaling (Wei et al., 1997).

Both PGRA and PGRB have been studied extensively in multiple species to determine their roles in the uterus during pregnancy, but the role of PGRC is still an enigma (Wetendorf and DeMayo, 2014).

Previous studies have described PGR localization in pigs during the estrous cycle and early pregnancy, but not beyond Day 18 of pregnancy (Geisert et al., 1994; Sukjumlong et al., 2005). Progesterone receptor B (PGRB) protein is expressed in the uterine LE, GE, stroma, and myometrium through Day 7 of the estrous cycle and pregnancy. During both the estrous cycle and pregnancy, prolonged exposure to P4 downregulated PGRB in uterine LE by Day 10 and in uterine GE by Day 12 (Ka et al., 2007). PGR is detected in the stroma and myometria through Day 18 of the estrous cycle and pregnancy. Progesterone receptor A (PGRA) protein has been detected by western blot in endometria from Days 0 to 10 of the estrous cycle and pregnancy (Geisert et al., 1994).

In addition to inducing uterine quiescence and suppressing uterine immune responses during pregnancy, P4 stimulates the production and secretion of histotroph, a complex mixture of hormones, growth factors, nutrients, and other substances that are required for growth and development of the conceptus (Knight et al., 1974; Roberts and Bazer, 1988; Bailey et al., 2010a). Two major protein components of histotroph, acid phosphatase 5 tartrate resistant (ACP5; uteroferrin) and secreted phosphoprotein 1 (SPP1; osteopontin), are produced and secreted by uterine GE during pregnancy in pigs (Renegar et al., 1982; Garlow et al., 2002). ACP5 is induced during the peri-implantation period in uterine GE by P4, while SPP1 is induced in uterine LE by

estrogen during the peri-implantation period, but induction in the GE between Days 30 and 40 is not solely dependent on P4 in pigs (Chen et al., 1973; Knight et al., 1973; Bailey et al., 2010a). P4 induces the production of histotroph through effects mediated via PGR; however, PGR are not expressed in uterine epithelia of mammals from just prior to implantation. At present, the mechanism of action of P4 to regulate functions of uterine epithelia is still unknown.

Therefore, the aim of this study was to quantify total endometrial mRNA and localize PGR protein in cells of the uterus throughout the estrous cycle and pregnancy in pigs. In addition, two well-established proteins in histotroph, ACP5 and SPP1, were localized in porcine uterine and placental tissues throughout gestation to gain physiological insight into the relationship between the pattern of PGR expression during mid- to late-pregnancy and the patterns of expression of ACP5 and SPP1.

Materials and Methods

Animals and Tissue Collection

Sexually mature, 8-month-old crossbred gilts were observed daily for estrus (Day 0) and exhibited at least two estrous cycles of normal duration (18 to 21 days) before being used in these studies. All experimental and surgical procedures were in compliance with the Guide for Care and Use of Agricultural Animals in Teaching and Research and approved by the Institutional Animal Care and Use Committee of Texas A&M University.

To evaluate the effects of pregnancy on temporal and cell-specific expression of mRNAs and proteins for PGR, ACP5, and SPP1, gilts were assigned randomly to either cyclic or pregnant status. Cyclic gilts were ovariohysterectomized on either Day 5, 9, 11, 13, 15 or 17 of the estrous cycle. Gilts in the pregnant group were bred and ovariohysterectomized on either Day 9, 11, 12, 13, 15, 17, 20, 25, 30, 35, 40, 50, 60, or 85 of pregnancy (n = 3 or 4 gilts/day/status). The lumen of each uterine horn of each gilt collected between Days 5 and 17 post-estrus was flushed with 20 ml physiological saline and flushings from mated gilts were examined for morphologically normal conceptuses. Tissue sections (~1cm thick) from the middle of each uterine horn of all hysterectomized gilts were fixed in fresh 4% paraformaldehyde in PBS (pH 7.2) and embedded in Paraplast-Plus (Oxford Laboratory, St. Louis, MO). Additionally, endometrium was physically dissected from the myometrium, snap-frozen in liquid nitrogen, and stored at -80°C for RNA extraction.

Progesterone Model

To evaluate effects of long-term P4 treatment without ovarian hormones on endometrial expression of PGR mRNA and localization of PGR protein, gilts were ovariectomized on Day 12 of the estrous cycle and assigned randomly to receive daily intramuscular injections of either corn oil (CO, 4 ml) or P4 (200 mg in 4 ml CO) on Days 12 through 39 post-estrus (n = 3/treatment) (Bailey et al., 2010c). All gilts were hysterectomized on Day 40 post-estrus and tissues collected as previously described.

RNA Extraction, cDNA Synthesis, and Primer Design

Total RNA was extracted from endometrial tissue samples using Trizol reagent (Life Technologies, Carlsbad, CA) according to manufacturer's recommendations (Appendix B). First strand cDNA was synthesized using Superscript III First Strand Kit (Life Technologies, Carlsbad, CA) according to manufacturer's instructions (Appendix B). First strand cDNA was diluted 10x for the qPCR reaction. Primers for qPCR were designed using NCBI Genbank sequences and Primer-BLAST (http://www.ncbi.nlm.nih.gov/). Primers were submitted to BLAST to test for specificity against the known porcine genome. The *PGR* forward 5'-GTGTCCTTACCTGTGGGAGC-3' and reverse 5'- TTCTAAGGCGACAAGCTGGG-3' primers were developed from NCBI reference NM_001166488.1 and have a product length of 138 nucleotides. Primer information for reference genes can be found in Table 5.1.

Quantitative PCR

Quantitative PCR assays were performed as previously described (Chapter III and Appendix B of this dissertation). Briefly, PerfeCta SYBR Green Mastermix (Quanta) was used in 10µl reactions with 2.5mM of each specific primer, on a Roche 480 Lightcycler (Roche) with approximately 60ng of cDNA per reaction. The PCR program began with 5 min at 95°C followed by 40 cycles of 95°C denaturation for 10 sec and 60°C annealing/extension for 30 sec. A melt curve was produced with every run to verify a single gene-specific peak. Standard curves with 2-fold serial dilutions were

run to determine primer efficiencies. All primer correlation coefficients were greater than 0.95 and efficiencies were 95-102%. The geometric mean of *TBP*, *SDHA*, and *ACTB* was used to normalize gene expression in endometrial tissue.

Immunohistochemistry

PGR, SPP1, and ACP5 proteins were immunolocalized in porcine uterine and conceptus tissues as described previously (Joyce et al., 2005)(Appendix B). A rabbit anti-human PGRA/PGRB polyclonal IgG (catalog no. RB-9017-P0; Thermo Fisher Scientific) was used at 5 µg/ml with a boiling citrate buffer antigen retrieval. A rabbit anti-bovine SPP1 affinity-purified polyclonal IgG was used at 25 µg/ml with a boiling citrate buffer antigen retrieval (Gabler et al., 2003). A rabbit anti-porcine ACP5 polyclonal IgG was used at 5 µg/ml with a boiling citrate buffer antigen retrieval (Chen et al., 1975; Bailey et al., 2010a). Purified non-relevant rabbit IgG, at a concentration equal to that for the primary IgG, was used as the negative control. Immunoreactive protein was visualized in paraffin-embedded sections (5µm thick) using the Vectastain ABC Kit (catalog no. PK-4001; Vector Laboratories, Inc., Burlingame, CA) according to kit instructions with 3,3'-diaminobenzidine tetrahydrochloride (catalog no. D5637; Sigma-Aldrich, St. Louis, MO) as the color substrate. Sections immunostained for SPP1 and ACP5 were counterstained with Harris modified hematoxylin (Fisher Scientific), whereas sections immunostained for PGRA/PGRB were not counterstained. Coverslips were affixed using Permount mounting medium (Fisher Scientific). Digital images of representative fields of immune-stained tissue were examined and recorded under bright-

field illumination using an Axioplan 2 microscope (Carl Zeiss, Thornwood, NY) interfaced with an Axioplan HR digital camera and Axiovision 4.3 software. Photographic plates were assembled using Adobe Photoshop (version 6.0, Adobe Systems Inc., San Jose, CA).

Statistical Analyses

The qPCR data for normal tissues were analyzed for effects of day, pregnancy status, and their interaction for Days 9, 11, 13, 15 and 17 by 2-way ANOVA via the General Linear Models (GLM) procedures of the Statistical Analysis System (SAS Institute, Cary, NC) with the least significant difference (LSD) multiple testing method. The qPCR data were also subjected to a sliding time window linear regression analysis to determine if there was an effect of day of gestation on the gene expression for the genes of interest throughout pregnancy (Days 9 to 85). The sliding time windows of the analysis were designed to detect effect of day on gene expression during three biologically relevant periods of time: the beginning, the middle, and the end of the study period. Each window analyzed contained a minimum of three days. Some windows contained greater than three days as long as the regression model showed a non-decreased performance in terms of the r^2 and the p-value of the F-statistics.

Results

Endometrial Expression of PGR Throughout Gestation

Endometrial expression of *PGR* mRNA was highest at Day 5 of the estrous cycle, decreased to Day 11, then increased again to Day 17 (Figure A.1; day x status $p<0.01$). Endometrial expression of *PGR* mRNA decreased from Days 13 to 40 of pregnancy ($r^2=0.847$, $p<0.01$). Endometria from gilts treated with P4 for 28 days had lower expression of *PGR* mRNA than that for CO-treated gilts (Figure A.2; $p<0.05$).

The antibody used to detect PGR in the present study was generated against both PGRA and PGRB antigens, but will be referred to as PGR. PGR protein was localized to uterine LE, GE, stroma, and myometrium on Day 5 of the estrous cycle and expression was maintained in those cells through Day 11 (Figure A.3). On Day 12, PGR protein was no longer detectable in uterine LE or superficial GE, but PGR protein was detected in the stroma, myometrium, and deep GE through Day 17 of the estrous cycle.

PGR protein was localized to uterine LE, GE, stroma, and myometrium on Day 9 of pregnancy with expression in LE being undetectable by Day 11 (Figure A.4), but expression of PGR was maintained in GE, stroma, and myometrium through Day 17 of pregnancy with deep GE appearing to have stronger immunostaining than superficial GE.

At Day 25, PGR protein was detected in some, but not all uterine GE, and GE in close proximity to areolae had stronger expression of PGR protein (Figure A.5 and Figure A.8). At Day 40, the proportion of cells in the GE with detectable PGR decreased

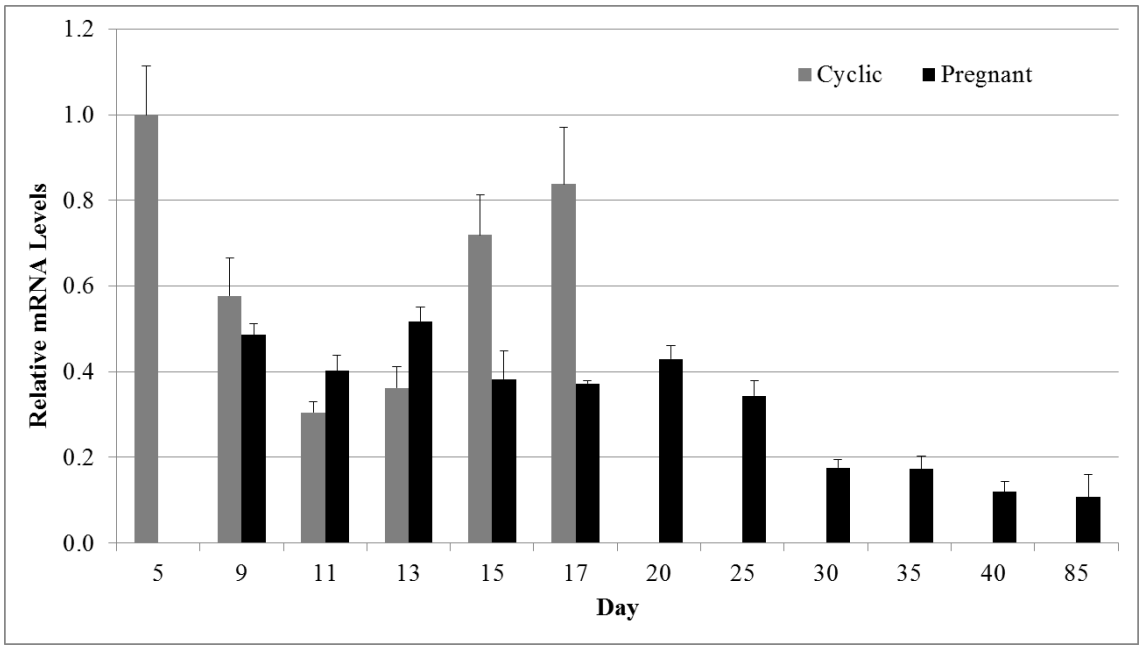

Figure A.1 Expression of *PGR* mRNA in endometrial tissue during the estrous cycle and pregnancy in pigs

Expression of *PGR* mRNA was greatest at Day 5, decreased until Day 11 during the estrous cycle, then increased again to Day 17 (day x status $p<0.01$). *PGR* mRNA in pregnant endometria decreased from Days 13 to 40 ($r^2=0.847$, $p<0.01$). Values are presented as mean±SEM.

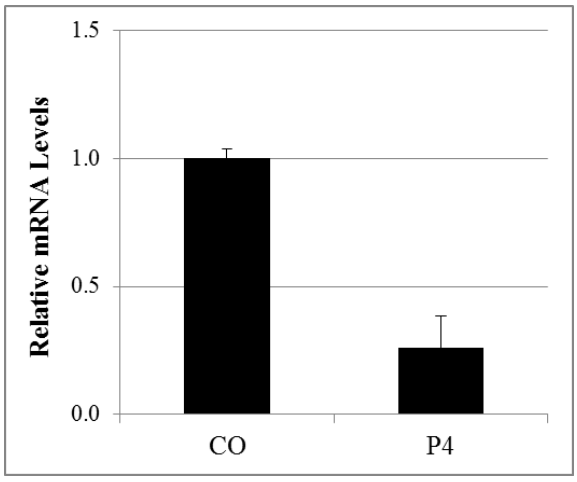

Figure A.2 *PGR* mRNA in endometria of P4-treated gilts

Endometrial expression of *PGR* mRNA was significantly less in the P4-treated than CO-treated gilts ($p<0.05$).

and this continued through Day 85. The stroma and myometrium continued to express PGR through Day 85 of pregnancy.

In endometria from ovariectomized gilts administered exogenous P4, PGR was only detected in the stroma and myometrium (Figure A.6). In contrast, endometria from control gilts had detectable PGR in uterine LE, stromal cells, and myometrium. Neither treatment group of gilts had detectable PGR in uterine GE.

ACP5 Protein Localizes to Uterine GE and Areolae For the Majority of Pregnancy

ACP5 protein was detected in uterine GE at Day 12 of pregnancy, the abundance increased by Day 25, and then remained in uterine GE to Day 85 (Figure A.6). At Day 25, ACP5 protein localized to the lumen and CE of the areolae, and expression in the areolae continued through Day 85. ACP5 protein was not detectable in endometria from cyclic gilts (data not shown).

SPP1 Protein Localizes to Uterine LE From Day 25, and Uterine GE From Day 35 to Day 85 of Pregnancy

SPP1 mRNA is induced in uterine LE by conceptus estrogens by Day 13 of gestation (Garlow et al., 2002). As expected, in the present study, SPP1 protein was detected in uterine LE at Day 25, and expression in uterine LE was maintained throughout gestation. Interestingly, SPP1 protein was only detectable in uterine LE in the interareolar region of the interface (Figure A.6). There was no detectable SPP1 in uterine LE proximal to areolae. On Day 35, SPP1 was barely detectable in uterine GE,

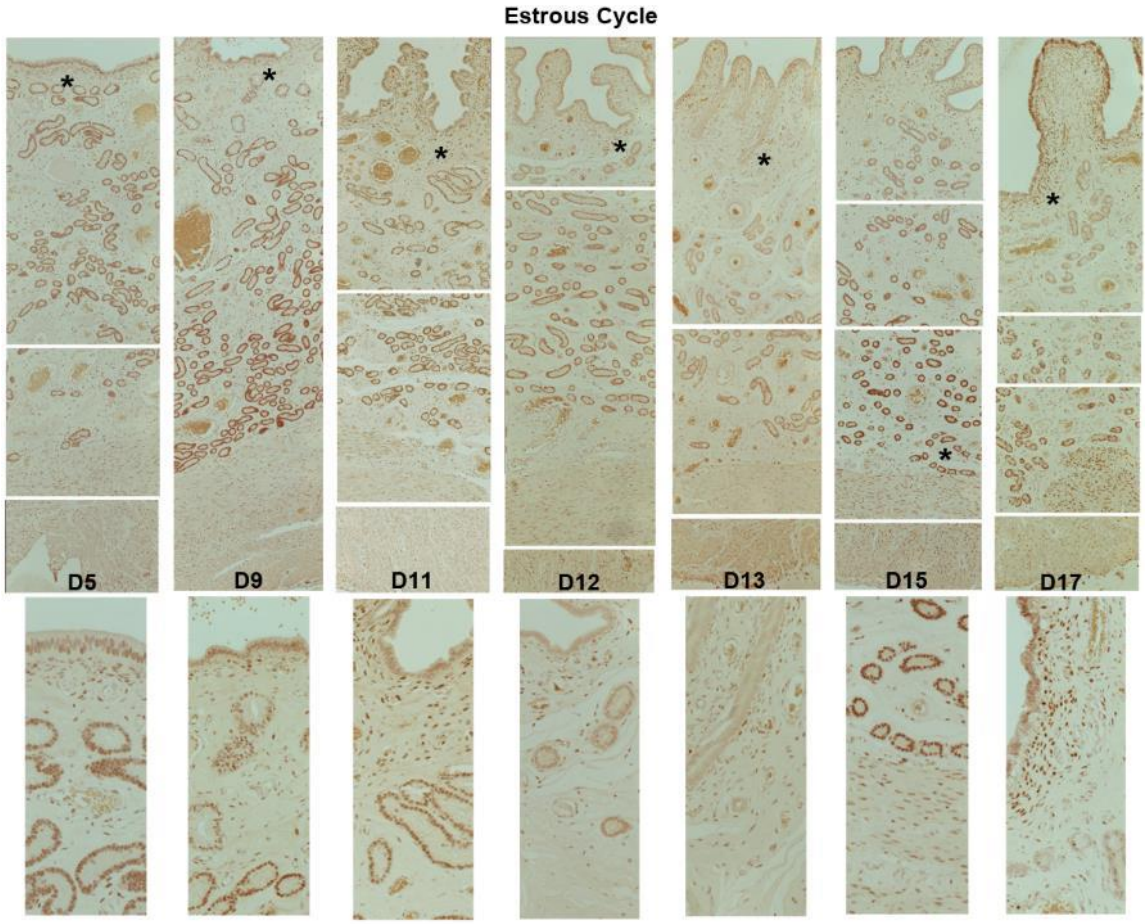

Figure A.3 Immunohistochemical localization of PGR in uteri of gilts during the estrous cycle

PGR protein localized to uterine LE, GE, stroma, and myometrium on Days 5 to 11 of the estrous cycle. At Day 12, protein was not detected in uterine LE, but was still detected in a few cells of the superficial GE, deep GE, stroma, and myometrium. At Day 17, PGR protein was detectable in uterine LE. Width of field is 570 µm. Asterisks represent area in magnified image below.

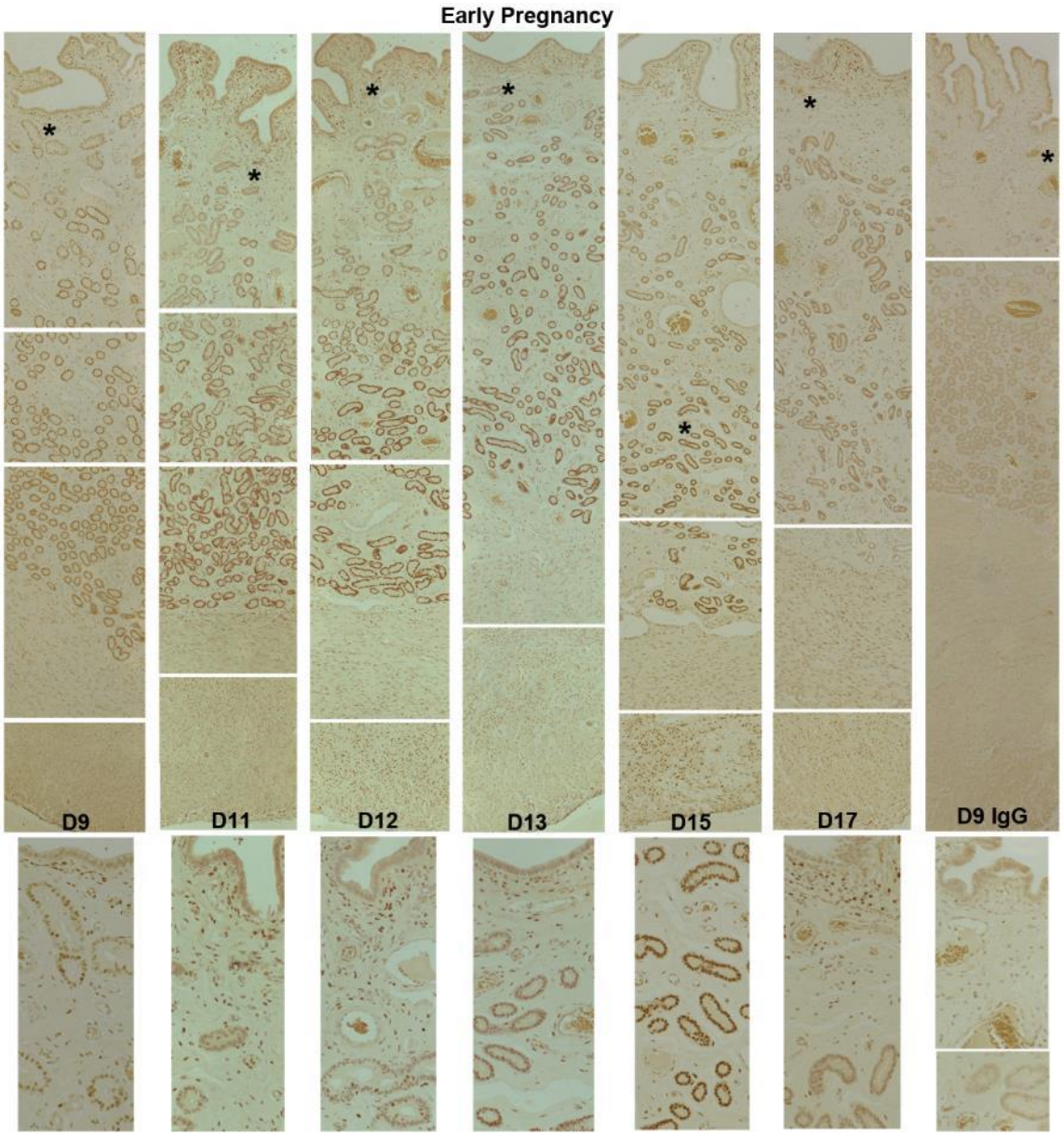

Figure A.4 Immunohistochemical localization of PGR in uteri of gilts during early pregnancy

PGR localized to uterine LE, GE, stroma, and myometrium at Day 9. By Day 11, PGR was not detected in uterine LE or the superficial GE, but was detected in deep GE, stromal cells, and myometrium through Day 17 of pregnancy. Width of field is 570 µm. The D9 IgG panel is the negative control. Asterisks represent area in magnified image below.

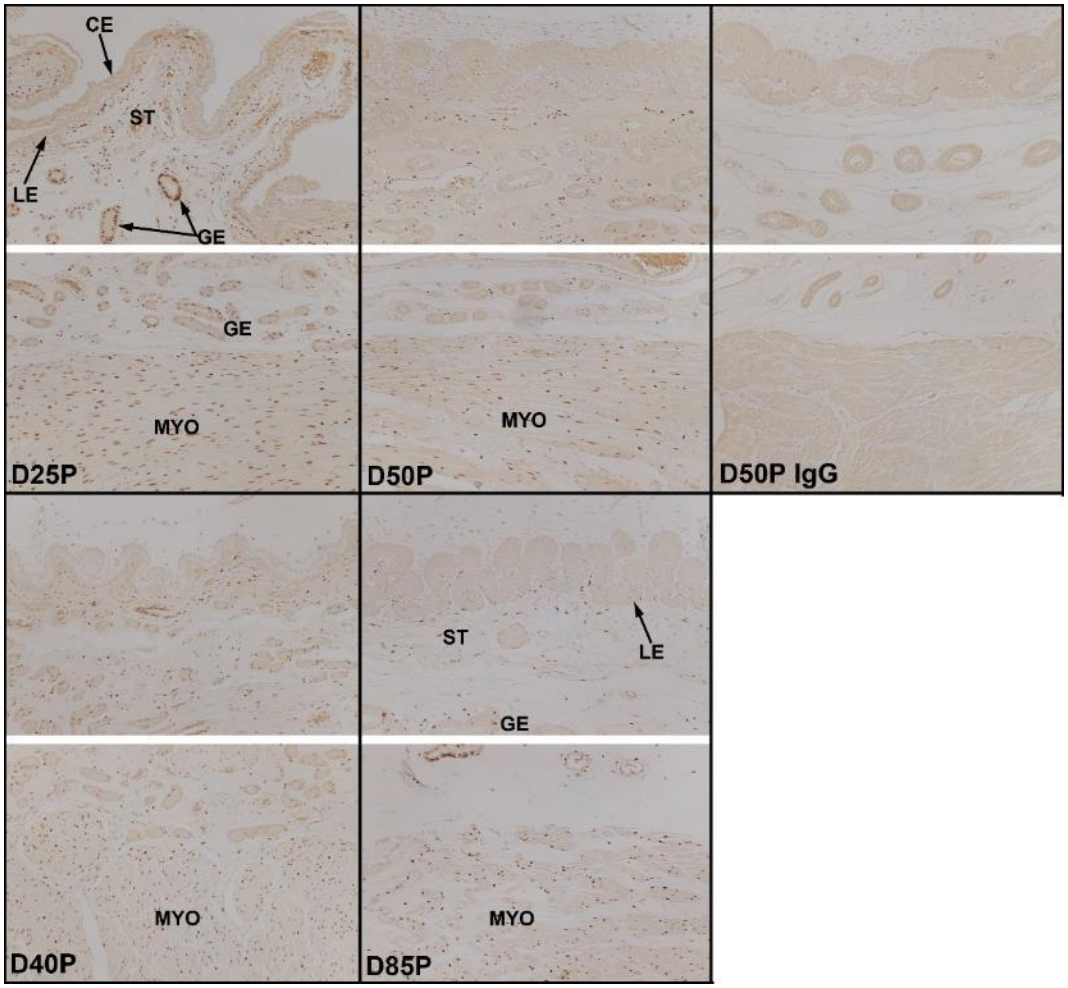

Figure A.5 Immunohistochemical localization of PGR at the uterine-placental interface during mid- to late-pregnancy in pigs

PGR localized to stromal cells and myometrium from Days 25 to 85 of pregnancy. Additionally, at Day 25, PGR localized to uterine GE, but not every GE cell. At Day 40, the proportion of GE with detectable PGR decreased and this continued through Day 85 of pregnancy. Width of field is 870 μm. The D50P IgG panel is the negative control. Legend: LE, luminal epithelium; GE, glandular epithelium; CE, chorion; ST, stroma; MYO, myometrium.

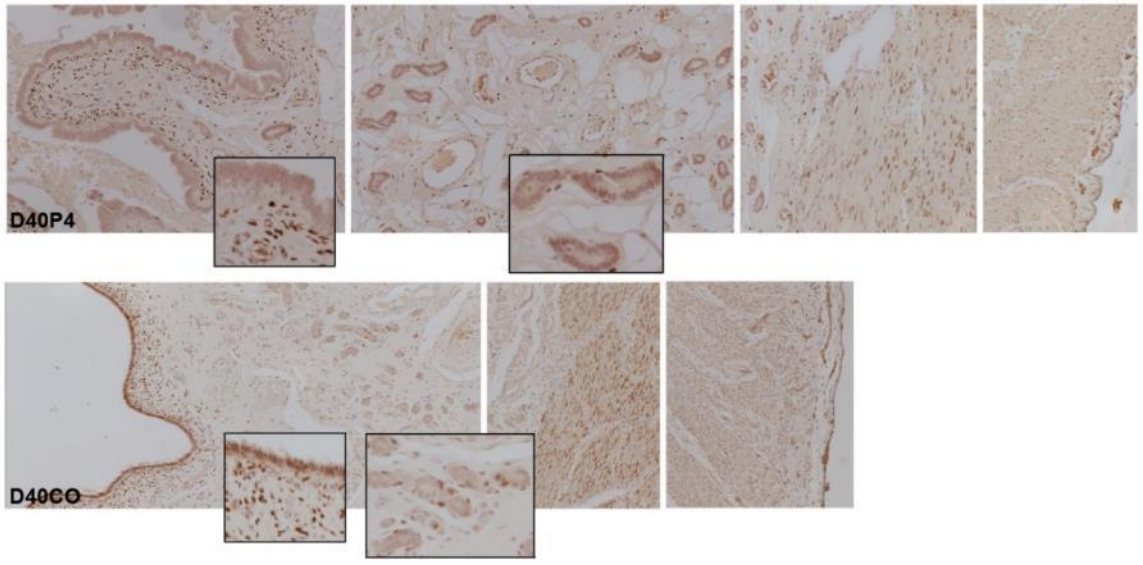

Figure A.6 Immunohistochemical localization of PGR in endometria of P4-treated gilts

In endometria of P4-treated gilts, PGR was detected in stromal cells and myometrium, while in the CO-treated gilts, PGR was detected in uterine LE, stromal cells, and myometrium. Height of field is 570 µm. The IgG negative control panel is in Figure A.4.

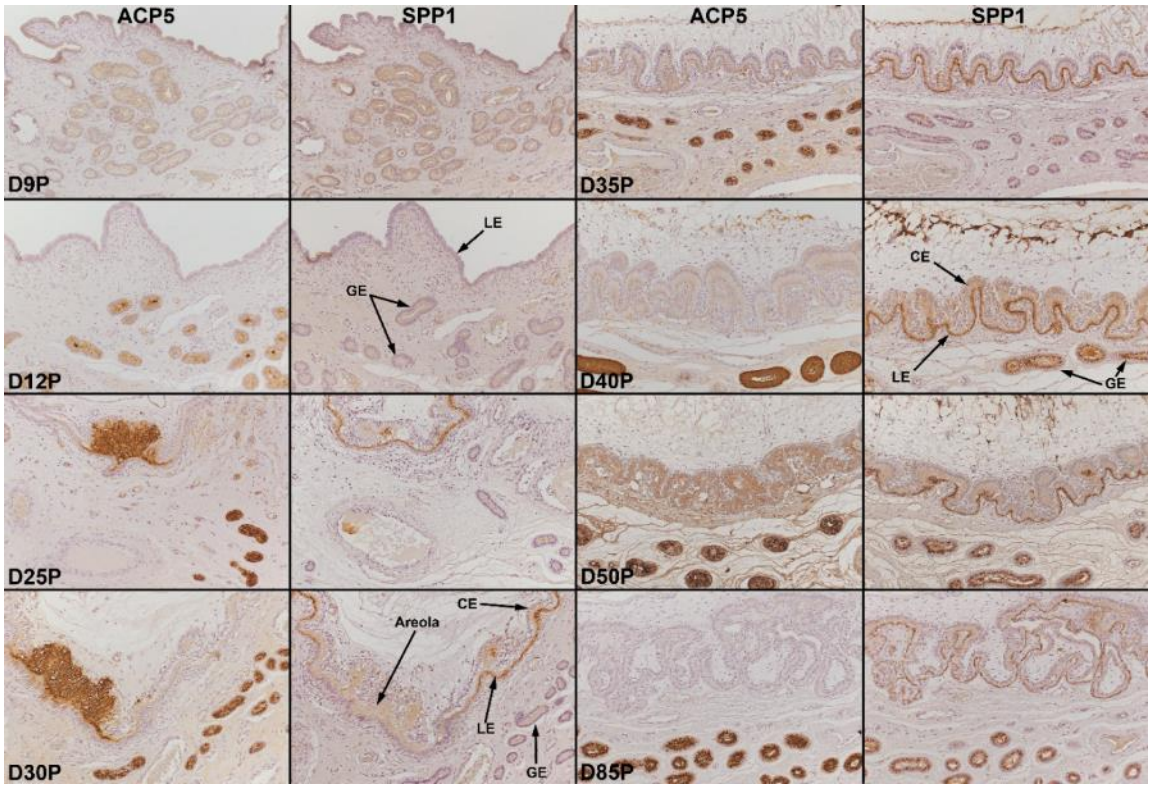

Figure A.7 Immunohistochemical localization of ACP5 and SPP1 at the uterine-placental interface during pregnancy

ACP5 protein was detected in uterine GE at Day 12 of pregnancy and in areolae at Day 25 with expression maintained through Day 85 of pregnancy in both tissues. SPP1 protein localized to uterine LE on Day 25, but was not detected in uterine LE proximal to areolae. SPP1 was detected in uterine GE at Day 35 and expression in LE and GE was maintained through Day 85 of pregnancy. Width of field is 870 µm. The rIgG negative control panel is in Figure A.8. Legend: LE, luminal epithelium; GE, glandular epithelium; CE, chorion.

but it was strongly expressed in uterine GE by Day 40. SPP1 was also detectable in the allantoic stromal cells at Day 40. GE and allantoic localization of SPP1 continued through Day 85. SPP1 was not detectable in endometria from cycling gilts (data not shown).

PGR, But Not ACP5 or SPP1, Localized to Uterine GE That Immediately Empty Into Areolae

PGR was expressed in uterine GE immediately adjacent to areolae, specifically uterine GE that opens directly into the areola, but not in any other GE (Figure A.7). Additionally, two protein components of histotroph, ACP5 and SPP1, were not detected in the GE that expressed PGR in serial sections at Day 40 of pregnancy. ACP5 was detected in the lumen of the PGR-positive GE, indicating that it was connected to GE that did secrete ACP5. Indeed, GE less than 200 μm away in the histological section clearly expressed ACP5 and SPP1.

Discussion

P4 is required for a successful pregnancy, yet the localization of PGR, an essential mediator for effects of P4, has not previously been evaluated beyond Day 18 of pregnancy in the pig. This study establishes that: 1) PGR expression in uterine LE returns by Day 17 of the estrous cycle; 2) PGR expression is maintained in the deep GE throughout the estrous cycle and early pregnancy; 3) PGR expression is maintained in the uterine stroma and myometrium through Day 85 of gestation; and, 4) PGR is

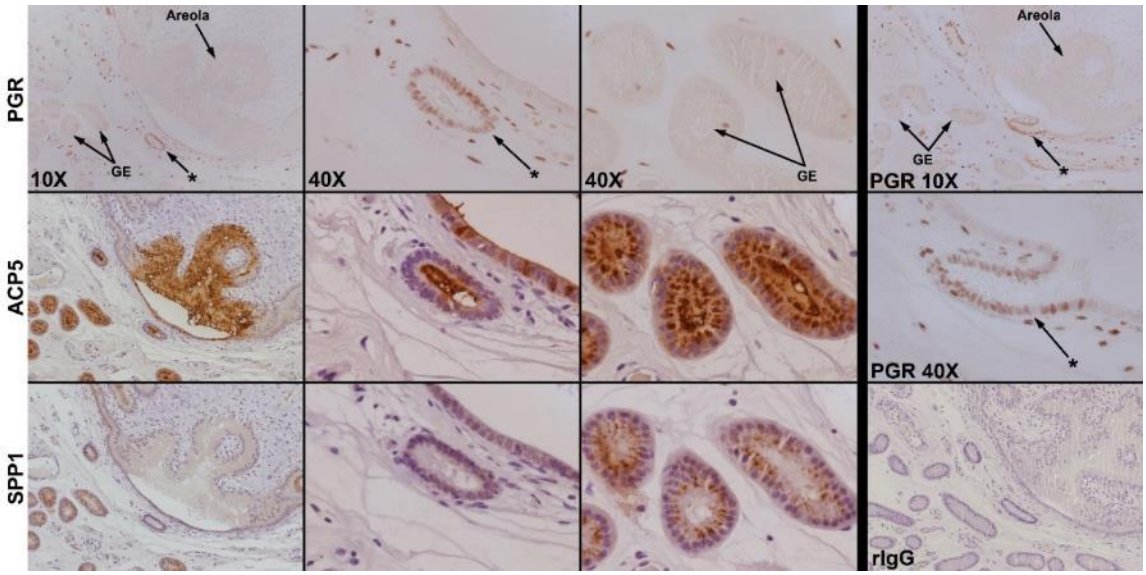

Figure A.8 Immunohistochemical localization of PGR, ACP5, and SPP1 in uterine GE proximal to areolae

PGR is detected in uterine GE directly beneath an areola (*), which open directly into the areola at Day 40 of pregnancy. GE not directly adjacent the areola do not express PGR. ACP5 and SPP1 are not detected in uterine GE that contain PGR, but both proteins are observed in the lumen of the uterine glands and in GE distant from the areola. Width of field is 870 µm. The rIgG panel is the negative control. Legend: GE, glandular epithelia.

expressed in the necks of uterine GE that empty into the areolae, suggesting that these regions of GE are excretory ducts that are not involved in the synthesis of histotroph, but serve as conduits for the passage of histotroph into the areolar lumen.

During the estrous cycle, uterine expression of *PGR* mRNA was high on Days 5 and 9, low on Days 11 and 13, and returned to high on Days 15 and 17. The protein localization for PGR confirmed that these changes are due to the loss of PGR from the LE and shallow GE by Day 11, which returned to LE and shallow GE by Day 17. The loss of PGR in uterine LE due to downregulation by its ligand, P4, has been described, but this is the first study to demonstrate the return of PGR protein in uterine LE late in the estrous cycle in the pig (Spencer et al., 2004; Mathew et al., 2011). This is expected due to decreasing concentrations of P4 as a result of luteolysis, and increasing concentrations of estrogen in blood during proestrus of the estrous cycle (Henricks et al., 1972).

The pattern of PGR expression during early pregnancy is similar to that observed for the estrous cycle with the a loss of detectable PGR from uterine LE around Day 11, and a decrease in detectable PGR in the superficial GE after Day 12, resulting in only a few sporadic cells in the shallow GE expressing PGR by Day 17. As expected, PGR remained detectable in stromal cells and myometrium through Day 17 of pregnancy. These results are similar to those reported by Geisert et al. in terms of uterine LE, stromal cells, and myometrium; however, in the present study PGR was expressed in GE beyond Day 12, particularly in the deep GE, although not in every gland or every GE cell. This could be partly attributed to the use of an antibody against PGRA and PGRB

in this study, while previous reports on cell localization of PGR in uteri utilized antibodies generated against PGRB (Geisert et al., 1994).

This study, for the first time, localized PGR in the uteri of pregnant gilts to Day 85 of gestation. At Day 25, some GE cells expressed PGR, but the proportion of cells expressing PGR decreased gradually until expression was undetectable at Day 50 and Day 85 of pregnancy. The loss of PGR in uterine GE from Days 25 to 50 corresponds to the stage in gestation when uterine GE is undergoing extensive hyperplasia and hypertrophy, which results in a dramatic increase in total uterine secretions after Day 30 of pregnancy (Knight et al., 1974; Basha et al., 1980; Perry and Crombie, 1982). The concurrent timing of PGR downregulation in uterine GE and activation of uterinr GE to increase secretion of histotroph suggests that PGR downregulation may be necessary for maximal production of histotroph. The uterine stromal cells and myometrium continued to express PGR from Days 25 through 85.

As expected, ovariectomized gilts treated with P4 long term exposure had downregulated expression of PGR in uterine LE and GE. However, surprisingly, there was no detectable PGR in GE of endometria from either the P4-treated or control gilts, suggesting that downregulation of PGR in GE may not be completely P4-dependent since PGR protein was not observed in endometria that had not been exposed to ovarian or exogenous steroid hormones. Conversely, estrogen may be required to upregulate and/or maintain PGR expression in GE and the endometria of the ovariectomized gilts in this study were not exposed to estrogens (Ing and Tornesi, 1997).

ACP5 and SPP1 protein had previously not been localized in porcine endometria throughout pregnancy. Immunohistochemistry was used previously to demonstrate that ACP5 is expressed by uterine GE of pigs at Day 60 of pregnancy, and is present in the areolae at Day 75 (Renegar et al., 1982). Results from the present study show that, in addition to expression of ACP5 in GE and areolae during mid-pregnancy, ACP5 is detected in uterine GE at Day 12 of pregnancy, in areolae by Day 25 when areolae are initially developing, and in uterine GE and areolae to Day 85 of pregnancy. *In situ* hybridization analysis demonstrated that estrogens secreted by the conceptus induce expression of SPP1 mRNA in discrete regions of uterine LE juxtaposed to the conceptus, and expression expands to the entire LE by Day 20, where expression is maintained through Day 85 (Garlow et al., 2002). Results from the present study provide further detail in that, unlike previously reported, SPP1 is not expressed in uterine LE adjacent to areolae. The physiological significance of this pattern of expression is not known, but SPP1 is proposed to attach uterine LE to chorion during implantation, and areolae are the only regions of the chorion that do not attach to uterine LE. The present results on localization of SPP1 protein are coordinate with results from *in situ* hybridization analyses showing that SPP1 is first detected in uterine GE at Day 35, increases through Day 40, and continues to be expressed in uterine GE through Day 85.

SPP1 is highly abundant in the allantoic stroma from Days 40 to 60 of pregnancy (Figure A.7). Although the exact cell type secreting SPP1 is unclear, the protein is located near the placental blood vessels. A similar pattern of SPP1 expression has also been observed in the allantoic stroma of the sheep. Interestingly, when ITGB3, an

integrin receptor for SPP1, was knocked down in sheep conceptuses, SPP1 mRNA was decreased in the placenta, and in those same conceptuses, fetal crown-rump length was decreased. These findings led to the hypothesis that SPP1 may enhance placental angiogenesis, which would allow for greater nutrient transport to the fetus (J.W. Frank and G.A. Johnson, unpublished results). The pattern of SPP1 expression in the allantoic stroma of the pig in this study suggests a similar role for SPP1 in angiogenesis.

Of interest is the observation that PGR was detected in the GE that directly open into the areolae. The epithelial cells that comprise the opening of the uterine glands have been hypothesized to have minimal secretory activity due to their cuboidal cytological form and small surface area (Friess et al., 1981; Leiser and Dantzer, 1994). Additionally, the capillary network that supplies the necks of the glands is a sparse, wide mesh of large capillaries, but as the gland tubule is followed down into the uterine stroma, toward the myometrium, the capillary bed becomes more intricate with smaller vessels indicative of transport occurring between the blood vessels and uterine GE (Leiser and Dantzer, 1994). Further, we observed that two histotroph proteins, ACP5 and SPP1, are not detected in uterine GE that express PGR, although immunoreactive secretory product for these proteins are present in the lumens of the necks of the glands. We propose that the necks of the GE that directly open into the areolae are classic excretory ducts, similar to many other glands in the body, that do not produce histotroph, but serve only to transport histotroph into the lumens of the areolae.

The presence of PGR in the necks of glands that do not synthesize ACP5 and SPP1, juxtaposed to the lack of PGR in uterine GE that does synthesize ACP5 and SPP1,

highlights the conundrum that P4 regulates the expression of genes in cells that do not express PGR, and that the presence of PGR in GE cells appears to prevent the ability of P4 to induce protein expression in those cells (Chen et al., 1975; Bailey et al., 2010a). Indeed, the presence of PGR appears to have an inhibitory effect on ACP5 and SPP1. The paradox of having gene and protein upregulation by P4 in cells lacking PGR has been discussed extensively, but no definitive explanation has been put forward. One hypothesis is that effects of P4 on epithelial cells are mediated through PGR-positive stromal cells that can respond to P4 and produce paracrine-acting factors (termed progestamedins) that then act on epithelial cells (Johnson et al., 2000; Ka et al., 2007). If this is the case, then the presence of PGR may block the effects of progestamedins on expression of genes in uterine GE adjacent to areolae.

In conclusion, these results are the first to show that PGR is maintained in uterine stromal cells and myometrium through Day 85 of pregnancy, but PGR expression is not detectable in epithelia beyond Day 50 of pregnancy, except in the necks of uterine GE that empty into areolae. PGR expression in the necks of uterine GE appears to inhibit the ability of GE to produce ACP5 and SPP1, which suggests that these regions are uterine gland excretory ducts that serve as conduits for the passage of histotroph into the lumen of the areola.

APPENDIX B

PROTOCOLS

RNA Extraction

An RNA extraction protocol for tissues.

1. Place frozen tissue samples (~1g) directly into 10 ml Trizol reagent (Life Technologies, Carlsbad, CA, USA) in a 50 ml conical tube on ice.
2. Homogenize the tissue using a Tissuemizer.
3. Incubate the homogenized tissue at room temperature (RT) for 5 min.
4. Centrifuge the samples at 12,000 x g for 10 min at 4°C.
5. Keep the clear supernatant and add 2 ml chloroform. Vortex and centrifuge at 12,000 x g for 10 min at 4°C.
6. Keep the aqueous phase and add an equal volume of isopropanol. Vortex, incubate at RT for 10 min, then centrifuge at 12,000 x g for 10 min at 4°C.
7. Aspirate off the liquid, wash the pellet with 10 ml 70% ethanol, and centrifuge at 7,500 x g for 5 min at 4°C.
8. Aspirate off the ethanol, let pellet dry, and re-suspend the pellet in 400 µl nuclease-free water. Incubate at 70°C for 5 min to completely dissolve the pellet.

DNase Treatment

A protocol to remove contaminating DNA from RNA samples.

For 1 reaction using DNase I (Qiagen):

87.5µl RNA from Trizol extraction
10µl RDD Buffer
2.5µl DNase I

Incubate for 15 min at RT and then 5 min at 70ºC.

cDNA Synthesis

A protocol for synthesis of cDNA using the Superscript III First Strand Kit (Life Technologies).

For 1 reaction: 5µg RNA
1µl oligo(DT)20
1µl 10mM dNTP
Nuclease-free water up to 10µl

Incubate for 5 min at 65ºC.

Add:
2µl 10x RT Buffer
4µl 25mM $MgCl_2$
2µl 0.1M DTT
1µl RNaseOUT
1µl Superscript III Reverse Transcriptase

Incubate at 50ºC for 50 min with the reaction being terminated at 85ºC for 5min. Add 1µl RNase H and incubate for 20 min at 37ºC.

Quantitative PCR

A protocol for determining mRNA expression in tissues.

1. Dilute cDNA from synthesis reaction 1:10 in nuclease-free water.
2. Use the following reaction mix, repeated in triplicate for each sample:
   5 µl PerfeCta SYBR Green Mastermix (Quanta Biosciences)
   1.25 µl Primers (forward and reverse, 10 mM stock)
   2.5 µl cDNA (~60ng)
   1.25 µl Nuclease-free water
   10 µl total
3. Pipette reactions into a 96-well plate and seal the plate.
4. Run the following PCR program:
   A. 5 min at 95°C
   B. 95°C denaturation for 10 sec
   C. 60°C annealing/extension for 30 sec
   D. Repeat B and C for 40 cycles
   E. Run a dissociation curve after every run

Immunohistochemistry

Immunohistochemistry is a tool for visualizing the cell localization of proteins in tissue sections.

1. Cut 5 µm thick sections from paraffin-embedded tissue blocks using a microtome. Place cut sections on 42°C distilled water, then move sections onto glass slides. Leave the slides at 37ºC overnight to ensure adhesion of the tissue to the glass slide.

2. Deparaffinize sections in Citrosolv, three washes for 4 min each, then rehydrate tissues through a series of ethanol washes (100% x3, 95% x2, 70% x2) for 30 sec each before placing slides in phosphate buffered saline (PBS pH 7.2).

3. Antigen Recovery:

A. Protease- Warm PBS to 37ºC, add Protease (0.5mg/ml), then submerge slides for 8 min. Rinse slides in distilled water and return them to PBS.

B. Boiling Citrate Buffer- Make a solution of 41ml 0.1M Sodium Citrate, 9ml 0.1M Citric Acid, and 450ml distilled water, then bring to a boil. Submerge the slides for 10 min, then remove the buffer from the heat, but leave the slides in the buffer for another 20 min. Return the slides to PBS.

C. No retrieval- Slides remain in PBS.

D. Note- When testing antibodies, test all three retrievals to determine the optimal one for the tissue of interest.

4. Quench the endogenous peroxidase activity by washing the slides in 1% H_2O_2 in methanol (6.7ml 30% H_2O_2 per 200ml methanol) for 15 min at room temperature. Rinse the slides in distilled water, then in PBS twice for 5 min.

5. Circle sections with a PAP pen, then lay the slides flat before adding a blocking solution to block nonspecific reaction sites. When using the Vectastain ABC Kit (either the Mouse or Rabbit IgG kit), add 3 drops (or 100 µl) normal serum to 10 ml of PBS to prepare the blocking solution. Add 60 µl per section to the slides to fully cover each section with solution and incubate for 10 min at room temperature. Rinse slides in PBS twice for 5 min.

6. The primary antibody will be diluted in a solution of PBS+1% BSA+0.1% Triton-X to 1-5 µg/ml (for pig tissues, start with 5 µg/ml, but the concentration may need to be adjusted). Purified IgG from the species that is the antibody host will be used as a negative control and will be used at the same concentration as the primary antibody it corresponds with. A negative control will need to be run with every batch that corresponds with each antibody and retrieval method. Add 60 µl of primary antibody or IgG control per section to the slides to fully cover each section with solution and incubate overnight at 4°C in a humidified chamber (leave a small amount of PBS in the bottom of the container holding the slides). Rinse slides in PBS twice for 5 min.

7. Prepare the secondary antibody by adding 3 drops normal serum and 1 drop biotinylated secondary (from the Vectastain kit) antibody to 10 ml of PBS. Add 60 µl per section to slides to fully cover each section with solution and incubate for 60 min at 37°C. Rinse slides in PBS twice for 5 min.

8. Prepare the detector reagent at the beginning of the secondary antibody incubation so that it can stand at room temperature by adding 2 drops of A, then 2 drops of B (from the Vectastain kit) to 5 ml PBS. Add 60 µl per section to slides to fully cover each section with solution and incubate for 30 min at 37°C. Rinse slides in PBS twice for 5 min.

9. Wash slides in 0.05M Tris-HCl (pH 8.8) for 5 min. Then, add 100mg 3,3'-diaminobenzidine tetrahydrochloride (DAB) and 50µl H_2O_2 to 200 ml Tris-HCl before submerging the slides. As the slides are incubating in DAB at room temperature, monitor the sections under a microscope until the desired color intensity is reached (2-10 min). Stop the reaction by placing the slides in tap water.

10. Counterstain slides with Harris modified hematoxylin (1-20 sec), rinse with distilled water until water is clear, then dehydrate sections through a series of alcohol washes (70% x2, 95% x2, 100% x3). Place slides in 3 washes of Citrosolv for 4 min each, then place coverslips on the slides with a drop of Permount mounting medium.

11. Let slides dry overnight on a flat, dry surface that is protected from light.

Isotope *In situ* Hybridization

In situ hybridization is a tool for visualizing the cell localization of a target mRNA in tissue sections.

1. Design primers for the gene(s) of interest with primers of 20-24 bases and a product length of 400-600 bases using known sequences for the species of interest (available through NCBI).

2. Generate partial cDNAs by RT-PCR using cDNA from a sample that will have an ample amount of the gene of interest. For each reaction:

2.5µl 10x PCR Buffer
0.5µl 10mM dNTP
0.75µl 50mM $MgCl_2$
1µl Forward Primer (10mM stock)
1µl Reverse Primer (10mM stock)
3µl cDNA from a 5µg total RNA reaction (~0.75 µg RNA)
Nuclease-free water up to 25µl total for the reaction

PCR amplification parameters are: 1) 95ºC for 5 min; 2) 95ºC for 45 sec, 60ºC for 30 sec, 72ºC for 1 min for 40 cycles; and, 3) 72ºC for 10 min.

3. Amplified PCR products will then be subcloned in the pCRII cloning vector using a TOPO TA Cloning Kit (Life Technologies):

A. Mix 4 µl of fresh PCR product with 1 µl salt solution and 1 µl TOPO vector, then incubate for 5 min at room temperature.
B. Add 2 µl of the mixture in (A) to one vial of bacteria from the kit. Keep bacteria on ice from removal from freezer to heat shock. Incubate for 5 min on ice.
C. Heat-shock the bacteria for 30 sec in a 42°C water bath without shaking, then transfer the vial back to the ice.
D. Add 250 µl of room temperature S.O.C. medium.
E. Shake the tube horizontally (200 rpm) at 37°C for 1 hr.
F. Spread 10-50 µl from each vial on a prewarmed (37°C) agarose plate (see below for plate instructions) and incubate overnight at 37°C to grow colonies.
G. Pick ~10 white colonies to transfer individually into glass tubes with 3 ml LB broth for propagation.

4. Preparation of LB broth and agarose plates:

A. LB Broth- 10 g Tryptone
5 g Yeast Extract
5 g NaCl
1 ml 1M NaOH

Up to 1L of ddH_2O

B. LB Broth + Agar- 1L LB Broth
15 g Agar

C. Autoclave both LB Broth and LB Broth + Agar for 30 min.

D. While still warm, pour LB Broth + Agar into 100mm polystyrene culture plates

E. After LB Broth has cooled, add 1 ml Carbenicillin (100 µg/ml) to 1L LB Broth

F. Before using plates, spread 40 µl X-gal (40 mg/ml) on each plate, then warm to 37°C

5. Propagate colonies from Step 3G in 3 ml LB Broth in glass tubes in a shaker (200 rpm) at 37°C overnight (tubes will a cloudy appearance have appropriate bacteria growth).

6. Collect 1 ml of media containing bacteria and perform a DNA extraction using the DNA MiniPrep (Macherey-Nagel, Germany) according to manufacturer's instructions. The other portion will be stored at 4ºC until a colony is determined to contain the desired insertion.

7. Purified DNA from the MiniPrep will be used for a restriction enzyme digest. For 1 reaction:

12.3µl water
2.0µl restriction enzyme buffer
0.2µl acetylated BSA(10µg/µl)
5µl DNA
0.5µl EcoR1(10U/µl)
20µl total

After a 2 hr incubation at 37ºC, run the digest on a 2% agarose electrophoresis gel for 30 min. Positive colonies will display a large vector band and a band at the product length of the primers used.

8. Sequence the DNA from positive colonies in both directions using an ABI PRISM Dye Terminator Cycle Sequencing kit and an ABI PRISM automated DNA sequencer (Applied Biosystems, Foster City, CA) to confirm sequence identity.

9. Propagate one clone for each gene with the correct sequence in 250 ml LB Broth at 37°C overnight on a shaker (200 rpm).

10. Collect the media containing the bacteria and extract the DNA plasmids using a MaxiPrep Kit (Macherey Nagel) according to manufacturer's instructions. Keep 500 µl of bacteria culture and add it to 500µl 80% glycerol for a stock that can be frozen and stored at -80°C.

11. Linearize the DNA plasmids by digestion with an appropriate restriction enzyme. Choose restriction enzymes that will not cut the gene sequence, but will cut on the appropriate side of the insert to create both sense and anti-sense strands. Use the vector map to help with this. For 1 reaction:

20µg of DNA
20µl Restriction Enzyme Buffer
20U Restriction Enzyme
Nuclease-free water up to 200µl

Incubate for 2 h. The temperature will depend on the enzymes used.

12. Purify the linearized DNA using the following Phenol:Chloroform Extraction:

A. Add 200 µl PCI pH 8.0 to linearized DNA, then centrifuge at 20,000 x g for 10 min.

B. Retain the top phase, add 200 µl Chloroform, then centrifuge at 20,000 x g for 10 min.

C. Retain the top phase, add 3 vol 100% ethanol, 1/10 vol 3M NaOAc, and 5µl dextran T500 (10mg/ml), then place in -80ºC freezer for 15 min to precipitate DNA.

D. Centrifuge the solution for 10 min at 20,000 x g at room temperature.

E. Remove liquid, wash the pellet with 150 µl of 70% ethanol, and centrifuge again.

F. Remove liquid and re-suspend the pellet in 40 µl nuclease-free water.

13. Generate the isotope-labeled antisense or sense cRNA probes with an *in vitro* transcription reaction.

A. Perform the following reaction for each probe:

1µg linearized DNA
5µl 5x Transcription Buffer
2.5µl 100 mM DTT
2.5µl 2.5mM rGAC
1µl RNasin
2.5µl [α-^{35}S]-UTP
1.5µl T7 or SP6 RNA polymerase
Nuclease-free water up to 25µl

B. Incubate the probe reaction at 37ºC for 2 hr.

C. Add 3µl RQ1-DNase I and 1.5µl RNasin, then incubate for 15min at 37ºC.

D. Add 25µl yeast tRNA (10mg/ml) and 100µl PCI pH 4.5, then centrifuge at 20,000 x g for 5 min.

E. Aspirate the top layer and place it into a new tube to do a second extraction with 100µl chloroform:isoamyl alcohol (24:1), then centrifuge at 20,000 x g for 5 min.

F. Place the top phase of the second extraction in the center of a NucAway (Ambion) gel column that was rehydrated with 650µl of nuclease-free water 30 min earlier and centrifuge for 2 min at 750 x g.
G. Add 60µl 3M NaOAc (pH 5), 2µl yeast tRNA, and 300µl 100% ethanol then place at -80ºC for 15min, followed by centrifugation for 10min at 20,000 xg at 4ºC.
H. Remove the supernatant, wash the pellet with 150 µl 70% ethanol, and centrifuge for 10 min at 20,000 x g at 4°C.
I. Aspirate the liquid and re-suspend the pellet in 50µl of 100mM DTT
J. Add 2 µl of the probe into a vial with 2 ml EcoLum and place the vial into a scintillation counter to determine the isotope count.

14. Cut 5 µm thick sections from paraffin-embedded tissue blocks using a microtome. Place cut sections on 42°C ddH_2O , then move sections onto glass slides. Leave the slides at 37ºC overnight to ensure adhesion of the tissue to the glass slide.

15. Deparaffinize sections in Citrosolv, three washes for 4 min each, then rehydrate tissues through a series of ethanol washes (100% x3, 95% x2, 70% x2) for 30 sec each before placing slides in phosphate buffered saline (PBS pH 7.2; RNase-free) and following this series of washes:

A. PBS, 5 min, 2 washes
B. Fresh 4% Paraformaldehyde, 20 min, 1 wash
C. PBS, 5 min, 2 washes
D. Proteinase K (20 µg/ml) in 50mM Tris, 5mM EDTA, 7.5 min, 1 wash
E. Fresh 4% Paraformaldehyde, 5 min, 1 wash
F. DEPC-treated water, 1 min, 1 wash
G. PBS, 5 min, 2 washes
H. 70% Ethanol, 30 sec, 2 washes
I. 95% Ethanol, 30 sec, 2 washes
J. 100% Ethanol, 30 sec, 2 washes
K. Air dry the slides at room temperature

16. Prepare the cRNA probe in hybridization solution containing 100 mM DTT calculating for $5x10^6$ CPM/slide and 75 µl of solution per slide. Incubate for 10 min at 70°C.

17. Add the hybridization solution containing the probe to each slide and gently place a coverslip on top with no bubbles. Hybridize overnight in a humidified chamber at 55°C.

18. After hybridization, the slides will be sent through a series of washes:

A. 5x SSC*/10mM βME, 30 min, 1 wash, 55°C
B. 50% Formamide/2x SSC/50mM βME, 20 min, 1 wash, 65°C
C. TEN (0.5M NaCl, 10mM Tris pH 8, 5mM EDTA), 10 min, 1 wash, RT
D. TEN, 10 min, 3 washes, 37°C

E. RNase A (10 µg/ml) in TEN, 30 min, 1 wash, 37°C
F. TEN, 15 min, 1 wash, 37°C
G. 50% Formamide/2x SSC/50mM βME, 20 min, 1 wash, 65°C
H. 2x SSC, 15 min, 1 wash, RT
I. 0.1x SSC, 12 min, 1 wash, RT
J. 70% Ethanol/0.3M Ammonium Acetate, 5 min, 2 washes, RT
K. 95% Ethanol/0.3M Ammonium Acetate, 1 min, 1 wash, RT
L. 100% Ethanol, 1 min, 2 washes
M. Air dry slides, then expose to Biomax film overnight in cassettes (16-18 hrs) to estimate emulsion exposure time
*20x SSC contains 3M sodium chloride and 0.3M sodium citrate at pH 7

19. All work with Kodak NTB2 emulsion must be done in the dark. Thaw emulsion at 42°C in a light tight container. Mix emulsion 1:1 with 42°C water. In the dark, dip slides in emulsion mix, wipe excess emulsion off the back of the slide and place in a slide box containing dessicant. Leave slide boxes in a light tight box overnight to dry at RT, the wrap slide boxes in foil and place at 4°C for 5-14 days (depending on exposure on films).

20. Develop slides in the dark, at RT, using the following series of washes:
A. Kodak D-19 Developer, 4 min, 1 wash
B. Water, 0.5 min, 1 wash
C. Kodak Rapid Fixer, 5 min, 1 wash
D. Water, 5 min, 2 washes (light can be turned on)
E. Hematoxylin, 20 sec, 1 wash
F. 50% Ethanol, 5 min, 1 wash
G. 70% Ethanol, 5 min, 1 wash
H. 95% Ethanol, 3 min, 2 washes
I. 100% Ethanol, 3 min, 3 washes
J. Citrisolv, 4 min, 3 washes
K. Affix coverslips with Permount, then allow slides to dry on a flat surface.

21. View slides using bright-field and dark-field illumination microscopy.